Transient Analysis of Diffusion and Adsorption under Reaction Conditions

Dipl. Ing. Peter Schwan

Submitted in fulfillment of the requirements for the degree of

Doctor of Philosophy

Department of Chemical Engineering
University of Cape Town
Cape Town, South Africa.

Supervisor: Dr. K.P.Möller

June 2001

Synopsis

During heterogeneous catalysis reactant molecules have to first diffuse through the porous catalyst and adsorb on the active site in order to react. Measuring these three processes simultaneously is of great importance for the development and design of catalysts and catalytic processes. The simultaneous measurement of these processes require the use of transient techniques.

The aim of this thesis is to measure diffusion and adsorption of hydrocarbons under reaction and non-reaction conditions in a jetloop reactor using a pulse technique. The jetloop is a recycle reactor approximating a CSTR. Cumene cracking to benzene and propene was chosen as test reaction. A key question in this thesis was, whether model parameters are theoretically measurable and what errors can be expected and how this information is applied in practice.

A minimum required theoretical recycle ratio of 20 was established, for which the recycle reactor approximates CSTR behaviour under the chosen conditions in this work. It was demonstrated in pulse RTD studies that this minimum recycle ratio can always be achieved, if flow rates are chosen high enough. The maximum measured recycle ratio of an empty reactor was 70. For the product analysis a semi-automated rotating Multi-Ampoule-System (MAS) was developed, that allowed sampling of the rapidly changing effluent concentration profiles at time intervals of 0.5-1s. The effluent concentration in the quickest case varied by over three orders of magnitude within 15s. A RTD study using the pulse responses in an empty CSTR, in which the MAS system and the online FID were both used was carried out. The MAS and online FID results were in excellent agreement with each other and with the theoretically expected response.

A theoretical study of reacting and non-reacting systems yielded the following results. An analytical solution for the pulse response curve of adsorbate under *non-reaction conditions* on biporous catalysts in a CSTR was presented, for which parameter estimations from experimental response curves can be achieved by calculating the first moment and the slope in the long time solution of a semi-logarithmic plot. It was shown that micropore and macropore diffusion mechanisms can only be distinguished, if either the pellet or the crystal size is varied.

For the case *with reaction* a linear macropore model with the following three key dimensionless parameters was developed:

1. α = reactor residence time / apparent (with adsorption) diffusion time
2. β = catalyst contact time / diffusion time
3. Thiele modulus φ = diffusion time / reaction time.

A ...meter sensitivity analysis revealed the following findings

Any variation of the three reactant
he groups $\beta_R\varphi$ and $\alpha_R\varphi^2$ are held

$\varphi^2 < 10^{-2}$.

t of α_R, if $\frac{\beta_R}{\alpha_R^2\varphi^3} < 10^{-2}$. The dynamic
. The only information that can be
ion.

ers can be estimated from a product
rption. Four highly correlated param-
ined. Two estimation procedures are

ieters have to be known a priori. The
ed.
alyst mass: At least one parameter has
ters can be estimated.

ns yielded the following results. The pa-
opane and butane on commercial zeolite
analytical solution are compared to pre-
surements of propane (T=55°C..200°C)
n a commercial ZSM-5 extrudate. The
= 875 at 75°C and an adsorption en-
values found in literature. Diffusion in
nd found to be independent of tempera-
ten times larger than that expected from
se experiments of benzene on the same
erage value of 0.015 cm^2/s, which was a
nate. Both deviations were attributed to
adsorption enthalpy of benzene was 120
strong adsorption behaviour of benzene
5. The benzene adsorption coefficient was

Pulse response curves of cumene showed no measurable effect of reversible adsorption (α_R negligible) with the system being diffusion limited ($\varphi \gg 3$). Benzene adsorption was found to be about ten times higher than propene adsorption. Two parameter estimation methods were thus possible (see above), using a least square method to fit the model to the experimental data:

- By assuming that (i) the ratio of diffusivities are given by Knudsen relation and (ii) the benzene diffusivity (β_{Be}) is known from benzene pulse experiments, the model could represent experimental data well, but the estimates of the first order reaction rate constant k_{eff} and the benzene adsorption K_{Be} had a scatter of more than an order of magnitude. k_{eff} was found to be dependent on conversion, which could be qualitatively explained by a Langmuir-Hinshelwood model. K_{Be} was about one order of magnitude smaller than estimated from benzene pulse experiments.

- Parameter estimation from simultaneous fit of all experiments as a function of catalyst mass, particle size and flow rate. Benzene diffusivity D_{Be} was the only parameter known a priori. Consistently good model fits could be achieved, however, a high degree of uncertainty in the parameter estimates can be seen in the table below.

	T=420°C			T=440°C		
	Low Estimate	Estimate	High Estimate	Low Estimate	Estimate	High Estimate
$D_{Cu}[cm^2/s]$	$4.6 \cdot 10^{-4}$	$7.3 \cdot 10^{-3}$	$1.2 \cdot 10^{-2}$	$2.4 \cdot 10^{-4}$	$1.0 \cdot 10^{-3}$	$4.2 \cdot 10^{-3}$
$K_{Pr}[/]$	22	32	48	26	31	38
$K_{Be}[/]$	240	370	560	550	740	1000
$k_{eff}[s^{-1}]$	201	303	458	870	3548	14474

Diffusivities of cumene were estimated from steady state experiments of cumene cracking on ZSM-5 extrudates. The average cumene diffusivity was $0.01\,cm^2/s$, which is consistent with the diffusivity calculated with the Knudsen relation from the measured benzene diffusion coefficient. Conversions during steady state experiments ($X \approx 50\%$) were two to three times higher than those measured under transient but otherwise same run conditions.

This work has shown that the measurement of transient rate parameters is not as attractive as it might seem from intuitive thinking. Far from being able to estimate all rate processes, it was found that all the parameters were highly correlated, from a theoretical analysis. Thus applying such analysis to experimental data reduces the success of parameter estimation even further by having an unacceptably large confidence interval on the estimated parameters. It is therefore clear that transient analysis of reacting and diffusing systems with no auxiliary data will not be possible.

Contents

List of Tables

List of Figures

Nomenclature

a_h	Langmuir Hinshelwood coefficient, eq. 6.9
a_i	linear dependency coefficient of s_{ij} of component i, eq. 5.55
a_s	specific catalyst surface area $[m^{-1}]$
b_h	Langmuir Hinshelwood coefficient, eq. 6.9
b_i	linear dependency coefficient of s_{ij} of component i, eq. 5.55
d_p	pore diameter [cm]
$\overrightarrow{j_c}$	micropore flux
$\overrightarrow{j_s}$	surface flux
$\overrightarrow{j_y}$	macropore or mesopore flux
k_{eff}	first order rate constant (gas phase concentration) [1/s]
k_{hinsh}	Langmuir-Hinshelwood pseudo-first order rate constant [1/s]
k_n	n-th order rate constant
k_{obs}	observed or apparent first order rate constant influenced by diffusion [1/s]
k_R	intrinsic first order rate constant (sorbate concentration) [1/s]
k_s	surface barrier mass transport coefficient [cm/s]
m_{cat}	mass of catalyst [g]

p^*	partial pressure (equilibrium) [atm]
q	sorbate concentration in micro-particles [g/ml]
r	radial coordinate of crystals [cm]
r_c	radius of crystals [cm]
r_p	macro or mesopore radius [cm]
s	Laplace transform variable
$s_{ij}(\tau)$	sensitivity function, eq. 5.54
$\|\|s_{ij}\|\|$	integral sensitivity, eq. 5.61 and 5.63
t	time [s]
w	dimensionless number, eq. 5.15 and 5.16
x	dimensionless number, eq.5.13
x_i	correlation exponent of component i, eq. 5.56
y	radial coordinate of macroparticles [cm]
$y\%$	mole fraction
y_i	correlation exponent of component i, eq. 5.57
$\tilde{C}$	Laplace transform of concentration
C_0	initial reactor concentration [g/ml] at time 0s
C_{S_t}	surface site concentration
C_t	total adsorption site concentration
C_y	local sorbate concentration in the macropores [g/ml]
C_z	concentration in the reactor [g/ml]
C_{Exp}	experimental dimensionless concentration

C_{Mod}	dimensionless reactor concentration calculated from model
D	macropore diffusivity in cylindrical pores $[cm^2/s]$
D_∞	intracrystalline self-diffusivity $[cm^2/s]$
D_{app}	apparent diffusivity, eq.5.24 $[cm^2/s]$
D_c	intracrystalline diffusivity $[cm^2/s]$
D_K	Knudsen diffusion $[cm^2/s]$
D_m	molecular diffusion
D_p	macropore diffusivity (only in gas phase) $[cm^2/s]$
D_s	surface diffusivity in macropores $[cm^2/s]$
D_y	intercrystalline diffusivity $[cm^2/s]$
D_{Be}	macropore diffusivity $[cm^2/s]$ of benzene
D_{Cu}	intercrystalline diffusivity $[cm^2/s]$ of cumene
D_{Pr}	intercrystalline diffusivity $[cm^2/s]$ of propene
Err	objective function eq. 3.3
$Err\%$	relative logarithmic error eq. 3.5
E_{eff}	Effective reaction rate (gas phase conc.) activation energy [kJ/mol]
E_{intr}	Intrinsic reaction rate (sorbate conc.) activation energy [kJ/mol]
E_s	surface diffusion activation energy [kJ/mol]
F	flow rate [ml/min]
ΔH_{ads}	Adsorption enthalpy [kJ/mol]
$I(s)$	denominator of $\tilde{C}$, eq. 5.39
K_c	dimensionless adsorption constant in the micropores, eq.5.9

K_y	dimensionless adsorption constant in the macropores
K_{Be}	dimensionless adsorption of benzene
K_{Cu}	dimensionless adsorption constant of cumene
K_{Pr}	dimensionless adsorption constant of propene
L	dimensionless number, eq.5.11
L_{mac}	dimensionless number, eq.5.27
L_{mic}	dimensionless number, eq.5.22
M	molecular weight $[g/mol]$
R	ideal gas constant $J/(molK)$
R	recycle Ratio
R^2	correlation coefficient eq. 3.4
Re	Reynolds number
Rf	carbon based response factor
R_y	radius of macroparticles [cm]
Sc	Schmitt number
Sh	Sherwood number
T	temperature [K] or [°C]
ΔV_{amp}	ampoule volume [ml]
V_{cat}	volume of catalyst [ml]
V_R	volume of reactor [ml]
X	conversion
Z	dimensionless number, eq.5.12

Greek

α	dimensionless number, eq. 5.37
β	dimensionless number, eq. 5.38
γ	dimensionless number, eq.5.11
γ_{mic}	dimensionless number, eq.5.22
γ_{mac}	dimensionless number, eq.5.27
ε_c	volume adsorbent / volume solid
ε_y	macropore pellet porosity
ζ	dimensionless crystal coordinate r/r_c
η	effectiveness factor, eq. 2.10
φ	Thiele modulus defined in eq. 2.11 and eq. 5.36
λ	dimensionless number, eq.5.11
κ	dimensionless number, eq.5.11
ϕ	eigenvalues, see eq.5.14, 5.21, 5.26
τ	dimensionless time t/τ_R
τ_{cat}	catalyst time constant V_{cat}/F [s]
τ_c	dimensionless time tD_c/r_c^2
τ_R	residence time of reactor V_R/F [s]
μ_0	zero moment, eq. 5.49
μ_1	first moment, eq.5.17 and 5.18
μ_2	second central moment eq. 5.51

ξ	Laplace function, eq. 5.40
ψ	dimensionless pellet coordinate y/R_y

Indices

R	Reactant
P	Product
Be	Benzene
Cu	Cumene
Pr	Product

Chapter 1

Introduction

The topic of diffusion in porous solids such as catalysts and adsorbents is of great practical importance to the chemical industry. In order to achieve a large specific surface area with high activity and capacity, solids with very small interconnected pores are used. Not only may the transport in these fine pores become the rate limiting process, it also opens the field for shape selective catalysis with micro-porous materials such as zeolites. A detailed understanding of the diffusional transport in porous materials is therefore fundamental for the design and optimisation of adsorption and catalytic processes. Contradictory results for diffusivities from different methods of measurements can be found in literature, which result not only from the different experimentation but also from different theoretical developments (Post, 1991; Chen et al., 1994). General assumptions made in simplifying models may only partly be true. In this sense, a considerable difference between steady state and transient methods can be observed. Dead end pores can contribute significantly to the capacity in a pulse experiment, but they are negligible in steady state experiments. Furthermore, large differences are to be expected, if the pore size distribution is large, but only one single effective diffusivity is used in the model (Kärger and Ruthven, 1992a). Comparative studies by Baiker et al. (1982), McGreavy and Siddiqui (1980) and Burghardt et al. (1988) show that diffusivities determined by transient experiments are in general somewhat smaller than those measured by steady state.

Park and Kim (1984a) reviewed the conflicting results found in literature from experimental as well as from theoretical consideration between diffusivities measured under inert and under reaction conditions. It was found for the isomerisation of cyclopropane on zeo-

lite Y and X that diffusion decreased by one order of magnitude under reaction conditions (Park and Kim, 1984b; Schobert and Ma, 1981a). In contrast, Hong et al. (1992) found in their NMR measurement that diffusivities under reaction conditions can be extrapolated from experiments under inert conditions. Diffusional studies under reaction conditions in micro-porous materials are however rare. In the preface of the recent book by Chen, Degnan and Smith *Molecular Transport and Reaction in Zeolites (Chen et al., 1994)*, the authors point out the "interdisciplinary gap existing between the study of diffusion in zeolites and the study of catalysis. Nearly all the excellent diffusion studies were made under conditions far away from reaction conditions using a single sorbate".

Regarding the discrepancies discussed above it is difficult to understand how little attention is paid to a detailed error analysis. Any parameter estimation from a model fit should provide (Press et al., 1988): (i) estimated parameters (ii) error estimates of the parameters (iii) a statistical measure of the goodness of the fit

It is unfortunate that in most diffusion works point (ii) and point (iii) are completely neglected. Confidence intervals of the parameters are an exception and the validity of the data is most of the time justified by a goodness of the temperature dependency. For models with more than two parameters this is however in no way acceptable. Secondly, transient experiments for which the concentration changes two to three orders of magnitude show characteristic kinetic time constants, if the response curves are shown in a semi-logarithmic plot. Even if a model fit is given, it is so often only presented in a normal concentration plot and thus disregards the often more important data points at lower concentrations in the long time solution. The following work will be focused on the measurability and errors of the estimated parameters during sorption pulse experiments in a CSTR.

The literature review in Chapter 2 defines the basic modes of transport in porous solids and present measurements of diffusion during reaction conditions. A review on different reactor types and methods of product analysis for pulse experiments is given. The experimental part is subdivided into two chapters. Chapter 3 describes the experimental apparatus and procedure, while Chapter 4 is dedicated to the performance evaluation of the two key components of the apparatus: the jetloop reactor (recycle reactor) and the Multi-Ampoule-Sampler. The theoretical part in Chapter 5 discusses the analytical solution of a pulse experiment on a biporous adsorbent, which is followed by a detailed discussion on the measurability of parameters during pulse experiments on macroporous catalysts. These analyses are used for the parameter estimation from pulse experiments of propane and ben-

zene on ZSM-5 extrudates under inert conditions and cumene cracking on the same catalyst in Chapter 6.

Chapter 2

Literature Review

2.1 Transport Mechanism in biporous Pellets

Commercial pelleted adsorbents or catalysts often consist of small micro-porous particles (like zeolites), which are aggregated together with a binder, such as alumina, to a convenient size. In general the particle size is a trade off between excessive pressure drop and high internal diffusional transport resistance. Pore size distributions can be expected in a range between micropores, mesopores and macropores. These are defined according to IUPAC as:

Micropore $d_p < 20$ Å

Mesopore 20 Å$<d_p<$ 500 Å

Macropore 500 Å$< d_p$

In most commercial zeolite pellets a well defined bimodal pore structure of a micropore size and a narrow macropore/mesopore pore size distribution is generally found.

The possible modes of transport in the different pores are described in the following section. Since experiments in this work are conducted only with highly diluted gases, transport by viscous flow, non isothermal and non-linear effects are not discussed. Excellent accounts for non-linearity effects, such as in Multicomponent systems with the Stefan-Maxwell equation are given by Do (1998), Yang (1987a) . The discussion will hence be focused on diffusion, which is understood to be the relative transport in a solid framework with reference velocity equal zero(Cussler, 1984).

2.1.1 Mode of transport in macropores/mesopores

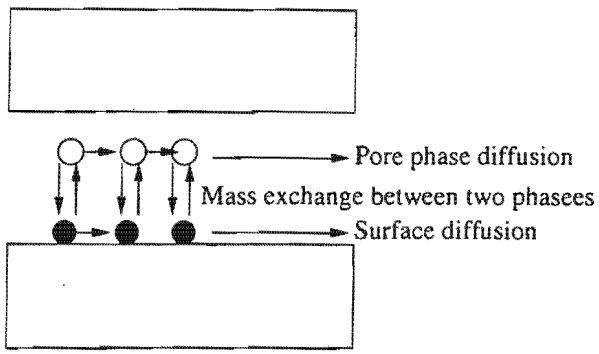

Figure 2.1: Sketch (Do, 1998) of the original idea by Dammköhler with parallel diffusion in the gas phase and on the surface.

The constitutional equation in the macropores of a pellet can be written in terms of Fick's law as:

$$\vec{j_y} = -D_y \varepsilon_y \left(\frac{\partial C_y}{\partial y}\right) = \varepsilon_y D_p \left(\frac{\partial C_y}{\partial y}\right) + (1-\varepsilon_y) D_s' a_s \left(\frac{\partial q_s}{\partial y}\right) \tag{2.1}$$

where y is the spatial coordinate, C_y is the concentration in the gas phase, D_y is the effective macropore diffusivity, D_p is the diffusivity in the gas phase, while D_s' denotes the surface diffusivity of the molecules adsorbed on the surface with specific area a_s. ε_y is the macropore voidage of the pellet. The incorporation of this factor takes into account the restriction of transport to the voidage space. The transport in the pores can according to eq. 2.1 be understood as the sum of two parallel mechanisms as illustrated in Figure 2.1. The partition between the flux in the gas phase and in the sorbed phase shall here be assumed to be linear, so that D_y is constant and can be written in the form:

$$D_y = \varepsilon_y D_p + (1-\varepsilon_y)\, a_s K_s D_s \tag{2.2}$$

, where $q_s = K_s C_y$.

2.1.1.1 Macropore diffusion in the gas phase

Two different modes of diffusion can be distinguished: *Knudsen* and *molecular diffusion*. Knudsen diffusion is the result of momentum transfer between molecules with the pore

wall, which becomes increasingly important for smaller pore sizes. For larger pores or high pressure momentum transfer occurs dominantly by collision between the gas molecules. The Knudsen diffusivity in a single cylindrical pore is given by:

$$D_K = \frac{2r_p}{3}\left(\frac{8RT}{\pi M}\right)^{\frac{1}{2}} = 9700 r_p \left(\frac{T}{M}\right)^{\frac{1}{2}} \tag{2.3}$$

where r_p = pore radius in cm, M = molecular weight in g/mol, T = temperature in K and $D_K = cm^2/s$.

There are various empirical equations for the estimation of *binary gas diffusivities* (Perry et al., 1997; Bird et al., 1960). In this work the equation by Fuller et al. (1966) has been employed. An estimated error of 5% can be expected for most gas mixtures at low pressure and with non-polar components:

$$D_m = D_{AB} = \frac{0.001 T^{1.75}\left(\frac{1}{M_A}+\frac{1}{M_B}\right)^{0.5}}{P\left[(\sum \nu_i)_A^{1/3} + (\sum \nu_i)_B^{1/3}\right]^2} \tag{2.4}$$

with the component indices A, B and the pressure P in bar. ν_i are the specific volume coefficient given in Table 2.1. The diffusivity is given in cm^2/s. In order to delineate the

Table 2.1: Volume coefficients according to (Fuller et al., 1966)

Structure	ν_i
C	16.5
H	1.98
aromat. ring	-20.2

regions of molecular and Knudsen domination, one has to compare the mean free path (Do, 1998) to the pore size. The mean free path is $mfp = \frac{1}{\sqrt{2}n\pi\sigma^2}$ with n being the molecules per volume and σ being the collision diameter, see (Perry et al., 1997). The following criteria for the diffusional regions are according to Do (1998):

$mfp/2r > 10$ Knudsen Mechanism

$0.01 < mfp/2r < 10$ Transition

$mfp/2r < 0.01$ Molecular Diffusion

In the transition state where the mean free path is comparable to the pore size both momentum transfers, molecule-wall and molecule-molecule, become important. Assuming the transfer to be additive one can show that the combined diffusivity for diluted gases and/or approximately equimolar counter diffusion may be simplified to

$$\frac{1}{D} = \frac{1}{D_k} + \frac{1}{D_m} \tag{2.5}$$

which is often called the Bosanquet relation being derived by several authors (Kärger and Ruthven, 1992b).

The *tortuosity factor* χ is a correction factor that allows to correlate the diffusivity D in a single cylindrical pore to that encountered in the actual pore network D_p, with a varying pore size distribution, different connectivity and geometry and thus larger diffusion pathway. The tortuosity factor is here defined as

$$D_p = \frac{D}{\chi} \tag{2.6}$$

It is a structural correction factor and as such not dependent on the sorbate (Kärger and Ruthven, 1992b). Although there have been several models for estimating the tortuosity factor, it is advisable to see this value as an empirical value, however, a rough estimate is $\chi \approx 1/\varepsilon_y$. For commercial zeolite pellets a value of 2-4 is generally found (Kärger and Ruthven, 1992b). For commercial pellets, Satterfield and Cadle (1968) measured tortuosity factors between 3 and 7, whereas tortuosity factors up to 78 were reported for laboratory pellets.

2.1.1.2 Surface diffusion

Surface diffusion can become important or even dominant, if the surface area is high and the relative concentration of the sorbate on the pore wall is very high. Costa et al. (1985) determined the effective diffusivities of light hydrocarbons on activated carbon at room temperature from uptake measurements. By plotting D_y versus the adsorption coefficient they separated the surface diffusivity from the gaseous diffusivity D_p. This, however, implies that all adsorbed molecules, on the external and internal surface, contribute to the surface flux. Surface diffusion counted for 40% to 80% of the flux in the macropores. Rivarola and Smith (1964) distinguished both transport mechanisms in the case of CO_2 diffusion

in alumina pellets, by first measuring the gaseous diffusivities of the non adsorbing gases N_2/H_2 in a Wicke-Kallenbach counter diffusion experiment, see Section 2.4. Since Knudsen diffusion is proportional to the square root of the molecular weight, they could then calculate the gaseous pore diffusion for CO_2 and estimate the influence of the surface flux from the CO_2 measurements. Here the surface diffusion contributed for about 40% of the macropore diffusion flux.

- Surface diffusion is generally considered of being an activated process, which strongly depends on adsorption. While the temperature dependence is modest for molecular diffusion ($\sim T^{1.5}$) and Knudsen diffusion ($\sim T^{0.5}$), the surface flux is commonly not and its temperature dependency can be written in accordance to eq. 2.9:

$$\vec{j_s} \sim \exp\left(-\frac{E_s + \Delta H}{RT}\right) \tag{2.7}$$

  The heat of adsorption ΔH is usually greater than the activation energy for the surface diffusivity E_s, with $-E_s - \Delta H > 0$. This generally leads to a rapid decrease of the surface flux with an increase in temperature (Do, 1998).

2.1.2 Micropore diffusion in molecular sieves

When the sorbate molecules are of a similar size as the pore diameter, they will always encounter the force field of the pore wall. Micropore diffusion differs in this sense from Knudsen diffusion and is similarly to surface diffusion an activated process (Kärger and Ruthven, 1992b; Yang, 1987a; Do, 1998; Ruthven and Derrah, 1972; Kärger et al., 1980), where the adsorbed molecules have to overcome a certain energy barrier in order to jump from one adsorption site to the other. The diffusional intracrystalline flux is hence commonly written in the sorbate concentration form of Fick's law:

$$\vec{j_c} = -D_c \frac{\partial q}{\partial r} \tag{2.8}$$

with an Arrhenius temperature dependence for the micropore diffusivity D_c

$$D_c(T) = D_\infty \exp\left(-\frac{E_A}{RT}\right) \tag{2.9}$$

It is commonly agreed on that the micropore diffusivity depends on the sorbate concentration (Do, 1998; Kärger and Ruthven, 1992b; Yang, 1987b). By arguing that the gradient of the chemical potential should rather be viewed as the actual diffusional driving force has lead to the Darken equation (Do, 1998; Kärger and Ruthven, 1992b; Yang, 1987b). However, this correction for the concentration dependence is very debatable (Yang, 1987c).

Due to the shape selective effect of zeolites, a vast amount of effort has been spent in the last 30 years to measure intracrystalline diffusion in zeolites. Many different methods have been employed for measuring intracrystalline diffusion, including, zero-length column (ZLC) (Eic and Ruthven, 1988), IR (Karge and Niessen, 1991), uptake measurements, pulse field gradient (PFG-NMR), frequency response (Yasuda, 1994) and pulse gas chromatography. Excellent reviews of these methods have been given by (Kärger and Ruthven, 1992b; Post, 1991). A few more recent methods are described in Section 2.4. Values for the measured diffusivities of the most common sorbate/zeolite systems can be found in (Kärger and Ruthven, 1992b). A scatter of 1-2 orders of magnitude for diffusivities of similar sorbate-sorbent systems prevails throughout literature.

2.1.2.1 Surface barrier

Adsorbing molecules may encounter an additional transport resistance at the pore mouth of the crystal (Magalhaes et al., 1996; Barrer, 1990). This so called surface barrier effect may have several reasons. The pore mouth may be blocked by coking, or hydrothermal treatment with removal of framework aluminium may result in the possible reduction of the pore mouth. Blocking or narrowing of the pore mouths through coating procedures such as CVD (Chemical Vapour Deposition) (Niwa et al., 1982), may help to tailor and control selectivity through diffusion. A non-equilibrium barrier may result in an apparent surface barrier, when adsorption equilibrium at the surface is not instantaneously achieved (Micke et al., 1994). From a modelling point, the flux through the surface barrier can be treated similarly to film diffusion as $\overrightarrow{j} = k_s(q^* - \overline{q})$, with k_s as the surface barrier mass transport coefficient, $\overline{q}$ the average sorbate concentration and $q^*$the equilibrium surface concentration (Kärger and Ruthven, 1992b; Magalhaes et al., 1996).

2.2 Measuring reaction, adsorption and diffusion in porous catalysts

In heterogeneous catalysis, most reactions that take place in these catalysts are pore diffusion controlled (Hill, 1977). The internal surface area of the catalyst is usually much greater than the external surface area, the reactant must therefore first diffuse through the pores, adsorb on the active sites in order to react. To understand the nature of the catalytic process, three phenomena have hence to be measured and understood: diffusion, adsorption and intrinsic reaction. Typically this diffusion-adsorption behaviour is measured under inert conditions at temperatures well below that at which reactions occur. The extrapolation of these parameters to reaction conditions has become a topic of debate (Chen et al., 1994). It is therefore preferred to study catalysts under reaction conditions. Such data can be interpreted by reaction-diffusion-adsorption models. The model parameters can be determined by using steady state or transient measurements.

The following section discusses the measurement of these parameters with the steady state 'Thiele modulus' approach and transient measurements.

2.2.1 Thiele modulus approach

The influence of internal diffusion on the reaction rate in a porous catalyst was first described by Thiele (1939). The easiest form of this Thiele modulus approach can be written in the case of a first order reaction in a spherical catalyst particle:

$$\eta = \frac{\text{reaction rate with diffusion}}{\text{intrinsic reaction rate}} = \frac{3}{\varphi^2}\left(\varphi coth\varphi - 1\right) \tag{2.10}$$

The effectiveness factor η describes the fraction with which the intrinsic reaction rate found for very small particles is reduced by the presence of internal transport limitation for larger particles. It is expressed by the Thiele modulus φ, which is the ratio between diffusion time and reaction time:

$$\varphi = \frac{k_R K_{ads}}{D_{eff}/R_y^2} \tag{2.11}$$

Adsorption of the reactant is here accounted for by the multiplication of the adsorption coefficient K_{ads} with the intrinsic reaction rate constant of sorbed molecules k_R. These

two parameters *cannot* be separated by steady state measurements. D_{eff} is the effective diffusivity of the gaseous molecules and R_y is the particle radius. Effects of the particle shape were incorporated (Aris, 1957) and internal effects of heat and mass transfer were further discussed by Weisz and Hicks (1962).

By measuring the reaction rate for significantly different particle sizes one can estimate the diffusivity and the intrinsic reaction rate. Many examples for this approach can be found in standard reactor design textbooks, such as in those of Levenspiel (1972), Fogler (1999), concerning the diffusional effect in macroporous particles. A vast list of about 1000 references can be found in (Aris, 1975). Early works by Weisz, Prater and coworkers (Prater and Lago, 1956; Weisz and Goodwin, 1963; Weisz and Goodwin, 1966; Weisz and Prater, 1954) applied the Thiele modulus approach for reaction works on macroporous materials such as silica-alumina, chromia-alumina, etc.. In the case of cumene cracking on silica-alumina, Weisz and Prater (1954) calculated the effective diffusivity of the reactant with the Thiele method. They compared this value to that obtained for helium in a Wicke-Kallenbach counter diffusion measurement using the Knudsen relationship, eq. 2.3. This extrapolated value was about 2.4 times higher than the value obtained during actual reaction conditions, which is according to Weisz and Prater (1954) a relatively small error.

Several authors measured the diffusivity of hydrocarbons in micro-porous zeolite crystals with the help of the Thiele modulus approach. The Thiele modulus can in principal be changed by either synthesising crystals with the same intrinsic activity but different particle size or changing the intrinsic activity while keeping the particle size constant.

Haag et al. (1982) in a famous paper, examined the transport and reactivity of $n-C_6$ to $n-C_9$, monomethyl isomers, dimethy isomers and respective olefins on ZSM-5 crystals with a diameter of 0.05 μm and 2.7 μm. The reaction rates of the n-alkanes and monomethyl paraffin isomers did not depend on the crystal size and were therefore not restricted by diffusion. The corresponding dimethyl isomers and olefins on the other hand showed diffusional restriction. The diffusivities reported by Haag et al. were very large, when compared to usual intracrystalline diffusion coefficients. Haag et al. referred the diffusion coefficient to the gas phase, while literature uses the sorbate concentration.

Swabb and Gates (1972) carried out the catalytic dehydration of methanol over zeolite H-mordenite crystals of varying sizes from 6 to 17 μm at 155°C and 205°C. No diffusional restriction could be observed at 155°C. With higher reaction rates at 205°C diffusion effects were observed and diffusivities could be estimated assuming pseudo-first order reaction

kinetics.

Post et. al. (1983) tried to compare diffusivities measured under reactive and non-reactive conditions. Intracrystalline diffusivities of 2,2-Dimethylbutane were measured at a low temperature (100°C) in gravimetric uptake experiments on ZSM-5 with different Si/Al ratios. No influence of the aluminium content could be observed. By having confirmed that the non catalytic silicalite yields the same diffusivity as the catalyst ZSM-5 at low temperature, chromatographic diffusion studies with silicalite were then conducted at higher temperature. In the same study conversion rates of n-hexane and 2,2-Dimethylbutane were measured for a series of HZSM-5 catalysts of different Al content and different crystal size. While n-hexane cracking was proportional to the Al content and independent of crystal size, cracking of 2,2-Dimethylbenzene depended on the crystal size, as was observed by Haag et al. (1982) earlier. The measured effectiveness factors η were correlated to the Thiele modulus, which had been estimated from the silicalite diffusion data.

Voogd and van Bekkum (1990) measured cracking rates of 3-methyl-pentane and n-hexane on ZSM-5 crystals. Samples of 5, 26, 61 and 150 μm of diameter were used. The use of big crystals enabled the authors to observe diffusion inhibition, which could not be measured by Haag et al. (1982). The authors point out the major disadvantage of the Thiele method. Preparation of different crystal sizes was bound to differences in activity and the non-uniform distribution of aluminium in the zeolites. However, the experiments fitted well the theoretical Thiele modulus function.

Instead of comparing reaction rates on different crystallite sizes, Garcia and Weisz (1993) changed the intrinsic rate constant of a pseudo-first-order reaction. This was achieved by changing the concentration of the second component in a second order reaction. This component was present in sufficient excess, so that no concentration gradient was to be expected. The authors wanted to examine the catalytic diffusivity of o-Xylene in ZSM-5. They observed the catalytic rate of the deuterium donation of o-xylene for different concentrations of per-deuterobenzene $C_8H_{10} + C_6D_6 \longrightarrow C_8H_9D + C_6HD_5$.

2.2.2 Transient measurement of diffusion/adsorption and reaction

Transient techniques have been developed (Kelly and Fuller, 1972; Schobert and Ma, 1981a,b; Park and Kim, 1984a,b; Miro et al., 1986,1987; Klemm and Emig, 1997a,b) , which allow the estimation of rate parameters using gradientless reactors. A general model for chro-

matography measurement in a fixed-bed was developed by Suzuki and Smith (1971), who used five parameters and presented the first three moments. It was claimed by Schobert and Ma (1981a,b) and Park and Kim (1984a,b) that all parameters can be derived from one pulse experiment by zero, first and second moment analysis. Miro et al. (1986, 1987) used weighted moments to eliminate the effects of tailing, while Park and Kim (1984 a,b) tried to overcome the excessive error in the tail by extrapolating the tail using an exponential function. It is clear from these studies that intracrystalline and intercrystalline effects in a biporous pellet cannot be separated without changing the particle sizes.

Schobert and Ma (1981b) obtained similar values between the diffusivity and adsorption constants of cyclo-propane in powdered zeolite A measured under reaction conditions to those extrapolated from gravimetric measurements. In contrast, Park and Kim (1984 a,b) studying the same system as Schobert and Ma, found that although the adsorption constants were similar, the diffusivities measured under reaction conditions were always at least one order of magnitude lower than those extrapolated from volumetric adsorption measurements. On the other hand, Miro et al. (1986) showed that the Thiele modulus measured under transient conditions was always much lower than that measured under steady state conditions, indicating that diffusion measured under transient conditions is larger than that at steady state. They studied the CO oxidation over CuY zeolite.

More recently Klemm and Emig (1997a,b) developed a diffusion model for the complex o-xylene isomerisation reaction on micro-porous material such as ZSM-5 catalyst during a step-up and step-down experiment. An intrinsic reaction model first proposed by Wei (1982) was employed. It was assumed that o-xylene and m-xylene had the same diffusivity and that the adsorption coefficients were known a priori. In a simulation study, Klemm and Emig (1997a) claimed that the Thiele modulus of o-xylene can be theoretically determined by fitting the location of the calculated reaction path, starting with 100% o-xylene, to the measured location of the path in a ternary concentration diagram of the xylene isomers. Values for the reaction and diffusion constant of the reactant could be determined by fitting the measured outlet concentration. A source of error, pointed out by the authors, is the necessary assumption that the diffusivities of ortho- and meta-xylene are set to be equal. Furthermore, the ratio of the diffusivities for para and ortho isomers could only be derived, if several different initial compositions of the isomers were used. In an experimental study Klemm and Emig (1997a) measured the diffusion coefficient of o-xylene on a non-active silicalite with a step-up of pure o-xylene and compared it to that of an xylene-equilibrium

mixture. The diffusivity for the single component measurement was approximately one order of magnitude lower than that of the multi-component system. This was mainly attributed to the speculative assumption that the adsorption coefficient is equal for all isomers.

2.2.2.1 Critical review on the moment analysis

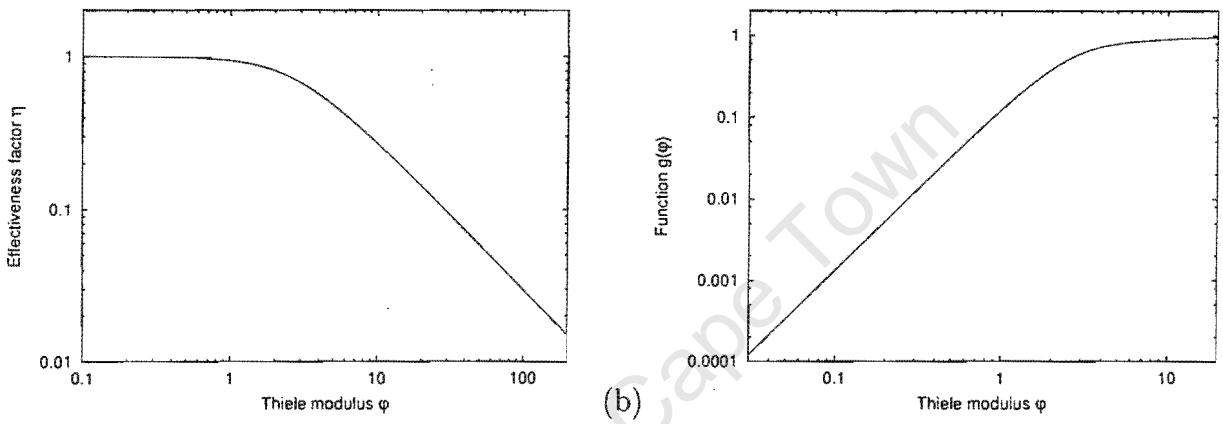

Figure 2.2: (a): Effectiveness factor eq. 2.10 as a function of the Thiele modulus eq. 2.11. (b) Combination of zero, dependent first and second moment to a function only dependent on Thiele modulus

As stated earlier, it was claimed by Schobert and Ma (1981a), Park and Kim (1984a) that all three parameters, e.g. diffusivity, adsorption and intrinsic reaction constant can be determined from one experiment in a mono disperse system, when the outlet concentration is analysed by the zero, first and second moment of a linear diffusion model. The three moments derived by both groups may be viewed in a dimensionless manner as:

$$\begin{aligned} \mu_0 &= f_1(\varphi, L) \\ \mu_1 &= f_2(\varphi, L, \gamma) \\ \mu_2 &= f_3(\varphi, L, \gamma) \end{aligned} \tag{2.12}$$

φ is the Thiele modulus, see Section 2.2.1. L, γ are dimensionless numbers containing adsorption and diffusion coefficients. All three functions f_i are hyperbolic functions of the Thiele modulus, which complicates the root finding algorithm and solution for all three parameters. It was however shown that these three functions can be combined, so that

$h(f_1, f_2, f_3) = g(\varphi)$. This means that the Thiele modulus could be extracted from the combination of the three experimental moments. Once the Thiele modulus is known, L is the only unknown parameter in the zero moment μ_0 and hence easy to determine. It was therefore argued that all three parameters were uniquely determined by the moment analysis.

The function $g(\varphi)$ is shown in Figure 2.2 together with the function of the effectiveness factor, as described in Section 2.2.1. On closer examination of the function $g(\varphi)$ it becomes apparent that $g(\varphi)$ is the most sensitive for low values of the Thiele modulus. At small φ (φ<1) however, the reaction becomes independent of diffusional effects. This signifies that even for a vanishing reaction rate one could still determine φ with a high accuracy. A second problem becomes apparent for values of φ>3. Here, the reaction process is controlled by diffusion and the effectiveness factor becomes inversely proportional to the Thiele modulus. In this regime $g(\varphi)$ tends to its asymptotic value of one and the estimation of φ becomes highly inaccurate.

It is thus clear that a thorough error analysis is necessary to establish the uniqueness of any parameter estimation and to establish the confidence intervals of these estimates.

2.3 Adsorption of benzene in Silicalite/ZSM-5 (MFI)

2.3.1 Crystal structure of MFI

ZSM-5 is a zeolite, which is a crystalline aluminosilicalite. Silicalite has basically an identical framework structure with an aluminium content close to zero. Both materials belong to the pentasil type family, so called because the secondary building unit is a five membered oxygen ring. Chains of these building blocks lead to the formation of a framework with a three dimensional bidirectional channel system, sketched in Figure 2.3. This channel system consists of two intersecting, ellipsoidal channels circumscribed by ten-membered oxygen rings. The free aperture of the almost circular straight channel is 5.4x5.6 Å and of the sinusoidal channel 5.1x5.5 Å. One unit cell has two straight channel sections (one in the centre, four 1/4 corner channels) and four zig-zag channels. The intersection cavity has a free diameter of ~9 Å(Meier and Olson, 1996). Depending on the temperature, Si/Al ratio and nature of guest molecules, monoclinic or orthorombic crystal symmetries can be observed (Song and Rees, 2000). The length of the straight channel, cell constant b, is 19.9

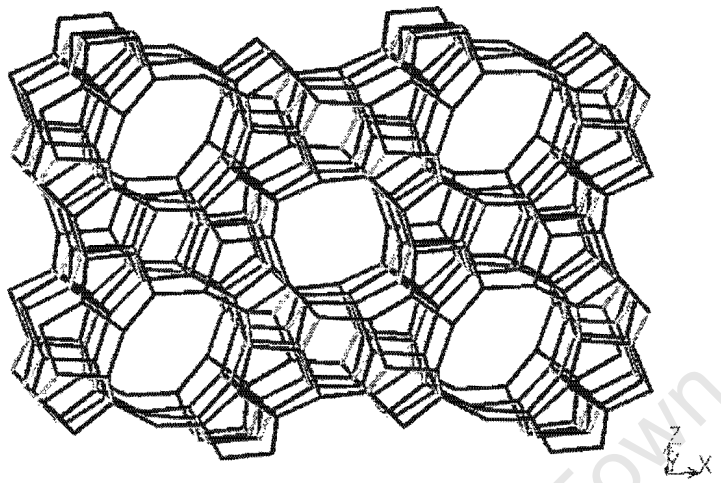

Figure 2.3: Structure of MFI [010] taken from (IZA Structure Comission, 2001)

Å, unit cell constants a =20.1 Å, c=13.4 Å (Szostak, 1992). This translates to $3.099 \cdot 10^{-4}$ mols unit cell /ml. The void volume is 0.10 ml/g. The framework density is 1.76 g/ml.

The silicon and aluminium atoms in the MFI structure are tetrahedrally bonded through oxygen atoms. The charge imbalance caused by the trivalent aluminium atom has to be compensated by the addition of cations such as Na^+ and H^+. This results in strong adsorption sites and if the cation is a proton the hydroxyl groups act as Brønsted acid sites.

2.3.2 Effect of heterogeneous acid sites on adsorption

This section reviews the anomalous adsorption behaviour of benzene in MFI and its dependence on temperature, crystal defects and sorbate concentration.

There are three possible adsorption sites for a benzene molecule in the MFI structure: the sinusoidal channel, the straight channel and the intersection of both channels. One unit cell can at most accommodate eight molecules. Two molecules have space in each of the two straight channels, while the other four benzenes can be situated in the zig-zag channels. For many sorbates, like smaller saturated hydrocarbons, the differences in the sorption sites energies may be negligible and the whole framework may be considered as energetically homogeneous (Song and Rees, 2000). This however changes with sorbates containing π electrons, such as aromatics, where the different acidic strengths of the heterogeneous hydroxyl groups play an important role in the hydrogen bonding of the OH group with the electron

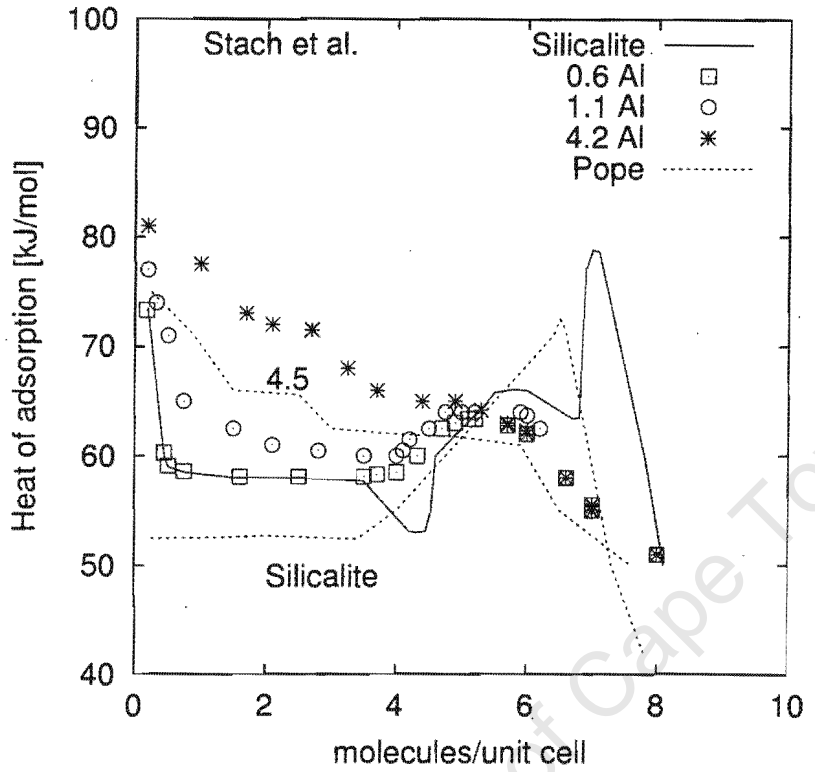

Figure 2.4: Comparison of the differential heat of adsorptions of benzene on H-ZSM-5 and silicalite as a function of sorbate concentration per unit cell. Measurements by Pope (1986) and Stach et al. (1984). Numbers in the legend of the graph refer to Al atoms per unit cell for experiments by Stach et al.. Dotted lines with labels refer to measurements done by Pope at different Al concentration per unit cell.

donor molecule. Datka et al. (1988, 1995) studied the heterogeneity of hydroxyl groups in zeolites by IR spectroscopy during adsorption of benzene on HNa-ZSM-5 and found at least four different hydroxyl groups. According to Hufton et al. (1995) heterogeneous sites are also found in aluminium free silicalite, which appear to be caused by two different defect sites: " isolated SiOH groups due to the fracture of a single Si-O-Si bond and silanol "nests" of four hydroxyls formed from the absence of a structural Si atom." Figure 2.4 shows the heat of adsorption of benzene on silicalite and H-ZSM-5 with a varying Al content. Pope (1986) pointed out the strikingly strong interaction of the sorbed molecules with each other in silicalite. He found a constant heat of adsorption until half of the maximum cell capacity was reached (4 molecules per unit cell.) so that no heterogeneity was indicated. At higher loadings till 6.5 m.p.u.c. (molecules per unit cell) benzene-benzene interactions begin to

dominate and a steep increase of the adsorption enthalpy and a decrease of the entropy is observed. This sorbate-sorbate interaction is inevitable since all channel intersections are occupied (Stach et al., 1984). The distinct decrease at 6 m.p.u.c. is possibly due to a reorganisation of the benzene molecules and a more efficient filling of pore space, at the expense of an optimum occupation on the adsorption sites. The constant adsorption enthalpy of $\sim$ 50 kJ/mol at low sorbate concentrations is confirmed by the results of Lechert and Schweitzer (1984) . A rapid increase in the heat of adsorption was observed at sorbate occupations smaller than 0.5 m.p.u.c. (Stach et al., 1984), (Thamm et al., 1988). This effect is caused by the heterogeneity of the sorption sites, which might be due to structural defects, as indicated by Hufton et al. (1995). This heterogeneity can also be caused by impurities of Al traces, which is indicated by the very similar behaviour of low Al content (0.6 Al per unit cell) ZSM-5, see Figure 2.4. As the aluminium content increases the effect of sorbate-sorbent interaction increases, so that this interaction is dominating at an aluminium content of 4.5 m.p.u.c. even at sorbate concentrations between 4-6 m.p.u.c. . The heat of adsorption increases dramatically with aluminium content. Heats of adsorption greater than $\sim$ 90 kJ/mol were measured (Lechert and Schweitzer, 1984; Hufton et al., 1995; Forni et al., 1986a,b).

Similar sorption behaviour can be found for other aromatics, where the heat of adsorption increases with the number of carbons and the number of alkyl groups on the aromatic ring, as it would be expected. The heat energies decrease with benzene < toluene < ethylbenzene < p-xylene (Pope, 1984; Lechert and Schweitzer, 1984; Hufton et al., 1995; Forni et al., 1986b; Stach et al., 1984; Thamm et al., 1987, 1988). According to Hufton et al. (1995) another indication for the strong impact of heterogeneous sorption sites due to surface defects is the greater sorption equilibrium and enthalpy of butene isomers versus the equivalent saturated isomers, which had already been measured earlier by Lechert and Schweitzer (1984) . It was therefore concluded by Hufton et al. (1995) that pulse response measurements, which are in general conducted at much higher temperatures, will lead to different results for adsorption (and diffusion), when compared to most other methods. It can also be concluded that the amount of aluminium present in the framework and the nature and amount of defect sites strongly influences the sorption behaviour. This will be of great importance, when sorption behaviour of unsaturated hydrocarbons are measured on commercial zeolite samples at very low concentrations.

2.4 Reactor types for pulse experiments

In order to simplify the mathematical model and minimise the number of model parameters, the basic requirements for a reactor type during transient experiments are that: (1) the flow pattern in the reactor is known and ideal, (2) external heat and mass transfer influences can be eliminated. The reactor types used in literature can be classified according to their flow pattern/mode of transport (Mills and Lerou, 1993):

- Fixed-bed reactors
- TAP (Temporal Analysis of Products) reactor
- Single Pellet reactor
- Ideally backmixed reactor

The popularity of the *fixed-bed pulse reactor* can be ascribed to its constructional and operational simplicity (Mills and Lerou, 1993). An example in the field of microporous zeolites is the gas chromatographic analysis, which was mainly used in the early works of diffusion/adsorption studies. A detailed review of these studies is given by Kärger and Ruthven (1992b). The disadvantages in this system lie in the concentration dependence upon the spatial reactor coordinates and the occurrence of axial dispersion. These complications of the applied transient model could be overcome by Eic and Ruthven (1988) with the development of the ZLC (zero-length-column) method. Duncan (2000) gives a criteria for the maximum bed length, where this reactor system is allowed to be treated as ideally mixed without concentration gradients. In a more recent development the group of van Santen (van Santen et al., 1996; Anderson et al., 1997, 1998) overcame the problem of unknown spatial concentration gradients by the use of positron emission tomography (PET), which is a non-invasive, in situ, radiochemical imaging technique. This method allows to monitor the concentration profiles along the reactor and was successfully used in a diffusional study of n-hexane on various zeolites. For all above mentioned methods special care has to be taken for malbehaviour of the flow pattern, e.g. deviation from the ideal plug flow reactor and channelling or bypassing of the catalyst.

The *TAP reactor,* which was developed by Gleaves and his group (Gleaves et al., 1986,1988), works in contrast to the fixed bed reactor without a carrier gas flow. The

pulse gas travels through a fixed bed of catalyst to the reactor exit which is exposed to high vacuum ($10^{-7} - 10^{-5} Torr$). The mode of transport along the reactor occurs primarily by Knudsen diffusion. Its advantage lies in the sub-millisecond time resolution and the opportunity to detect short-lived intermediates after they desorb from the surface into the gas phase (Mills and Lerou, 1993). This opportunity arises due to the molecules greater mean free path length at very low pressures as opposed to atmospheric pressures in conventional reactors. The reactor system, here called *Multitrack,* was used for the diffusional study of hydrocarbons in zeolites(Nijhuis et al., 1997). The major disadvantage in both the TAP and the PET reactor lie in their apparative and operational complexity and their high cost of investment and maintenance.

An alternative is provided by the *Single Pellet reactor.* The most commonly used among these reactor types is the Wicke-Kallenbach diffusion cell, first introduced by Wicke and Kallenbach in 1941 (Wicke and Kallenbach, 1941). The pellet embedded in epoxy is placed as a membrane between two chambers of different concentration but same pressure. By ensuring efficient mixing at both faces of the pellet this method provides the opportunity to reduce the necessary model parameters to those of the catalyst membrane. The major disadvantage of this method is the difficulty of manufacturing a membrane, especially when small catalyst and/or non planar shapes are used. This method was used by Smith and coworkers (Do and Smith, 1984; Dogu and Smith, 1975, 1976) for diffusion/adsorption measurements in pelletized zeolite crystals. The need to pelletize crystals was overcome (Wernick and Osterhuber, 1985; Hayhurst and Paravar, 1988; Paravar and Hayhurst, 1984; Sun et al., 1996) using zeolite crystals with a size of 100μm for diffusion measurements of light alkanes.

The major benefit of the *Ideally Backmixed reactor* is that the model equations may be developed as independent of the spatial coordinates of the reactor. The flow path and the flow rates are known. Appealing though from these theoretical points, the backmixed reactor bears several experimental disadvantages. Achieving perfect backmixing and eliminating heat and mass transfer in the catalyst bed may prove difficult, especially when flow resistances in the catalyst bed increase according to Darcy's law with increasing bed length and decreasing pellet sizes. The power needed for ideal mixing is furthermore inversely proportional to the square of the pressure in the reactor (Mills and Lerou, 1993). Although sometimes found in literature, it is impossible to use fine catalyst powder at these high mixing rates without securely attaching the fine particles to a support. This support, how-

ever increases the possibility of flow resistance in the bed. Another problem arises with the relatively large inner surface of the reactor, where the metal parts may contribute itself to the reaction. In most of these reactors moving/rotating parts are involved. This inherently leads to constructional difficulties, high costs in investment and maintenance.

The recycle reactors used as ideally mixed reactors can be subdivided in external and internal recycle reactors depending on the location of the circulation mechanism. Pistons and propellers are utilised as agitators in the internal recycle reactors.

Carberry (1964) developed the spinning basket reactor in which the catalyst particles are held in place in a four-bladed basket. This basket is attached to a shaft which spins with up to 2500 rpm. However, Ruthven and Kärger (1992c) point out that the fluid-solid mass transfer is unsatisfactory as a result of the hydrodynamic drag, which is caused by the fluid phase tending to follow the spinning basket. Ma and Schobert (1981a) used this reactor for the transient measurement of diffusion in biporous adsorbent zeolite pellets during reaction conditions. Berty et al. (1974) designed an internal radial blower system with a fixed catalyst basket. For operation at atmospheric pressure modifications to this basic concept were necessary (Mills and Lerou, 1993). By combining a magnetic stirrer with a turbine and operating at shaft speeds in excess of 10,000 rpm high recycle ratios could be achieved. Unfortunately no transient reaction works could be found for this reactor system. A bennet reactor, which is similar to the berty reactor but with an axial blower, was used by Miro et al. (1986, 1987).

A much simpler recycle reactor is the jetloop reactor first developed by Luft and coworkers for catalytic purposes in different designs: In stainless steel (Schermuly and Luft, 1978) and in a glass construction by Dreyer and Luft (1982, 1984). The major advantage of the jetloop reactor is its simplicity with no moving parts being used. This results in low investment and maintenance costs and simplifies the operation of the apparatus. Since the reactor can be totally built of quartz, inertness of the reactor can be ensured.

2.4.1 Jetloop reactor concept

The operation of the jetloop reactor is based on the principle that the gas enters the reactor with high pressure and high velocity through a nozzle. This creates a jet stream, which entrains the recycling gas into a draft tube as a result of the jet's venturi effect. The draft tube is centred in the middle of the reactor. (see Figure 3.3, pg. 29). In a modification

to the construction by Luft and coworkers, Möller et al. (1995) designed a jetloop reactor, where the catalyst is passed upstream in the annulus between reactor and centre tube. This reduces the possibility of bed channelling. Blenke et al. (1965) and Sommers (1971) found during initial fluid dynamic experiments that the recycle ratio is strongly dependent on the geometry of both center tube and reactor size. Sommers recommended a ratio of length of the inner tube to its diameter of 7 to 1 (Schermuly and Luft, 1978). Möller et al. (1995) studied extensively the influence of the nozzle diameter, flow rate, temperature and catalyst particle size. The recycle ratio is increased by increasing the momentum transfer with decreasing nozzle diameter and increasing flow rate. The friction in the nozzle and in the catalyst bed is the smallest at low temperatures. Decreasing the temperature thus increases the recycle ratio.

2.5 Product analysis during transient experiments

Transient experiments with more than one component necessitate fast sampling techniques with the ability to separate and quantify all components. Online measurement are from a modelling point of view the most desirable methods ensuring a representative number of samples. Such measurements can be achieved with mass spectrometry methods such as commercially available TOF-MS (Time of flight mass spectroscopy) or an assemblance of several mass spectrometers in line. The latter method was utilised by Nijhuis (1998) using 4 quadrapole mass spectrometers. The disadvantage of these techniques in addition to the enormous costs is that only relatively simple product compositions can be analysed without extra product separation.

Complex product compositions, however, require a time consuming separation by capillary chromatography. Samples have thus to be taken and stored for further analysis. For systems in the gas/vapour phase two methods are practicable.

One method is the use of a commercially available but very expensive multiport valve, e.g. 34 ways, with 16 gas sampling loops as described by Weitkamp (1988). The multiport valve can be heated. During an experiment the product gas flows through a sample valve loop. The valve is turned to its next position, whereby a product sample is captured in the loop. After the experimental run is finished, the gas samples can be analysed in a gas chromatograph. The advantage of this method is that both sampling and analysing can be fully automated, which reduces the source of error and labour time. It allows fast

sampling in the range of one second. Besides the high cost, the major drawback of this method is that sampling and analysis can not be decoupled, which reduces the flexibility for further analytical work and reduces the number of experiments per time. Another factor arises in the difficulty of maintenance and keeping the valves free from leaks especially at high temperatures. The multiport valve technique was used for pulse diffusion/reaction work (Miro et al., 1987) with sampling times between 5 to 10 seconds. Unfortunately no evaluation of the accuracy of their analysis was given.

A cheaper but yet not commercially available method is the ampoule sampling technique, which was first developed by Pichler and Gärtner (1962). A preevacuated glass ampoule is broken at its capillary tip, whereby a sample is instantaneously taken, and is then sealed with a flame, see Section 3.2.1.3. This technique allows the complete decoupling of sampling and analysis. It's major benefit is its flexibility in the type of product analysis, storage and transportability. The technique is very robust involving little maintenance. Sample sizes can be easily changed. However, a drawback of this method is that microprobes of light/combustion gases get sucked into the ampoule sample during the melting process. During the capillary chromatography analysis slight broadening and tailing of the peaks may occur.

The major disadvantage of this method is that it has yet not been fully automated, which makes this method more labour intensive and inaccurate if fast sampling is required. A semi-automated version of this technique was therefore developed in this work, Section 3.2.1.3.

2.6 Objectives of this work

The aim of this work is the measurement of diffusion and adsorption of hydrocarbons on a porous catalyst under non-reaction and reaction conditions. A pulse technique in a CSTR is used to achieve this goal.

This aim can be subdivided into:

Apparatus

- Verify the good recycle behaviour of the jetloop reactor and establish a criteria for the approximation of CSTR behaviour.

- Design of an automated Multi-Ampoule-Sampler. Testing of the performance to be sufficient for fast pulse techniques.

Theoretical using simple linear continuum models

- Non-reaction conditions: Find an analytical solution for a biporous adsorbent. How can parameters be estimated using the analytical solution?
- Reaction conditions: Can all parameters be simultaneously estimated from one pulse experiment? What is the criteria for which parameters become insignificant to pulse response curves ? Are parameters strongly correlated?

Measurement of diffusion, adsorption (and reaction) as a function of flow rate , mass of catalyst, particle size and temperature

Non-reaction conditions:

- Measurement of macropore diffusivity and adsorption of propane and benzene on zeolite ZSM-5 extrudates.
- Diffusion analysis of pulse experiments by Möller and O'Connor (1994) of propane and butane on zeolite 5A.

Reaction conditions:

- Measurement of macropore diffusion, adsorption and reaction of propene, benzene and cumene during cumene cracking on commercial ZSM-5 extrudates
- What is the error in the estimates? Are the results consistent in temperature, mass of catalyst, flow rate?
- Can pulse experiments be compared to steady state experiments?

Chapter 3

Experimental

3.1 Materials

3.1.1 Chemicals

The chemicals listed in 3.1 were used without any further purifications.

Table 3.1: Sources and purities of chemicals used in this project

Chemical	Source	Purity, mass%
Benzene	Aldrich	99.9
Cumene	Riedel-de Haen	99
n-Decane	Aldrich	99
n-Heptane	Aldrich	99
Propane	Fedgas	99.5
Argon	Fedgas	99.999
Helium	Fedgas	99.99
Air	Fedgas	99.99

3.1.2 Catalyst

All the catalysts used in this project were commercial ZSM-5 zeolites, which were supplied by Suedchemie. The samples came in powder and in extruded form. According to the supplier, the commercially available T4480 was extruded with 25% (weight % after calcination)

aluminium hydroxide binder. A not commercially available sample P1 was formed to its extrudates E1, E2, E3 with 22 -23.5% aluminium hydroxide binder by utilising three different peptising agents. The Si/Al ratio (atomic) was 45 according to the supplier.

The diameter of all extrudates was 1.5 mm. They were sorted out into sizes of the same length . Smaller sized extrudates were obtained by crushing these samples and the sieving into size fractions, (1) -1180 + 1000 μm, (2) -1000 + 710μm and (3) -710 + 500μm.

3.1.2.1 X-ray diffraction

The ZSM-5 structure was verified for both powder samples with X-ray diffraction (XRD) . The XRD was obtained from a Phillips X-ray diffractometer using Cu-Kα radiation with a wavelength of 1.542Å at 40kV and 25mA. The scan range was $6<2\Theta<48$ at a 2Θ step size of 0.1°, 1000 counts/s and a time constant of 1s.

The ZSM-5 morphology is confirmed with the two large peaks at 24° and the two peaks at 45° (see Appendix A).

3.1.2.2 Scanning electron microscopy

Micrographs were obtained using a Leica S440 Scanning Electron Microscope with an acceleration voltage between 10-40kV at a working distance of 11-15 μm.

Both powder samples exhibit a typical morphology expected from commercial samples (see Figure 3.1 and 3.2) . A highly intergrown crystalline structure with a size of $\sim$0.2 μm and mesoporous channels in the range of 100 nm.

3.1.2.3 BET surface area analysis

Nitrogen adsorption was carried out to characterise the pore volumes and surface areas using a Micromeritics ASAP 2000. 0.5 g of the extrudate was dried at 120 °C at a pressure of 0.5mmHg for 12 hours. Nitrogen was then adsorbed at the boiling temperature of liquid nitrogen (77K). 150 pressure points were taken between 0.5mmHg and ambient pressure. BET Isotherms and desorption plots can be found in Appendix B

3.1.2.4 Mercury porosimetry analysis

The macropore voidage was according to the supplier about 0.3 for all extrudates. The bulk density was 1.17 g/ml. The volume percentage of zeolite to total solid volume (binder +

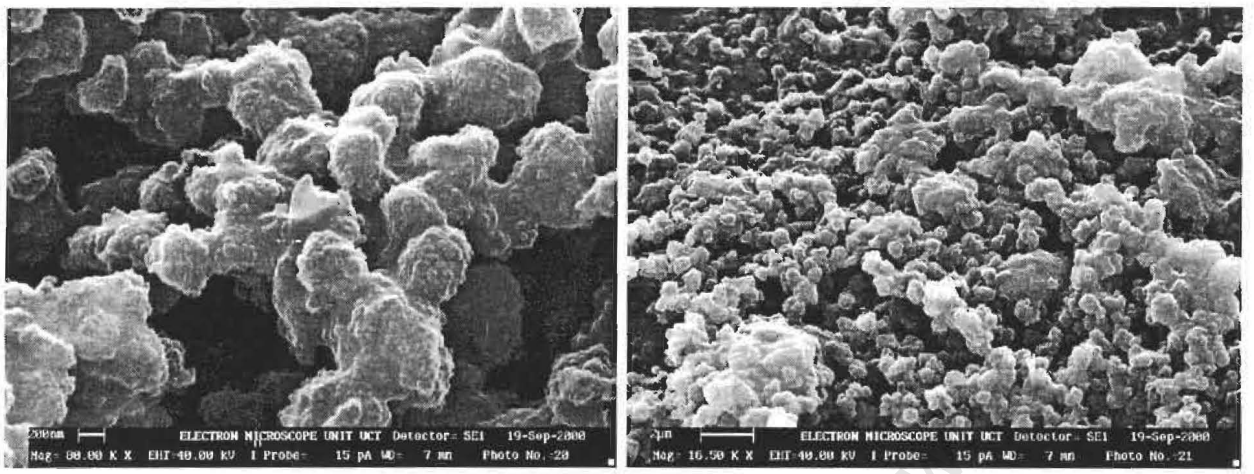

Figure 3.1: SEM micrographs of the ZSM-5 powder T4480

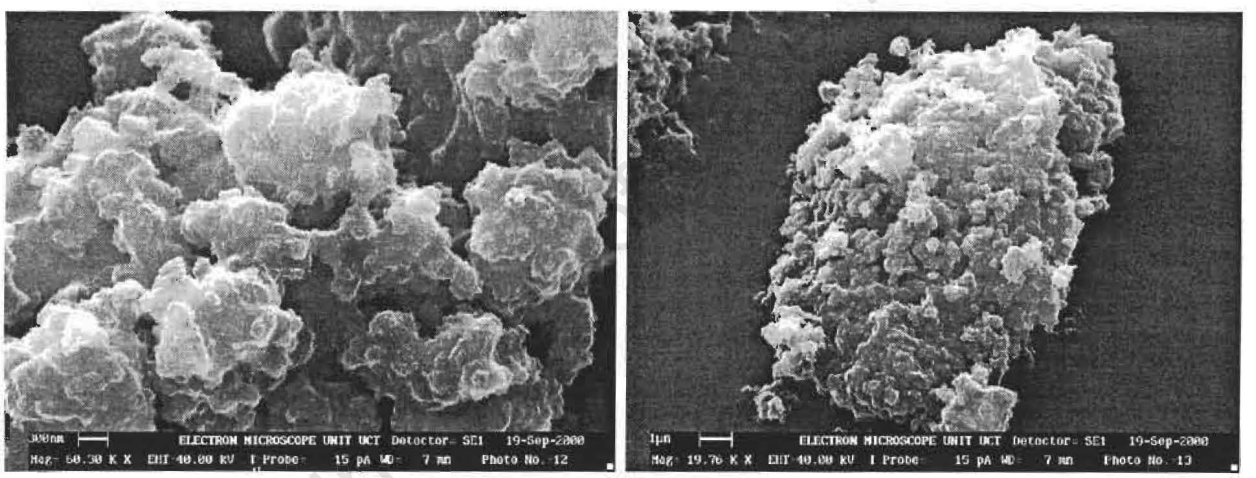

Figure 3.2: SEM micrographs of the ZSM-5 powder P1

zeolite) is then calculated as 74 %.

Introduction to experimental apparatus and procedures

Two reactor systems were utilised in this work. The jetloop reactor system was used for the transient measurement of diffusion and adsorption of propane, propene, benzene and cumene on ZSM-5 extrudates under reaction and non reaction conditions. Additionally, steady state reactions of cumene on extrudates were conducted with this reactor system.

3.2 Jetloop reactor measurements

In principal there are two streams entering the jetloop reactor (JLR). A jet stream of inert gas enters the reactor via a nozzle and causes the internal recirculation. The perturbation of the system is achieved by a hydrocarbon/inert gas stream flowing into the reactor via an injector port. Pulse as well as step experiments can be conducted. The total hydrocarbon stream of the reactor outlet is measured online by an FID. If product separation is needed, the stream is sampled by an Multi-Ampoule-Sampler and analysed by gas chromatography.

3.2.1 Experimental Apparatus

Figure 3.3 shows the flow sheet of the experimental apparatus. All gases were purified through molecular 13X sieves and in the case of the carrier gas additionally with activated carbon. Depending on whether a calcination/regeneration gas or carrier gas was needed, air or argon (99.999%) could be optionally fed via the three way valves (TWV 2) and (TWV 3).

The carrier gas jet stream (Inlet 1) was controlled by a Brooks (Series 5890, range 0-500ml/min at 25 °C) mass flow controller (MFC 1). The stream entered the JLR through a nozzle with an approximate inside diameter of 0.1mm. The head pressure varied between 1 and 8 bar, which was monitored by a pressure gauge.

The feed line to the injector port of the reactor was equipped with two feed dosing systems (Inlet 2) and (Inlet 3), which could be selected through a 1/16" four port Valco valve. The stream not entering the JLR went either to the vent or flowed through a bypass line, which had to be additionally assembled for steady state experiments. Both flows were controlled through Porta (range 0-200 ml/min at 25 °C) flow controllers (FV 1) and (FV 2) respectively. Both flows passed a 1/16" six port Valco valve, which was equipped with a 150μl sample loop. The inlet stream (2) consisted of either pure carrier gas or gaseous hydrocarbon, which could be selected through the three way valve (TWV 1). The inlet stream (3) consisted either of hydrocarbon (vapour)/carrier gas or pure carrier gas. Here, carrier gas flowed either through a glass saturator or through the bypass line depending on the three way valves (TWV 4) and (TWV 5). The temperature of the glass saturator could be controlled by a water jacket. As injector port a Swagelok 1/8" T-piece was used, which was sealed with a high temperature silicon septum. The injector port was heated to 300 °C controlled by a UNITEMP temperature controller. This allowed the dosing and rapid

evaporation of liquid hydrocarbon injected via syringe. In order to keep backmixing and dead time low, 1/16 " tubing was used for the lines between 6 port valve and reactor. These lines, Valco valves and the feed dosing system (Inlet 3), were heated by heating tape to 200 °C +/-1 °C using an RKC REX-C100 PID temperature controller.

The jetloop reactor was heated by four 120 Watt 60x8mm heating elements placed in the reactor wall using an RKC REX-C100 PID temperature controller. A more detailed description of the JLR is given in Section 3.2.1.2.

The exit line out of the reactor was split using a needle valve (NV 2), where approximately 10 % of the flow passed through a 1/16" OD stainless steel tubing of length 30 cm to a Flame Ionization Detector (FID), while the major stream proceeded to the Multi-Ampoule-Sampler (MAS). The pressure was measured prior to the transient experiments and did not exceed 25 mbar above atmospheric pressure. No pressure sensor was used to monitor the pressure during transient experiments, since it was found to be an inevitable source of error due to an increased dead volume or possible condensation from the vapour phase.

The FID was mounted on a heating block and the temperature was maintained at 290 °C within ±1°C using a RKC REX-C100 PID temperature controller. The FID was connected to the Electrometer (Gow-Mac model 40-900) operated between ranges 10^{-9} and 10^{-11}. The signal was further amplified in an APC50-card (Intelec Systems) and sent to an onboard 24 bit analog-digital converter with a sampling rate of 10 Hz. Baseline corrections were automatically made prior to each experiment. The flow rate of air through the FID was set to 300 ml/min, whereas the hydrogen flow rate had to be varied between 30 ml/min and 40 ml/min in order to achieve maximum sensitivity and to avoid that the FID flame was blown out at higher flow rates.

For the ampoule sampler analysis an internal standard was fed into the product gas stream using a Unit (range 0 to 20 ml/min at 25°C) mass flow controller (MFC 2) in combination with a glass saturator at atmospheric pressure. The temperature of the glass saturator was controlled within ±0.2 °C of deviation by a water jacket using a refrigerated circulating water bath. The final product stream flowed through the MAS, which is equipped with a stepper motor to allow automatic sampling (Section 3.2.1.3).

In order to simultaneously capture the data of the FID and control automatically the sampling via MAS a computer program (APC50JIR.EXE) was written.

All product lines, internal standard line and MAS were heated with heating tape using

RKC REX-C100 PID temperature controller. The temperature in the MAS was controlled at 120°C.

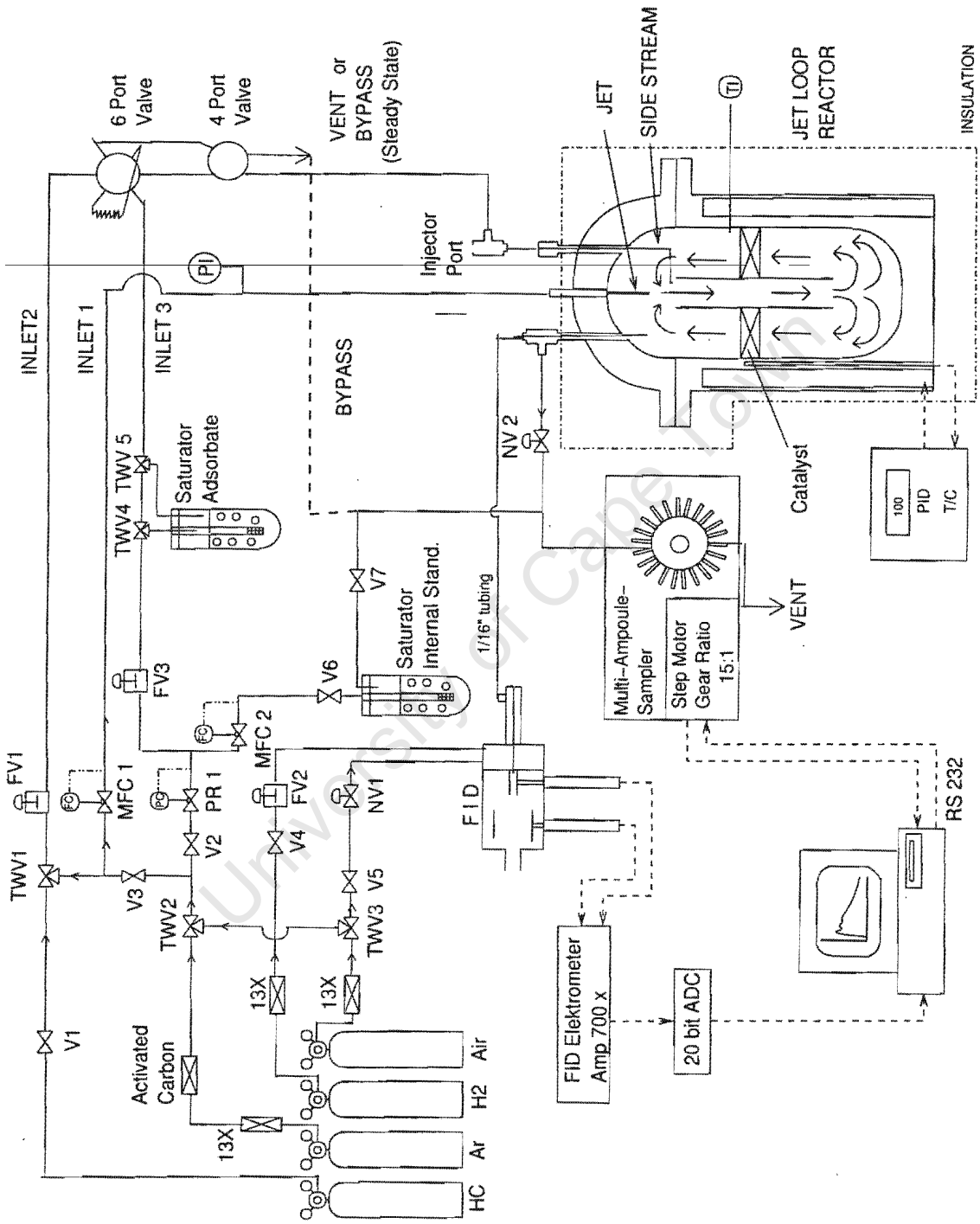

Figure 3.3: Flowsheet of the jetloop reactor system used for transient measurements and steady state reaction (with bypass line)

3.2.1.1 Jetloop reactor residence time and recycle measurements

In order to accurately measure recycle ratios, it was necessary to achieve sharp input pulses and to avoid backmixing in the exit line to the FID. This was achieved by modifying the apparatus described earlier in Section 3.2.1. The propane tracer (150 μl) was injected directly via the 6-port into the jet stream, as opposed to the injection to a low flow rate injector stream. The input pulse time was estimated to be within 0.1-0.2 s. For the determination of the recycle ratio (R) the time lag had no influence on the time difference between the recycle pulses. As exit line to the FID a 50 cm long inert fused silica capillary tube with an inside diameter of 0.32 mm was used. The capillary was directly inserted into the FID flame tip so as to channel the flow directly into the flame. The other end of the capillary was inserted into the JLR through the reactor discharge line and was placed about 5mm above the central draft tube (Section 3.2.1.2). This position was found (Möller et al., 1995) to be the optimum point to measure sharp peaks, since flow disturbances and mixing were observed in the upper hemisphere of the JLR. To ensure a flow through the capillary the system pressure was set by a needle valve to 200 mbar above atmospheric pressure. The FID signal was recorded every 0.01 to 0.05 sec. The following effects were investigated: carrier gas (helium, nitrogen, argon), flow rate, catalyst bed resistance simulated by 40 mesh glass beads.

3.2.1.2 Jetloop reactor (JLR)

Figure 3.4 shows the drawing of the jetloop reactor with its dimensions. The reactor has a volume of 49 ml. The gas flows through the jet, thereby entraining bulk gas into the jet stream. The gas flows through the draft tube and proceeds upwards through the outer annulus, passing through the catalyst bed. The catalyst is placed between two annular sieves of 0.2mm opening. A split ring fixes the bed on the top. For best recycle ratios the jet should be positioned flush to the draft tube in the center of the reactor. This results in higher entrainment of bulk gas and avoids that the jet stream bypasses the draft tube (Möller et al., 1995). Two different jets were used for diffusion work: (1) An HPLC stainless steel capillary (Length 25 mm, ID 0.10 mm) was used for RTD measurements and diffusion work at low temperature (T $<$ 200 °C). (2) A "bulk head" jet previously used (Möller et al., 1995) is illustrated in Figure 3.4. Its orifice (Length 0.2mm, ID 0.12 mm) offers a lower pressure resistance and was hence used at elevated temperatures.

The reactor was insulated with ceramic wool (thickness 10 cm). Isothermal conditions in the reactor could be achieved within 0.2 °C.

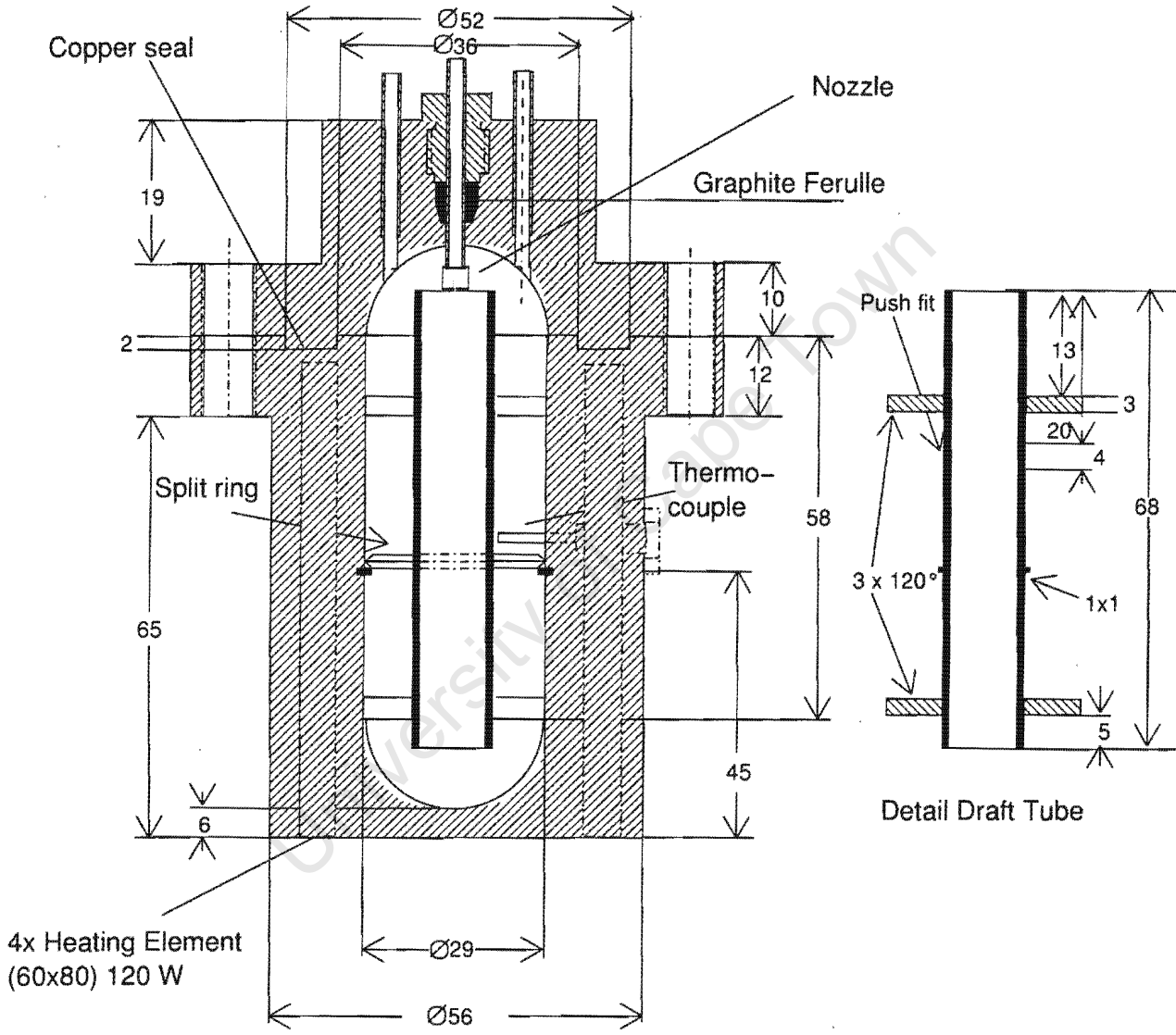

Figure 3.4: Drawing of the jetloop reactor

3.2.1.3 Multi-Ampoule-Sampler (MAS)

The method of capturing and analysing gas samples was first described Pichler and Gärtner (1962) and further developed by Schulz et al. (1984). A pre-evacuated glass ampoule is broken at the tip of its capillary ending and hereby samples a product volume, which can then be captured by sealing the tip again with a gas flame. Product samples can be stored over a long time period. The Multi-Ampoule-Sampler (MAS) technique is based on this principle and is a modification, which allows automated and faster sampling. Figure 3.5 shows the schematic drawing of the MAS.

The product gas flows through 1/8" tubing from the sampler body to the conical rotor through a small channel (diameter=1.5mm) into the annular gas sampling space between rotor and body. This annulus has a volume of 2.1 ml. The gas stream exits through a second channel to the hollow axis (1/4" OD tubing). The rotor and the MAS body are sealed off from each other by three o-rings.

20 cylindrical brass cartridges are screwed on the outer diameter of the MAS body. The capillary ending of an ampoule is inserted through the rubber seal of the cartridge into the annular gas sampling space. Next to the gas entrance is the breaker tooth, which is placed on the rotor. This pin breaks the ampoule tip, when the rotor is turned. After breaking, the ampoules have to be sealed off manually by a torch flame. The hollow axis of the rotor is connected to a gear box (Bonfiglioli MVF 30/A, gear ratio 15:1), which is driven by a stepper motor (1.8 VDC, 4.7 Amp, The Superior Electric Company, USA, 110 OZ 144S/R 65', C-Class B Insul.).

The driver for the stepper motor is controlled by a standard PC using an Intel SBC8032 I/O processor. A detailed description of the communication protocol is given in (Randal et al., 1993). The driver step size for one ampoule sample step is 98 with a driver step rate of 5 ms.

The sampling rate for the MAS is mainly limited by the gear ratio of the gear box, which was necessary due to the friction of the large o-rings. The mechanically maximum possible sampling rate was 0.5-1 s. At this high sampling frequency large errors in the time resolution have to be taken into account: Before the start of the experiment the breaker tooth was directly positioned at the tip of the first glass ampoule, in order to reduce the delay of the sampling. The maximum distance between the breaker tooth and the glass tip was 0.1mm. The maximum delay of the sampling time can then be estimated to about 0.2

s.

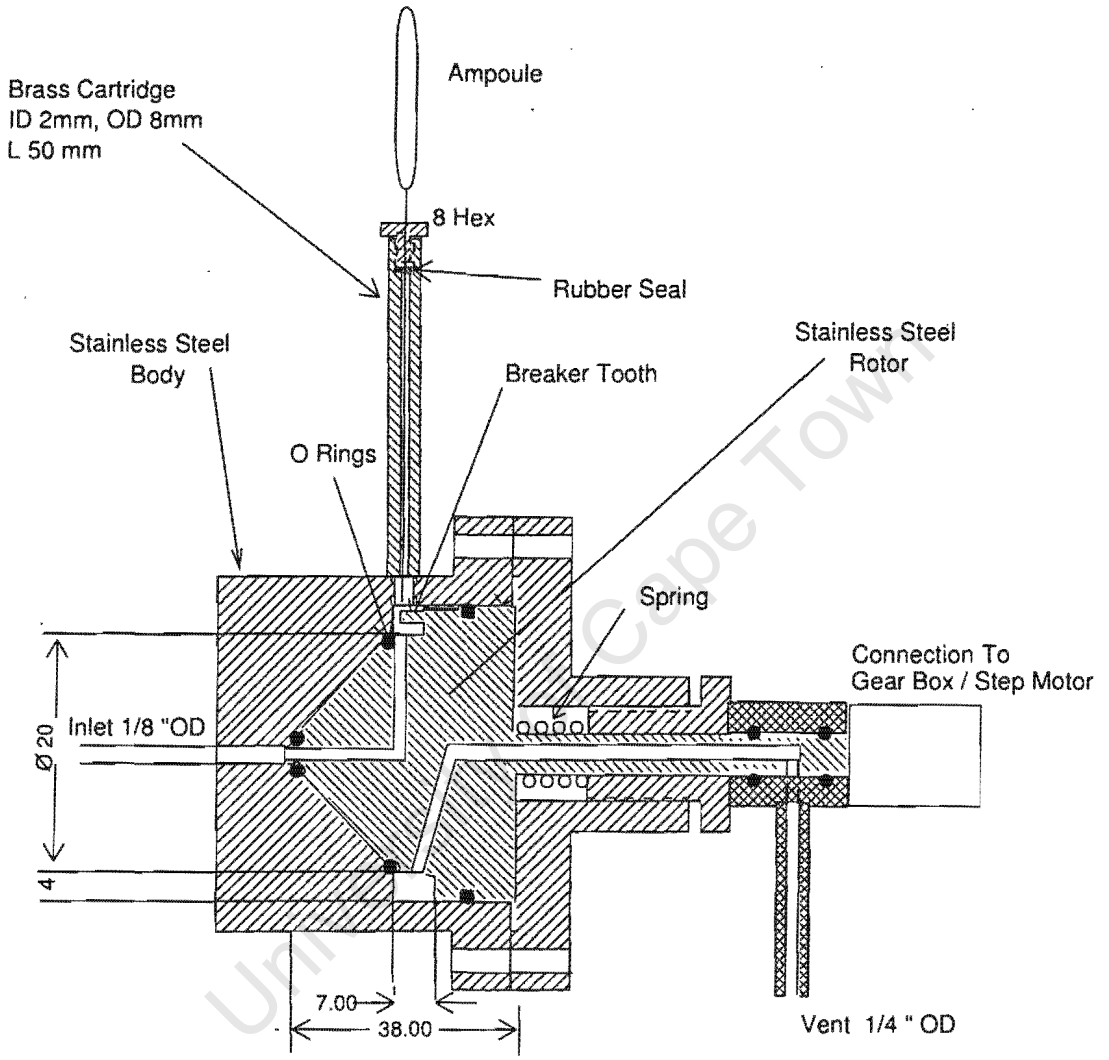

Figure 3.5: Schematic drawing of the Multi-Ampoule-Sampler

3.2.2 Experimental procedures

After loading the reactor the catalyst was, prior to any experiment, calcined for at least 6 hours at 500° C in air. Each time a leak check was performed around the JLR. For this the reactor lines had to be dissembled and blocked with a stop nut at two points: the FID inlet and after the needle valve (NV2). The six port valve was closed and the system was filled with argon to a pressure of 9 bar. Valve (V3) was then closed and a possible pressure drop was monitored for an hour.

3.2.2.1 Transient sorption experiments without reaction

After cooling the reactor to experimental temperature the flow rate for the jet stream and the injector purge flow were set. The reactor was left to stabilise for two hours. The flow rate of the hydrocarbon stream passing the sample loop into the vent was set. The data capture program was started and the sample valve was switched.

The carrier flow rate through the jet was varied between four different flow rates, e.g. 170 to 500 ml/min (at 0°C, 1atm), in order to check for external film resistance and non idealities of the reactor behaviour. Sorption experiments were exclusively carried out on crushed extrudates of T4480 HZSM-5 adsorbent catalyst with a diameter of 0.66 and 1.1 mm. The mass of catalyst was 0.5 and 2.0 g. As adsorbate propane and benzene were investigated. The adsorbate pulse volume was 150 μl. The flow rate of the hydrocarbon line passing the sample loop, as well as, the carrier flow rate purging the sample loop were 20 ml/min (at 0°C, 1atm).

In the case of propane a temperature range between 75 - 200 °C was investigated. In order to check for non-linearities two concentrations were fed, pure propane and a 100 fold dilution with argon.

Benzene sorption measurements were carried out at the actual reaction condition of cumene (Section 3.2.2.2) at temperatures between 390 - 470 °C. The benzene saturator was operated at room temperature and atmospheric pressure. The initial molar concentration of benzene can be calculated, from the injected volume, a partial pressure in the sample loop of 100 mmHg (taken from (Sandler, 1989)) and the reactor volume, as 16 μmol/l.

3.2.2.2 Transient cracking experiments of cumene

As described in Section 3.2.2.1 the reactor was stabilised and set to the same range of the jet flow rate. The Muli-Ampoule-Sampler was loaded with 20 ampoules and the individual sample times were programmed into the data capture routine. The internal standard was switched in line and stabilised for two hours. A carrier gas flow of 20 ml/min (at 0°C, 1atm) was purging the injector port, when a pulse of liquid cumene (0.5 μl) was injected. Monitoring the FID-online signal the MAS sampling routine was started, when a rise of the FID signal was detected. The effluent concentration was sampled until the total carbon concentration was detected to be 1/1000 of the initial concentration.

Concentration gradients differ substantially during the run time. This demands small sample volumes at the steepest concentration gradients in order to minimise broad averaging (see detailed discussion in Section 4.2). Larger sample volumes for a higher sensitivity were chosen otherwise. In order to measure representative concentration curves a logarithmic sampling time sequence was applied. Six small samples with an ampoule volume of about 0.5 ml were therefore broken every second. The last 14 samples were taken with decreasing sample frequency and had an ampoule volume of about 2 ml.

The internal standard saturator filled with n-heptane was operated at 15 °C and atmospheric pressure and was flushed by an argon flow of 15 ml/min. Pulse reaction studies were carried out on uncrushed/crushed extrudates of T4480 HZSM-5 with diameters of 0.066, 0.084, 1.1 and 1.5 mm. Sample weights were 0.2, 0.5 and 3 g. The HZSM-5 extrudates E1-E3 were studied for the uncrushed sample 1.5 mm with a sample weight of 0.5 g.

The initial molar concentration of cumene can be calculated, from its density as 7.2 mol/l (Perry et al., 1997) the injected volume and the constant reactor volume to 72 μmol/l. This is equivalent to an initial partial pressure of 0.4 kPa at 1atm and 400°C assuming ideal gas law.

Additional, cumene pulses were conducted, where a stream of benzene had been cofed for two hours into the jetloop reactor (mole fraction of 0.15% in the reactor), after which 0.5 μl of liquid cumene was injected.

3.2.2.3 Steady state cracking experiment of cumene

After the reaction temperature was reached, the carrier gas flow through the jet and the injector purge flow were set. The internal standard was switched in line. The carrier gas flow

through the cumene saturator was set. This flow was mixed with the effluent JLR/internal standard stream via the four way valve and the bypass line. The system was then left to stabilise for two hours. Afterwards bypass samples were taken over a time period of two hours. The cumene flow was then fed into the JLR by switching the four way valve. Six reaction samples were taken with a gas syringe within three hours.

The amount of T4480 ZSM-5 extrudates was 0.5 g. The different diameters were 0.66, 1.1 and 1.5 mm. The saturators of the internal standard (n-decane) and of cumene were thermostated to 15 °C. Both carrier gas flows through the saturator were adjusted to 20 ml/min (at 0°C, 1 atm). The flow rate of the jet stream was varied between 200 and 500 ml/min (at 0°C, 1atm), in order to study the reaction kinetics.

The range of the mole fraction in the feed stream can be calculated from eq. 3.8 on pg. 40 with a partial pressure of cumene in the saturator of 4 mmHg (taken from (Sandler, 1989)). The mole fraction ranged with the above given conditions between 0.02% and 0.05%.

3.3 Gas chromatographic analysis

The samples contained in the glass ampoules were analysed by breaking them in a heated ampoule breaker device (Schulz et al., 1984), which was connected to the gas chromatograph via a six port sampling valve. The GC carrier gas could thus either bypass the ampoule breaker or transport the product sample to the column when both were switched in-line (Figure).

A Hewlett-Packard HP 5890A gas chromatograph equipped with an OV1 (15m x 0.32 mm, film-thickness 0.5 μm) was used. A flame ionization detector was used. The carrier gas was helium. Further specifications, temperature programmes and representative chromatograms are given in Appendix C.

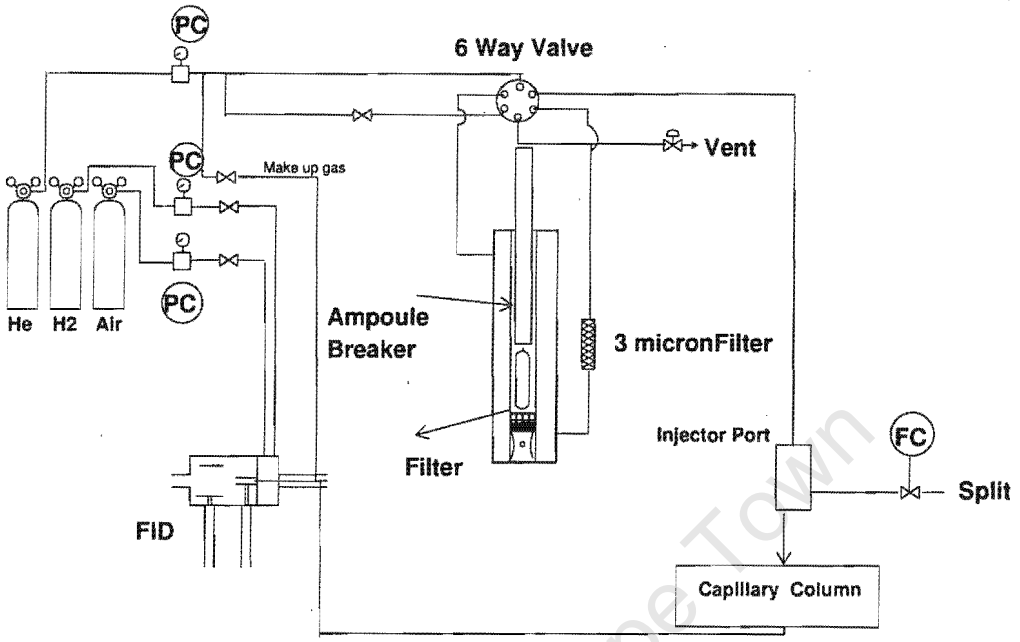

Figure 3.6: Flow sheet of ampoule breaking device and gas chromatograph

3.4 Evaluation of experimental data

3.4.1 Normalisation of transient measurements

In the case of sorption experiments without reaction, the signal response was normalised to the dimensionless concentration by

$$C(t) = \frac{Signal(t)}{\int_0^\infty Signal(t)dt} \cdot \tau_R \tag{3.1}$$

The first term on the right hand side represents the residence time distribution. τ_R is the residence time. It should be noted that this normalisation is preferred to setting the maximum signal to 1, where the largest experimental error is to be expected.

In the similar case of transient reaction experiments, the concentration curve of each component is normalised by the residence time distribution of total carbon and the residence time of the reactor. The units of the unnormalised concentrations are therefore in moles carbon / ml.

Similar to eq. 3.1 the signal response was normalised by

$$C_i(t) = \frac{Signal_i(t)}{\int_0^\infty \sum Signal_i(t)dt} \cdot \tau_R \tag{3.2}$$

The signal of component i is obtained from the relative peak area of component i to the area of the internal standard in the GC-chromatogram. The relative response factor on molar carbon basis for an FID signal is assumed to be equal to one for hydrocarbons containing no hetero atoms (Dietz, 1967).

3.4.2 Data analysis of transient reaction runs

The parameter estimation routine Greg96 (Stewart and Associates Engineering Software Inc Madison Wisconsin, 1996) was used to fit the diffusion model, as described in Section 5.3.1, to the experimental concentration curves. Greg96 handles the optimisation at each iteration by minimising a quadratic approximation to the objective function. The algorithm is based on a Gauss-Newton method and has been extended to handle simple parameter bounds. Furthermore, a trust region strategy is implemented in order to handle singular Hessians, which occur when there are parameter dependencies. This method is one of the most efficient and robust optimisation strategies available for parameter estimation (Iauw-Bieng and Biegler, 1991).

The objective function chosen for the optimisation was an ordinary relative least-squares estimation:

$$Err = \sum_{j=1}^{3} \sum_{i=1}^{N(j)} \left(\frac{C_{Exp}(j,i) - C_{Mod}(j,i)}{C_{Exp}(j,i)} \right) \tag{3.3}$$

The least-squares optimisation is hence simultaneously conducted for all three components (index j) with $N(j)$ collected data points for component j. Normalised concentrations greater than 0.001 were taken into account for propene and benzene, while for cumene only concentrations greater than 0.01 were considered because of the lower accuracy observed in the blank run (see Section 4.2).

Standard 95% confidence intervals for each estimated model parameter were computed by the Greg routine assuming a normal density distribution. These intervals were based on the maximum likelihood of the logarithmic (base 10) value of the model parameter. Giving the optimisation routine a logarithmic value of the parameter has the advantage that no meaningless negative physical values can be computed, which are a source for numerical

instability.

In order to express the goodness of the model fit standard correlation coefficient R^2 between the experimental and model data points (i) are calculated for each component (j):

$$R(j)^2 = \frac{\left(N(j,i)\sum C_{Mod}(j,i)C_{Exp}(j,i) - \sum C_{Mod}(j,i)\sum C_{Exp}(j,i)\right)^2}{\left(N(j,i)\sum C_{Mod}^2(j,i) - \left(\sum C_{Mod}(j,i)\right)^2\right)\left(N(j,i)\sum C_{Exp}^2(j,i) - \left(\sum C_{Exp}(j,i)\right)^2\right)} \tag{3.4}$$

Minimum and maximum relative errors in the model fit of the logarithmic concentration curves are computed according to

$$Err\% = \left|\frac{\log\frac{C_{Exp}(j,i)}{C_{Mod}(j,i)}}{\log C_{Exp}(j,i)}\right| \cdot 100\% \tag{3.5}$$

3.4.3 Evaluation of steady state experiments

3.4.3.1 Calculation of conversion and carbon balance

Carbon balances were performed for both, fixed bed and recycle reactor, by comparing the flow of carbon in the feed to the flow of carbon in the product stream. The carbon feed flow was determined from the reactor bypass samples. Using the peak areas on the chromatogram and assuming relative response factors on molar carbon basis of one, the carbon balance is:

$$C - balance = \frac{\sum_i \frac{\text{Area}_{\text{i,out}}}{\text{Area}_{\text{IStd,out}}}}{\frac{\text{Area}_{\text{feed,bypass}}}{\text{Area}_{\text{IStd,bypass}}}} \tag{3.6}$$

Carbon balances better than 95% were achieved with only a few exceptions, which were discarded for further analysis.

The conversion of cumene is calculated assuming 100% carbon balance

$$X = 1 - \frac{\text{Area}_{\text{Cumene,out}}}{\sum_i \frac{\text{Area}_{\text{i,out}}}{\text{Area}_{\text{IStd,out}}}} \tag{3.7}$$

3.4.3.2 Calculation of molar feed fraction

The molar feed fraction of cumene can be calculated from the partial pressure of cumene (assuming equilibrium) p^*_{Sat}, the pressure in the saturator p_{Sat} and the dilution ratio of saturator flow to total flow rate.

$$y\% = \frac{p^*_{Sat}}{p_{Sat}} \frac{F_{Ar,Sat}}{F_{Ar,dil} + F_{Ar,Sat}} \tag{3.8}$$

Chapter 4

Characterisation of apparatus

4.1 Jetloop reactor (JLR)

4.1.1 Introduction

The reactor behaviour, e.g. the recycle ratio, depends strongly on the flow rate, temperature, geometry of the nozzle, friction in the catalyst bed and the carrier gas. Hence operation parameters have to be found that ensure the reactor's approximation of an ideally mixed reactor (CSTR) with negligible temperature and concentration gradients.

4.1.1.1 Definition and determination of the recycle ratio

The standard model for a recycle reactor is shown in Figure 4.1. The recycle ratio R is defined as the recycled flow over the exiting flow. It can be estimated from the residence time distribution (RTD) measurement of a Dirac delta function δ(t) input. The average time needed to pass the reactor volume is $V_{Rctr}/((1+R)*F) = \tau_R/(1+R)$, where τ_R denotes the residence time in the reactor. The RTD consists of an infinite series of delta functions, whose magnitudes decrease as a geometric series (Rippin, 1967),

$$f(t) = \sum_{i=1}^{\infty} \frac{1}{1+R} \left(\frac{R}{R+1}\right)^{i-1} \delta\left(i - \frac{i\tau_R}{1+R}\right) \tag{4.1}$$

for which the RTD reduces with large R to that of a CSTR :

$$\frac{1}{\tau_R} exp(-t/\tau_R) \tag{4.2}$$

The recycle ratio can thus be evaluated from the time interval between two peaks, with

$$R = \frac{\tau_R}{\Delta t} - 1 \tag{4.3}$$

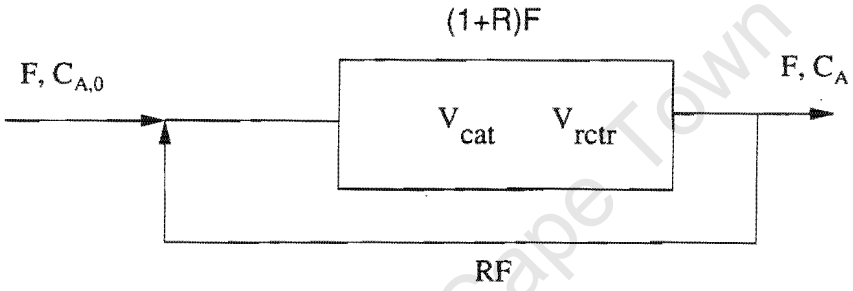

Figure 4.1: Recycle reactor model neglecting volume expansion

Möller et al. (1995) found that using a dispersion model yielded recycle ratios within 10% of those estimated from the above stated method.

4.1.1.2 Criteria for minimum recycle ratios

When modelling a recycle reactor as a perfectly backmixed CSTR, it is essential to determine the effect of the recycle ratio on the degree of backmixing. It was demonstrated (Luft and Herbertz, 1969) that a criterion for this recycle ratio is sufficient, if the catalyst bed can be treated as differential. Hence, the concentration gradient and the temperature gradient ΔT in the catalyst bed should not exceed certain limiting values depending on the desired experimental accuracy. The following criteria were given:

concentration gradient

$$R \geq \frac{X}{\text{rel. conc.gradient}} - 1 \tag{4.4}$$

temperature gradient

$$R \geq \frac{Xy\%\,(-\Delta H_R)}{c_p \Delta T} \tag{4.5}$$

The minimum recycle ratio is thus dependent on the conversion X, the reaction enthalpy ΔH_R, the molar feed fraction $y\%$ and the specific heat capacity c_p of the feed Total.

For the estimation of the minimum recycle ratio for this work the following data is used: ΔH_R(Cumene,700K) of 95.7 kJ/mol (Sandler, 1989), a maximum molar cumene percentage of 0.5%, heat capacity for argon of 20.9 J/(molK) and a maximum conversion of 90%.

By allowing a maximum relative error of 5% in the measurement of concentration, the minimal recycle ratio may be estimated by eq. 4.4 to be 17. At a maximum acceptable deviation of 1°C, the minimal necessary recycle ratio, according to eq. 4.5, is 20.

A rule of thumb commonly used is that a recycle ratio greater than 20 is sufficient to ensure that the reactor performance corresponds to that of a CSTR (Mills and Lerou, 1993). It is, however, obvious from eq. 4.5 that much higher recycle ratios are required for reactions with a high reaction enthalpy and high molar feed fractions.

4.1.1.3 Estimation of external film diffusion

Möller and O'Connor (1996) studied the mass transfer rates of naphthalene beads in the same JLR that was used in this work. They conducted their experiments at 20 °C with residence times varying between 0.02 to 0.1 s, where recycle ratios lie between 30 and 70. The mass transfer coefficient was found to be independent of the flow rate, but inversely proportional to the bead diameter. The corresponding Sherwood number $Sh = \frac{k_f d}{D_{Naph}} = f\,(Re, Sc)$, appeared thus to be independent of the Reynolds number Re. From the data presented in that work, a Sherwood number of 70 is obtained, which is similar to the values reported for a Berty-type reactor. Considering that the Schmidt number Sc for ideal gases does not vary significantly with temperature (Bird et al., 1960), mass transfer coefficients at elevated temperatures can therefore be extrapolated from these experiments.

4.1.2 Results of RTD studies

The RTD of a propane tracer pulse was measured on-line by an FID, as described in Section 3.2.1.1. Figure 4.2 shows a typical response curve. In general peaks broadened and dampened out after the second recycle. The time difference Δt between the two first peaks was used in order to calculate the recycle ratio according to eq. 4.3. A disadvantage of the RTD method arises with the upper limitation for recycle measurements. For an empty reactor the upper range of measurability was 70, after which peaks fused together. This upper range

is further reduced with increasing temperature leading to a higher degree of dispersion due to faster molecular diffusion. Additionally, increasing the flow resistance in the bed due to turbulent backmixing in the catalyst bed, as well as, in the lower and upper hemisphere of the reactor decreases the range of measurability. Hence, RTD studies above 350°C were not conducted. However, after surpassing the upper measurability a perfect CSTR response could always be observed, see Figure 4.3. The reactor volume can be estimated from the flow rate and the measured residence time. The error between actual and estimated reactor volume never exceeded 5%.

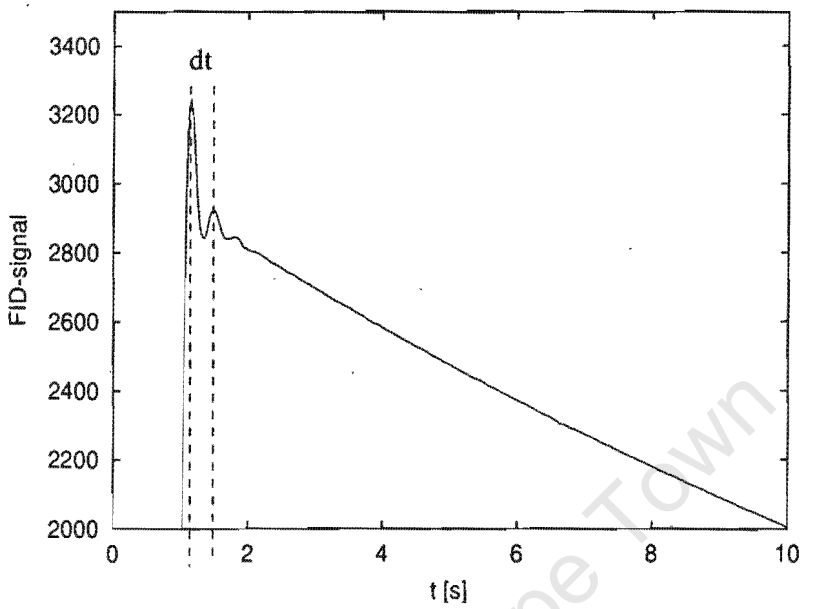

Figure 4.2: Determination of the recycle ration by measuring the time between two recycle peaks. T=22°C, τ_R=23.45 s, R=70

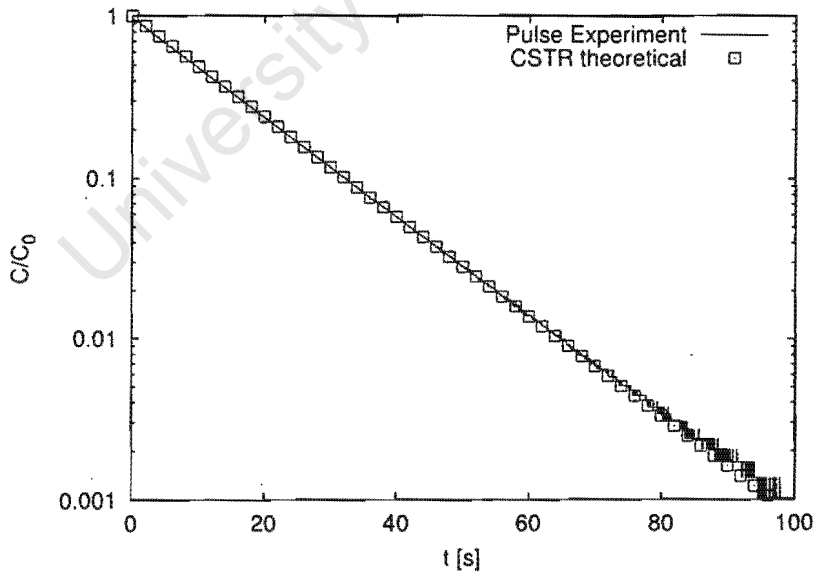

Figure 4.3: Comparison of the pulse experiment to the theoretical CSTR response.T=22°C, τ_R=14 s, R>70

4.1.2.1 Influence of the jet geometry

In addition to the "bulk head" nozzle depicted in Figure 3.4, which was studied by Möller et al. (1995), two alternative nozzles were investigated: (a) A "Laval-nozzle" made out of 1/8" quartz tubing with a minimum inner diameter of 0.1mm; (b) A 2cm long stainless steel HPLC capillary with an inner diameter of 0.1mm. It was suggested (Schnitzler, 1997), that a Lavall-jet design should result in higher recycle ratios, since this design permits supersonic gas velocity and hence maximum momentum transfer. The HPLC capillary was investigated, because it offered less obstruction at the center draft tube promising a possible enhancement in bulk fluid entrainment. Since the internal recirculation of the jetloop reactor is exclusively

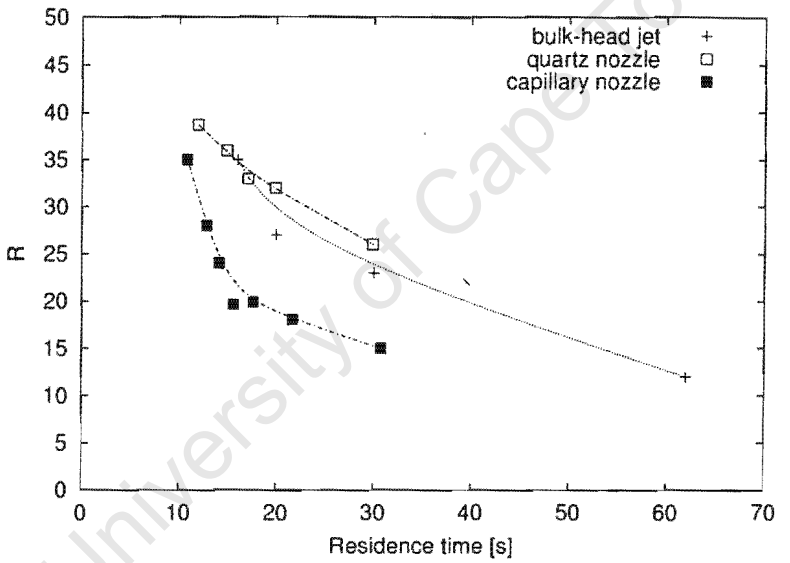

Figure 4.4: Effect of jet type on the recycle ratio. 2g 40 mesh glass beads, 25 °C, carrier gas nitrogen. Bulk-head jet measurements taken from (Möller et al., 1995)

caused by the momentum transfer of the jet stream to the bulk fluid, one expects a strong dependence of the recycle ratio on the flow rate, which is shown in Figure 4.4

Figure 4.4 also illustrates that the "Lavall-jet" yielded only slightly higher recycle ratios than the bulk-head nozzle. The quartz jet was also found to be impracticable because it was fragile. The capillary nozzle proved to be inferior to the bulk-head nozzle. Compared to this nozzle, the capillary jet needed half the residence time in order to achieve same recycle ratios. This might be understood by the higher loss of energy due to friction in the long tube, which leaves less energy to achieve recirculation.

4.1.2.2 Effect of temperature and flow rate on recycle ratio

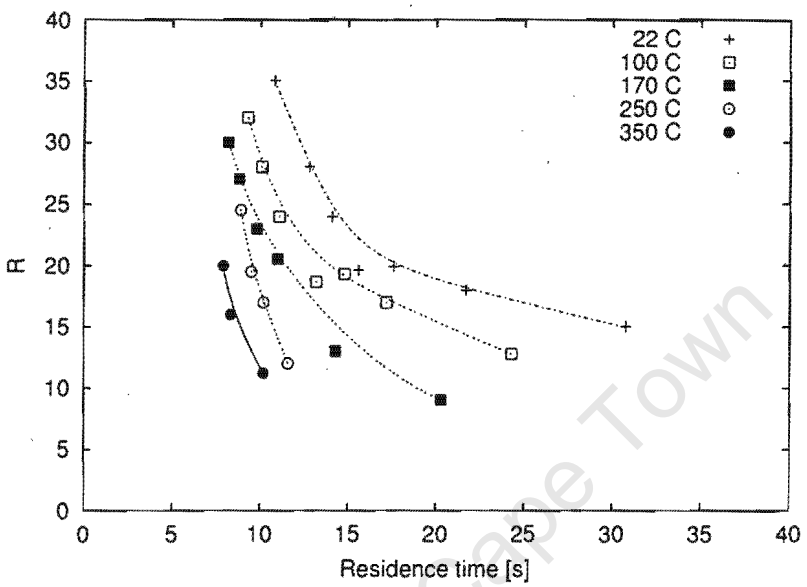

Figure 4.5: Effect of temperature/bed resistance on the recycle ratio, capillary jet, 2 g 40mesh glass beads, carrier gas nitrogen

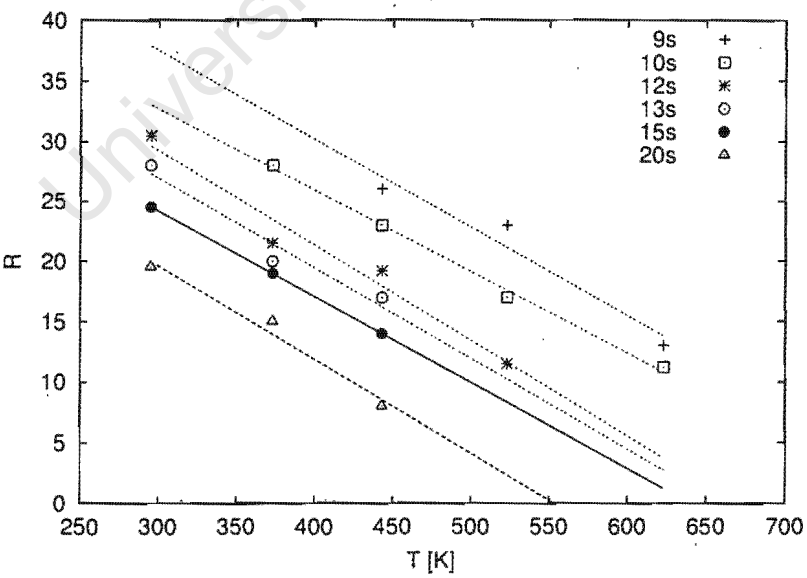

Figure 4.6: Linear dependence of the recycle ratio to the temperature with reactor residence time being constant. Data interpolated from Figure 4.5.

Figure 4.5 shows that increasing the temperature reduces the recirculation. For constant temperatures the recycle ratio is inversely proportional to the residence time, e.g. proportional to the flow rate with the recycle ratio increasing by 10 for every 100 ml/min increase in flowrate at all temperatures. The linear relationship between temperature and recycle ratio at constant residence times is represented in Figure 4.6 with data interpolated from Figure 4.5. For all residence times, the recycle ratio decreases by ten for every 150°C. A maximum achievable recycle ratio could not be measured, which suggests that higher recycle ratios could be obtained at lower residence times and a minimum required flow rate can be extrapolated from these data.

Möller et al. (1995) remarked that at a certain maximum recycle in relation to the flow rate exists, when the frictional loss of energy in the recycle loop outweighs the increase in jet energy. This maximum recycle ratio was 70 for an empty reactor, which was close to the experimental limitations. Dreyer and Luft (1982) measured recycle ratios with an anemometer and observed that after an optimum was reached the recycle ratio declined with the same rate as it increased.

4.1.2.3 Influence mass catalyst on recycle ratio

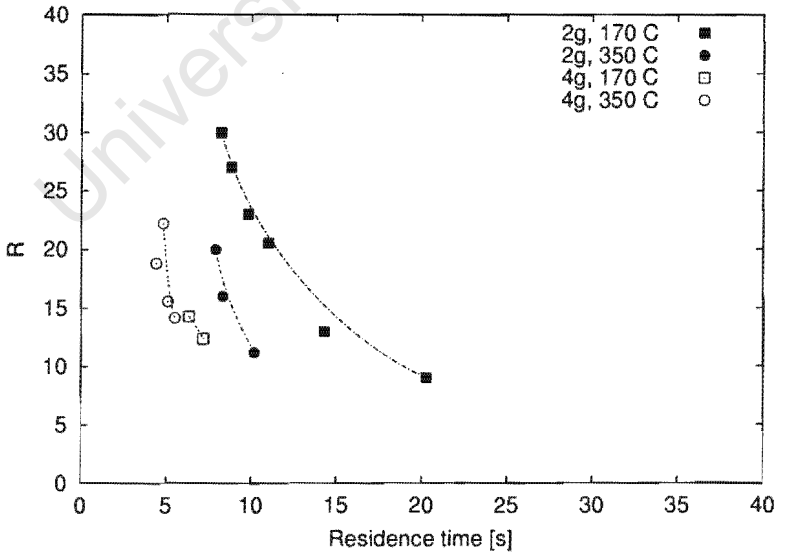

Figure 4.7: Effect flow resistance in the bed on the recycle ratio: Comparison: 2g vs. 4 g 40mesh glass beads, (capillary jet,carrier gas nitrogen)

The recycle ratio decreases with increasing friction in the catalyst bed. This decrease of recirculation is represented in Figure 4.7. In order to achieve the same recycle ratio with twice the mass of glass beads approximately half the residence time was needed. However higher recycle ratios are to be expected, if bigger particle sizes are used which offer less pressure drop in the particle bed. These results can be regarded as a worst case, since the catalyst particle diameters used in this work are at least a factor two bigger than of those utilised in the above RTD study. In the same sense it should be noted that the "bulk-head" will perform even better as it has a much flatter decline of the recycle ratio with residence time (Figure 4.4).

4.1.2.4 Influence of the carrier gas

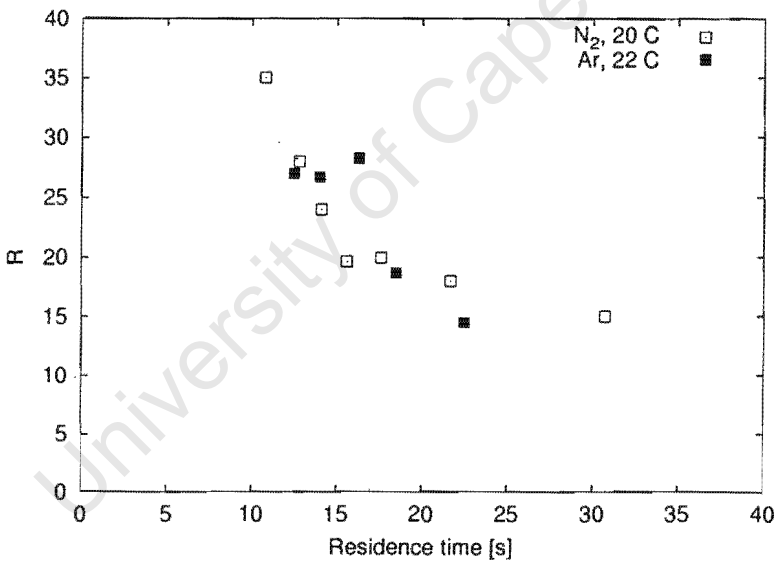

Figure 4.8: Comparison of the recycle ratios achieved with nitrogen vs. argon as carrier gas. 22 °C, 2g 40 mesh glass beads, capillary jet

The only driving force for recirculation in the JLR is the momentum from the jet stream, which is a product of mass throughput and the jet velocity. It is equal to the frictional force in the reactor at steady state. To achieve the necessary momentum is therefore difficult, if carrier gases with a low molecular weight are used. No recirculation behaviour could be achieved, when helium was used as carrier gas in the presence of 2g; 40 mesh glass beads. Here, the lower mass throughput would have to be compensated for a seven times higher

jet velocity. When argon was used as carrier gas, similar recycle ratios compared to those with nitrogen were observed, since the molecular weights only differ by 40 %. This is shown in Figure 4.8.

4.1.3 Conclusion

To justify the assumption of a CSTR a minimum recycle ratio is necessary to ensure gradientless behaviour in the reactor. The required recycle ratio for this work was calculated to be 20, according to the equations by Luft and Herbertz (1969) . Recycle ratios decrease with:

- decreasing catalyst particle size
- increasing mass of catalyst
- increasing temperature
- decreasing flow rate

Limiting operating parameters had thus to be found. As a worst case, RTD studies were conducted with glass beads of half the diameter in comparison to the smallest catalyst pellet used in this work.

Linear dependencies between the recycle ratio and the operating parameters flow rate and temperature were established. It was proven that the required minimum recycle ratio can be achieved, if small enough residence times are used. These can be estimated from the inverse and linear dependency plots of recycle ratio vs. residence time and recycle ratio vs. temperature (Figures 4.5 and 4.6).

4.2 Multi-Ampoule-Sampler (MAS)

4.2.1 Introduction

In order to ensure transient product analysis, the new MAS technique had to be evaluated for its accuracy and a feasible range of residence times had to be established. The technique was tested by injecting 500 μl of pure propane or benzene (vapour) or 0.5μl of liquid cumene into an empty jetloop reactor. The pulse responses obtained from the MAS method were compared to the online FID signal and the theoretically expected CSTR response curve. This was also a test for the correctness of the CSTR behaviour and plausibility of an ideal pulse injection.

The modelling of transient reactions required that concentrations were measured with mole fractions decreasing three orders of magnitude within 10 to 60 s. It was therefore crucial that sample volumes were sufficiently small in order to ensure differential sampling, but on the other hand being large enough to secure a representative sample at low concentrations for further analysis in the GC.

4.2.2 Theoretical criteria for differential sampling

For the development of a criteria for differential sampling, it is assumed that the sampling time (time of breaking ampoule tip) is exact. The fastest allowable sampling rate depends then on the rate of decline of concentration, the sample volume ΔV_{Amp} and the flow rate through the MAS (see Figure 4.9).

One can estimate a worst case criteria by assuming that the MAS is in plug flow, where samples are taken exclusively downstream from the sampling point. A sample volume ΔV_{Amp} is taken. This sample captures the effluent gas which has passed the sampling point within a time period of $\Delta t_{sample} = \Delta V_{Amp}/F$. With the effluent concentration of the CSTR being $C/C_0 = \exp(-t/\tau_R)$, one can introduce a maximum acceptable deviation $\frac{C(t-\Delta t_{sample})-C(t)}{C(t)} < 5\%$. The corresponding maximum sampling rate $1/\Delta t_{sample}$ can then be calculated using

$$\Delta t_{sample} = \frac{\Delta V_{amp}}{F} < \tau_R \ln(1+0.05) \approx \frac{\tau_R}{20} \tag{4.6}$$

where τ_R is the residence time of the JLR. Note, the actual deviation between the concentra-

tion in the ampoule and the concentration $C(t)$ at the sampling time t is smaller than 5%, because the sample has an averaged effluent concentration, which is taken as well upstream from the sampling point.

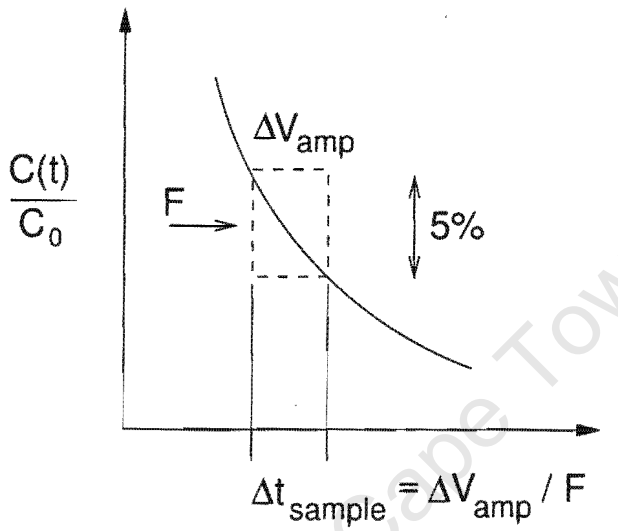

Figure 4.9: Criteria for maximum sample volume with 5% deviation in concentration

Approximate maximum sampling rate:

The biggest ampoules used had a volume of $\sim$ 2ml and the highest achievable flow rate was $\sim$ 500 ml/min (STP). Taking gas volume expansion in both MAS and JLR into account, the residence time τ_R has a value of 2.2s at 440°C, for which the 2ml ampoule proves to be 70% too big. In the crucial initial region, where the steepest concentration gradient and the highest concentrations are to be expected, smaller samples of 0.4-0.6 ml could be taken without a compromise on accuracy.

Similar to the above considerations of differential sampling, one can estimate the error caused by the maximum observed delay of the sampling time, which was approximately 0.2s (Section 3.2.1.3). Taking again a reactor residence time of 2.2s, a relative error of 10% can be calculated according to eq. 4.6.

4.2.3 Results

The measured pulse responses of propane and benzene for three different residence times are shown in Figure 4.10, where a good reproducibility is demonstrated. However, on average four out of 20 samples were not successful. Reasons were that the ampoules were fragile and that mistakes occurred during the pre-evacuation process. A detailed list of the areas in the chromatogram, evaluation of the concentration and errors is given in Appendix D. Traces of light hydrocarbon/combustion gases probably due to the sealing process of the glass ampoule, were always found to be present, even if an evacuated ampoule was sealed in a blank test. These gases were not separated during the GC analysis and contribute therefore to the propane peak resulting in a minimum concentration of $C/C_0 = 6 \cdot 10^{-4}$, which results in a slight tailing at concentration levels close to 10^{-3}.

A good agreement between MAS and FID is demonstrated in Figure 4.10. At higher flow rates (τ_R =2.2s) , where FID inlet flows could not be controlled below 60 ml/min, non linearities of the detector response were observed, which were probably caused by non-constant flow rates. However, the results obtained from the MAS are in excellent agreement to the expected theoretical CSTR response. For a system with such small residence times, it is difficult to achieve an ideal pulse. Considering the goodness of the response behaviour, this non-ideality of the pulse appeared to be negligible, although the injection volume was large.

Residence times are obtained from the FID and the MAS response by a least square fit of the exponential decay. These residence times are compared to the theoretical time of the CSTR. Table 4.1 shows that the deviation between experimental and theoretical residence time did not exceed 12% for both FID and MAS measurements. The average error of the concentration for each tracer experiment varies between 18%-31% in the normalised concentration range between 10^{-3} and 1. At low concentration regions the maximum error exceeds 100%. A more evenly weighted error distribution is obtained, when the error of the logarithmic concentration is calculated. The average error of the concentration varies then between 6% to 14%. However, when injecting 0.5μl of liquid cumene deviations between the theoretical CSTR response and the measured concentration curve of the MAS became apparent, as can be seen in Figure 4.11. Table 4.2 collates the residence times, which were calculated at concentrations greater than 0.01, where the measured response curve matched the expected CSTR curve. Excessive tailing at concentrations below 10^{-2} can be noticed

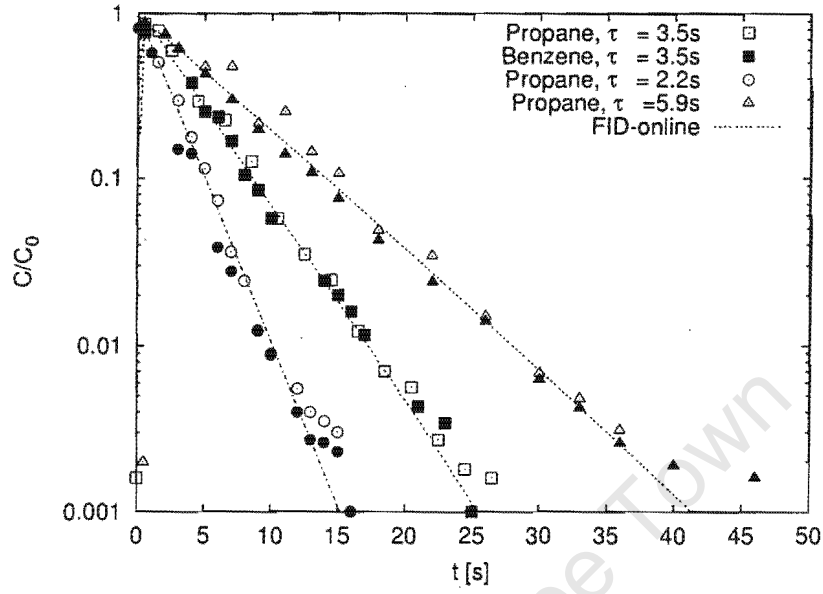

Figure 4.10: Comparison between the pulse responses (pulse size 500μl) obtained in parallel by the MAS technique and FID online as a function of residence time. Tracer gas: propane or benzene, empty JLR. (Line for τ_R=2.2s theoretical CSTR curve)

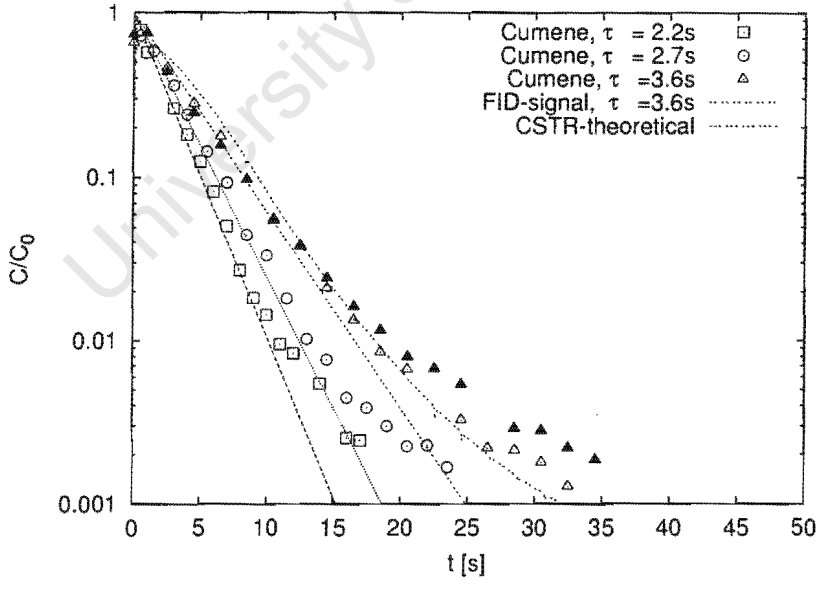

Figure 4.11: Comparison between pulse response obtained by MAS to theoretical CSTR curve. 0.5 μl liquid cumene injected in empty JLR with different residence times τ_R

Table 4.1: Comparison of the theoretical CSTR residence time τ_R[s] to those obtained from the measured slopes of the FID and MAS responses. Tracer gases propane and benzene

CSTR	FID	MAS #1	MAS #2	Error % FID	Error % MAS #1	Error % MAS #2
2.21	-	2.34	2.27	-	5.9	2.8
3.51	3.60	3.67	3.85	4.0	5.9	11.1
5.85	6.01	6.01	6.06	2.7	3.6	3.0

Table 4.2: Comparison of the theoretical CSTR residence time τ_R [s] to those obtained from the measured slopes of the MAS response. Injection: 0.5μl liquid cumene

CSTR	MAS #1	Error % MAS #1	MAS #2	Error % MAS #2
2.19	2.36	7.4	-	-
2.73	2.90	6.3	-	-
3.61	4.09	13.3	4.24	17.4

from both FID and MAS. This suggest that the large errors at lower concentrations are partly a consequence of poor injection and evaporation. However, increasing the temperature of the injector port and increasing the flow through the injector port by a factor three could not alter this behaviour.

4.2.4 Conclusion

The automated Multi-Ampoule-Sample (MAS) proved to be an excellent sampling technique for transient experiments. The fastest sampling rates were 1 sample per second. For pulse injections of propane and benzene concentrations curves could be monitored successfully, even if concentration levels decreased three orders of magnitude in 15 seconds. The error in the measurement of the CSTR residence time corresponds to that measured in parallel with an online FID. The minimum measurable concentration level for light hydrocarbons is determined by the presence of traces of these gases in the ampoules due to the ampoule making/melting procedure. When cumene was injected response curves could be reliably measured for normalised concentration levels above 10^{-2}.

Chapter 5

Theoretical

5.1 Introduction

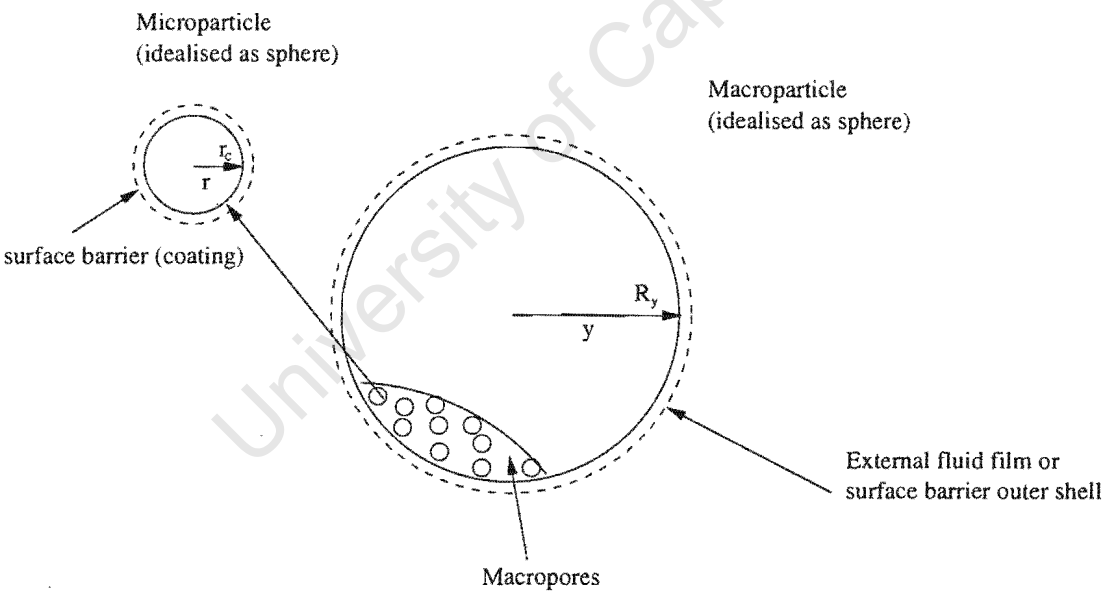

Figure 5.1: Illustration of a biporous catalytic particle (Not to scale). Note, micropore particles are about 100 times smaller than macropore particles.

Commercial catalysts, such as zeolites, consist of microporous crystals, which are formed using a binder into pellets or extrudates, see illustration in Figure 5.1. Such catalysts exhibit a bipore distribution, where the molecules have to diffuse first through the randomly distributed macropores, adsorb on the crystals and then migrate through the microporous

channels within the crystals. Additionally to this inter and intracrystalline diffusional restriction, the adsorbate may encounter transport restrictions on entering the crystals in the form of a surface barrier due to coating and possible pore mouth narrowing or pore mouth blocking. During the pelletisation process a dense outer shell can be formed around the pellet. This surface resistance is mathematically similar to that of external film resistance. Adsorption and reaction may occur in both micropores and macropores. In a general continuum model the transport resistances in the bipore structure are thus in series, whereas the adsorption and reaction processes may occur in parallel within the microporous and macroporous structure

Film resistance and surface barriers concerning crystals or pellets are not incorporated in the following continuum models. A discussion of a general model, which incorporates all remaining six model parameters (diffusion, adsorption and reaction in micropores and macropores), would be too complex. Two simplified models are hence examined in detail with the key issues being: Parameter estimation and uniqueness of model parameters, see Table 5.1. Sorption experiments on a biporous adsorbent are discussed in Section 5.2. In Section 5.3 a first order reaction term is integrated for a macroporous catalyst with adsorption and reaction in the micropores but without diffusional resistance in the micropores.

Table 5.1: Key features and parameters of the two continuum models presented in Chapter 5

	Model without reaction	Model with reaction
Linear Model	Yes	Yes
Micropore Diffusion D_c	Yes	No
Macropore Diffusion D_y	Yes	Yes
Micropore Adsorption K_c	Yes	Yes
Macropore Adsorption K_y	Yes	No
First order rate const. k_R	No	Yes
Solution	Analytic	Numerical
Parameter estimation	Analytic + Moment Analysis	Optimisation, Least Square
Parameter Uniqueness Test	Analytic + Moment Analysis	Numerical Sensitivity Analysis

5.2 Pulse response without reaction

In this section a theoretical model describing the diffusion and adsorption on biporous catalysts during a pulse experiment in a CSTR is presented.

Ruckenstein et al. (1971) were the first to develop analytic solutions for uptake measurements with such bipore adsorbing catalysts. For the analysis of ZLC (Eic and Ruthven, 1988) measurements, Silva and Rodrigues (1996) and Brandani (1996) independently developed an analytic solution. Where Brandani incorporated the effect of fluid hold-up, Silva and Rodrigues investigated the significance of the long time solution on the analysis of experimental data.

This model is similar to those discussed above, but it incorporates the effect of external surface adsorption in the macropores. The analytical solution for dual and single resistance and their long time solutions are developed. It will be demonstrated that the first moment and the long time solution of the response curve can be used to estimate the parameters. This method avoids the use of inaccurate higher moments. The uniqueness of the solution and its parameters is examined in detail.

5.2.1 Mathematical model

The mathematical model is based on the work of (HSU and Haynes, 1981) with the following assumptions:

- the adsorbent pellet has a uniform biporous structure
- the pellets and the crystals have spherical geometry
- adsorber behaves like a CSTR
- linearity: isothermal operation, adsorption equilibria in micropores and macropores are linear
- micropore and macropore diffusion mechanisms are in series and given by Fick's law
- no external film resistance

In general, the assumption of linearity is reasonable for low inlet pulse concentrations, where only a small percentage of the surface is covered. Nevertheless, non-linearity effects might

occur due to different strength of adsorption sites. The transport mechanism in series holds true, if the radius of the microparticle is much smaller than the radius of the macroparticle. CSTR behaviour can in general be assumed with the jetloop reactor having a recycle ratio greater than 20 (Section 4.2), in which case external film resistance is also eliminated.

Model equations are as follows.

Micropore mass balance:

$$\frac{\partial q}{\partial t} = D_c \left(\frac{\partial^2 q}{\partial r^2} + \frac{2}{r} \frac{\partial q}{\partial r} \right) \tag{5.1}$$

Macropore mass balance:

$$(1 + K_y)\, \varepsilon_y \frac{\partial C_y}{\partial t} + (1 - \varepsilon_y)\, \varepsilon_c \frac{\partial \overline{q}}{\partial t} = \varepsilon_y D_y \left(\frac{\partial^2 C_y}{\partial y^2} + \frac{2}{y} \frac{\partial C_y}{\partial y} \right) \tag{5.2}$$

with

$$\frac{\partial \overline{q}}{\partial t} = 3 \frac{D_c}{r_c} \left(\frac{\partial q}{\partial r} \right)_{r=r_c} \tag{5.3}$$

Reactor mass balance:

$$-C_z - \frac{3 V_{cat} D_y \varepsilon_y}{F R_y} \left(\frac{\partial C_y}{\partial y} \right)_{y=R_y} = \frac{V_R}{F} \frac{\partial C_z}{\partial t} \tag{5.4}$$

The initial conditions are

$$C_y\,(y, t < 0) = q\,(r, t < 0) = 0 \tag{5.5}$$

$$C_z\,(t < 0) = C_0 \tag{5.6}$$

and boundary conditions

$$\left(\frac{\partial C_y}{\partial y} \right)_{y=0} = \left(\frac{\partial q}{\partial r} \right)_{r=0} = 0 \tag{5.7}$$

$$C_y\,(R_y, t) = C_z\,(t) \tag{5.8}$$

$$q(y, r_c, t) = K_c C_y(y, t) \tag{5.9}$$

5.2.2 Analytical solution

If adsorption in the macropores is negligible one can readily obtain the analytical solution of the pulse response by differentiation of the step response given by Brandani (1996).

In the more general case the set of equations 5.1 to 5.9 can be solved in the Laplace domain. By inverting to the time domain through the use of the method of residues or Heaviside theorem one obtains the analytical solution:

$$\frac{C_z(t)}{C_0} = \sum_{n=1}^{\infty} \frac{4\gamma\phi_n^2 \exp\left(-D_c/r_c^2\phi_n^2 \cdot t\right)}{4\gamma\phi_n^2 + \frac{1}{x_n}\left((\gamma\phi_n^2+1-L)^2 - x_n - \gamma\phi_n^2 - 1 + L\right)} \cdot \frac{1}{\left(-2\kappa(1+K_y)\phi_n^2 - \lambda(Z_n^2+\phi_n^2-Z_n)\right)} \tag{5.10}$$

with the dimensionless parameters

$$\kappa = \frac{D_c/r_c^2}{D_y/R_y^2} \qquad \lambda = \frac{3(1-\varepsilon_y)\varepsilon_c}{\varepsilon_y}\kappa K_c$$
$$\gamma = \frac{\kappa}{3}\frac{V_R}{\varepsilon_y V_{cat}} \qquad L = \frac{1}{3}\frac{FR_y^2}{\varepsilon_y V_{cat} D_y} \tag{5.11}$$

with

$$Z_n = \frac{x_n + \kappa\left(1+K_y\right)\phi_n^2}{\lambda} + 1 \tag{5.12}$$

and

$$x_n = -\left(1+K_y\right)\kappa\phi_n^2 + \lambda\left(\phi_n \cot\phi_n - 1\right) \tag{5.13}$$

The values of ϕ_n are given by the positive real roots of:

$$-\gamma\phi_n^2 + L - 1 + \sqrt{x_n}\coth\sqrt{x_n} = 0 \tag{5.14}$$

where in the case of $x_n < 0$ eq. 5.14 simplifies to:

$$w_n \cot w_n - \gamma\phi_n^2 - 1 + L = 0; \quad x_n = -w_n^2 \tag{5.15}$$

if $x_n > 0$, then

$$w_n \coth w_n - \gamma\phi_n^2 - 1 + L = 0; \quad x_n = w_n^2 \tag{5.16}$$

The derivation of eq. 5.10 can be found in Appendix E on page 173

In each π interval of ϕ_n there is an infinite number of roots that is a solution to the transcendental eq. 5.14.

A detailed description of how to determine the roots of eq. 5.14 is given by Brandani (1996) for the solution of the ZLC-model, whose characteristic equation is equivalent to that of a pulse response.

Moment Analysis

The first moment may be determined from the Laplace solution (Appendix eq.E.8) by using van der Laan's theorem;

$$\mu_1 = \lim_{s \to 0} \frac{\partial \widetilde{C}_z(s)}{\partial s} = \frac{\int_0^\infty C_z(t) t dt}{\int_0^\infty C_z(t) dt} \tag{5.17}$$

yielding

$$\mu_1 = \frac{V_R}{F} + \frac{V_{cat}}{F} \left(\varepsilon_y \left(1 + K_y\right) + \left(1 - \varepsilon_y\right) \varepsilon_c K_c\right) \tag{5.18}$$

5.2.3 Theoretical analysis of pulse curves

Finding the roots of the transcendental eq. 5.14 is a numerically strenuous task. Eq. 5.1 to 5.9 are preferably solved by the method of collocation (Finlayson, 1973) or by inverting the Laplace solution, see Appendix eq. E.8 with the Fast Fourier Transform (Brigham, 1988). In Figure 5.2 the convergence of the response by using the method of collocation and the calculation by the analytical solution is demonstrated.

5.2.4 Long time solution

For the analysis of the ZLC response in a single pore system, Eic and Ruthven (1988) used the long-time solution. This was further developed by Silva and Rodrigues for a bipore system.

In the longer time region, only the first term of the series in eq. 5.10 has to be considered, and the solution can be approximated by:

$$\frac{C_z(t)}{C_0} = \text{intercept} \cdot \exp(-D_c / r_c^2 \phi_1^2 \cdot t) \tag{5.19}$$

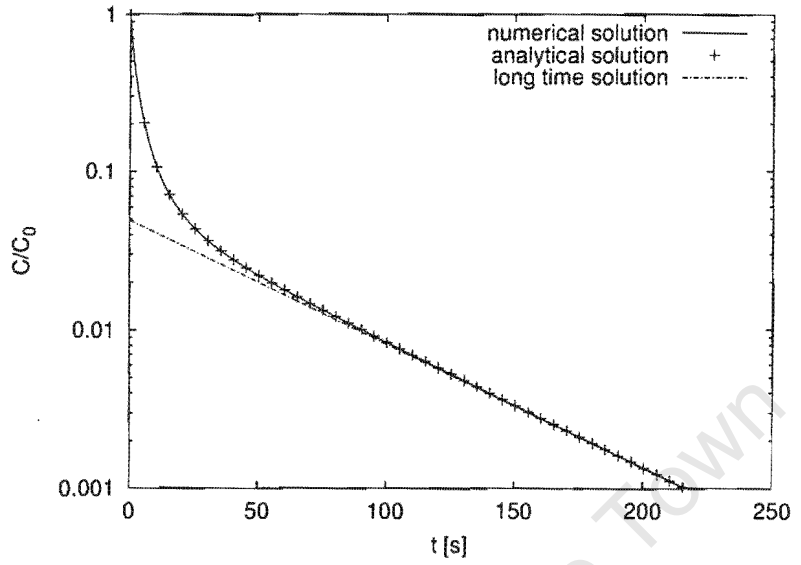

Figure 5.2: Analytical solution eq. 5.10 in comparison to method of collocation using 9 collocation points and the long time solution according to eq. 5.19 to 5.15 $\kappa = 3.17 \cdot 10^{-4}$, $\gamma = 0.073$, $L = 2.51$ and $\lambda = 2.63$

with

$$\text{intercept} = \frac{4\gamma\phi_1^2 \exp\left(-D_c/r_c^2\phi_1^2 \cdot t\right)}{4\gamma\phi_1^2 + \frac{1}{x_1}\left(\left(\gamma\phi_1^2 + 1 - L\right)^2 - x_1 - \gamma\phi_1^2 - 1 + L\right)} \cdot \frac{1}{\left(-2\kappa\left(1 + K_y\right)\phi_1^2 - \lambda\left(Z_1^2 + \phi_1^2 - Z_1\right)\right)} \tag{5.20}$$

where ϕ_1 is the first root of eq. 5.15

5.2.4.1 Micropore or macropore diffusion control

The general solution may be simplified, if either micropore diffusion ($\lambda \ll 0.1$) or macropore diffusion ($\lambda \gg 10$) is rate controlling. The solutions can be obtained either by solving the simplified Laplace solutions or by a Taylor expansion of the characteristic equations (Brandani, 1996). In the case of intracrystalline diffusion control, where λ and κ are small, x_n tends to zero. The characteristic equation then simplifies to:

$$\phi_n \cot \phi_n - 1 + L_{mic} - \gamma_{mic}\phi_n^2 = 0 \tag{5.21}$$

where the modified dimensionless numbers are

$$L_{mic} = \frac{1}{3}\frac{r_c^2 F}{D_c K_c \overline{V}_{cat}}; \quad \gamma_{mic} = \frac{1}{3}\frac{\overline{V}_R}{K_c \overline{V}_{cat}} \tag{5.22}$$

with the effective volumes:
$\overline{V_R} = V_R + \varepsilon_y(1+K_y)V_{cat}$; $\overline{V}_{cat} = V_{cat}\cdot(1-\varepsilon_y)\,\varepsilon_c$
and the analytical solution for micropore diffusion is:

$$\frac{C_z(t)}{C_0} = \sum_{n=1}^{\infty} \frac{2\gamma_{mic}\phi_n^2}{\phi_n^2 + (1 - L_{mic} + \gamma_{mic}\phi_n^2)^2 + L_{mic} - 1 + \gamma_{mic}\phi_n^2} \exp\left(-\frac{\phi_n^2 D_c t}{r_c^2}\right) \tag{5.23}$$

Once the solution for micropore diffusion control is known, it is easy to deduct the case of macropore diffusion control by introducing, according to Ruthven (1984) , an apparent diffusion coefficient;

$$D_{app} = \frac{D_y \varepsilon_y}{(1+K_y)\,\varepsilon_y + (1-\varepsilon_y)\,\varepsilon_c K_c} \tag{5.24}$$

Similar to the reasoning made by Ruthven and Xu (1993) the solution for macropore diffusion control is:

$$\frac{C_z(t)}{C_0} = \sum_{n=1}^{\infty} \frac{2\gamma_{mic}\phi_n^2}{\phi_n^2 + (1 - L_{mac} + \gamma_{mac}\phi_n^2)^2 + L_{mac} - 1 + \gamma_{mac}\phi_n^2} \exp\left(-\frac{\phi_n^2 D_{app} t}{R_y^2}\right) \tag{5.25}$$

with the characteristic equation:

$$\phi_n \cot\phi_n - 1 + L_{mac} - \gamma_{mac}\phi_n^2 = 0 \tag{5.26}$$

and the corresponding dimensionless numbers

$$L_{mac} = \frac{1}{3}\frac{R_y^2 F}{\varepsilon_y D_y V_{cat}}; \quad \gamma_{mac} = \frac{1}{3}\frac{V_R}{V_{cat}\left((1+K_y)\,\varepsilon_y + (1-\varepsilon_y)\,\varepsilon_c K_c\right)} \tag{5.27}$$

In both micropore and macropore control, the long-time solution can again be found by only considering the first term of the infinite sum.

Parameter estimation from experimental curve:

In order to estimate the two model parameters diffusivity and adsorption from an experimental response curve, it is sufficient to calculate: **(i) first moment, (ii) slope of**

long time solution (of the semi-log plot). This estimation procedure is similar to the ZLC method, but it offers additionally the possibility to check the validity of the model by comparing the experimental and the theoretical intercept of the long time region.

5.2.5 Uniqueness of parameters

It was shown (Silva and Rodrigues, 1996) that micropore and macropore diffusivity cannot be simultaneously extracted from the measured slope and intercept in a semi-log plot during ZLC experiments, even if the microporous adsorption constant is known.

In the case of a pulse experiment, the uniqueness of the response curves shall be investigated for a system with micropore adsorption only and a system where both micropore and macropore adsorption become important. For both sections the following parameters stay constant: $V_{cat}/F = 0.0268s$, $V_R/F = 5.925s$ $R_y = 0.0254cm$, $\varepsilon_y = 0.32$, slope of the long time solution $= 0.008s^{-1}$.

5.2.5.1 Micropore adsorption only

When $K_y = 0$, the micropore adsorption K_c is uniquely defined by the first moment (eq. 5.18), which is not a function of diffusivity. Intuitively, it might be assumed that in a system with transport resistances in series and adsorption only happening in the last member of the chain, an infinite number of combinations of diffusivities with same overall resistance yield exactly the same response curve. Additionally, if the first moment and the long time solution (slope) are identical, the response curves should be identical. This is investigated in Figure 5.3 with the parameters given in Table 5.2 for three different adsorption constants. For a given slope and an arbitrary diffusivity D_y the corresponding micropore diffusivity D_c can be determined by solving the characteristic eq. 5.15 (note that eq. 5.16 does not have a root in the first π interval, see (Brandani, 1996)). ϕ_1 and D_c were simultaneously solved by Newton's method.

Response curves ranging from intracrystalline ($\lambda \leq 0.1$) to intercrystalline ($\lambda \gg 10$) diffusion control are shown in Figure 5.3. The solutions for single transport resistance have the same eigenvalues (roots of eq. 5.21 and 5.26) and are thus mathematically identical, compare Table 5.2. A proof for the limiting value of ϕ_1, if $\lambda \to \infty$, is given by Brandani (1996) . The solutions of the bipore model differ slightly but not significantly enough to be distinguished from each other experimentally. This observation is irrespective of the

adsorption capacity. However, as remarked already by (Silva and Rodrigues, 1996) for the case of ZLC experiments, the intercepts of the long time solutions are uniquely determined by its slope and the adsorption constant.

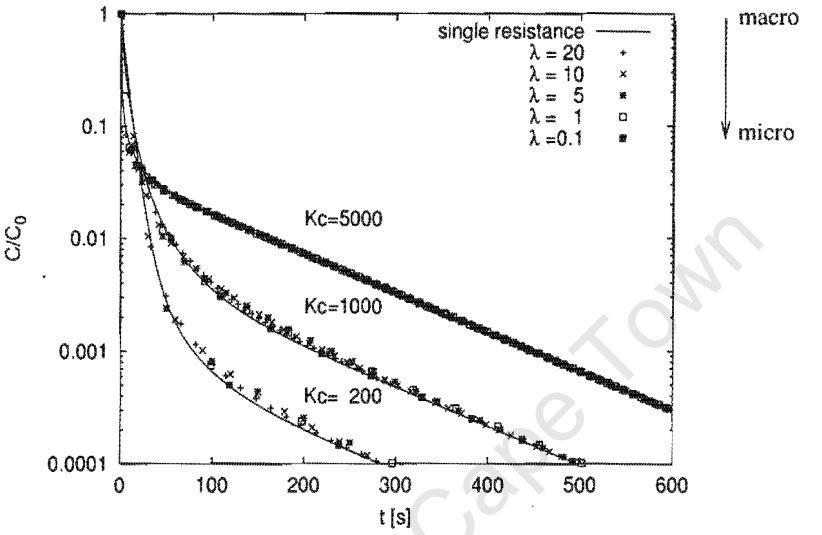

Figure 5.3: Effect of λ on three sets of response curves with different micropore adsorption coefficients K_c. Diffusivities for same slopes in long time solution range from macropore to micropore diffusion control, see Table 5.2.

Table 5.2: Model parameters used for Figure 5.3. Three sets of different first moments, e.g. different K_c, but same slopes in the long time solution.

	$K_c = 200$			$K_c = 1000$			$K_c = 5000$		
λ	D_c	D_y	ϕ_1	D_c	D_y	ϕ_1	D_c	D_y	ϕ_1
∞	-	0.227	3.112	-	1.235	2.980	-	17.23	1.784
20	17.59	0.250	1.115	19.15	1.362	1.099	54.62	19.43	0.651
10	9.666	0.275	1.547	10.53	1.498	1.482	30.50	21.70	0.871
5	5.777	0.329	2.000	6.287	1.790	1.918	18.55	26.40	1.116
1	2.926	0.833	2.811	3.166	4.506	2.702	9.344	66.49	1.573
0.1	2.430	0.691	3.086	2.645	37.64	2.957	7.462	531.0	1.760
0	2.388	-	3.112	2.603	-	2.980	7.262	-	1.784

D_c $[cm^2/s \cdot 10^{11}]$
D_y $[cm^2/s \cdot 10^3]$

5.2.5.2 Micropore and macropore adsorption

If additionally adsorption in the macropores occurs, not all adsorbing species necessarily enter the micropores but might only get adsorbed (parallel process) in the macropores. This should result in two exponential decays in the long time solution, if macropore diffusion is not the transport limiting process. In the following discussion, this deviation from the response curve with macropore diffusion control is investigated. Note that for diffusional control in the macropores it is irrelevant, whether the adsorption capacity is in the macropores or micropores.

In Table 5.3 four different groups are given with sets of model parameters that yield response curves with *same slope* in the long time solution and *same first moment*, e.g. same overall adsorption capacity. The different curves are:

A	Macropore diffusion control
B-D	Approximately same diffusivities but increasing contribution of macropore adsorption
E-G	Constant micropore and macropore adsorption but increasing ratio D_c/D_y, e.g. increasing λ
H	Curve that is fitted to curve C with $C/C_0 > 0.001$ assuming macropore diffusion control.

The first moments for curves A to G are calculated according to eq. 5.18:

$$\mu_1 = 5.925s + 0.0268s(0.32(1 + K_y) + (1 - 0.32)K_c)) = 24.15s$$

In Figures 5.4 and 5.5 two distinct straight lines in the semi-logarithmic plot can be identified for the curves B to G in contrast to the curve A.

In Figure 5.4 this effect is emphasised by decreasing κ (the ratio of micropore/macropore diffusivity). With decreasing κ - from curve G to E - the existence of two straight lines becomes more pronounced and the intercept of the long time solution is shifted towards lower concentrations.

In Figure 5.5 the fraction of the micropore adsorption in the overall adsorption capacity is lowered from curve B to curve D. With smaller ratios of K_c/K_y the response curves exhibit two very distinct straight lines in the semi-logarithmic plot.

If κ and K_c/K_y are small, adsorption and diffusion in the macropores dominate the initial sorption dynamics without a significant contribution from the dynamics in the microporous crystals. Sorption in the micropores becomes important in the long time region, when the sorbed molecules slowly diffuse out of the crystals into the macropores. One can thus distinguish theoretically between micropore and macropore parameters, as shown for curve C and H. Curve H is fitted with a macropore diffusion model to the initial part of curve C, for which sorption in the micropores only plays an insignificant role. The estimated adsorption coefficient K_y is about 5% smaller and the macropore diffusivity is 25% smaller than the respective values of the bipore model.

The response curve B of the bipore model, however, approaches the macropore controlled response curve A. Here, micropore and macropore dynamics are comparable. In any case, it is not possible to fit curve B with a simple micropore or macropore model of two parameters. A parameter estimation using the first moment and the slope of the long time solution, as described in Section 5.2.5.1, will consequently always lead to a model response which is below the actual response curve in the initial region and above in the long time region.

Furthermore, it should be remarked that the logarithmic scale of C/C_0 from 1 to 10^{-5} was chosen out of theoretical interest, whereas the measurability of concentration is generally restricted to 10^{-3}.

Table 5.3: Model parameters used for Figure 5.4 and 5.5.

	K_c	K_y	$D_c[cm^2/s]10^{11}$	$D_y[cm^2/s]10^3$	$\kappa(1+K_y)$	λ
A	1000	-	-	1.24	∞	∞
B	500	1062	2.567	10.0	0.061	0.183
C	100	1911	2.387	10.0	0.101	0.034
D	50	2018	2.365	10.0	0.107	0.017
E	250	1593	2.454	10.0	0.087	0.0873
F	250	1593	2.526	5.00	0.1798	0.1797
G	250	1593	3.048	2.00	0.542	0.542
H	-	1900	-	7.55	∞	∞

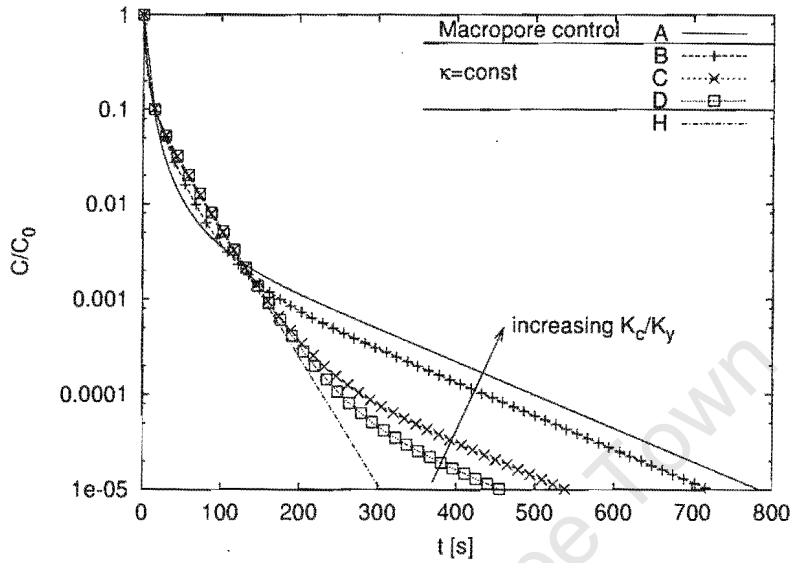

Figure 5.4: Effect of K_c/K_y on response curves with the same slope=$0.008s^{-1}$ and the same first moment. Model parameters for curves A to H are listed in Table 5.3. Macropore diffusion controlled curve H approximates initial region of curve C.

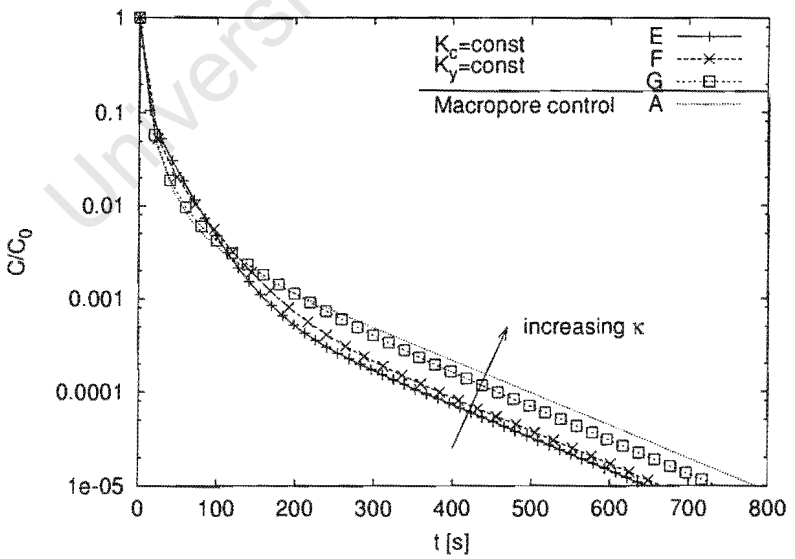

Figure 5.5: Effect of diffusivities on response curves with the same slope=$0.008s^{-1}$ and same adsorption coefficients. Model parameters for curve A to G are listed in Table 5.3.

5.2.6 Summary

An analytical solution for the pulse response curve of adsorbate on bipore catalysts in a CSTR was developed. For the regimes, where either micropore or macropore resistance is dominant solutions are presented. In this case, a parameter estimation from an experimental response curve can be achieved by calculating the first moment and the slope in the long time solution of a semi-logarithmic plot.

For the case where there is only adsorption in the micropores, it was demonstrated that response curves do not differ significantly, when their first moment and slope in the long time solution are the same. One can therefore only distinguish between the two diffusion mechanisms, if either the pellet or the crystal size is varied. When adsorption in the macropores is significant the response curve exhibits two distinct straight lines on a semi-log plot. In this case, model parameters cannot be directly estimated from the first moment and the long time solution and parameter estimations will in general not be possible due to inappropriate experimental sensitivity.

5.3 Pulse response with reaction

It was demonstrated in the previous section that the contribution of micropore diffusion and macropore diffusion can be easily accounted for, if these resistances are considered to be in series in a continuum model. Models for such a biporous system including first order reactions were developed by Schobert and Ma (1981a,b), Park and Kim (1984 a,b). As it was pointed out in Section 2.2.2.1 it is questionable, whether diffusion, adsorption and reaction coefficients can be extracted from one pulse experiment, as claimed by Schobert and Ma (1981a,b), Park and Kim (1984 a,b). It was, however, mentioned by both groups that macropore and micropore kinetics cannot be distinguished in a single experiment without changing particle sizes. This result was confirmed in the previous section. Hence, in order to simplify matters only diffusion in the mesopores is considered to be important for the following model and parameter sensitivity analysis. The results can be readily applied to the similar microporous system.

The analysis of the sorption systems with only one diffusivity and adsorption coefficient in the previous section was simple and elegant in a way that only two supposedly easy calculations were necessary for the parameter estimation: first moment and the long time solution. Despite the simplicity of this method, one has to bear in mind the (possible) inadequacies of this approach, especially for more complex systems involving multi-component and multi-parametric problems:

- The calculation of moments is very inaccurate, especially for higher moments needed in multi-parametric systems
- A theoretical moment analysis in the Laplace domain suggests the possibility of a parameter estimation irrespective of the range of measurability
- Model parameters can be highly correlated. This is, because of the naturally high degree of nonlinearity in the moment equations, a difficult mathematical problem
- A meaningful error analysis, e.g. confidence intervals, of the estimated parameters is not possible
- The system has to be linear

The introduction of the reaction term as a third parameter in the sorption model complicates the analysis under these aspects in two ways. Firstly, the method of parameter analysis has to account for an experimentally higher degree of error in the response curves analysis of a multi-component system. Secondly, the reaction term may lead to estimated parameters which are strongly correlated.

Numerical methods are more versatile in handling complex multi-component systems. For the reaction model a numerical parameter sensitivity using the first order parameter derivatives of the outlet concentration curve of reactant and product was thus used to clarify the question of parameter uniqueness and sensitivity. A review on the application of sensitivity analysis is given by Rabitz et al. (1983).

5.3.1 Model description

The mathematical model and its assumptions are similar to those from the previous chapter, except that transport resistance in the micropores or at the pore mouth of the crystals is considered to be insignificant. Additionally, an irreversible first order reaction occurs exclusively in the zeolite crystals. The active sites for adsorption and reaction are assumed to be homogeneous. The adsorption behaviour is linear and reversible.

The mass balances are nondimensionalised, as in Section 5.2, with the difference that the independent dimensionless time τ is the real time t divided by the reactor residence time τ_R, which does not contain any unknown model parameters. The dimensionless spatial coordinate ψ is the particle coordinate divided by the particle radius R_y.
Model equations are as follows.

Macropore mass balance:

Reactant

$$\frac{\partial C_R}{\partial \tau} = -\varphi^2 \alpha_R C_R + \alpha_R \left(\frac{\partial^2 C_R}{\partial \psi^2} + \frac{2}{\psi} \frac{\partial C_R}{\partial \psi} \right) \tag{5.28}$$

Product

$$\frac{\partial C_P}{\partial \tau} = -C_R \frac{\varphi^2}{Rf} \frac{\beta_R}{\beta_P} \alpha_P + \alpha_P \left(\frac{\partial^2 C_P}{\partial \psi^2} + \frac{2}{\psi} \frac{\partial C_P}{\partial \psi} \right) \tag{5.29}$$

Rf is the response factor on a carbon number basis (e.g. $Rf(Propene) = -3/9$, $Rf(Benzene) = -6/9$).

Reactor mass balance:

Reactant

$$\frac{\partial C_R}{\partial \tau} = -C_R(1) - \beta_R \left(\frac{\partial C_R}{\partial \psi}\right)_{\psi=1} \tag{5.30}$$

Product

$$\frac{\partial C_P}{\partial \tau} = -C_P(1) - \beta_P \left(\frac{\partial C_P}{\partial \psi}\right)_{\psi=1} \tag{5.31}$$

The initial conditions are

$$C_i\left(\psi < 1, t < 0\right) = 0 \tag{5.32}$$

$$C_R\left(\psi = 1, t < 0\right) = 1 \tag{5.33}$$

$$C_P\left(\psi = 1, t < 0\right) = 0 \tag{5.34}$$

and boundary conditions

$$\left(\frac{\partial C_i}{\partial \psi}\right)_{\psi=0} = 0 \tag{5.35}$$

The dimensionless groups in eq.5.28 to 5.31 are:

φ is the Thiele modulus, which signifies the relation of reaction time over diffusion time and is here defined as

$$\varphi^2 = \frac{\left(1-\varepsilon_y\right) k_R K_{c,R} \varepsilon_c}{\varepsilon_y D_{y,R}/R_y^2} = \frac{\text{reaction time constant}^{-1}}{\text{diffusion time constant}^{-1}} \tag{5.36}$$

k_R is the intrinsic first order rate constant of the sorbed reactant. $K_{c,R}$ is the dimensionless adsorption coefficient and $D_{y,R}$ is the macropore diffusivity of the reactant, ε_c is the zeolite volume fraction of total solid volume, ε_y is the void fraction.

α_i can be interpreted as the ratio of the reactor residence time over the interparticle diffusion time, which is often referred to as apparent diffusivity, and is defined as

$$\alpha_i = \frac{\tau_R}{R_y^2\left(\varepsilon_y + \left(1-\varepsilon_y\right)\varepsilon_c K_{c,i}\right)/\left(\varepsilon_y D_{y,i}\right)} = \frac{\text{residence time}}{\text{apparent diffusion time}} \tag{5.37}$$

β_i is the ratio of the catalyst contact time over the diffusional purge time at the boundary. It is defined as

$$\beta_i = \frac{3V_{cat}\varepsilon_y D_{y,i}}{F R_y^2} = \frac{3\tau_{cat}}{R_y^2/\left(\varepsilon_y D_{y,i}\right)} = \frac{\text{catalyst contact time}}{\text{diffusion time}} \tag{5.38}$$

The system of PDEs was solved by the method of collocation. The collocation coefficients were calculated according to the method by Villadsen and Michelsen (1978). 50 collocation points proved to be sufficient even at values for the Thiele modulus close to 1000. The resulting ODEs were integrated by Gear's method using the LSODE algorithm by Hindmarsh (1980).

5.3.2 Uniqueness of parameters

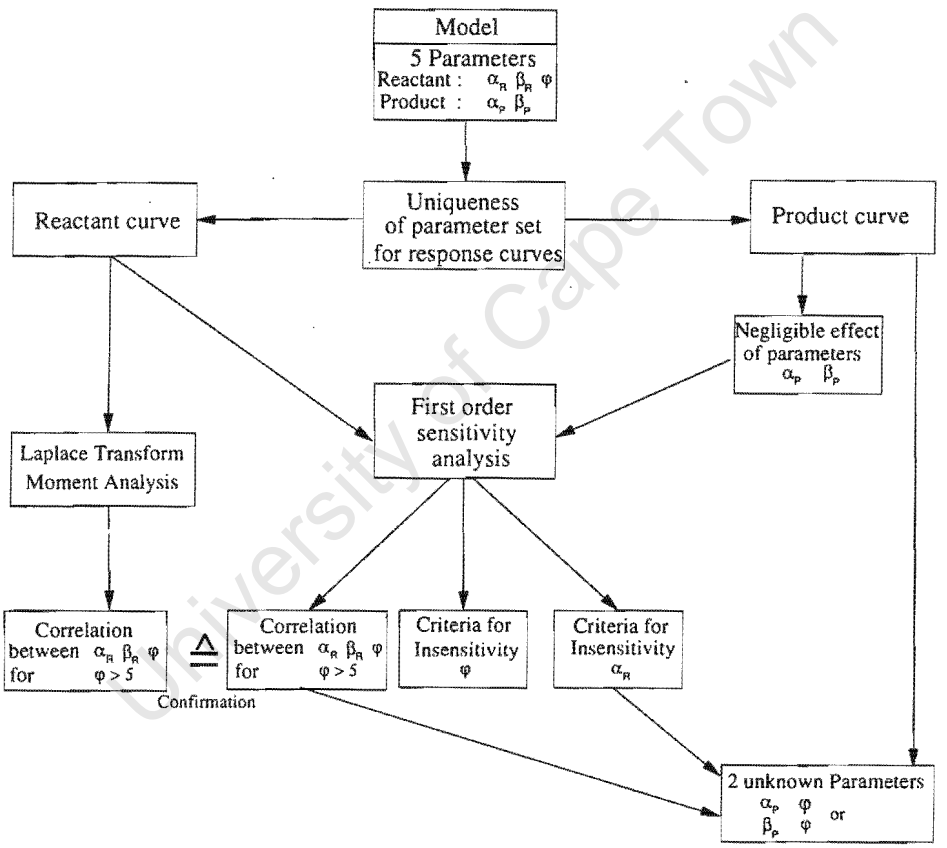

Figure 5.6: Methodology used for the investigation of the parameter uniqueness for the irreversible first order reaction $R \rightarrow P$.

In every parameter estimation problem the question of the uniqueness of a set of model parameters for given observations has to be clarified. In other words, can any other set of these model parameters describe the observations? Two questions hereby arise:

- Is there a correlation between the parameters? Can the model describe the observa-

tion with different model parameters, if this correlation is fulfilled. The number of measurable parameters is then reduced.

- When does a model parameter become insignificant and the response curve insensitive to this parameter ? In this case, the parameter can be eliminated from the model.

Figure 5.6 illustrates the methodology used in this section to answer these questions for the above outlined reaction model.

There are three parameters for the reactant concentration curve: α_R, β_R and φ. Since the continuum model is linear and reaction is not influenced by the product, the reactant curve is independent of the product concentration and the product parameters. The product curve, however, is dependent on the reactant concentration and the reactant parameters. This leads to five parameters for the product: Three reactant parameters $\alpha_R, \beta_R, \varphi$ and two product parameters α_P, β_P.

In a first step only product curves with negligible diffusion and adsorption, e.g. negligible product parameters α_P and β_P, are investigated. In this way, one can compare directly the information which can be extracted from both curves. One can then clarify, which response curve is more sensitive to the model parameters.

The reactant curve is analysed in two ways: Firstly, in order to find possible correlations between the model parameters, as hypothesised in Section 2.2.2.1 for large values of φ, a moment analysis is conducted. This result is confirmed by a first order sensitivity analysis. Secondly, the sensitivity analysis is used to establish criteria for the insensitivity of the reactant and product response curves towards model parameters.

Finally, product curves with significant adsorption and transport resistance of the product, are examined. Special cases for experiments with only two unknown parameters, but large values of the Thiele modulus φ, are discussed in detail.

5.3.2.1 Laplace Transform and moment analysis

The zero, first and second moment of the transient system can be calculated via the Laplace Transform for the reactant concentration. The solutions differ only in the nomenclature to those obtained by Schobert and Ma (1981a), Park and Kim (1984 a). The solution of the Laplace transform is:

$$\widetilde{C}_R(s) = \frac{1}{s + 1 + \beta_R \left(\xi \coth \xi - 1\right)} = \frac{1}{I(s)} \tag{5.39}$$

s is the Laplace variable and ξ is defined as

$$\xi = \sqrt{\frac{s + \varphi^2 \alpha_R}{\alpha_R}} \tag{5.40}$$

The limiting value of is $\xi(s = 0) = \varphi$.
The moments are calculated by the van der Laan's theorem. The zero moment of C_R is:

$$\mu_0 = \lim_{s \to 0} \tilde{C}_R(s) = \lim_{s \to 0} \frac{1}{I(s)} \tag{5.41}$$

The normalised first moment is:

$$\mu_1 = \lim_{s \to 0} \frac{\partial}{\partial s} \left(\tilde{C}_R(s) \right) = \lim_{s \to 0} \frac{I'(s)}{I^2(s)} \tag{5.42}$$

The second normalised central moment is:

$$\mu_2 = \lim_{s \to 0} \frac{\partial^2}{\partial s^2} \left(\tilde{C}_R(s) \right) = \lim_{s \to 0} \frac{I(s)''}{I(s)^2} - 2I(s)\mu_1^2 \tag{5.43}$$

The limiting values for $I(s)$ and its derivatives are:

$$I(0) = 1 + \beta_R \left(\varphi \coth \varphi - 1 \right) \tag{5.44}$$

$$I'(0) = \frac{\beta_R}{2\varphi\alpha_R} \left(-\frac{\varphi}{\sinh^2 \varphi} + \coth \varphi \right) \tag{5.45}$$

$$I''(0) = \frac{\beta_R}{2\varphi\alpha_R} \left(\frac{\coth \varphi}{\alpha_R \varphi \sinh^2 \varphi} - \frac{1}{\alpha_R \varphi^2 \sinh^2 \varphi} + \frac{\coth \varphi}{2\alpha_R \varphi^3} \right) \tag{5.46}$$

Question of uniqueness

If all moments for different sets of the model parameters α_R, β_R, φ are the same, then the concentration curves $C(t)$ should be identical. Since the moments only depend on $I(s)$ and its derivatives, it is sufficient to show that those equations can have multiple solutions for the model parameters. The first three moments, eq. 5.44 to 5.46, are strongly nonlinear. But this nonlinearity is only caused by the hyperbolic functions of the Thiele modulus. These hyperbolic functions have limiting values for large values of the Thiele modulus with $\varphi \gg 3$:

$$\lim_{\varphi \to \infty} \{\coth \varphi\} \to 1 \tag{5.47}$$

and

$$\lim_{\varphi \to \infty} \{\sinh^2 \varphi\} \to \infty \tag{5.48}$$

In general for values $\varphi \gg 3$ the nonlinear equations eq. 5.44 to 5.46 reduce to:

$$I(0) - 1 = \beta_R (\varphi - 1) \tag{5.49}$$

$$I'(0) = \frac{\beta_R}{2\varphi\alpha_R} \tag{5.50}$$

$$I''(0) = -\frac{\beta_R}{4\alpha_R^2\varphi^3} \tag{5.51}$$

It is evident that these equations are not independent of each other for large enough values of φ. This analysis holds true for any higher moments (without proof).

The condition for which different sets of parameters (with $\varphi \gg 3$) yield the same response curves are therefore:

$$\beta_R\varphi = const \tag{5.52}$$

$$\alpha_R\varphi^2 = const \tag{5.53}$$

For large values of the Thiele modulus one can hence only measure two lumped parameters.

In dimensional terms conditions of eq. 5.52 and 5.53 are equivalent to the lumped parameter $D_y K_c k_R = const$ and the intrinsic rate constant of the adsorbed molecules $k_R = const$.

5.3.3 Parameter sensitivity analysis

The integration of the PDEs with simultaneous calculation of the first order derivatives of the outlet concentration was achieved with the FORTRAN package PDASAC (Caracotsios and Stewart, 1995) using a method of lines procedure.

The resulting sensitivity functions $s_{ij}(\tau)$ for the component i and the parameter θ_j are defined as

$$s_{ij}(\tau) = \frac{\theta_j}{C_i}\frac{dC_i(\tau)}{d\theta_j} = \frac{dlnC_i(\tau)}{dln\theta_j} \tag{5.54}$$

The double logarithmic form of the sensitivity coefficient is essential, because concentration

and parameters may range over several orders of magnitude.

Plots of the parameter sensitivities versus time can be of considerable use (Caracotsios and Stewart, 1985). They are an elegant instrument to compare the effect of the parameters on the observed function and to show at what point of time the observed function is most sensitive. Secondly, they can reveal over-parameterisation of the model if the sensitivities are zero, or the sensitivities are linear dependent over the observed time range. This work concentrates on the latter, in order to clarify the question of parameter uniqueness and verify the result obtained from the moment analysis in the previous section.

5.3.3.1 Linear dependence of sensitivities

An unsophisticated approach for the check of linear dependent sensitivity functions can be chosen, when only three unknown parameters are involved. $s_{ij}(\tau)$ for j=1..3 are linearly dependent, if

$$\frac{s_{i3}(\tau)}{s_{i2}(\tau)} = a_i + b_i \frac{s_{i1}(\tau)}{s_{i2}(\tau)} \tag{5.55}$$

form a straight line. It means that the model parameters are correlated and the model is thus over-parameterised for the chosen set of parameters.

This is illustrated for the above described diffusion model. If the sensitivities are linearly dependent, one may establish a set of two correlations, for which the concentration curves $c_i(\tau)$ remain the same, when the model parameters are varied.

Since the two correlations (eq. 5.52 and 5.53) are already known from the moment analysis, similar power relations, eq. 5.56 and 5.57 were chosen with the difference that the two constants x_i and y_i are the unknown exponents of the correlation. (K_1 and K_2 are like in eq. 5.52 and 5.53, two arbitrary constants).

$$\left(\varphi_i^2\right) \alpha_i^{x_i} = K_1 \tag{5.56}$$

and

$$\left(\varphi_i^2\right) \beta_i^{y_i} = K_2 \tag{5.57}$$

In order to find the unknown exponents x_i and y_i and confirm the correlations found with the moment analysis a first order Taylor expansion is applied on the response curve $C_i(\tau)$:

$$\frac{\partial C_i(\tau)}{\partial \varphi_i^2} + \frac{\partial C_i(\tau)}{\partial \beta_i} \frac{\partial \beta_i}{\partial \varphi_i^2} + \frac{\partial C_i(\tau)}{\partial \alpha_i} \frac{\partial \alpha_i}{\partial \varphi_i^2} + Res = 0 \tag{5.58}$$

When neglecting the second order terms *Res* the relation

$$\frac{\partial C_i(\tau)}{\partial ln(\varphi_i^2)} = \frac{1}{x_i}\frac{\partial C_i(\tau)}{\partial ln\alpha_i} + \frac{1}{y_i}\frac{\partial C_i(\tau)}{\partial ln\beta_i} \tag{5.59}$$

can easily be shown.

The exponents x_i, y_i of the correlation conditions eq. 5.56, 5.57 can hence be found from the intercept with $a_i = 1/y_i$ and the slope $b_i = 1/x_i$ of eq. 5.55.

5.3.3.2 Parameter sensitivity of response curves

In many reactions, especially during cracking of hydrocarbons, light products are produced which diffuse relatively fast and exhibit no measurable adsorption effects. The two model parameters for the product α_P and β_P become in this case relatively large. The outlet concentration curves for these products are independent of those parameters and depend only on the model parameters of the reactant. Sensitivities of reactant and product curves can thus be directly compared.

In the following sections a sensitivity analysis is performed for the reactant and its light product. The following product model parameters are assumed:

1. *Carbon based response factor* $Rf = 1$
2. $\alpha_P = 100$
3. $\beta_P = 100$.

Sensitivity functions are calculated for outlet concentrations between C/C_0= 0.001..1, which is the experimental range of measurability.

9 sets with three different conversions X= 0.1, 0.5 and 0.9, and three different values for α_R 1, 0.01and 0.0001, are investigated. For each of these sets the Thiele modulus is varied from φ=50 to $\varphi\approx$1. Mass balances were checked and the validity of the response curves could be confirmed even for response curves with steep initial drop and a long tail at concentrations smaller 0.001, see for example parasens43 in Appendix I.

Each time a test for linear dependency is conducted by fitting a straight line through the sensitivity function obtained from eq.5.55. The degree of linearity is validated by the least square error and the correlation coefficient R^2. The intercept a_i and the slope b_i

are calculated from this fit. The results can be found in Appendix I. The corresponding plots of the sensitivity functions and linear dependency can be found on the CD-ROM in the Appendix F. The method exhibits numerically erratic behaviour, when the sensitivity coefficient for φ tends to zero.

The sensitivity functions for product and reactant are used to investigate the following:

- What are the experimental conditions to achieve an accurate parameter estimation, or the highest sensitivity? What is the influence of conversion on this condition?
- Confirmation of parameter correlation obtained from moment analysis. Are sensitivity functions linearly dependent?
- Are there criteria for the insensitivity of the response curves towards model parameters? When do sensitivity functions become zero for the entire time period?

5.3.3.3 Influence of conversion on parameter sensitivity ($\alpha_P = 100 = \beta_P$)

The most accurate parameter estimations can be achieved, when the response curves are the most sensitive to the parameters. It is hence of great interest for the experimentalist to analyse in which parameter regions sensitivities are the highest and at what times data points should be primarily collected.

Measuring the reactivity, adsorption and diffusion properties of the system for a given temperature and pressure without changing the particle size of the catalyst, leaves only two parameters that can be easily changed by the experimentalist: the flow rate F and the catalyst volume V_{cat}, or in dimensionless terms α_R and β_R. α_R is dependent only on the flow rate and can only be varied in a relatively small range, when considering the limitations of a recycle reactor. β_R depends on both experimental parameters with a greater range of variability and the possibility for the experimentalist to change β_R without changing α_R and φ.

The influence of β_R on the sensitivity functions for α_R and φ is thus investigated. This is equivalent to the investigation of the effect of the catalyst volume or conversion on the sensitivity with otherwise fixed parameters.

The effect of conversion on the reactant curve is demonstrated for a varying Thiele modulus and constant α_R in Figures 5.7.a and b with a conversion of $X = 90\%$ in Figure 5.7.a and $X = 10\%$ in Figure 5.7.b. The respective response curves for the product are shown

in Figures 5.8.a and b (with the product parameters $\alpha_p = \beta_P = 100$). The corresponding sensitivity functions are to be found in Figures 5.9.a and b and 5.10.a and b.

It should be noted that the area μ_0 underneath the concentration curves in a non-logarithmic plot are the same at constant conversion X with

$$X = 1 - \mu_0 \tag{5.60}$$

Description response curves

The reactant curve in Figure 5.7.a approximates a straight line at $\varphi = 50$ with an intercept close to one, but becomes increasingly skewed for smaller values of φ with a steeper decline of concentration in the initial region and stronger tailing in the long time solution. At a lower conversion in Figure 5.7.b, product response curves can be represented by a straight line for smaller values of the Thiele Modulus ($\varphi > 10$). A straight line in a semi-logarithmic plot means that the concentration curve can be described by a simple exponential function with only one time constant. An increase of conversion leads, in such a case, to a more complex system with numerous time constants. A similar conclusion can be drawn for the product curve in Figure 5.8.a and b for which the concentration curves become better separable at higher conversions when comparing the responses for $\varphi = 10$.

Sensitivity functions

$s_{R,\alpha}$ and $s_{P,\alpha}$

The reason for this degeneration of the system response can be found in the sensitivity function of α_R in Figure 5.9.a. The sensitivity function for the reactant goes to zero in the entire time range, if the Thiele modulus is high and the conversion low enough. Increasing the conversion level leads to higher absolute values of the sensitivity function $s_{R,\alpha}$. The trend in $s_{R,\alpha}$ is enhanced in the long time region and only deviates substantially from zero in the initial region, when the Thiele modulus is low enough. In a physical sense, this can be interpreted as an insignificant effect of adsorption at initial times of the pulse experiment, where the reaction is so fast that the process is dominated by diffusion and contact time of the fluid and the catalyst. The opposite, however, holds true for the product sensitivity functions $s_{P,\alpha}$, which indicate larger effects of α_R on the product curves at initial times, that vanish at longer times. The sensitivity of the product curve for α_R is again enhanced

by increased conversion, which is best observed in Figure 5.9.b for a Thiele modulus of ten.

s_{R,φ^2} and s_{P,φ^2}

The effect of conversion on the sensitivity functions, as shown in Figure 5.10, for the square of the Thiele modulus φ^2 is more diverse. The sensitivity of both reactant and product curve is in general enhanced by increased conversion. But for very low values of φ this enhancement of sensitivity for reactant and product curve becomes very small, see concentration curves with $\varphi = 1, 2$. At these values the sensitivity function for the reactant s_{R,φ^2} tends to zero, whereas the sensitivity function for the product s_{P,φ^2} tends to one. A more detailed discussion regarding the consequences for the concentration curves is given in Section 5.3.3.5.

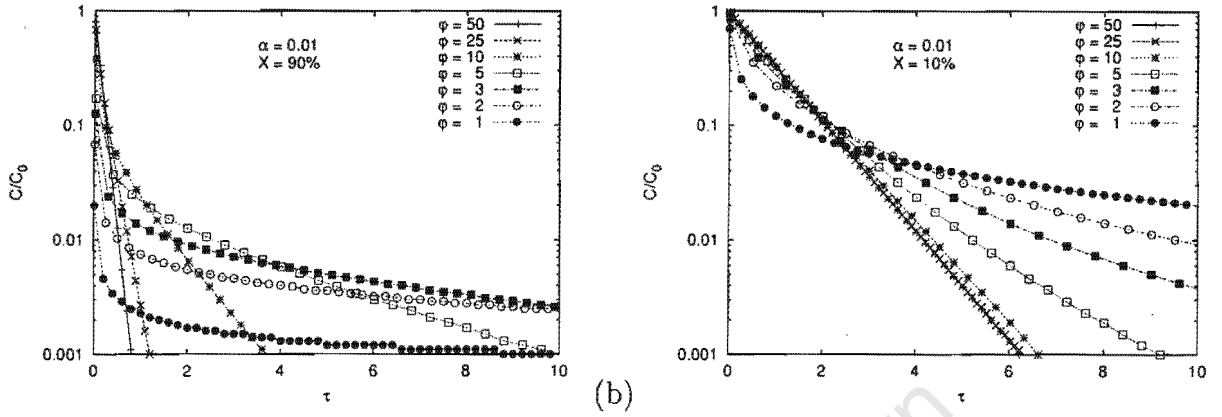

Figure 5.7: Response curve of reactant. Model parameter α=0.01, Figure (a): conversion $X = 90\%$, Figure (b) conversion $X = 10\%$

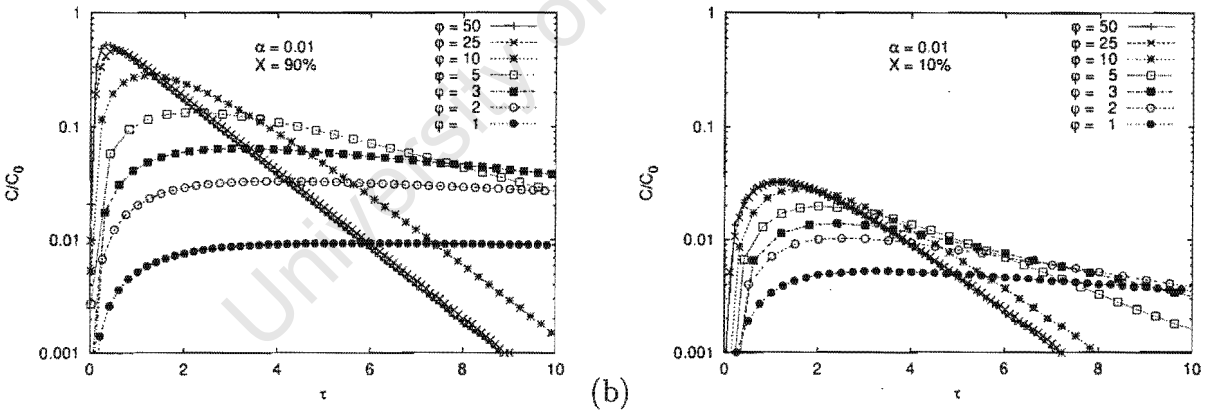

Figure 5.8: Response curve of product. Model parameter α=0.01, Figure (a): conversion $X = 90\%$, Figure (b) conversion $X = 10\%$. Product parameters: $\alpha_P = \beta_P = 100$, Carbon based response factor $Rf = 1$

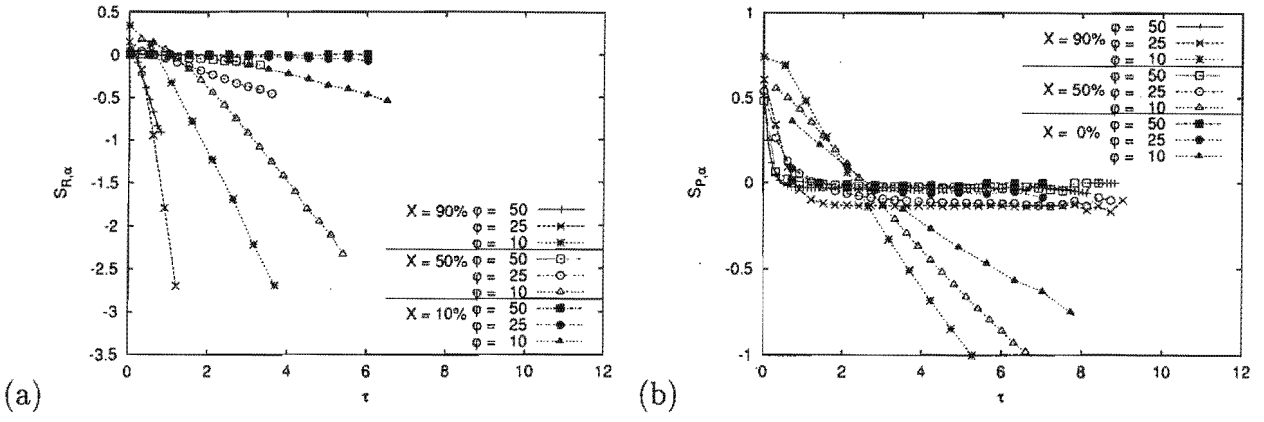

Figure 5.9: Effect of conversion on the sensitivity coefficient $s_{i\alpha}$ in the reactant (Figure a) and product (Figure b) response curve at different values of the Thiele modulus.

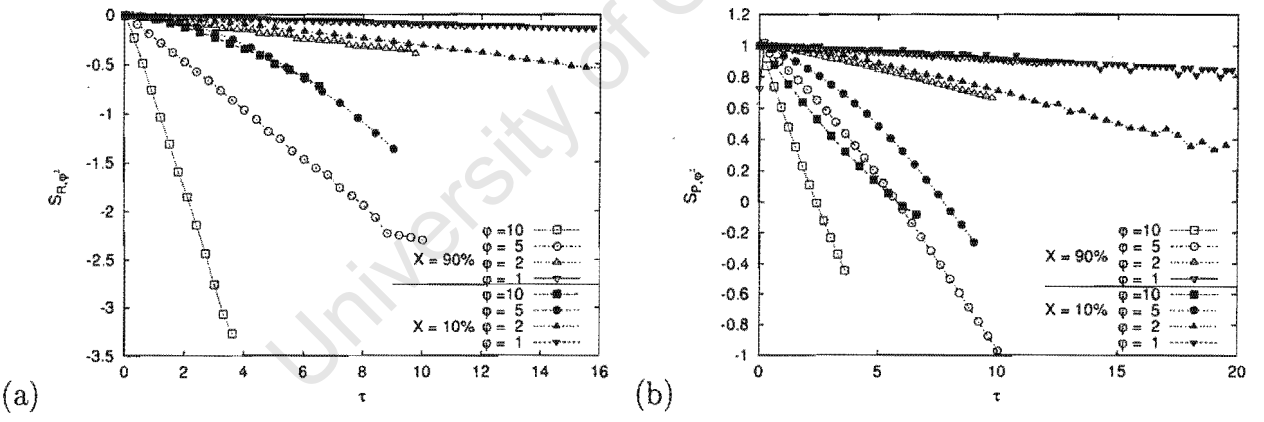

Figure 5.10: Effect of conversion on the sensitivity coefficient $s_{i\varphi^2}$ in the reactant (Figure a) and product (Figure b) response curves at different values of the Thiele modulus.

5.3.3.4 Response curves with fast reaction/slow diffusion (large φ)

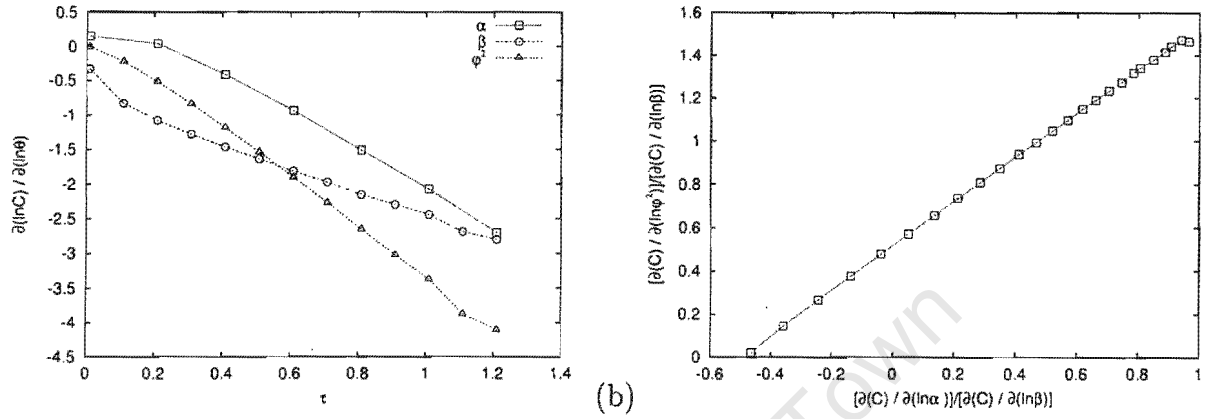

Figure 5.11: Test for linear dependency of sensitivity functions according to eq. 5.59 for reactant model curve with Thiele modulus 25. Model Parameters see I.1 File parasens31.

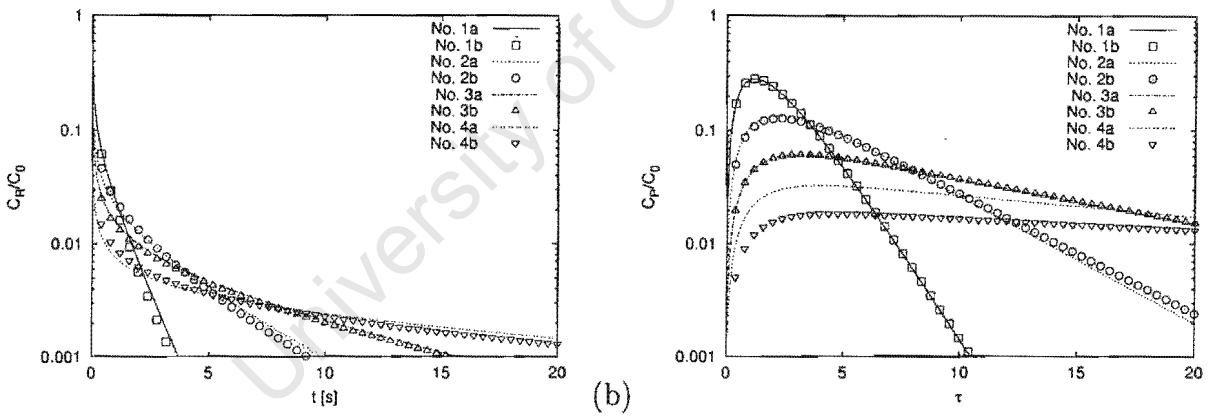

Figure 5.12: Good agreement of response curves, even when Thiele modulus is changed by factor 10. Model parameters of the reactant according to Table 5.4. Product parameters: $\alpha_P, \beta_P = 100$, Carbon based response factor $Rf = 1$, Conversion 90%

The existence of lumped model parameters was demonstrated in Section 5.3.2.1 for large values of the Thiele modulus, see eq. 5.52 and 5.53. This is to be confirmed by the sensitivity analysis.

Figure 5.11.a shows the three sensitivity functions for a reactant curve with a Thiele Modulus of 25. The sensitivity functions are of the same order of magnitude, but they show a linear dependency towards each other in Figure 5.11.b according to eq. 5.55. The straight

Table 5.4: Model parameters used in Figure 5.12

No.	α_R	β_R	φ	
1a	10^{-2}	1.0	10	actual
1b	10^{-4}	0.1	100	fitted
2a	10^{-2}	2.25	5	actual
2b	$9.55 \cdot 10^{-5}$	0.167	50	fitted
3a	10^{-2}	4.467	3	actual
3b	$9.55 \cdot 10^{-5}$	0.317	30	fitted
4a	10^{-2}	8.375	2	actual
4b	$5.33 \cdot 10^{-5}$	0.437	20	fitted

line in Figure 5.11.b has an intercept a_i of 0.5 and a slope b_i of 1.0. With $x_i = 1/b_i = 1.0$ and $y_i = 1/a_i = 2.0$ the correlation in eq. 5.56 results to $\varphi^2\alpha_R = K_1$ and the correlation in 5.57 gives $\varphi_R^2\beta_R^2 = K_2$ (or $\varphi\beta_R = K_2'$). This finding is identical to the one from the moment analysis in Section 5.3.2.1.

The values of the exponents a_i, b_i are compiled in Appendix I, where $a_i = 0.5$ and $b_i = 1.0$ for both the reactant and the product curve can in general be established for values of φ greater than 10. Deviations to these values are observed, if the sensitivity functions for φ^2 or α become very small.

Analysis for $\varphi < 10$

One weakness of the above outlined sensitivity analysis is that a simple first order Taylor analysis becomes too inaccurate at values of the Thiele modulus $\varphi < 10$, in order to reflect the more complex parameter dependency. Additional to the first order sensitivities, higher order terms would be required in this case for an exact Taylor analysis.

In Table 5.4 four sets of model parameters are listed with values of $\varphi = 10, 5, 3, 2$. The reactant and product concentration curves are plotted in Figure 5.12. These response curves are fitted by alternative concentration curves with a ten fold higher φ. The corresponding values of α_R and β_R are found by simple iteration, see Table 5.4. The comparison between the response curves and their counterparts with ten fold higher φ in Figure 5.12 shows almost identical curves, although the values of α_R change by two orders of magnitude and values for β_R and φ are within one order of magnitude. This illustrates that the model parameters -accepting a relatively small experimental error- are indeed not unique. This even holds true for $\varphi = 3$. For a Thiele modulus of two, however, the product curves deviate,

while the response of the reactant shows no significant difference. An estimation of all three parameters should here be possible, if both reactant and product curve are simultaneously fitted.

5.3.3.5 Insignificance of φ / Adsorption control for (small α)

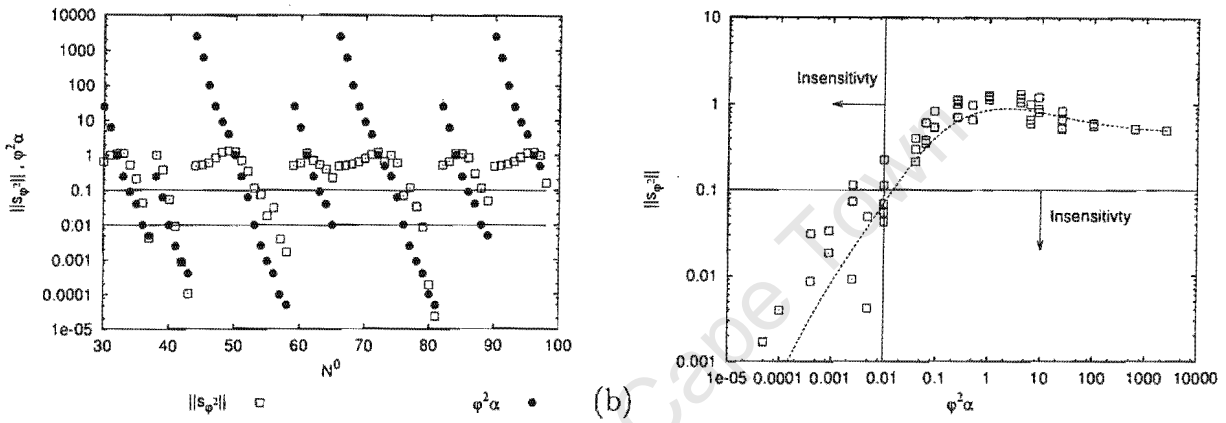

Figure 5.13: Criterion for insensitivity with respect to the Thiele modulus φ. Figure (a): Number of sensitivity test (Appendix I) versus $\|s_{R,\varphi^2}\|$ and versus $\alpha\varphi^2$. Figure (b) Correlation function $\alpha\varphi^2$ versus integral sensitivity $\|s_{R,\varphi^2}\|$. Limiting values for insensitivity $\|s_{R,\varphi^2}\| < 0.1$ and $\alpha\varphi^2 > 0.01$.

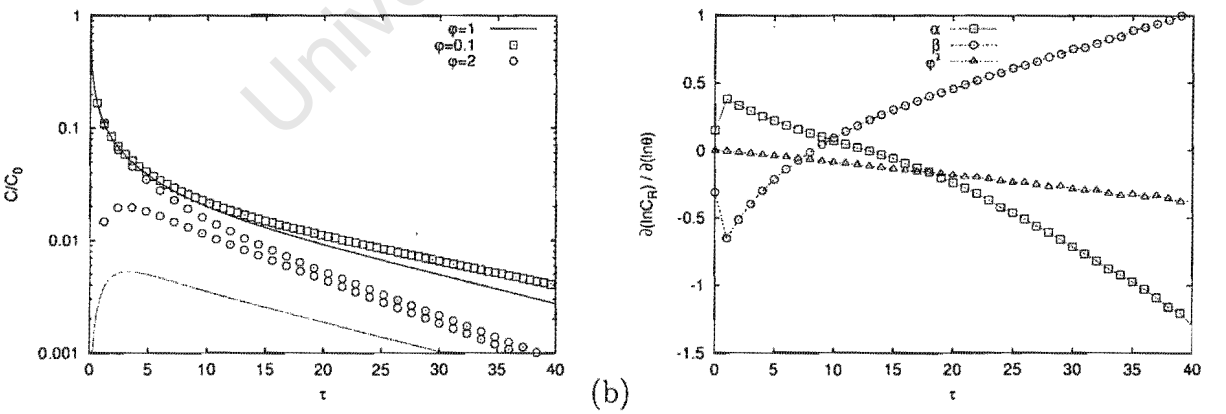

Figure 5.14: Analysis of sensitivity test for file parasens65 (Appendix I) Figure (a): Reactant and product response curves with $\alpha = 0.01$, $\beta = 0.355$, $\varphi = 1$ and variations of φ with values of 0.1 and 2.0. Figure (b): Sensitivity functions for reactant curve, $s_{R,\varphi^2}(\tau) \rightarrow 0$

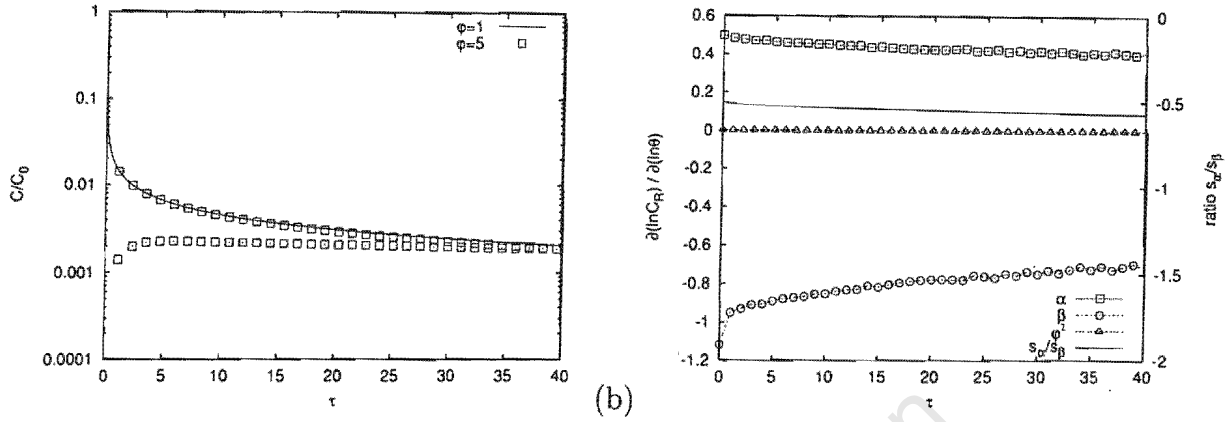

Figure 5.15: Figure (a): Reactant and product response curves with $\alpha = 0.0001$, β, φ as in Figure 5.14 and increased value of φ= 5.0. Figure (b): Sensitivity functions for reactant curve, $s_{R,\varphi^2}(\tau) \rightarrow 0$.

It was demonstrated in Section 5.3.3.3 that reactant sensitivity functions $s_{R,\varphi^2}(\tau)$ with respect to φ^2 can tend to zero. But this indicates that changing the reactivity in the Thiele modulus does not alter the reactant concentration curve. This is of course not true, since it leads to a change of conversion and therefore necessarily to a different response curve. The question is rather whether this difference is measurable. In the following a criterion is established, for which the reactant sensitivity with respect to φ^2 reaches a certain lower limit. The consequence of this insensitivity for the parameter measurability is then discussed:

Criterion

In order to establish a criterion for which $s_{R,\varphi^2}(\tau)$ tends to zero, it is useful to calculate a relative integral sensitivity $\|s_{R,\varphi^2}\|$:

$$\|s_{R,\varphi^2}\| = \frac{\int s^2_{R,\varphi^2}(\tau)d\tau}{\int s^2_{R,\alpha}(\tau)d\tau + \int s^2_{R,\beta}(\tau)d\tau + \int s^2_{R,\varphi^2}(\tau)d\tau} \tag{5.61}$$

An empirical analysis reveals that the reactant response curve becomes relatively independent of φ, if the integral sensitivity $\|s_{R,\varphi^2}\|$ is smaller than 0.1.

It was already noted in Section 5.3.3.3 that changing the value of β_R with α_R, φ being constant, does not significantly alter the relative insensitivity of the reactant towards φ^2. A criterion should thus be independent of β_R. The term $\alpha\varphi^2$ - already known from the

correlation eq. 5.53 - was used to find a relation between the model parameters and the integral sensitivity. The values of $\alpha\varphi^2$ and $\|s_{R,\varphi^2}\|$ for the numerical sensitivity runs in Appendix I are summarised in Figure 5.13.a. The correlation between $\alpha\varphi^2$ and $\|s_{R,\varphi^2}\|$ is shown in Figure 5.13.b. The scatter of the data points suggests that this correlation can only be considered a rough approximation of the integral sensitivity. It however reveals that $\|s_{R,\varphi^2}\|$ becomes smaller than 0.1, if the value of $\alpha\varphi^2$ is approximately smaller than 0.01.

A criterion for which $s_{R,\varphi^2}(\tau)$ tends to zero is therefore:

$$\text{if } \alpha\varphi^2 < 10^{-2} \text{ then } s_{R,\varphi^2}(\tau) = \frac{\partial \ln C_R(\tau)}{\partial \ln \varphi^2} \to 0 \tag{5.62}$$

Interpretation of $s_{R,\varphi^2}(\tau) \to 0$

In the sense of a Taylor expansion the first order derivative s_{R,φ^2} is only an approximation of the sensitivity in the region of the parameter used. The region for which this approximation is valid cannot be quantified directly without the calculation of higher derivatives. $s_{R,\varphi^2}(\tau) \to 0$ alone can hence not serve as a proof for insensitivity. But since a criterion for $s_{R,\varphi^2}(\tau) \to 0$ was established for the entire parameter region, a change of φ will not affect the reactant curve significantly, if $\alpha\varphi^2$ remains small enough.

This is demonstrated in Figure 5.14. The analysis (parasens65, Appendix I) shows that the sensitivity function s_{R,φ^2} is relatively small compared to those of α and β. The value of $\alpha\varphi^2$ is 0.01, but the integral sensitivity is $\|s_{R,\varphi^2}\| = 0.23$ (see Figure 5.14.a, Run 65) slightly above the criterion for insensitivity. The insensitivity is confirmed, when the reactant response curve is compared to that with a ten times smaller φ, but otherwise same model parameters. The concentration curve for $\varphi = 0.1$ is slightly above the original curve at longer times, which is in perfect agreement to the negative values of s_{R,φ^2}. These small deviations are from an experimental view point well within the expected error margin. It should be noted, however, that this deviation causes a decrease of conversion from 10% to 0.1%, which is also reflected in the vanishing of the product for the smaller value of φ.

If the Thiele modulus, on the contrary, is increased by a factor of two, the concentration curves differ substantially.

For a response curve with a smaller value of α, the criterion for insensitivity to the Thiele modulus in eq.5.62 should be met also for larger values of φ. This is illustrated in Figure 5.15 with the sensitivity analysis test parasens57, Appendix I. The same parameters as for

the original response curves in the previous Figure 5.14 are used, with the difference that α is a hundred times smaller, $\alpha = 0.0001$. The integral sensitivity $\|s_{R,\varphi^2}\|$ is with 0.004 (see Figure 5.14.a, Run 57) very small. This is confirmed by the plot of the sensitivity function in Figure 5.15.b. In contrast to the response curve with α=0.01 an increase of the Thiele modulus by a factor 5 still leads here to a reactant curve that is almost identical to the original curve. The slight decrease of concentration is consistent with the small but negative values of the sensitivity function.

When furthermore the response curve with an original value of $\varphi = 1$ can be approximated by a larger Thiele modulus of $\varphi \gg 3$, the correlations eq. 5.56 and 5.57 as outlined in Section 5.3.3.4, should hold. This requires the linear dependency of the sensitivity functions. Because $s_{R,\varphi^2}(\tau)$ is close to zero, $s_{R,\alpha}(\tau)$ and $s_{R,\beta}(\tau)$ should directly correlate with each other, so that the ratio of the sensitivity functions is constant. The sensitivities and their ratio are plotted in Figure 5.15.b. The ratio of the sensitivities shows only a deviation of 10%, which is an indication of a strong correlation between the model parameters α_R and β_R. This leads to a further degeneration of the model, where only one lumped parameter α_R/β_R^2 can be estimated from the reactant curve only. The same conclusion obviously also holds true for inert experiments without reaction and $\varphi = 0$.

The reason for this degeneration of the parameter measurability lies in the strong adsorption which overshadows a slow reaction. This phenomena is best visible in the extreme case of the product curve in Figure 5.15.a. The product curve rises quickly to the concentration level 0.002 and only declines extremely slowly. With very small values of α_R the large adsorption capacity in the catalyst causes long retention times of the reactant with excessive tailing in the long time region. A slow reaction in this long time region will therefore not be accurately measurable in the concentration curve of the reactant.

It should finally be remarked that mass balances for all concentration curves were verified. From an experimental view point however, it would be difficult to ensure the correctness of the mass balance, which is important when normalising the concentration curves.

5.3.3.6 Absence of adsorption effects (large α_R)

It was demonstrated in Section 5.3.3.3 that the reactant sensitivity function with respect to α_R, $s_{R,a}(\tau)$, can tend to zero. Similarly to the sensitivity analysis with respect to φ^2 one can find a criterion for which $s_{R,\alpha}(\tau)$ tends to zero. For the quantification of an overall

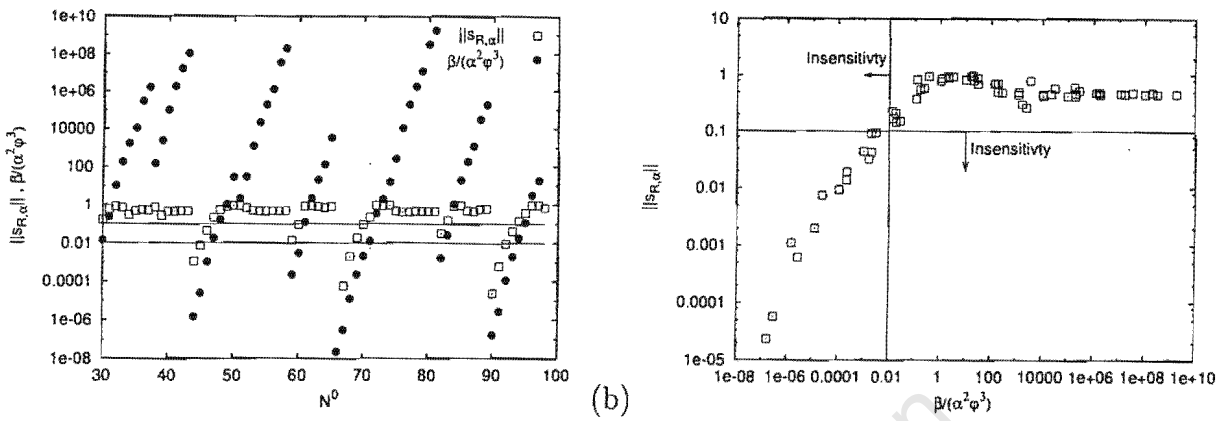

Figure 5.16: Criterion for insensitivity with respect to α_R. Figure (a): Number of sensitivity test (Appendix I) versus $\|s_{R,\alpha}\|$ and versus $\frac{\beta_R}{\alpha_R^2\varphi^3}$. Figure (b) Correlation function $\frac{\beta_R}{\alpha_R^2\varphi^3}$ versus integral sensitivity $\|s_{R,\alpha}\|$. Limiting values for insensitivity $\|s_{R,\alpha}\| < 0.1$ and $\frac{\beta_R}{\alpha_R^2\varphi^3} < 0.01$.

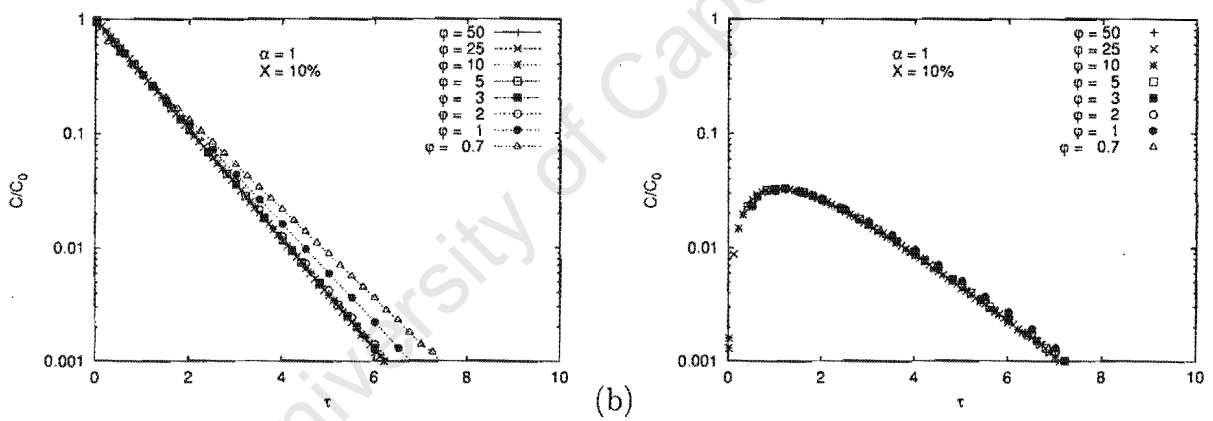

Figure 5.17: Response curve of reactant and product. Model parameter $\alpha_R = 1$, $\mu_0 = 0.9$. criterion for insensitivity of α_R is fulfilled for curves with $\varphi \geq 3$.

sensitivity, a relative integral sensitivity $\|s_{R,\alpha}\|$ is defined as:

$$\|s_{R,\alpha}\| = \frac{\int s_{R,\alpha}^2(\tau)d\tau}{\int s_{R,\alpha}^2(\tau)d\tau + \int s_{R,\beta}^2(\tau)dIl\tau + \int s_{R,\varphi^2}^2(\tau)d\tau} \tag{5.63}$$

Values of the integral sensitivity $\|s_{R,\alpha}\|$ smaller than 0.1 proved in an empirical analysis to be a good indication for an insensitivity of the response curves towards the parameter α_R.

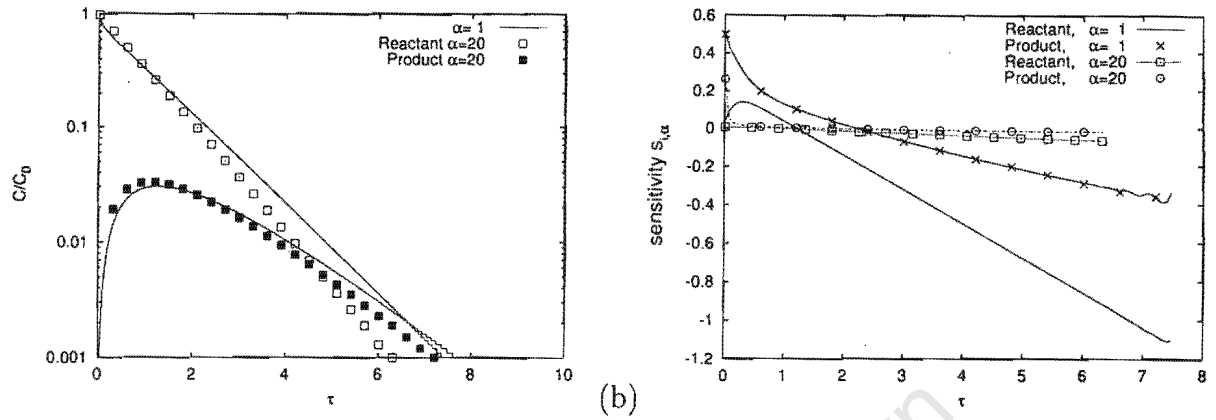

Figure 5.18: Examination of sensitivity for α_R for response curve presented in Figure 5.17 with φ=0.7. When α_R is increased to 20, the criterion 5.64 is fulfilled; only one time constant measurable.

Criterion for $s_{R,\alpha}(\tau) \to 0$

In contrast to the sensitivity function for φ^2, it was already noted in Section 5.3.3.3 that changing the value of β_R with α_R, φ being constant, does significantly alter the relative insensitivity of the reactant towards α_R. A criterion should thus be dependent of β_R. As a correlation parameter $\frac{\beta_R}{\alpha_R^2\varphi^3}$ was intuitively found from the limiting second moment term in eq. 5.51. The values of $\frac{\beta_R}{\alpha_R^2\varphi^3}$ and $\|s_{R,\alpha}\|$ for the numerical sensitivity simulations in Appendix I are summarised in Figure 5.16.a.

Figure 5.16.b shows a good correlation between $\frac{\beta_R}{\alpha_R^2\varphi^3}$ and $\|s_{R,\alpha}\|$. The sensitivity $\|s_{R,\alpha}\|$ becomes smaller than 0.1, if the value of $\frac{\beta_R}{\alpha_R^2\varphi^3}$is below 0.01. The criterion for insensitivity is hence:

$$\text{if } \frac{\beta}{\alpha^2\varphi^3} < 10^{-2} \text{ then } s_{R,\alpha}(\tau) = \frac{\partial \ln C_R(\tau)}{\partial \ln \alpha} \to 0 \tag{5.64}$$

This implicates that adsorption is best measured with larger values of β_R, e.g. with increased catalyst volume and thus increased conversion.

Interpretation of sensitivity function and response curves

When the system response is not affected by adsorption of the reactant, e.g. $s_{R,\alpha}(\tau)$ tends to zero, the reactant response curve exhibits a straight line with an intercept of one. This is shown in Figure 5.17. The reactant curve can thus be described by an exponential function

$\frac{C(\tau)}{C_0} = \exp(-\tau/tc)$ with only one time constant tc, which is identical to the zero moment μ_0 given by eq. 5.49. In the case of the insensitivity for φ^2, the product curves differed while reactant curves overlapped when varying φ. This is in contrast to the case of insensitivity for α_R, where both reactant and product curves become insensitive towards α_R.

The criterion of eq. 5.64 is validated with the sensitivity analysis test for parasens73 (see Appendix I), which has the smallest Thiele modulus of 0.7 and thus the highest sensitivity for α_R in Figure 5.17. The integral sensitivity $\|s_{R,\alpha}\|$ is, as shown in Figure 5.16.b, 0.95 and is thus of comparable magnitude to the sensitivity for β_R and φ_R. The effect of increasing α_R by a factor 10, while keeping β_R and φ_R constant is investigated in Figure 5.18. The concentration initially increases for both reactant and product and decreases in the long time region. This is consistent with the initial positive sensitivity function (for $\varphi = 1$), which becomes negative in the long time region. The reactant and product sensitivity function is approximately zero for the entire time, when α_R is increased to 20. The correlation parameter $\frac{\beta_R}{\alpha_R^2\varphi^3}$ is hereby decreased by a factor 400 to 0.005 and is therefore well within the region of $\|s_{R,\alpha}\| < 0.1$.

If for $s_{R,\alpha}(\tau) \to 0$ the product curve does not exhibit any contribution of adsorption itself, e.g. $\alpha_P \ll 1$, no more information can be extracted from the concentration curve of the product. Since $1 - \mu_0$ is nothing else but the conversion at steady state, a pulse experiment cannot, in this case, deliver more information than a simple steady state experiment. It is in the same sense impossible to distinguish, whether the system is in a region of strong diffusion limitation $\varphi \gg 3$ or without any diffusional limitations.

5.3.4 Product analysis with diffusion limitation($\varphi \gg 3$) and large α_R

It was demonstrated in the previous section that a pulse experiment, which lacks the contribution of adsorption to the system dynamics, does not offer any advantage over a simpler steady state experiment. In both cases only conversion can be measured, with the consequence that the terms for diffusion, adsorption and reaction can not be separated.

Imagine a case, for which the product exhibits a dynamic behaviour caused by adsorption, while adsorption dynamics from the reactant side can be neglected. The subsequent discussion investigates the use of possible product adsorption for parameter estimation. The special case for a fast reaction with slow diffusion ($\varphi \gg 3$) and large α_R is investigated. As

will be shown, this special case is applicable to the system of cumene cracking studied in this work. Important conclusions from the previous sections can be summarised as follows:

1. **Large α_R (Section 5.3.3.6):** The adsorption dynamics of the reactant are insignificant. The only information that can be extracted from the reactant curve is the conversion $X = 1 - \mu_0$, which is identical to the area under the product curve. *It can hence be concluded that only the product curve has to be analysed for a parameter estimation.*

2. $\varphi \gg 3$ **(Section 5.3.3.4):** Reactant concentration curves with large α_R are unchanged, if the parameters β_R and φ are varied in such a way that the product $\beta_R\varphi$ remains constant, e.g. same conversion:

$$\beta_R\varphi = const \tag{5.65}$$

3. **This leaves four unknown parameters:** β_R, β_P, α_P and φ

Point 2 is not valid for small values of α_R. In such a case the product $\alpha_R\varphi^2$ has to remain constant, to ensure an unchanged response curve for varying parameters, see Section 5.3.3.4. Thus a reactant system of initially three independent parameters α_R, β_R and φ is reduced to two lumped parameters.

Analogous to the finding for the reactant, one can imagine for the case of product adsorption that the system of four parameters is over-parameterised, e.g. large values of φ should as well here lead to a "lumping" of the model parameters. One can try to reduce this problem and intuitively find a correlation between α_P and β_P, which is similar to the term $\alpha_R\varphi^2 = const$ and which is therefore an analogy to the findings for the reactant. For such a possible correlation $\alpha_P\varphi^{*2} = const$, one can compare the two reaction terms in the mass balance for the macropores, which are for the reactant $\varphi^2\alpha_R C_R$ and for the product $C_R\varphi^2\frac{\beta_R}{\beta_P}\alpha_P$, see eq. 5.28 and eq. 5.29, pg. 71. φ^* would thus have to be $\varphi^* = \varphi\sqrt{\frac{\beta_R}{\beta_P}}$.

In order to achieve same product concentration curves with varying model parameters one has to additionally preserve a similarity in the boundary condition. This is achieved, if *the ratio between reactant and the product diffusivity* $\frac{\beta_R}{\beta_p}$ *is constant*:

$$\frac{\beta_R}{\beta_P} = const \tag{5.66}$$

With a constant ratio of $\frac{\beta_R}{\beta_p}$, φ^*can be written as $\varphi^* = \varphi \cdot const.$ The following simple correlation can hence be introduced:

$$\alpha_P \varphi^2 = const \tag{5.67}$$

Table 5.5: Model parameters for Figure 5.19

φ	β_R	β_P	α_P	$\beta_R\varphi$	$\frac{\beta_R}{\beta_P}$	$\alpha_P\varphi^2$
20	0.01	0.01	0.01	0.2	1	4
200	0.001	0.001	0.0001	0.2	1	4

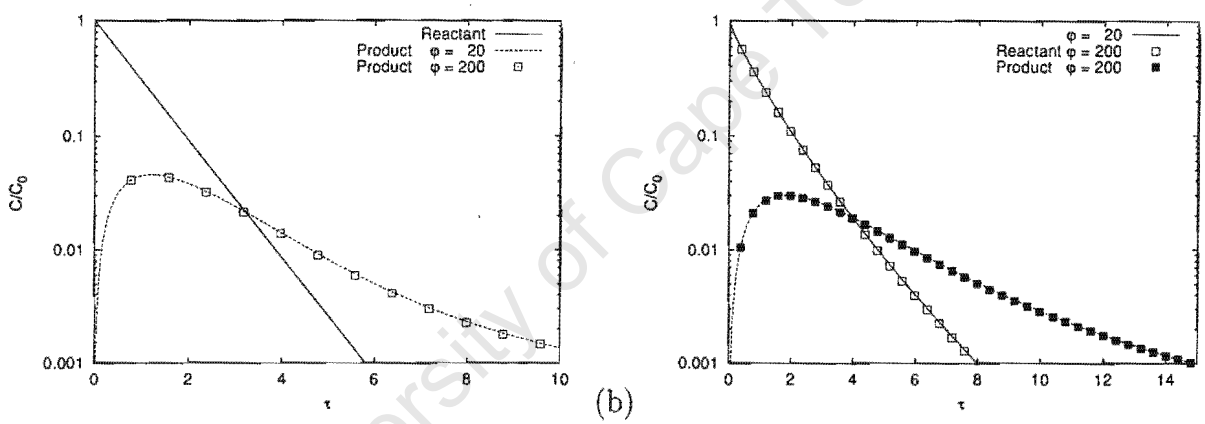

Figure 5.19: Verification of the correlation between reactant and product parameters. Model parameters from 5.5: (a) Negligible reactant adsorption dynamics, (b) with reactant adsorption dynamics

The system response curves should therefore be the same for any variation of the four model parameters, if the following four conditions are fulfilled: $\varphi \gg 3$, eq. 5.65, eq. 5.66 and eq. 5.67. This finding is validated in Figure 5.19 for a system with negligible reactant adsorption dynamics $\alpha_R = 1$. The model parameters are given in Table 5.5. The reactant and the product response curves are calculated for two parameter sets with values of Thiele modulus φ differing by a factor 10. β_R, β_P, α_P are changed according to the correlations eq. 5.65, eq. 5.66 and eq. 5.67 with the consequence that the response curves are identical. This confirms the above derived correlations.

The conclusion can be extended to the case, where the adsorption dynamics of the reactant become important. When the fifth parameter α_R is introduced, the additional

correlation $\alpha_R\varphi^2 = const$ can ensure that the response curves remain unchanged. This is demonstrated in Figure 5.19.b with the same model parameters as above, but with $\alpha_R = 0.001$ for $\varphi = 20$ and $\alpha_R = 0.00001$ for $\varphi = 200$. The values of the constants for the four correlations are for both parameter sets the same, which results in identical response curves.

Consequence for parameter estimation of systems with $\varphi \gg 3$, large α_R

The above outlined system of a product response curve with $\varphi \gg 3$ and large α_R is sufficiently described by three correlation functions consisting of four parameters. If one of the four model parameters β_R, β_P, α_P or φ is known a priori, the remaining three parameters are thus at least theoretically uniquely determined by the product response curve. One could hence determine all four parameters, if for example β_P is measured by a second experiment. In the case of cumene cracking to benzene and propene, the additional measurement of the benzene diffusivity with a pulse experiment of pure benzene would have to be conducted, in order to estimate the remaining parameters.

The subsequent discussion will deal with the validity of the above drawn conclusion, if the parameter estimation is complicated by a certain experimental error.

Table 5.6: Model parameters for Figure 5.20

No.		φ	β_R	$\frac{\beta_P}{\beta_R}$	α_P
1	original	20	0.01	1	0.01
2	fitted	20	0.01	10	0.05
3	original	20	0.1	1	0.01
4	fitted	20	0.1	0.1	0.0011
5	bad fit	20	0.1	10	0.05
6	bad fit	20	0.01	0.1	0.0011

Two original product curves and their approximating curves are shown in Figure 5.20 with model parameters listed in Table 5.6. Product curve (1) has a value for β_R of 0.01. Product curve (3) has a ten times larger value $\beta_R = 0.1$. Both original curves have the same value for φ, α_P. The ratio of $\frac{\beta_P}{\beta_R} = 1$ is the same for both curves. The system, which generates curve (3), can hence be interpreted as being identical to that of curve (1), except that the catalyst volume is increased by a factor ten.

One can now try to approximate these original curves with a response curve of unchanged parameters φ and β_R but a ten times larger or smaller ratio β_P/β_R. In order to find an

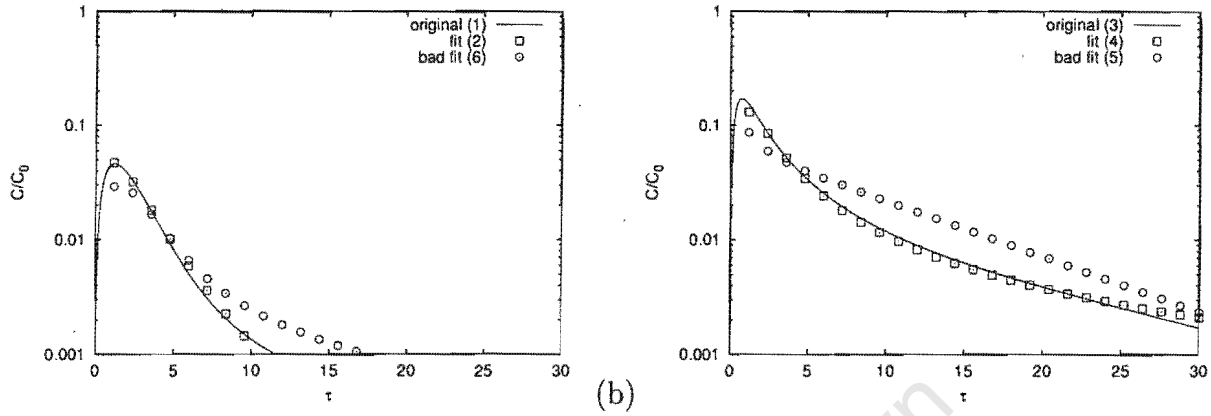

(a) (b)

Figure 5.20: Comparison of product curves (1) or (2) with their best approximation (2) or (4), when $\frac{\beta_P}{\beta_R}$ deviates by factor then. Figure (a) $\beta_R = 0.01$, Figure (b) $\beta_R = 0.1$ ($\hat{=}$10x more catalyst). Curve (6) is wrong fit with parameter estimates from (4). Curve (5) is wrong fit with parameter estimates from (2).
Model parameters listed in Table 5.6.

optimised approximation to the original curve, the remaining parameter α_P is used as a fitting parameter. It is clearly shown in Figure 5.20 that both original curves can be well approximated. The original curve (1) can be fitted by curve (2) with a ten times larger ratio of β_P/β_R. Curve (3) with a ten times larger amount of catalyst can be well approximated by curve (4) with a ten times smaller ratio of β_P/β_R. The deviations from the original response curves are in both cases well below the expected experimental error. It is hence not possible to accurately estimate three parameters from only one experiment, as it was suggested from the theoretical considerations mentioned above.

It is however not possible to approximate simultaneously curve (1) and curve (3), which differ only in their amount of catalyst. This is shown with curve (5) and curve (6): In curve (5) the fitting parameters β_P/β_R and α_P are taken from curve (2). Although these parameters led to a good approximation of curve (1), they cannot be used at the same time to fit curve (3), which has a ten times larger amount of catalyst but same Thiele modulus as curve (1). The large deviation between curve (3) and (5) is shown in Figure 5.20.b. In the same way parameters β_P/β_R and α_P, which are taken from curve (4), do not lead to a good approximation of curve (1).

One can therefore conclude that it should be possible to accurately measure three of the four unknown model parameters, if two experiments with substantially different mass

of catalyst (different β_R and β_P) are conducted.

Special case of Knudsen diffusion

As an alternative to the parameter estimation from product curves with different masses of catalyst, one can estimate the model parameters, if a second parameter, the ratio of β_P/β_R, is known a priori. This ratio is equal to the ratio between product and reactant diffusivity. In some special cases like the Knudsen diffusion regime, see pg. 4, a good approximation of this ratio should be possible. It should, however, be noted that the validity of this assumption nevertheless has to be verified by experiments using different amounts of catalyst, since a good model fit of the experimental response curve cannot guarantee the validity of this assumption from one experiment only.

5.3.5 Conclusion

It was shown that an accurate simultaneous estimation of all diffusion, adsorption and reaction parameters is not possible from one pulse experiment.

This inaccuracy can be caused by a high insensitivity of the response curve in respect to a model parameter.

Secondly, for large values of the Thiele modulus ($\varphi \gg 3$) the parameter estimates become highly correlated, which causes the confidence intervals of the estimated parameters to become infinite.

For smaller values of the Thiele modulus, the adsorption dynamics are likely to dominate the response curve of the reactant, which become then insensitive towards a change of the Thiele modulus. In this case, the product curve has to be analysed in order to estimate the value of the Thiele modulus. Even if such an estimation was theoretically possible, it would be difficult to ensure a correct mass balance since the loss of reactant due to conversion is difficult measure, when the sorption process dominates the reactant response curve.

If the response curves lack any contribution of the reactant adsorption to the dynamics of the system, only the conversion of the reactant is measurable. No more information can then be extracted from the analysis of the reactant curve than from a simple steady state experiment. If, however, the product curves are significantly influenced by adsorption, it should be possible to accurately measure three model parameters , if the fourth parameter is known a priori and if experiments with different catalyst volumes are conducted.

Chapter 6

Results and Discussion

6.1 Sorption measurements without reaction

6.1.1 Sorption measurements on T4480 (ZSM5) extrudates

The experimental procedure for sorption experiments of propane and benzene on T4480 (ZSM-5) extrudates are outlined in Section 3.2.2.1, 3.4.1. The pulse experiments of propane and butane on commercial 5A pellets were conducted by Möller and O'Connor (1994) in an apparatus similar to this work, which is described in more detail therein.

6.1.1.1 Propane on HZSM-5

Due to the small crystal size of $\sim 0.2\mu m$ the diffusional resistance in the macropores / mesopores was assumed to be dominant. The response curves of propane on HZSM-5 were analysed according to the long time solution of eq. (5.24-5.27) and with the help of the first moment eq. 5.18. A list of all experimental results can be found in the Appendix G. Figure 6.1 shows a comparison between experimental and model response curves at four different flow rates while keeping the *model parameters constant*. Figure 6.2 illustrates the effect of increasing the mass of adsorbent on the pulse response curve. The good agreement between experiment and model curves demonstrates the validity of the model and the ideal behaviour of the recycle reactor. It indicates that external film resistance is not significant. This is supported by experiments with different diameters yielding similar diffusion coefficients (at least within error limitations) as shown in Figure 6.3, since the recycle ratio decreases

strongly with decreasing pellet size in the catalyst bed and thus decreasing the linear velocity of the fluid around the pellets, see Section 4.1.2.3.

The degree of the model's validity may be expressed in the relative error of the intercept in the long time solution obtained from the least-square fit and the model intercept obtained from eq. (5.24-5.27). This is shown in Figure 6.4. The maximum error never exceeded 12% and was in average 4%. As can be seen from Figure 6.3 deviations of the macropore diffusivity are within 25% at lower temperatures. The adsorption coefficients at temperatures above 420K become small enough that the adsorbate concentration in the entire particle is in equilibrium with the gas phase. The average deviation of D_y at 420K exceeds 50%. Diffusivities cannot be measured at temperatures above 420K, where response curves clearly exhibit only one time constant, see Figure 6.5. Due to this relatively large error neither a temperature dependency of the macropore diffusivity nor a possible contribution of transport resistance in the micropores or of a surface barrier could be estimated.

Adsorption coefficient

The average deviation in K_c did not exceed 15 % as shown in Figure 6.6. The heat of adsorption ΔH_c was found to be 35.5 kJ/mol, which is in good agreement to values reported in literature (Nijhuis et al., 1997). The adsorption coefficients compare very well with those measured by Hampson and Rees (1993) using an isosteric method and to those by Hufton and Danner (1993), who used a pulse chromatography method.

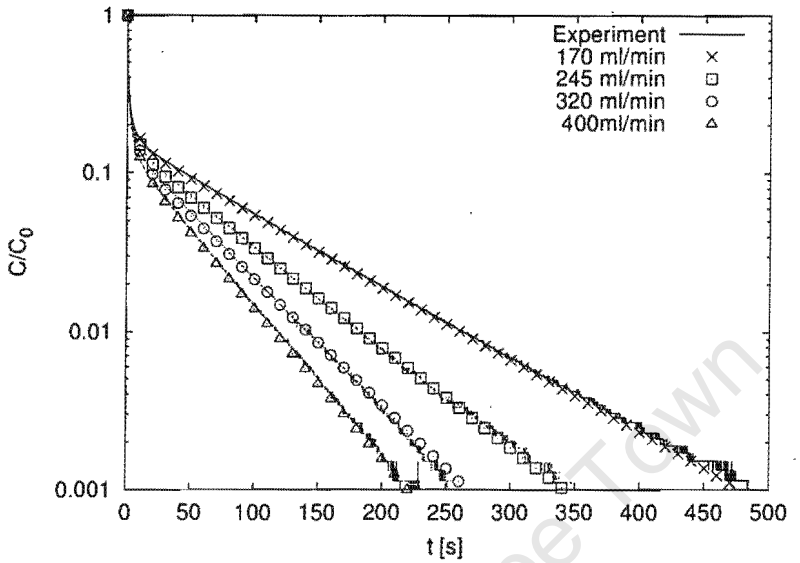

Figure 6.1: Pulse response of propane on 0.5 ml ZSM5 extrudates (r=0.06cm) at $350K$ at different flow rates. Model parameters are constant: $D_y = 3.5 \cdot 10^{-2} cm^2/s$ and $K_c = 875$.

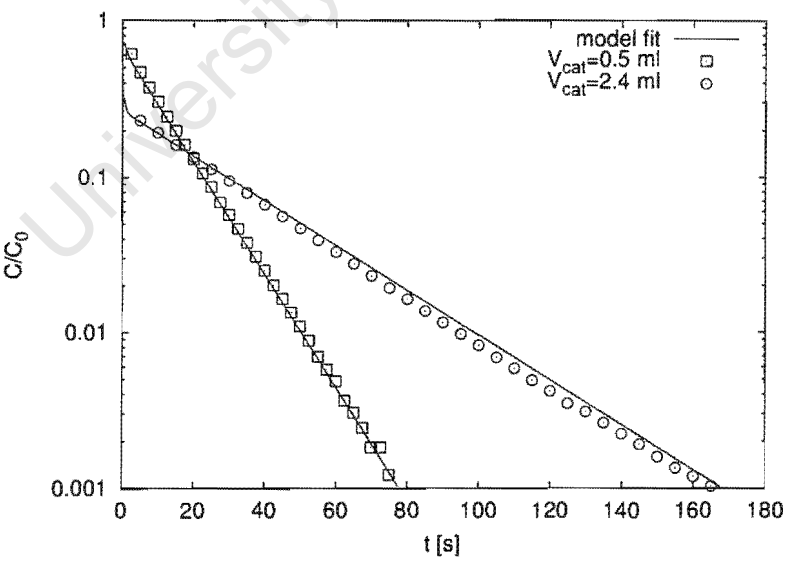

Figure 6.2: Comparison of response curves of propane/ZSM-5 with 0.5 ml and 2.4 ml of adsorbent. T=423K, F=360 ml/min; Run data: propan19 and propan44 (Appendix G)

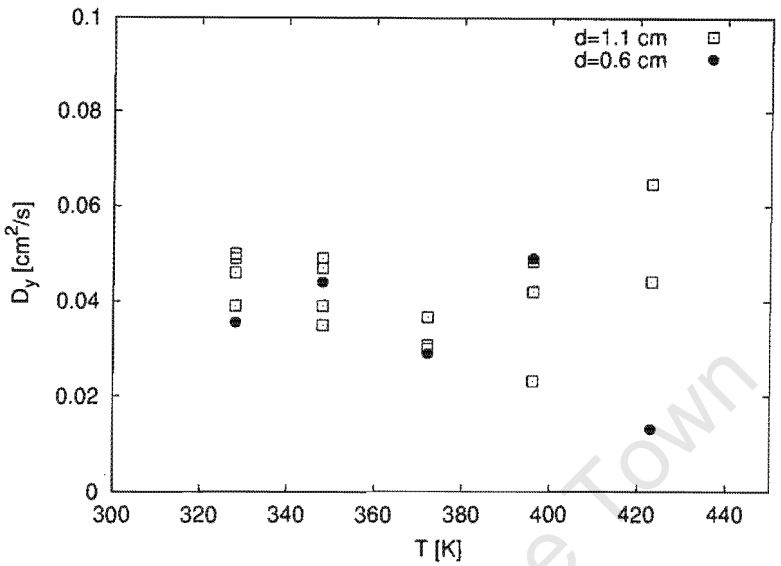

Figure 6.3: Macropore diffusion of propane in ZSM5 extrudates with two different pellet sizes as a function of temperature.

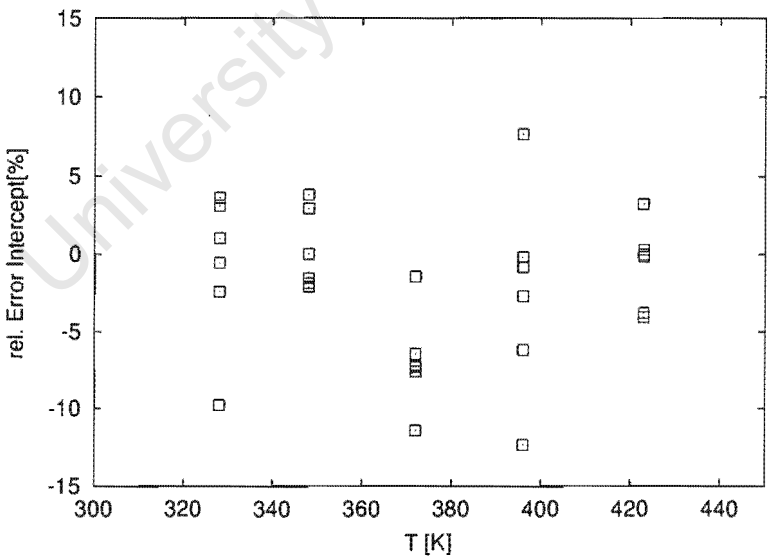

Figure 6.4: Error of intercept in the semi-log plot calculated from the long time solution of eq. 5.25 compared to the intercept obtained from the least square fit of the experimental long time solution of propane pulse experiments. $(C_{exp,long} - C_{theo})/C_{exp,long}100\%$

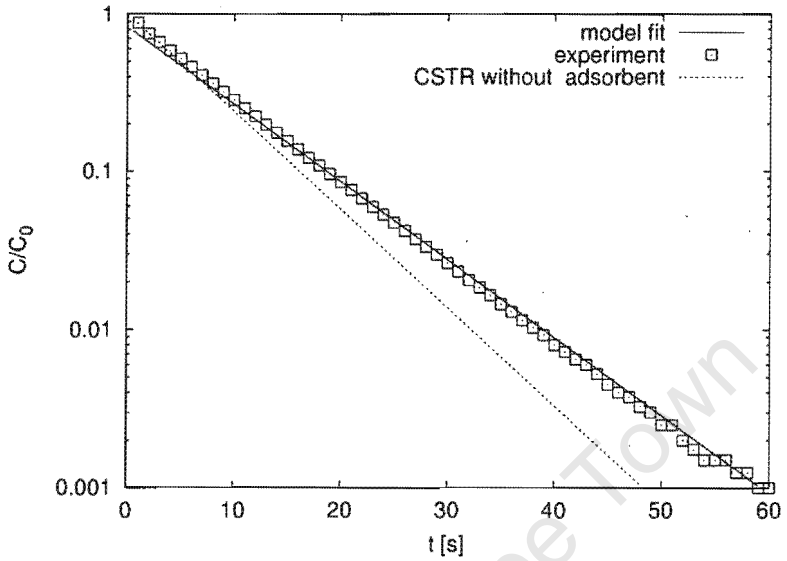

Figure 6.5: Response curve of propane/ZSM-5 at T=473K. Only one time constant observed. No diffusional transport resistance. Run data: propan22 (Appendix G)

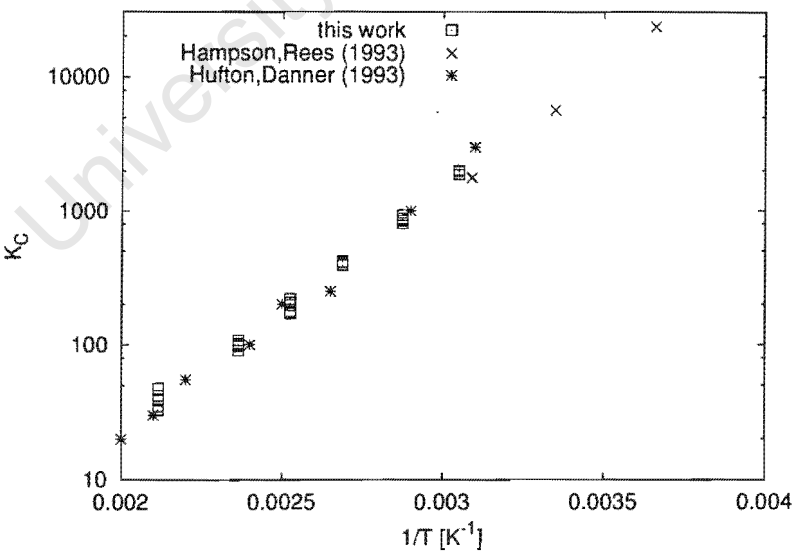

Figure 6.6: Van't Hoff plot for the adsorption coefficient of propane on ZSM5 extrudates calculated from the first moment of the pulse experiment.

6.1.1.2 Benzene on HZSM-5

In the same way as for the system propane/ZSM-5, it was assumed that diffusional resistance in the macropores/mesopores was dominant. The response curves were therefore analysed according to the long time solution of eq. (5.24-5.27) and the first moment eq. 5.18. A list of all experimental results can be found in the Appendix H.

Figure 6.7 shows that the model compares very well with the experimental data over the entire temperature range. The degree of the model's validity may again be expressed by the relative error of the intercept in the long time solution as explained above. The results are shown in Figure 6.8. The error in this system is, however, slightly higher than in the propane/ZSM-5 system with a maximum error of 35% and an average error below 10%. As can be seen from Figure 6.9 deviations of the macropore diffusivity are bigger than in the case of propane. Diffusivities measured for the particle size of 0.033cm were in general a factor two smaller than those measured for particles of 0.055 cm. However, due to the curvature and tailing of the long time solution and a relatively insensitive model parameter D_y, a minimum error of ± 50 % is to be expected. This is demonstrated in Figure 6.10, where the experimental data is modelled with different diffusivities but constant adsorption coefficient. Hence, in order to check experimentally, whether transport resistance in the micropores or at the pore mouth play an important role, a much greater variation of the particle diameter should be employed. This however was not feasible in the recycle reactor, due to the decrease in the recycle ratio and elution of small particles.

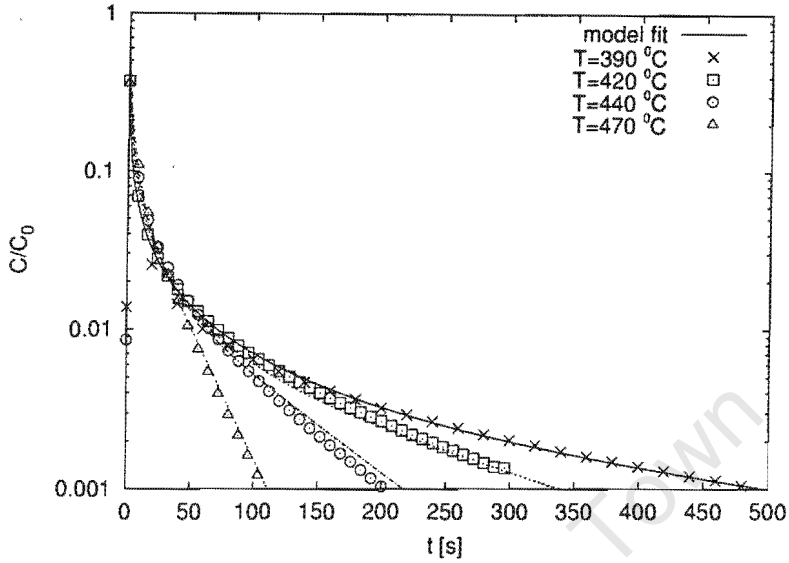

Figure 6.7: Measurement of the pulse response of benzene on T4480 extrudates at four different temperatures. Run data from: bem40a5 (390°C), bem42a5 (420°C), bem45a5 (440°C), bem48a5 (470°C) in Appendix H

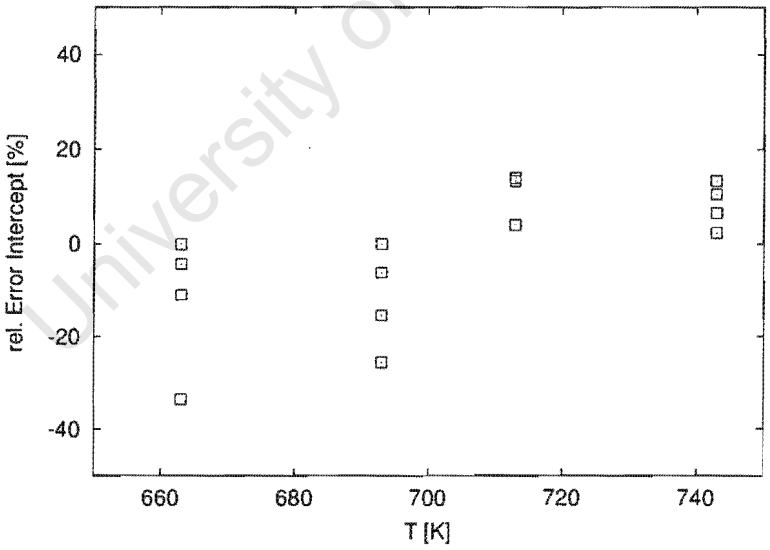

Figure 6.8: Error of intercept in the semi-log plot calculated from the long time solution of eq. 5.25 compared to the intercept obtained from the least square fit of the experimental long time solution of benzene pulse experiments. $(C_{exp,long} - C_{theo})/C_{exp,long}100\%$

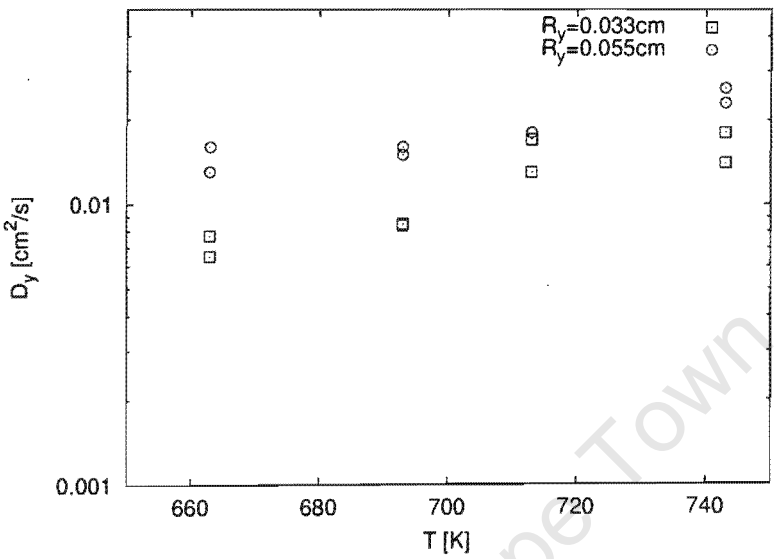

Figure 6.9: Macropore diffusion of benzene in T4480 extrudates with two different pellet sizes as a function of temperature.

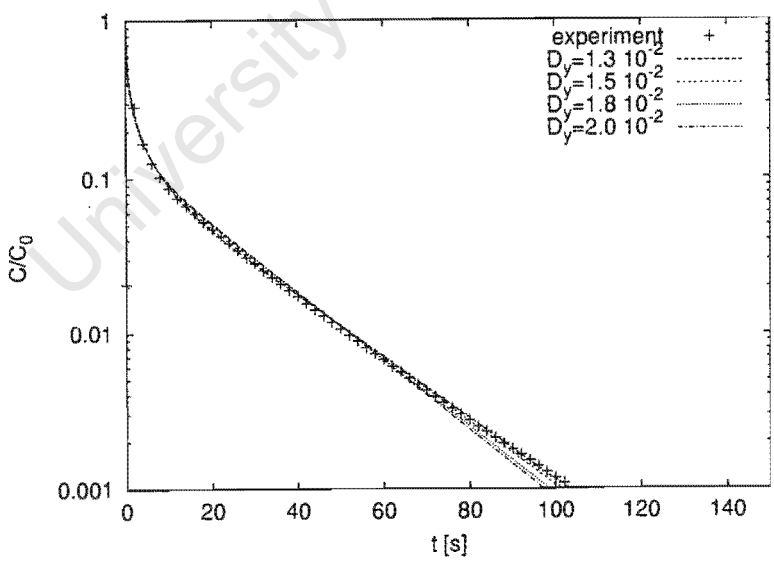

Figure 6.10: Parameter insensitivity of estimated diffusion coefficient $D_y = 1.3 \cdot 10^{-2} cm^2/s$ Run data: see Appendix H

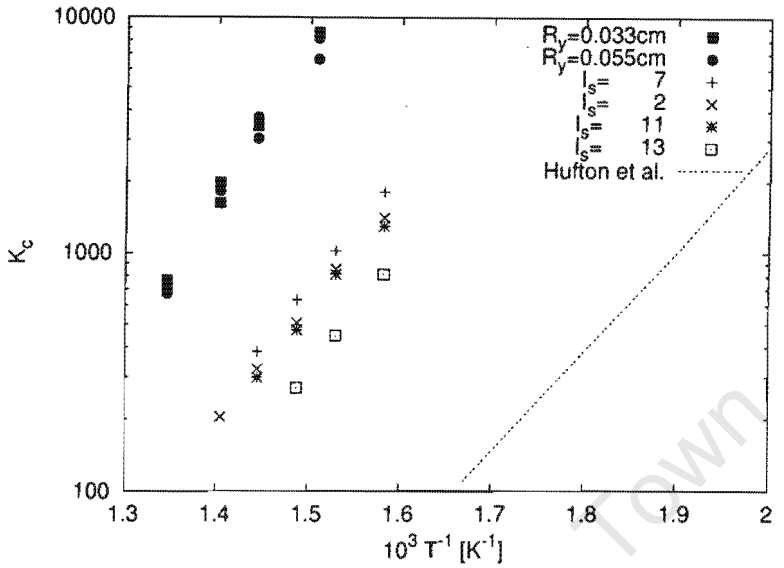

Figure 6.11: Van't Hoff plot for the adsorption of benzene on ZSM-5. Comparison with chromatographic measurements by Forni et al. (1986b), who investigated the effect of Na-exchange on laboratory HNaZSM-5 crystals with I_s being the severity Index of Ion-exchange and results by Hufton et al. (1995)

Adsorption coefficient

When the sorbate concentration is very low, extremely strong adsorption and enhanced heats of adsorption can be expected for molecules with electric dipole or quadrupole moments, such as in the case of aromatics containing π-electrons (see Section 2.3). The heat of adsorption of benzene on ZSM-5 increases dramatically at sorbate concentrations below 0.1 molecules per 1/4 unit cell, where enthalphies greater than 80 kJ/mol were measured (Thamm et al., 1988).

Due to this effect at very low sorbate concentrations, adsorption coefficients measured in this work are only compared to the pulse chromatography measurements done by Forni et al. (1986a,b) , Hufton et al. (1995). The measured adsorption coefficients in this work were within an error of 15%. Figure 6.11 compares the adsorption coefficient measured to those obtained by Forni et al. and Hufton et al. as a function of temperature. It can be seen that the adsorption equilibrium observed at the commercial ZSM-5 extrudates is about one order of magnitude higher than those measured by Forni et al.. Much lower, however, are the results by Hufton et al. on large silicalite crystals. However, in all cases

extremely high adsorption enthalphies of similar magnitude were established with 97 ± 3 kJ/mol by Forni et al., 88 kJ/mol by Hufton et al. and 120 ±4 kJ/mol in this work. The slightly greater adsorption enthalpy is in line with the increased adsorption coefficients on the commercial T4480 sample, which reflects the presence of stronger adsorption sites. The maximum sorbate concentration at a temperature of 390°C can be calculated from the initial gas phase concentration (see Section 3.2.2.1) and a Henry constant of adsorption of 8500 to $q \leq 0.1$ molecules per 1/4 unit cell, which is well in the region, where enhanced adsorption is to be expected.

Forni et al. investigated the effect that the different degrees of Na-exchange of a HNaZSM-5 sample have on the benzene adsorption constant. They reported a three fold smaller Henry constant of adsorption for the most severely Na-exchanged crystals, see Figure 6.11. However, in contrast to this observation, pulse responses on HZSM-5 samples from the same batch showed strong non-linear behaviour, so that adsorption equilibrium constants could only be estimated qualitatively from the smaller retention times in relation to those retention times measured with samples in the sodium form. The extremely strong influence of even small amounts of Al in silicalite was demonstrated by Thamm, see Section 2.3. Commercial ZSM-5 samples have in general a higher grade of impurities and undergo often severe hydrothermal treatment. Possible structural changes of the crystals may thus lead to the creation of stronger acid sites, for which the extremely high adsorption enthalpy and equilibria observed in this work are conceivable. Unfortunately no sorption experiments on commercial ZSM-5 could be found in literature for low sorbate concentration.

6.1.2 Transport mechanism of propane and benzene in T4480 extrudates

The numerical values for the average experimental pore diffusivity are given in Table 6.1. They are compared to theoretical values of molecular, Knudsen and effective pore diffusion, which are calculated according to eq. 2.3 to 2.6 in Section 2.1.1.

In order to confirm the dominance of intercrystalline diffusion, possible influences of external film resistance and intracrystalline diffusion have to be evaluated.

Table 6.1: Average estimated diffusivities $\overline{D}_{Exp}$ of propane and benzene on T4480 in comparison to molecular (D_m, Knudsen D_K and pore diffusivity D_y excluding surface diffusion and assuming a tortuosity factor of one and a measured pore radius 40Å(BJH desorption). [Diffusivities $\times 10^2 cm^2/s$]

Propane					Benzene				
$T[°C]$	$\overline{D}_{Exp}$	D_m	D_K	D_y	$T[°C]$	$\overline{D}_{Exp}$	D_m	D_K	D_y
55	3.7	11	1.1	1.0	390	1.1	31	1.5	1.4
75	3.7	12	1.1	1.0	420	1.2	34	1.5	1.5
100	3.8	13	1.1	1.0	440	1.6	36	1.6	1.5
125	4.2	15	1.2	1.1	470	2.0	38	1.6	1.5
150	4.1	16	1.2	1.1					

6.1.2.1 External film resistance

If mesopore and external film resistances are dominant, a significant contribution from the external film resistance can only be expected, if there is a substantial contribution from surface diffusion in the mesopores (Kärger and Ruthven, 1992d). The slower Knudsen diffusion in the mesopores will otherwise dominate over the faster molecular diffusion in the external film. A simple criterion for the relative importance is $\frac{5D_{exp}}{k_f R_y} \ll 1$ (Yang, 1987b), for which film diffusion becomes insignificant. Assuming a minimum Sherwood number of 2, a particle size of 0.03 cm and diffusivities D_m and D_{Exp} taken from Table 6.1, a maximum number of the left hand side of this criterion results to 0.35. Considering now that Möller and O'Connor (1996) measured Sherwood numbers of 70 in the jetloop reactor, the presence of significant film resistance can be excluded.

6.1.2.2 Intracrystalline diffusion

Diffusion of propane in very small ZSM-5 crystals is rapid even at low temperatures. To confirm the dominance of mesopore diffusion the ratio of the diffusional time constants λ has to be greater than 10 (Section 5.2.4.1). Diffusivities for propane in ZSM-5 crystals have been fairly consistently measured by macroscopic methods to be approximately $10^{-7} cm^2/s$ (T=334K) (Hayhurst and Paravar, 1988; Eic and Ruthven, 1989; Bülow et al., 1986) with exceptions of NMR measurements (van den Begin et al., 1989) and square wave measurements (Caro et al., 1985), which are two orders of magnitude higher. With $K_c = 100$,

the value of λ is greater than $8 \cdot 10^4$ which clearly proves the dominance of mesoporous resistance.

The diffusivity of benzene has been extensively studied by numerous workers (Niessen and Karge, 1993; Eic and Ruthven, 1989; Bülow et al., 1986; van den Begin et al., 1989; Beschmann et al., 1987; Doelle et al., 1981; Qureshi and Wei, 1990; Shah et al., 1988, Brandani et al., 2000). Diffusivities of $\sim 10^{-9} cm^2/s$ (T=386K) with an activation energy of $\sim 25 kJ/mol$. The diffusivity at 400°C can be calculated with the Arrhenius equation as $\sim 10^{-7} cm^2/s$, so that the value of λ is in the same order of magnitude as in the previous case of propane. One might argue that strong interaction between sorbent and sorbate at very low concentrations of benzene might lead to smaller diffusivities. It was however shown (Song and Rees, 2000), that diffusivities of benzene increase at very low concentrations. This is a clear indication that mesoporous transport resistance prevails in this system.

6.1.2.3 Surface diffusion

For the calculated pore diffusivities in Table 6.1 an unrealistic tortuosity factor of one was used, which would signify diffusion in a straight unconnected cylindrical pore. A more realistic value for the tortuosity factor for small pore systems is three to four, see Section 2.1.1. This however means that the theoretically estimated diffusivity in the macro/mesopores is ten times smaller in the case of propane and three times smaller in the case of benzene than the experimentally observed diffusion coefficient. This large discrepancy can not be explained by the estimated ±50% error in the diffusion coefficients. One could assume that the discrepancy is due to a large pore size distribution, this would however mean that the effective pore size is required to be three to four times larger in the case of benzene, where Knudsen diffusion prevails at high temperatures, but 40 times larger in order to explain the propane measurements due to a transition from Knudsen to molecular diffusion regime. It is therefore evident that the enhanced pore diffusion can only be explained by a parallel transport mechanism such as surface diffusion, see Section 2.1.1.2. This translates to a very high contribution of surface diffusion in the range of 90% in the effective pore diffusion of propane and 55 to 75 % of enhanced benzene diffusion.

Since surface diffusion is an activated process it is however striking that no activation energy for the effective pore diffusivity could be observed for propane. Despite the experimental error it is indicated that the effective diffusivity for benzene even increases with

temperature, although the activation energy for benzene adsorption is very high. The latter should lead to a strong decrease of the diffusivity, since the surface flux is proportional to the adsorption coefficient. Nevertheless, there is no other explanation for the enhanced effective diffusivity.

6.1.3 Propane/Butane on 5A zeolite pellets

The properties of the commercial Linde zeolite 5A pellets used by Möller and O'Connor (1994) are summarised in Table 6.2.

The pulse response curves were analysed with the help of the long time solution assuming intracrystalline diffusion control, while K_c was independently estimated from the first moment.

The results for D_c and K_c are shown in Figure 6.12-6.14. The accuracy of the parameter estimation is comparable to the ZSM-5 systems. The diffusivities and adsorption constants of propane and butane on 5A compare well with those found in the literature measured on commercial samples. In all cases the measured diffusivities of laboratory crystals were between one and two orders of magnitude greater than those of commercial samples.

Values for D_c were also estimated by applying the long time solution of the bipore model. Macropore diffusion had thus to be estimated from Knudsen and molecular diffusion using eq. 2.3 to 2.6 in Section 2.1.1, assuming a tortuosity factor of 3.

Table 6.2: Parameters for Linde Zeolite 5A (30/40 mesh Lot No. 4780841), reported by Möller and O'Connor (1994)

PARAMETER	
density [g/ml]	1.15
pore voidage	0.32
pellet radius [cm]	0.254
pore radius [cm]	3.3E-5
crystal radius [cm]	1.7E-4

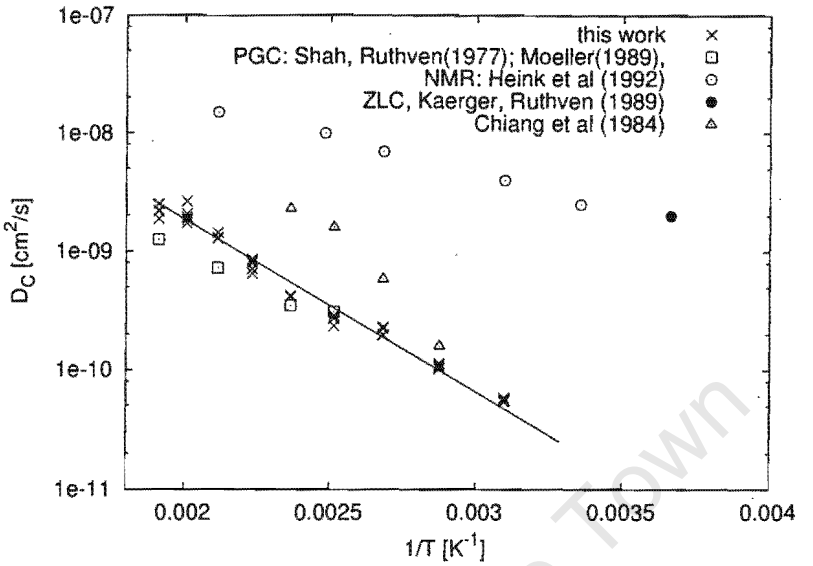

Figure 6.12: Diffusion of propane in 5A pellets (assuming transport resistance in the micropores is dominant) compared to the literature.

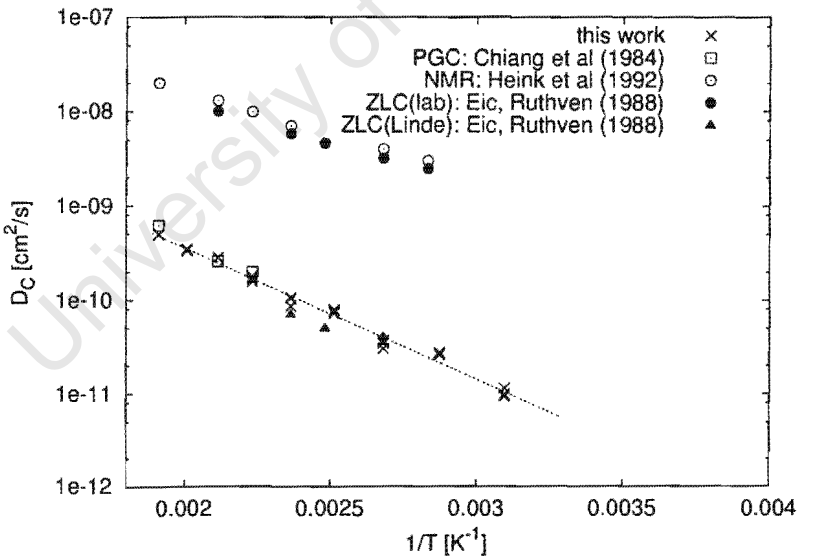

Figure 6.13: Diffusion of butane in 5A pellets (assuming transport resistance in the micropores is dominant) compared to the literature.

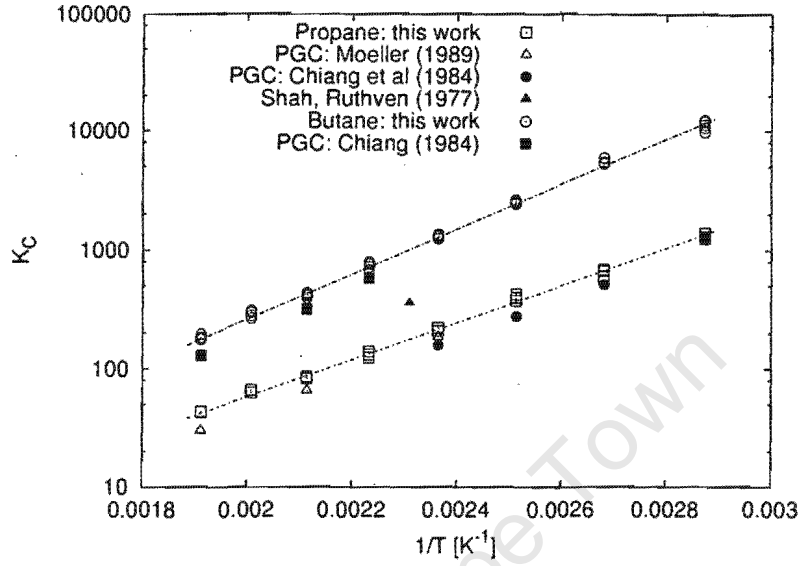

Figure 6.14: Adsorption of propane/butane on 5A pellets estimated from first moment of pulse response curves.

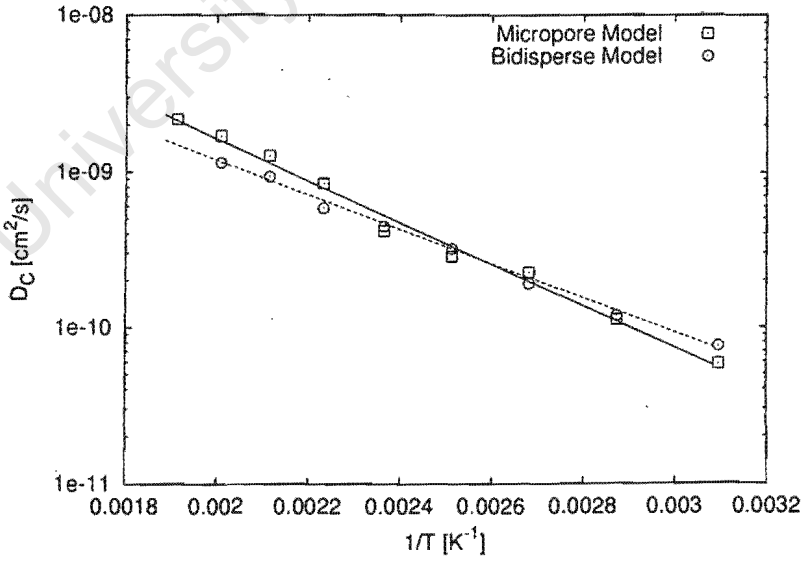

Figure 6.15: Estimated values of micropore diffusivities of propane on 5A pellets assuming bipore or micropore diffusion model.

6.2 Pulse experiments of cumene on ZSM-5

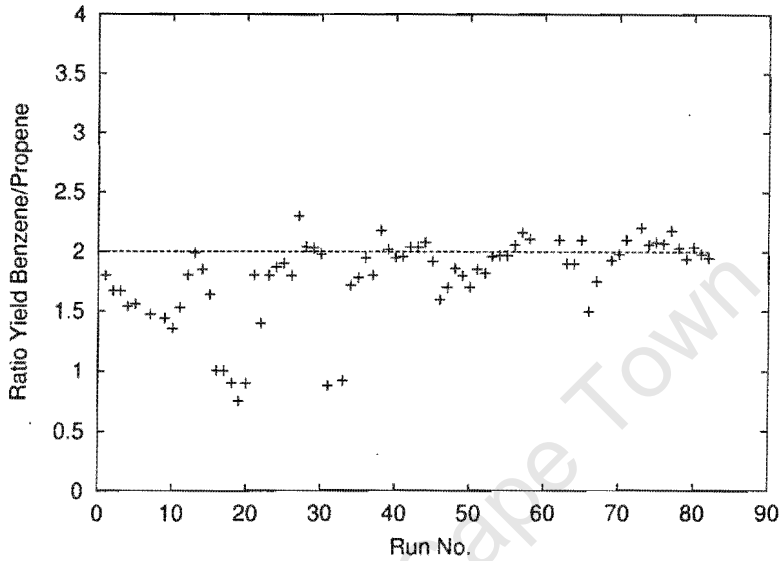

Figure 6.17: Ratio of the integrated carbon concentration curves for benzene and propene for all pulse reactions of cumene on T4480 ZSM-5 catalyst. (Theoretically expected value 2)

Response curves of the pulse injection of cumene on ZSM-5 were measured according to the experimental procedure described in section 3.2.2.2. The outlet concentration curves were normalised with the initial total carbon concentration, as outlined in section 3.4.1. The normalisation for each transient reaction run was performed in an Excel spreadsheet using a simple trapezoidal rule for integrations, see spreadsheets in Appendix F. Reaction run data and results are listed in detail in Appendix K. The gas chromatographic analysis of the effluent gas composition revealed a very clean reaction of cumene to benzene and propene, see chromatogram in Appendix C. The integral amount of primary and secondary byproducts was well below 1% of total products and was hence discarded in the further analysis. A measure for the goodness of the product analysis is the ratio of the yields for benzene and propene. This ratio of the integrated carbon concentration curves of benzene to propene is plotted in Figure 6.17 for all pulse measurements. The measured ratios deviate in general only by 10 % from the theoretically expected value of two. Shortages of benzene can be found for the reaction runs 2-11 with a relatively low conversion of 20 % and reaction runs 15-20 at low temperatures with the largest amount of catalyst used. In these runs

the adsorption of benzene is strong and the residual amount of benzene is expected to be in the long tail of the benzene curve at low concentrations. Normalisation of the effluent concentrations in these cases is preferably conducted by only taking the concentrations of cumene and propene into account and assuming a theoretical ratio between benzene and propene of two. The formation of "coke" during the cracking of cumene was investigated by Fukase and Wojciechowski (1986), who found that only small amounts of coke below 1% were formed by propene oligomerisation. It should be noted that the formation of "coke" during a pulse experiment can however not be excluded, since strongly adsorbing products may not be detectable.

The good repeatability of the pulse experiments is demonstrated in Figure 6.18 for two sets of comparative runs with same batches of catalyst (without regeneration in between) being used each time. This emphasises again the good accuracy of the product analysis with the new MAS technique. The reproducibility of the experiments was evaluated

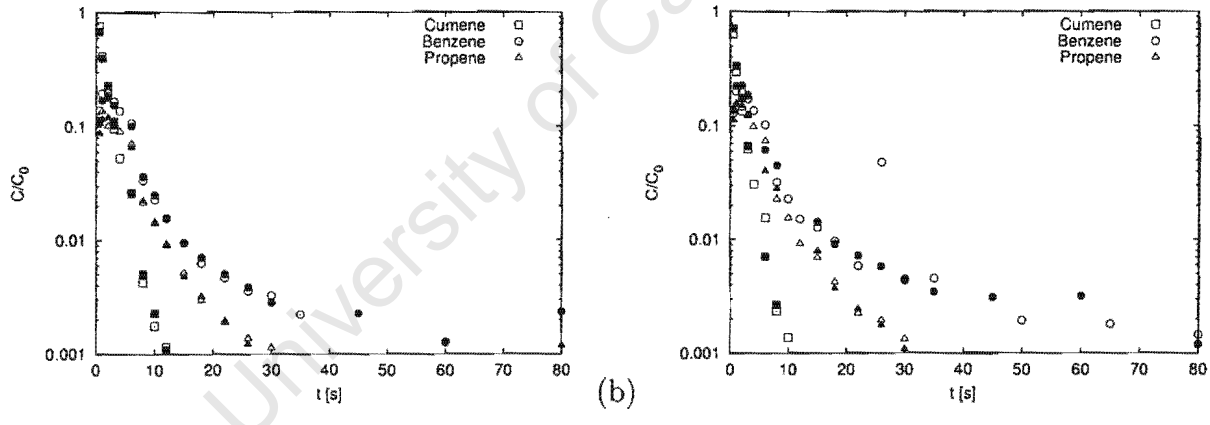

Figure 6.18: Repeatability of cumene pulse experiments on E1, E2 ZSM-5 extrudates at 350°C. (a) Run 83/84, (b) Run 85/86. Same catalyst packing for each comparative runs.

by testing samples of extrudates that were separately crushed, sieved, and calcined. The reproducibility of the measurements was very good. An example is given in Figure 6.19. While the propene and cumene response curves are in reasonable agreement with each other, the benzene curve deviates in run 31 substantially from the other two runs 71 and 81, especially with regard to the excessive tailing in run 31. This large discrepancy of benzene was however unusual and could not be explained.

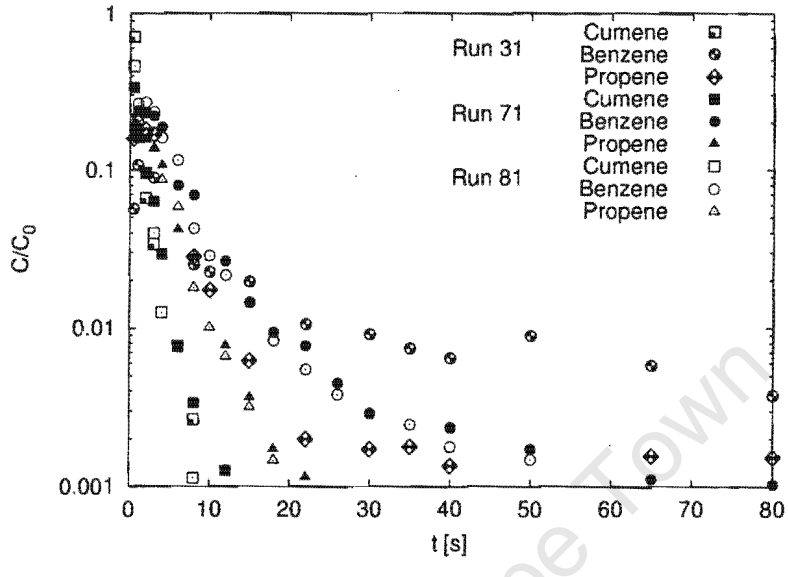

Figure 6.19: Reproducibility runs of cumene pulse experiments on T4480 ZSM-5 extrudates. Run react31, 71, 81 see Appendix K. Different catalyst batches for all comparative runs.

6.2.1 Parameter sensitivity and discrimination

A typical system response is plotted in Figure 6.20. The cumene concentration curve is represented by a straight line in the semi-logarithmic plot. The presence of only one time constant for the reactant curve was attributed to the lack of adsorption dynamics from the reactant (see Section 5.18). It means that the adsorption coefficient for cumene is sufficiently small with α_{Cu} being relatively large, so that the criterion $\frac{\beta_{Cu}}{\alpha_{Cu}^2 \varphi^3} < 0.01$ of eq. 5.64 is fulfilled and the response curve is not influenced by any reversible adsorption dynamics. Since additionally propene adsorbs only weakly on the catalyst surface (see quantification below), only one parameter can be extracted from both transient concentration curves, e.g. $\beta_{Cu}\varphi$ or in dimensional form $D_{Cu}k_{eff}$. k_{eff} is here denoted as the effective rate constant referred to the concentration in the gas phase and is hence the product of adsorption and intrinsic rate constant.

$$k_{eff} = K_{Cu}k_R \tag{6.1}$$

Differences to this absence of adsorption dynamics seems to occur, when conversion levels are relatively low. The cumene concentration curve in Figure 6.21 exhibits only one time constant until $c/c_0 \simeq 0.01$ and it then slowly tails off. Figure 6.22 illustrates the influence of reversible adsorption of cumene on the concentration curves of propene and cumene.

Note that the reaction term k_{eff} was constant and independent of adsorption K_{Cu}. While keeping $\beta_{Cu}\varphi$ and therefore the conversion constant, an increase of the adsorption constant leads to a slightly improved representation of the reactant, which however is accompanied by a large error with respect to the product concentration curve. In this simulation the value of φ was 11 and the adsorption coefficient of propene has been assumed to be zero. Furthermore, increasing the adsorption coefficient of propene the model curve shifts further away from the experimental curve. Increasing the Thiele modulus φ while keeping the conversion constant has the opposite effect on the reactant and product curves (see Figure 5.7 and 5.8), which makes the simultaneous fitting of the propene concentration curve and the tailing of cumene response impossible. This tailing can therefore be attributed with confidence to the error observed in the blank runs described in section 4.2. Given the fact that the cumene concentration curves do not tail off at high conversion and are therefore reliably measured by the MAS technique indicates that the source of this error is in the jetloop reactor/injector port.

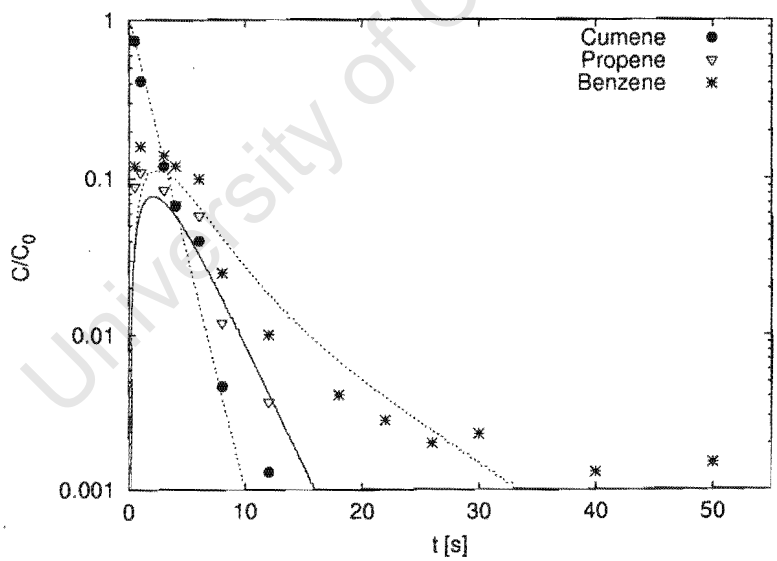

Figure 6.20: Cumene pulse experiment Run react52: T=440°C; Catalyst Mass=0.5g; Flow(@STP) = 410 ml/min; Particle radius=0.075cm. X=60%

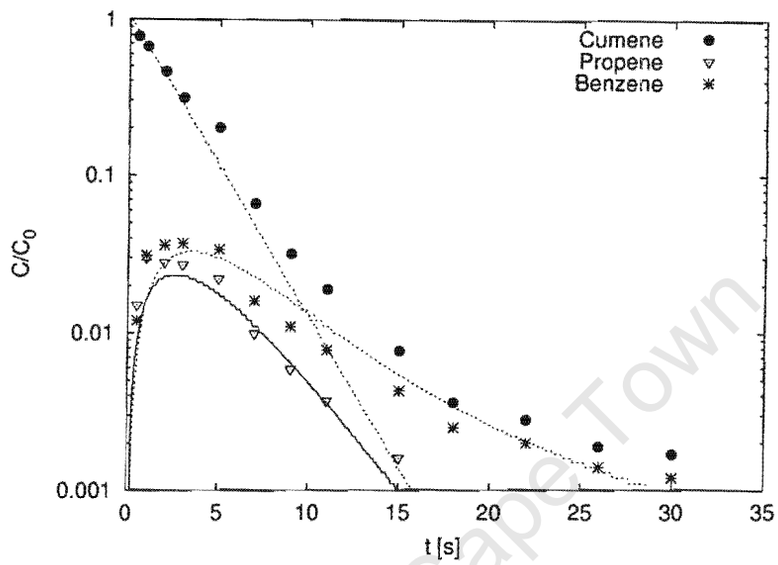

Figure 6.21: Cumene pulse experiment Run react2: Catalyst Mass=0.2g; X=19%; otherwise run conditions as in Figure 6.20.

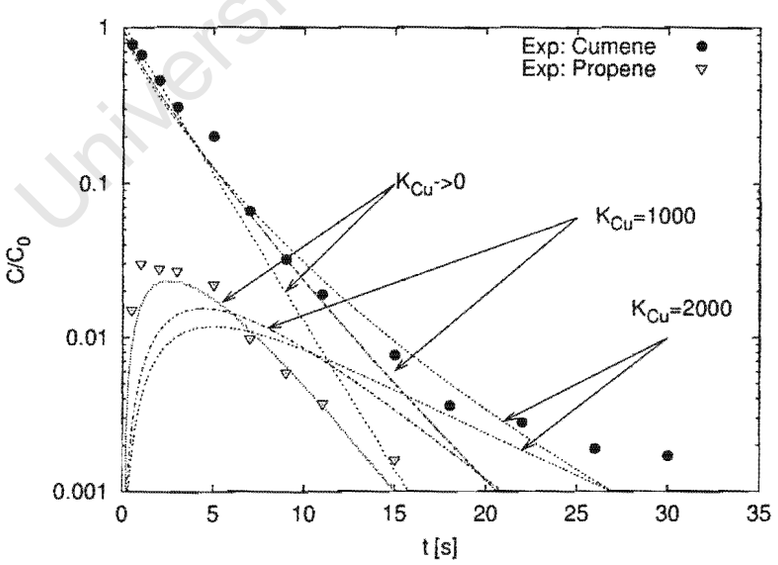

Figure 6.22: Influence of cumene adsorption parameter K_{Cu} on the response of cumene and propene. Run react2 with conditions as in Figure 6.21. Model curves with same conversion, e.g. $\beta_{Cu}\varphi = 0.22$ (constant k_{eff}, D_{Cu}), but different α_{Cu} with varying K_{Cu}.

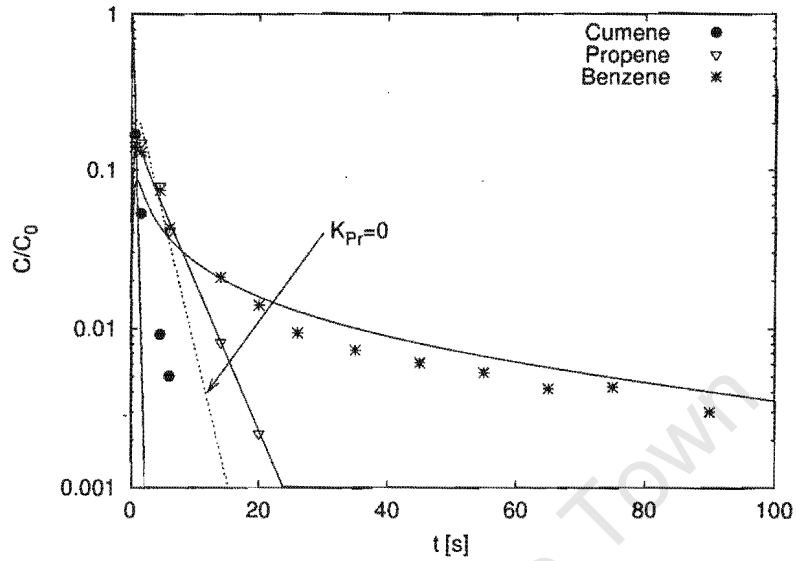

Figure 6.23: Cumene pulse experiment Run react14: Catalyst Mass=3.0g; X=85%; otherwise run conditions as in Figure 6.20.

The shape of the benzene curve with its tailing at lower concentration is however indicative of adsorption. This is confirmed, when the mass of catalyst is increased, see Figure 6.23. Since additionally no significant extraneous tailing was measured during benzene blank pulse experiments in Section 4.2, it can be concluded that reversible adsorption influences the benzene response curves.

Figure 6.23 also shows that the adsorption behaviour of propene becomes significant when the mass of catalyst is sufficiently large. This finding is similar to the earlier discussed correlation of the sensitivity of the reactant curve for α_R (see Section 5.3.3.6). For small values of the correlation $\frac{\beta_R}{\alpha_R^2 \varphi^3}$ the reactant curve was found to be insensitive towards the parameter α_R. Higher sensitivities were achieved by increasing β_R (increasing mass of catalyst) and thus increasing the value of this correlation.

The parameter discrimination and measurability can be summarised as follows:

- Reactant curves are independent of α_R. A reversible adsorption of the reactant is not measurable.
- Thiele modulus $\varphi \gg 3$
- Adsorption of propene K_{Pr} is small and only measurable, if larger amounts of catalyst are used.

- Adsorption dynamics for benzene are measurable.

Parameter estimation

It becomes clear from the above observations and the earlier discussed parameter sensitivity analysis that further assumptions have to be made, if any of the desired parameters D_i, K_i and k_{eff} are to be extracted from the transient experiments. It was concluded in the sensitivity analysis (Section 5.3.4) that only the product curve has to be analysed in a parameter estimation, if the reactant exhibits no reversible adsorption, as in the case of cumene. It is therefore necessary to rely on the analysis of the benzene response curves. Two possible approaches for a parameter estimation can be deduced for the analysis of the benzene response curves:

1. One of the benzene parameters, D_{Be} or K_{Be} is known a priori. Furthermore, the ratio of the diffusivities is known. The two unknown parameters are then: k_{eff}, D_{Be} or K_{Be}. Only a single pulse experiment is necessary.

2. One of the benzene parameters, D_{Be} or K_{Be} is known a priori, but the ratio of the diffusivities is unknown. The three unknown parameters are then k_{eff}, D_{Cu}, D_{Be} or K_{Be}, which have to be simultaneously estimated from experiments with different values of β_R (different catalyst masses).

One has therefore to rely on the sorption experiments of benzene on ZSM-5 which were presented earlier in Section 6.1.1.2. It is possible to either incorporate the measured adsorption or the diffusion coefficient into the reaction model. It was however shown that the adsorption behaviour of benzene molecules is strongly influenced by the heterogeneity of the active sites in ZSM-5. In the presence of a reacting species the adsorption may change in such a system, so that it is more reasonable to assume the diffusivity as being unchanged by reaction. An average value of $0.015 cm^2/s$ for the benzene diffusivity is assumed, which is taken from inert pulse experiments over all temperatures (Figure 6.9). A temperature dependency of the diffusivity is not incorporated in the model, because of the relatively high uncertainty of the experimental value.

In the following both approaches for the parameter estimation are used during the investigation of cumene pulse experiments on T4480 catalyst.

6.2.2 Parameter estimation using Knudsen relation

Additional to the diffusivity of benzene, one has to know the ratio of the different diffusivities in order to unambiguously estimate the unknown model parameters k_{eff} and K_{Be} from a single experiment. Although it was shown that surface diffusion of benzene was enhancing the mass transport in the mesopores, the ratio of the diffusivities shall as a first approximation follow Knudsen diffusion, e.g. inversely proportional to the square root of the molecular weight of the molecules.

For reaction runs with high catalyst loading (run react12-react20, see Appendix K) adsorption of propene becomes significant so that its adsorption has to be estimated in these runs as well.

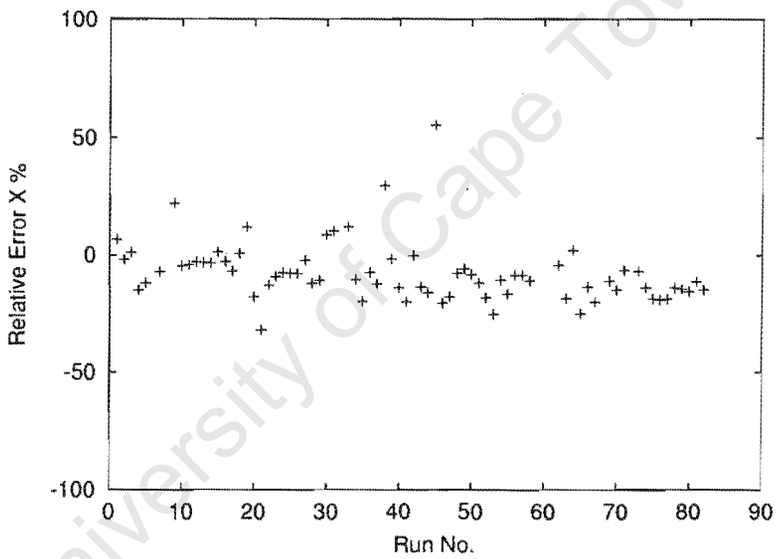

Figure 6.24: Relative error of calculated model conversion and experimental conversion.

Figure 6.24 shows the relative error of the conversion calculated from the model parameters and the experimental error. The estimated model conversion is systematically about 10% smaller than the conversion calculated from the experiments. The systematically smaller value of the model conversion is due to the oversimplification of the model, because short time and long time solutions cannot be fitted simultaneously with the same accuracy. Product concentrations were always predicted to be lower in the initial region, while the reactant curve deviated the most at longer times. Nevertheless, the error is acceptably small considering the large experimental uncertainty.

The maximum error of the logarithmic concentrations between experiment and model were calculated using eq.3.5 and were about 50%. Examples of these model fits are given in Figures 6.20, 6.21 and 6.23, while all model fits are shown in Appendix K. An indication for the goodness of the fit is the correlation coefficient R^2 between model and experimental data. This value was for all three components close to one (~ 0.94), which was considered to be an indication of a relatively good fit regarding the simplicity of the model and the experimental inaccuracy. The relative least square error was about 0.1.

6.2.2.1 Adsorption

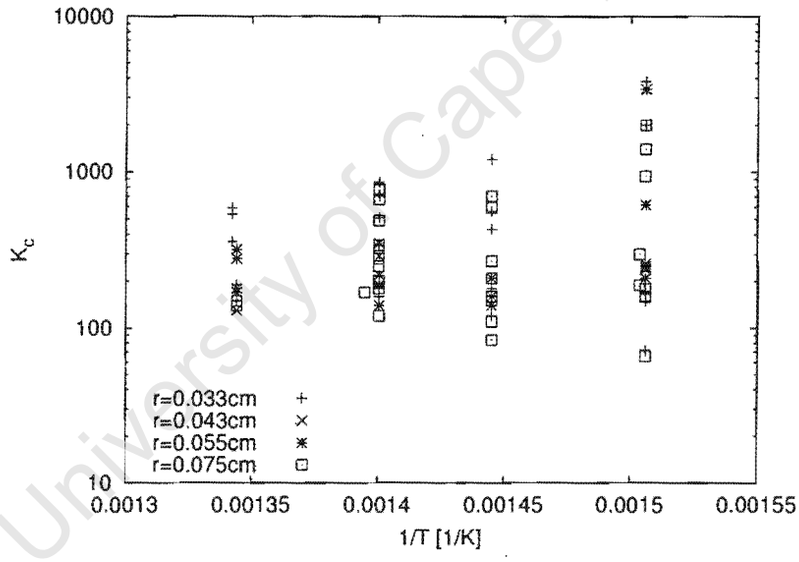

Figure 6.25: Van't Hoff plot of benzene adsorption estimated from cumene pulse experiments on T4480 catalyst.

From the Van't Hoff plot in Figure 6.25, it is evident that no temperature dependency can be deduced for the estimated benzene adsorption, due to the large error of the estimates. Moreover, a trend of increasing variance can be observed for lower temperatures. The results for the estimated adsorption coefficients of benzene are plotted against the conversion in Figures 6.26 to 6.27 with no correlation between adsorption and conversion being apparent. The 95% confidence interval for the estimated adsorption coefficient of benzene in each model estimation is approximately 100% below and above the estimated value, see results in Appendix K. This reflects the relatively large error margin observed in Figures 6.26 to

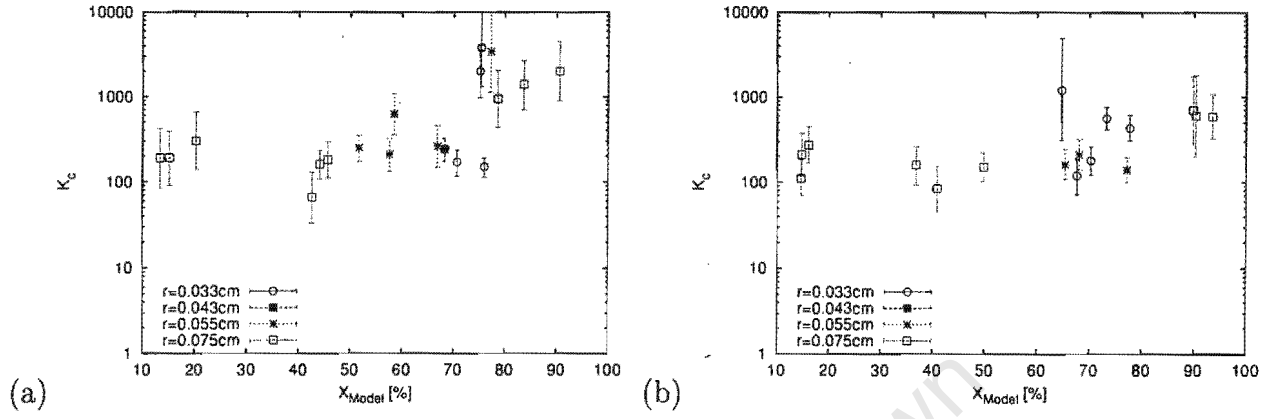

Figure 6.26: Estimation of the adsorption coefficient from transient reaction response curves at: (a) T=390°C; (b) T=420°C

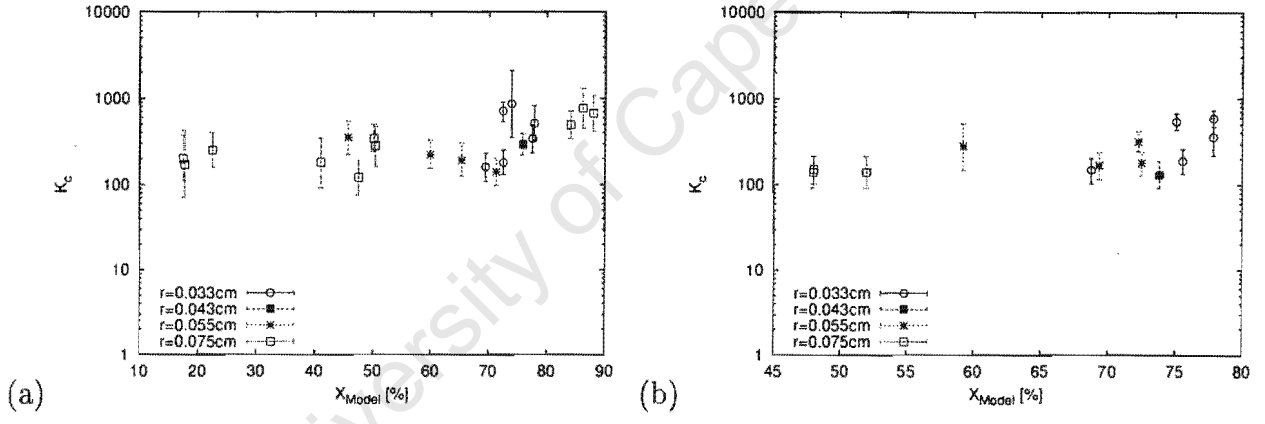

Figure 6.27: Estimation of the adsorption coefficient from transient reaction response curves at: T=440°C; T=470°C

6.27. Three times larger confidence intervals were however observed at conversions greater than 70%. In comparison to the extremely strong dependence of the benzene adsorption coefficient on the temperature during pulse experiments without reaction, adsorption during reaction conditions at the same temperature range does not depend significantly on temperature. The benzene adsorption coefficient at 390°C is approximately 200, which is forty times smaller than the value obtained from the single component sorption experiment. It can hence be speculated that the strong active sites, which were responsible for the extremely strong adsorption of benzene molecules, are now occupied by irreversibly adsorbing cumene molecules i.e. competitive adsorption. This hypothesis is supported by two experiments,

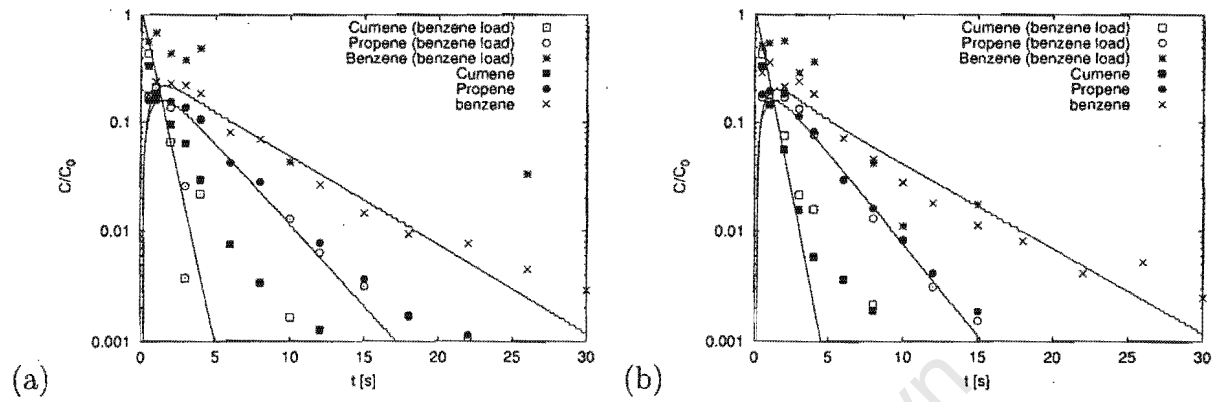

Figure 6.28: Comparison of cumene pulse experiments with an without benzene co-feed. (a) T=390°C (react71) (b) T=470°C (react74)

where a steady stream of benzene had been cofed into the system, which was perturbated by a pulse of liquid cumene. Figure 6.28 shows that the response curves for propene and cumene were not affected by the prior presence of benzene on the catalyst. A significant enhancement of the benzene concentration in the initial region can be clearly found in Figure 6.28, which proves that cumene molecules flush off adsorbed benzene molecules from the catalyst surface.

Adsorption coefficients for propene obtained for measurements with 3g of catalyst (run react12-react20) were approximately 15 to 30 times lower than those of benzene (see Table 6.3).

Table 6.3: Adsorption coefficient of propene estimated from reaction runs react12-react20

Run	T_R[°C]	K_{Pr}	K_{Be}/K_{Pr}
12	440	33	15
13	440	29	26
14	440	23	29
15	420	37	16
16	420	29	21
17	420	161	(4)
18	390	62	22
19	390	74	27
20	390	65	15

6.2.2.2 Effective rate constant k_{eff}

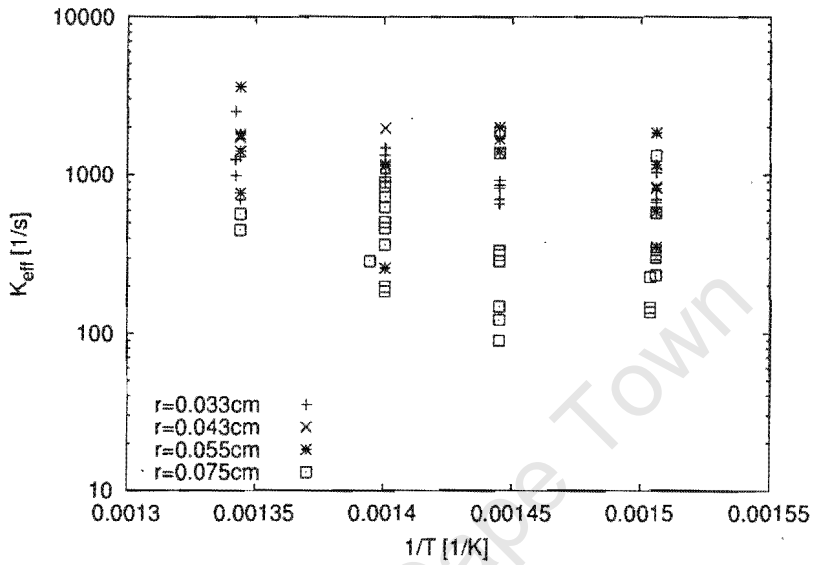

Figure 6.29: Arrhenius plot of the estimated effective rate constant k_{eff} estimated from cumene pulse experiments on T4480 catalyst.

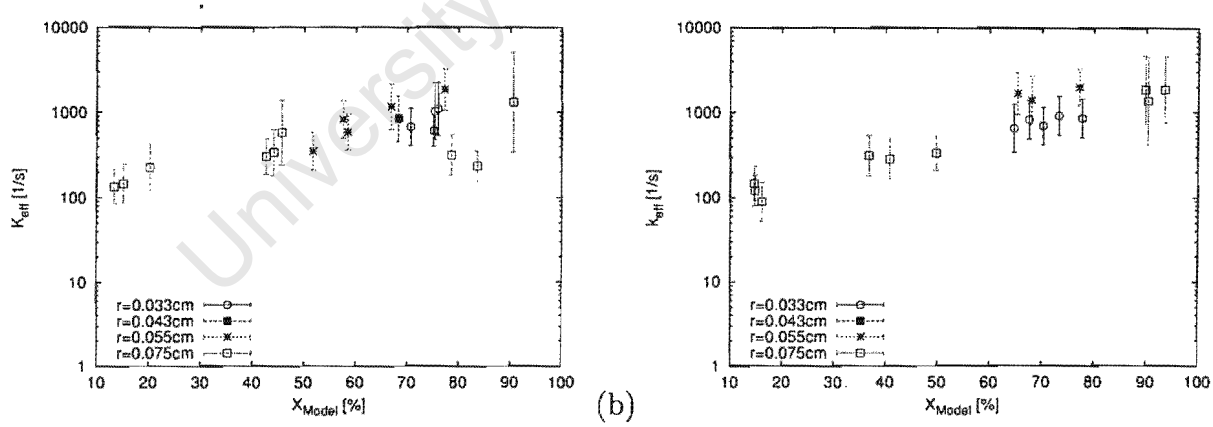

Figure 6.30: Estimation of the effective rate constant k_{eff} from transient reaction response curves at: (a) T=390°C; (b) T=420°C

From the Arrhenius plot in Figure 6.29, it is evident that no temperature dependency can be deduced for the estimated rate constant, due to the large error of the estimates. The effective rate constant shows however a dependence on conversion. The rate constant increases from 100/s at a conversion of 10% to approximately 1000/s at a conversion of

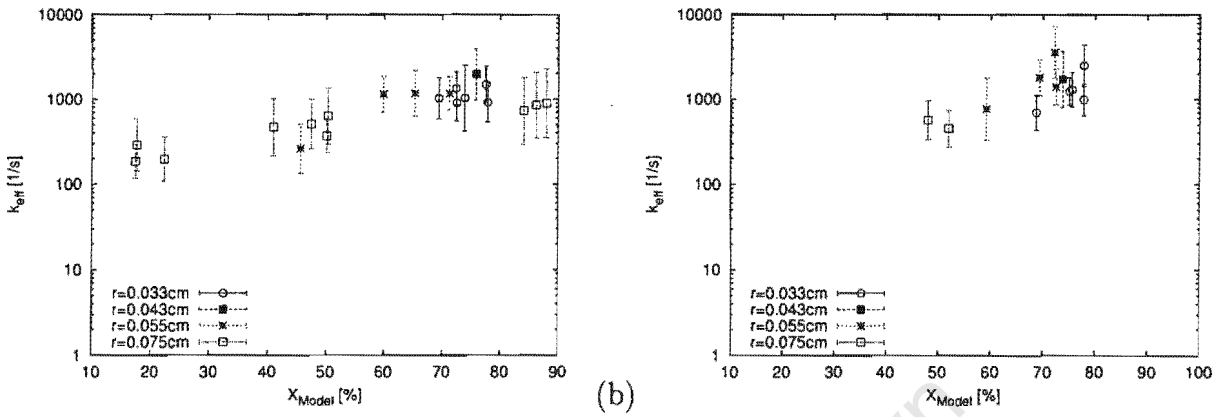

Figure 6.31: Estimation of the effective rate constant k_{eff} from transient reaction response curves at: (a) T=440°C ; (b) T=470°C.

90%. When comparing Figures 6.30 to 6.31 one can conclude that this observation is within a small error margin irrespective of temperature. The 95% confidence intervals are in the same range as those computed for the adsorption coefficient. The approximately linear dependence of k_{eff} on the conversion is observed irrespective whether the conversion is changed by varying pellet size, mass of catalyst or flow rate. It is therefore an effect of the actual reaction mechanism. It is important to note that this result is inconsistent with the model assumption of a first order reaction, despite the fact that experiments were in general well represented by the model.

The actual reaction order must be less than one, because the observed first order rate constant increases with conversion. This can be seen by comparing the observed pseudo first order rate with its concentration dependent rate "constant" k_{eff} to an n-th order rate equation with a rate constant k_n.

$$rate = k_{eff}(1 - X) \tag{6.2}$$

$$rate = k_n(1 - X)^n \tag{6.3}$$

The pseudo first order rate "constant" can thus be written as

$$k_{eff}(X) = k_n \frac{1}{(1 - X)^{n-1}} \tag{6.4}$$

This leads to an increase of $k_{eff}(X)$ for larger conversions X. Cumene cracking, however, is

a well known first order reaction (Fogler, 1999), which cannot plausibly be explained by an n-th order reaction rate. A model that preserves the first order mechanism with respect to cumene, but which leads to a reaction order smaller than one, is the Langmuir-Hinshelwood approach.

6.2.2.3 Langmuir-Hinshelwood approach

So far it was assumed that the reaction system is linear and not dependent on the surface coverage, which seemed reasonable due to the relatively low concentrations in the gas phase. Taking the surface coverage into account leads to a Langmuir-Hinshelwood approach which was used by Corrigan et al. (1953) for the cracking of cumene on silica-alumina catalyst. A more simplified approach is used here:

$$\begin{aligned} Cu + S &\rightleftharpoons CuS \quad (a) \\ CuS &\rightarrow Be + Pr + S \quad (b) \end{aligned} \tag{6.5}$$

The symbol S in eq. 6.5 denotes the catalytic site and CuS is the adsorbed cumene molecule. The reactant molecules are regarded as being the only adsorbed molecules on the catalytic sites, because of the negligible effect of the benzene concentration on the cumene and propene response curves. With the adsorption/desorption rate in eq. 6.5.a being fast, equilibrium between the gas phase and the surface can be assumed. The surface concentration of cumene is written with the equilibrium constant K_{Cu} :

$$C_{CuS} = K_{Cu} C_{Cu} C_S \tag{6.6}$$

The concentration of unoccupied surface sites C_S can then be expressed in terms of the total number of sites $C_t = C_S + C_{Cu}$:

$$C_S = \frac{C_t}{1 + C_{Cu} K_{Cu}} \tag{6.7}$$

The reaction of the adsorbed cumene molecules can then be written as a simple first order reaction in terms of concentration or conversion X as:

$$r = \frac{k_r C_t C_{Cu}}{1 + K_{Cu} C_{Cu}} = \frac{k_r C_t C_{Cu,0}(1 - X)}{1 + K_{Cu} C_{Cu,0}(1 - X)} \tag{6.8}$$

One can now try to correlate the observed conversions from the transient experiments with the Langmuir-Hinshelwood reaction rate (eq. 6.8) assuming, as a first approximation, steady state. Since the initial concentration was constant for all experiments at a given temperature, one can simplify eq. 6.8 in terms of the normalised concentration of cumene C'_{Cu}, as defined earlier $C'_{Cu}(t=0)=1$, as

$$r = \frac{a_h C'_{Cu}}{1 + b_h C'_{Cu}} = \frac{a_h(1-X)}{1+b_h(1-X)} \tag{6.9}$$

Writing the Langmuir-Hinshelwood equation as a "pseudo" first order rate one can derive the "constant" $k_{hinsh}(X)$ by setting $k_{hinsh}(1-X) = \frac{a_h(1-X)}{1+b_h(1-X)}$ to

$$k_{hinsh} = \frac{a_h}{1+b_h(1-X)}. \tag{6.10}$$

The correlation of k_{hinsh} is compared to the rate "constants" k_{eff} obtained from the model fits of the pulse experiments at T=440°C with different mass of catalyst and pellet radius. The coefficients a_h and b_h were estimated in a simple iteration to $a_h = 1500s^{-1}$ and $b_h = 5$ by fitting k_{hinsh} to the experimental k_{eff} . It can be seen that the Langmuir-Hinshelwood approach can at least qualitatively approximate the observed behaviour in k_{eff}. In or-

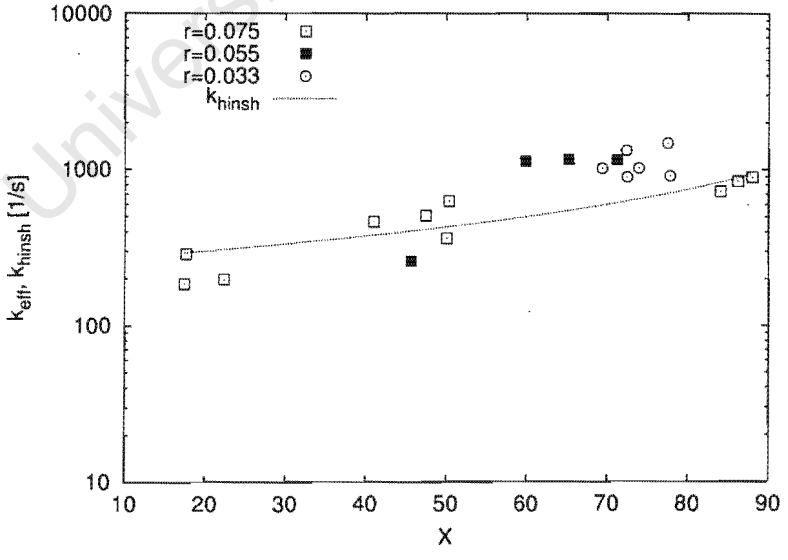

Figure 6.32: Comparison of k_{eff} approximated by eq.6.9 to experimental estimates from first order fit. Experiments at T=440°C

der to evaluate whether the Langmuir-Hinshelwood approach is suitable for explaining the transient reaction data, the term of the first order rate in the continuum model was substituted by eq. 6.9. The diffusion and adsorption parameters were unchanged and the above values for a_h and b_h were used. It can be seen from Figure 6.33 to 6.35 that the Langmuir-Hinshelwood model approximates first order *model* curves well. It should however be noted that a proof for the validity of the Langmuir-Hinshelwood approach would require the variation of the initial concentration. Furthermore, a parameter sensitivity and error analysis over a wide range of initial concentrations and conversions level would be required in order to justify any physical meaning of the obtained parameters. A quantitative analysis of the pulse experiments with a Langmuir-Hinshelwood model was hence not conducted.

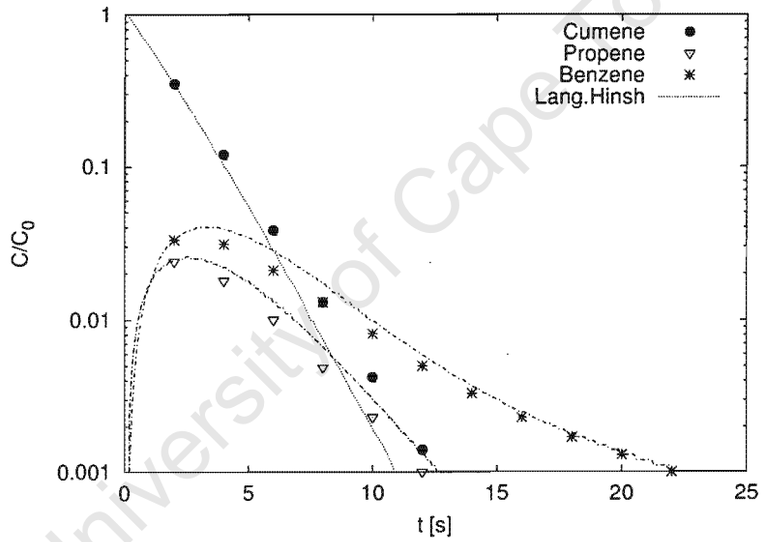

Figure 6.33: Comparison of first order reaction *model* fit to Langmuir-Hinshelwood approach. Model and run data from reaction run react3. Mass of catalyst 0.2g, Flow rate (@STP)=510 ml/min, Temperature 440°C.

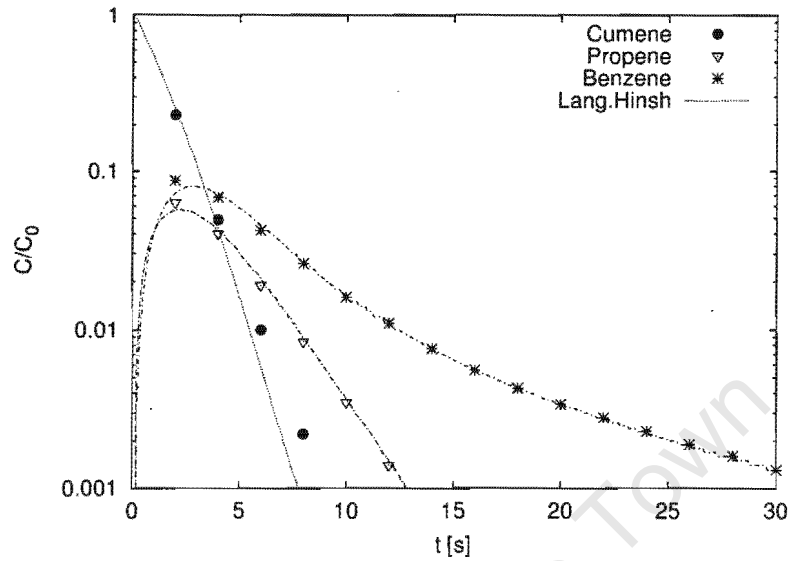

Figure 6.34: Comparison of first order reaction *model* fit to Langmuir-Hinshelwood approach. Model and run data from reaction run react53. Mass of catalyst 0.5g, Flow rate (@STP)=510 ml/min, Temperature 440°C.

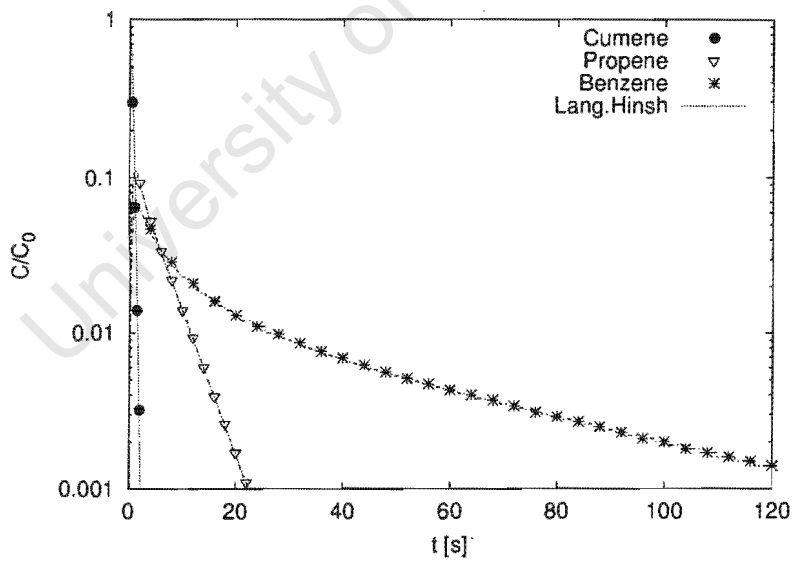

Figure 6.35: Comparison of first order reaction *model* fit to Langmuir-Hinshelwood approach. Model and run data from reaction run react12. Mass of catalyst 3g, Flow rate (@STP)=510 ml/min, Temperature 440°C.

6.2.3 Simultaneous parameter estimation

The assumption, that the ratio of the diffusivities β_{Cu}/β_{Pr} is known by the use of the Knudsen relation, may be wrong because of two reason: Sorption measurements of benzene showed that the transport in the macropores was enhanced by surface diffusion. It is as well possible that the bulkier cumene molecule is hindered at the pore mouth or at the intracrystalline channel of the zeolite crystals. The introduction of such an additional transport resistance would lead to a substantially lower value of an "effective diffusivity" than it is observed for benzene molecules.

The dependence of the parameter estimates on conversion, observed by the linear model assuming Knudsen diffusion, can either be explained by a non-linear model, as it was demonstrated above with the Langmuir-Hinshelwood approach, or by the invalidity of the Knudsen relation.

If the diffusivity of benzene is the only parameter that is known a priori , one has to find the remaining parameters k_{eff}, D_{Cu} and K_{Be} by simultaneously fitting experimental benzene curves of different values β_R (different catalyst). The estimation from a single experiment would lead to parameter estimates with too large error margins (see Section 5.3.4). Because of the small value of propene adsorption, any transport resistance of propene becomes negligible, so that the diffusivity D_{Pr} can be approximated by the Knudsen relation. The only additional unknown parameter is here K_{Pr}.

The parameter estimates from the simultaneous fit of all experiments (with different mass of catalyst, particle size and flow rate) are given in Table 6.4 for T=420°C and Table 6.5 for T=440°C. The corresponding model fits for experiments with different catalyst masses in Figure 6.36 to 6.38 demonstrate that the given parameter estimates allow a consistently good representation of the system. The confidence intervals for the adsorption parameters are well within a factor two to both sides. This relatively good confidence in the parameters also holds for the cumene diffusivity and the effective rate constant at T=420°. Much higher uncertainties for both parameters are however observed at T=440°C (see Table 6.5).

The qualitative analysis of the parameters suggests that benzene adsorption increases with temperature while the diffusion of cumene decreases significantly with temperature. Given the fact that adsorption is an exothermic process and diffusion is supposed to increase with temperature, this finding is physically not reasonable.

Furthermore, the simultaneous fit of all experiments at a temperature of 390°C was

not possible. Correlation coefficients R^2 below 0.4 were observed, which reflects the model inadequacy. This can be attributed to the increased error in the measurement of benzene concentration curves at longer times at lower concentration. This was shown in Figure 6.17 with the run react17-react20 and the highest loading of catalyst (3g), where the ratio of the total carbon yield of benzene and propene detected in the effluent stream was below one in comparison to the theoretical value of two.

At a temperature of 470°C, a simultaneous fit of all experiments was possible but no parameters could be estimated, because confidence intervals became infinite and parameter estimates were arbitrary. The reason for the degeneration of the parameter estimation is that at this temperature no experiments with a large amount of catalyst were conducted. The variation of the flow rate and the particle size by a factor two to three, proved to be insufficient for a parameter estimation.

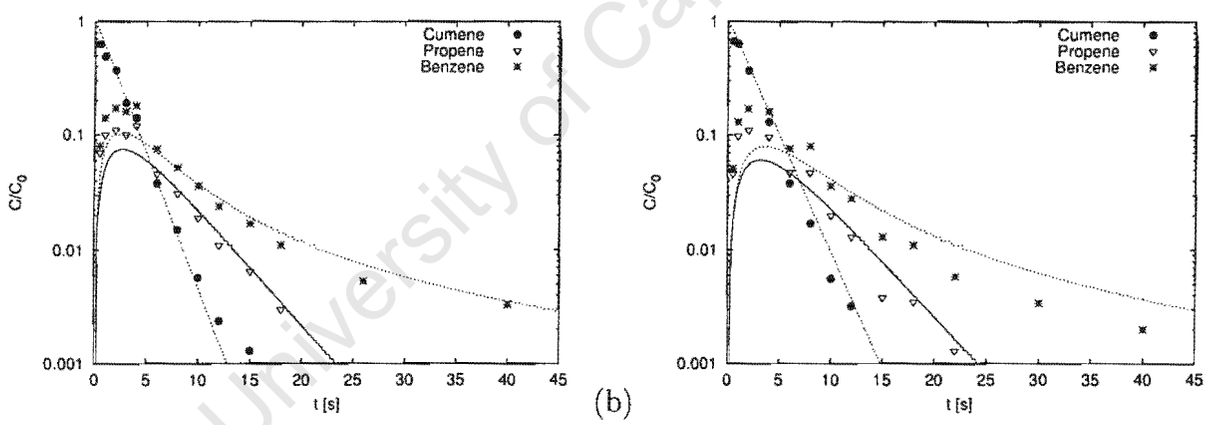

Figure 6.36: Model curve fit with parameters simultaneously estimated from all cumene pulse experiments at (a) T=440°C (react51) and (b) T=420°C (react48).
Catalyst Mass=0.5g; Flow(@STP)=310ml/min, Particle radius=0.075cm. $X \approx 60\%$

Table 6.4: Parameters estimated from simultaneous fitting of all pulse experiments at T=420°C. 95% confidence intervals given from the logarithmic value.

	Low Estimate	Estimate	High Estimate
$D_{Cu}[cm^2/s]$	$4.6 \cdot 10^{-4}$	$7.3 \cdot 10^{-3}$	$1.2 \cdot 10^{-2}$
$K_{Pr}[/]$	22	32	48
$K_{Be}[/]$	240	370	560
$k_{eff}[s^{-1}]$	201	303	458

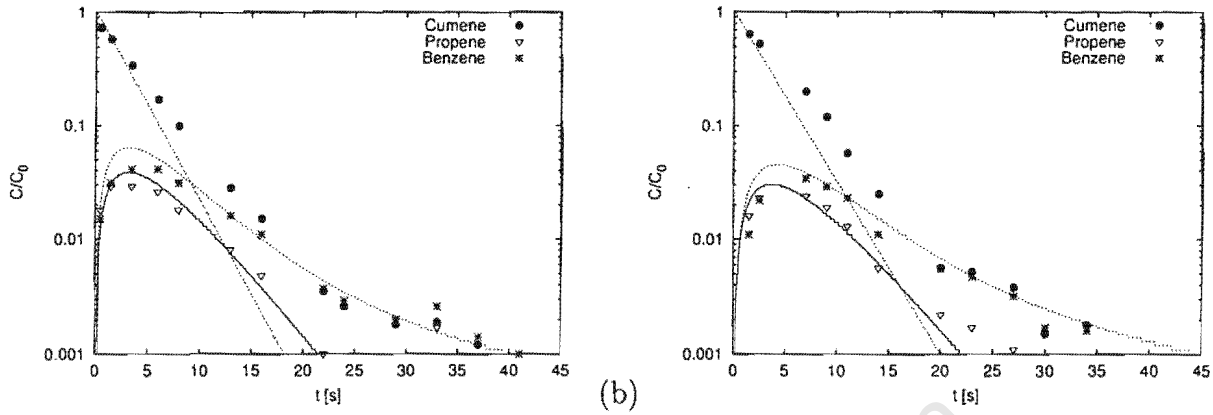

Figure 6.37: Model curve fit parameters simultaneously estimated from all cumene pulse experiments at (a) T=440°C (react1) and (b) T=420°C (react4).
Catalyst Mass=0.2g; $X \approx 20\%$; otherwise run conditions as in Figure 6.37.

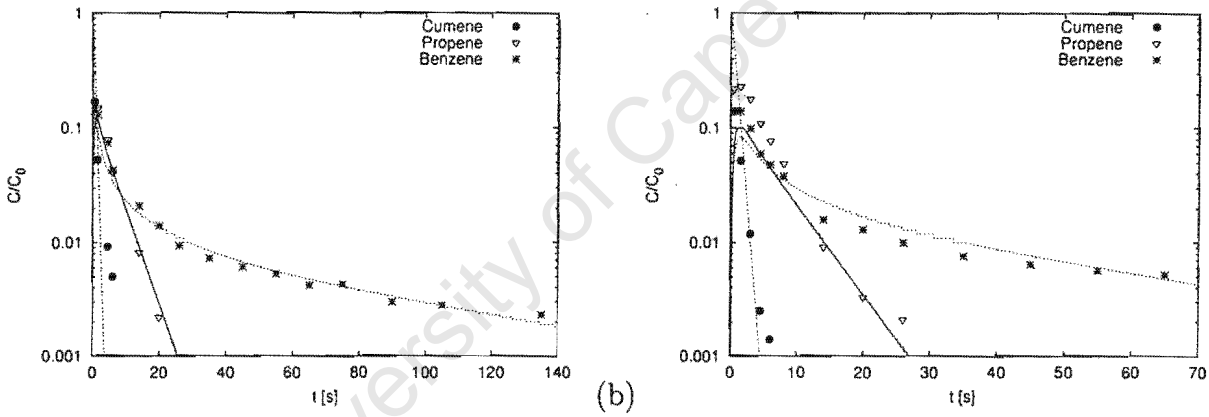

Figure 6.38: Model curve with parameters simultaneously estimated from all cumene pulse experiments at T=440°C (react14) and (b) T=420°C (react16).
Catalyst Mass=3.0g; $X \approx 85\%$; otherwise run conditions as in Figure 6.37.

Table 6.5: Parameters estimated from simultaneous fitting of all pulse experiments at T=440°C. 95% confidence intervals given from the logarithmic value.

	Low Estimate	Estimate	High Estimate
$D_{Cu}[cm^2/s]$	$2.4 \cdot 10^{-4}$	$1.0 \cdot 10^{-3}$	$4.2 \cdot 10^{-3}$
$K_{Pr}[/]$	26	31	38
$K_{Be}[/]$	550	740	1000
$k_{eff}[s^{-1}]$	870	3548	14474

6.2.4 Qualitative analysis of pulse experiments on E1-E3

The previous sections have demonstrated that a quantitative analysis of cumene pulse experiments on T4480 extrudates lead to parameter estimates with a high degree of error and uncertain temperature dependencies. Model fits could nevertheless represent a single pulse experiment well. Even if a reasonable quantitative analysis is not possible, a pulse analysis could hence be used for a fast screening of different catalyst with a test reaction.

In this sense, three extrudates E1-E3 were "screened" with pulse experiments of cumene at T=350°C at same run conditions (see Appendix L). The extrudates have, according to the supplier, the same zeolite content (75%) but have undergone different extrusion processes. Nevertheless, BET desorption plots in Appendix B show approximately same average pore diameters with 105, 96 and 98Å, where the samples E1 and E2 show a slightly bimodal form of the pore volume plot. It should thus be expected that the pulse response curves are similar.

In order to fit the response curves, the assumption that the *ratio* of the diffusivities can be calculated according to the Knudsen relation is made as in Section 6.2.2. Since the intrinsic activity can be expected to be the same for all three samples, k_{eff} is assumed to be constant. For a qualitative analysis it is sufficient to set the unknown parameter k_{eff} to an arbitrary value, here $k_{eff} = 2500s^{-1}$. This leaves three parameters to be unknown, D_{Cu}, K_{Be} and K_{Pr}, which have to be estimated from the response curves with a fitting routine.

For each extrudate two repeatability runs were conducted, as it has been already shown in Figure 6.18. The repeatability was in all cases excellent. Figure 6.39 shows that the model can represent the response curves very well. All model fits are given in Appendix L. The estimated parameters are shown in Table 6.6. (Note that the absolute values of the

Table 6.6: Parameter estimates from pulse experiments on E1-E3 extrudates. Numbers in brackets are the lower and higher 95% confidence intervals (logarithmic basis).

run ID	Extrud.	$D_{Cu}[cm^2/s] \cdot 10^3$	K_{Pr}	K_{Be}
react83	E1	(2.9) **7.0** (17)	(26) **74** (205)	(66) **254** (971)
react84	E1	(4.2) **9.1** (19)	(39) **80** (166)	(161) **408** (1034)
react85	E2	(2.3) **5.3** (12)	(10) **38** (132)	(41) **126** (386)
react86	E2	(2.5) **5.1** (11)	(23) **55** (133)	(37) **123** (407)
react87	E3	(1.9) **5.0** (13)	(14) **31** (69)	(22) **73** (245)
react88	E3	(2.9) **6.2** (13)	(0) **8** (126)	(34) **68** (126)

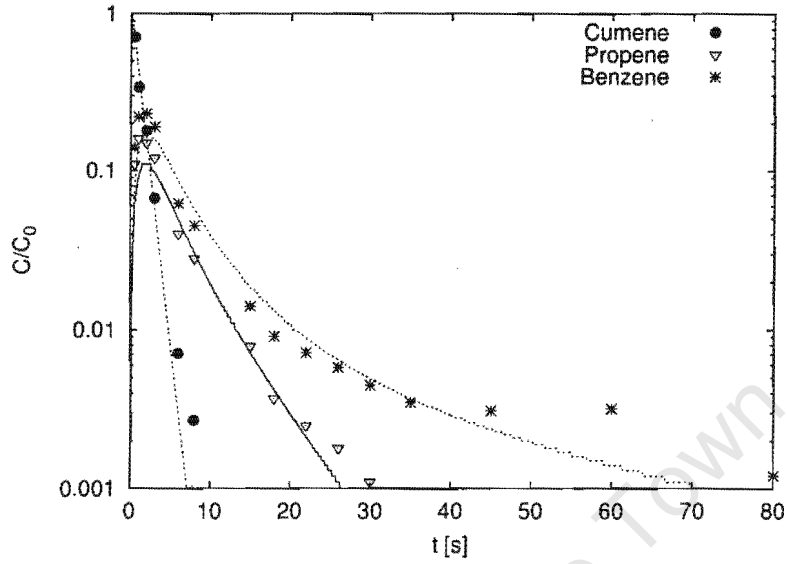

Figure 6.39: Model fit of cumene pulse experiment on extrudate E1, run react84 (see Appendix L. Conversion X=67%; T=350°C; mass of catalyst=0.5g; $R_y = 0.075cm$; F(@STP)=420ml/min

parameters are not physically meaningful, since the value of k_{eff} is arbitrary.) The results suggest that the diffusivity measured for extrudate E1 with the largest pore diameter is more than 50% higher than those estimated for extrudates E2 and E3. It is also indicated that the adsorption for benzene and propene is a factor 2 to three larger for extrudate E1. This relatively large discrepancy in the adsorption coefficients is questionable and cannot be explained by a change of physical properties due to a different extrusion process. The discrepancy in estimated adsorption can be explained by an examination of the confidence intervals. Confidence intervals for the estimated adsorption coefficient with a difference between the lowest and the highest estimate of a factor ten can be found. A more accurate estimation is suggested for the diffusivity within a factor four. Considering the uncertainty of the estimated parameters, differences in the response curves are thus too small in order to make any inferences on the effect of the extrusion process on the performance of the catalyst.

It can hence be concluded that a qualitative screening of catalysts with a pulse technique is only reasonable, if relatively large differences in the performance are to be expected, since the uncertainty in the parameter estimates will in general be very high.

6.3 Steady state experiments on T4480

Diffusion coefficients of cumene in T4480 extrudates are estimated from steady state experiments and are compared to those obtained from the transient experiments. Steady state experiments of cumene cracking on T4480 extrudates (3 sizes: 0.075cm, 0.043cm and 0.03cm) were conducted according to Section 3.2.2.3 in the jetloop reactor at four different temperatures (440°C, 420°C, 390°C and 350°C).

The Thiele modulus approach is used to calculate the diffusivities. The effectiveness factor, η, is obtained by dividing the observed first order rate constant for the pellets k_{obs} by the rate constant of the T4480 powder k_{eff} taken from experiments by Henry (1998). In order to compare data from powder experiments to those from extrudates, it has to be assumed that the alumina binder (25% weight) in the extrudates does not contribute to the catalytic behaviour. The inactivity of alumina in respect to cumene cracking is well documented in literature (Zdenek, 1985; Kania, 1981), so that the catalytic activity can be attributed only to the zeolite ZSM-5.

6.3.1 Carbon balance

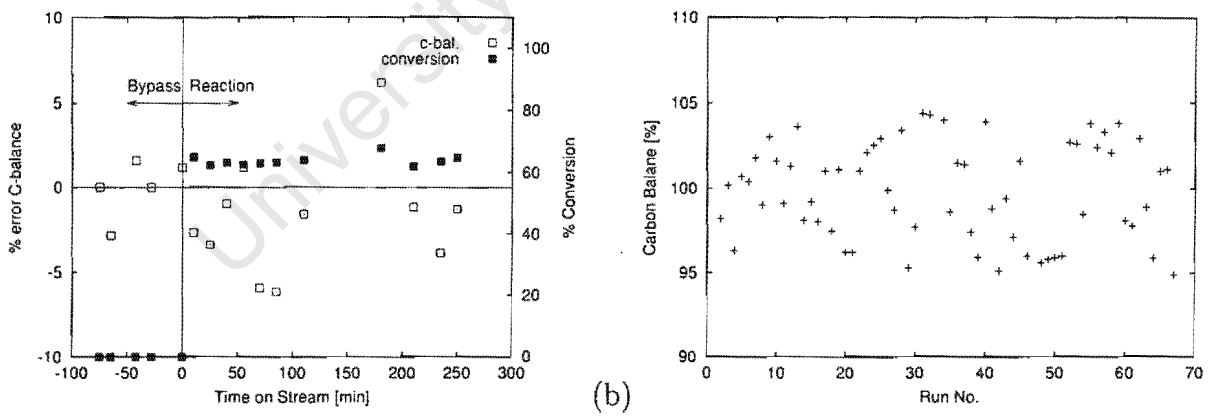

Figure 6.40: (a)Carbon balance and conversion as a function of time on stream. For run conditions and analysis see Table J.1. (b) Error in the carbon balance for all steady state runs.

Carbon balances and conversions were calculated by eq. 3.6 and eq. 3.7. A sample spreadsheet for the evaluation is given in Figure J.1 in the Appendix. All reaction run evaluations can be found in the Excel spreadsheets on the CD-ROM (see Appendix F).

A typical reaction run with the conversion and the error in the carbon balance can be seen in Figure 6.40.a. The error in the carbon balance is within 6% with an average carbon balance of 98.2%. The average carbon balance in Figure 6.40.b is for all steady state runs within an error of 5%.

6.3.2 Kinetic evaluation

6.3.2.1 Rate constant k_{eff} for powder

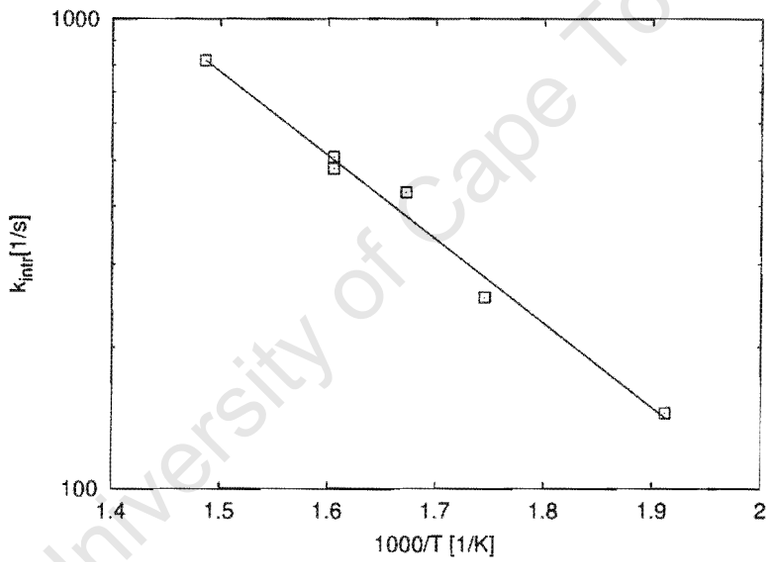

Figure 6.41: Arrhenius plot of effective rate constant k_{eff} taken from steady state experiments in a fixed bed by Henry (1998). Cracking of cumene over T4480 powder at a contact time of $m_{cat}/F_{Cumene} = 0.7g\,cat/(g/hr)$

Henry (1998) conducted kinetic experiments of cumene cracking on T4480 powder in a fixed bed reactor. Figure 6.41 shows the Arrhenius plot of the rate constant k_{eff}. The reported activation energy appears to be quite low with 34.2 kJ/mol. Such low values have been explained by Wei (1996): The effective rate constant is given by the intrinsic rate constant k_R multiplied by the adsorption constant K_c. Its activation energy is thus the sum $E_{eff} = E_{intr} + \Delta H_{ads}$. Similar activation energies for cumene cracking on ZSM-5 with different Si/Al ratios were observed by Malecka et al. (1987) with values between 33.9 to 50.7 kJ/mol.

6.3.2.2 Measurement of pellet rate constant k_{obs}

The pellet rate constant k_{obs} is based on the volume of zeolite powder V_{zeol} in the pellet. The value of k_{obs} can be calculated using the mass balance of the CSTR for a first order reaction in eq. 6.11

$$\begin{aligned} \frac{X}{1-X} &= slope \cdot \frac{1}{F} \\ slope &= V_{zeol} \cdot k_{obs}, \end{aligned} \tag{6.11}$$

from the slope through the origin of a plot $\frac{X}{1-X}$ vs. $\frac{1}{F}$. Such a plot is shown in Figure 6.42 with conversions X measured for four different flow rates at T=420°C and a particle size $R_y = 0.03cm$ and constant mass of catalyst 0.2g (or $V_{zeol} = 0.086ml$).

The results for the so calculated slopes and rate constants k_{obs} from all steady state experiments are given in the spreadsheet in Figure J.2 in the appendix. The estimated values are in good agreement to the results obtained in a fixed bed reactor by Henry (1998), who measured k_{obs} to be 50 1/s for $R_y = 0.075cm$ and 160 1/s for $R_y = 0.033cm$ as opposed to 80 1/s and 167 1/s in this work at a temperature of 350°C.

The Arrhenius plot of the estimated rate constant k_{obs} is shown in Figure 6.43. The respective activation energies can be determined as follows: $13.9\,kJ/(molK)$ for $R_y = 0.075cm$, $15.1\,kJ/(molK)$ for $R_y = 0.043cm$ and $12.5\,kJ/(molK)$ for $R_y = 0.033cm$. The lowest theoretically expected apparent activation energy of the observed rate constant is half the value of the intrinsic activation energy, if macropore diffusion is the limiting ($\varphi \gg 3$) process with a negligible activation energy (Fogler, 1999). The estimated activation energies are slightly smaller than this theoretically expected value of $17\,kJ/mol$, which reflects that the reaction is in the diffusion limiting regime.

The measured conversions X and the rate constants k_{obs} directly calculated from only one experiment are shown in Table J.1 in the appendix for all reaction runs. From these results it can be seen that the estimated rate constants were always smaller at flow rates lower than 235ml/min (@STP), which can be attributed to smaller recycle ratios at this flow rate and thus a possible intrusion of film resistance.

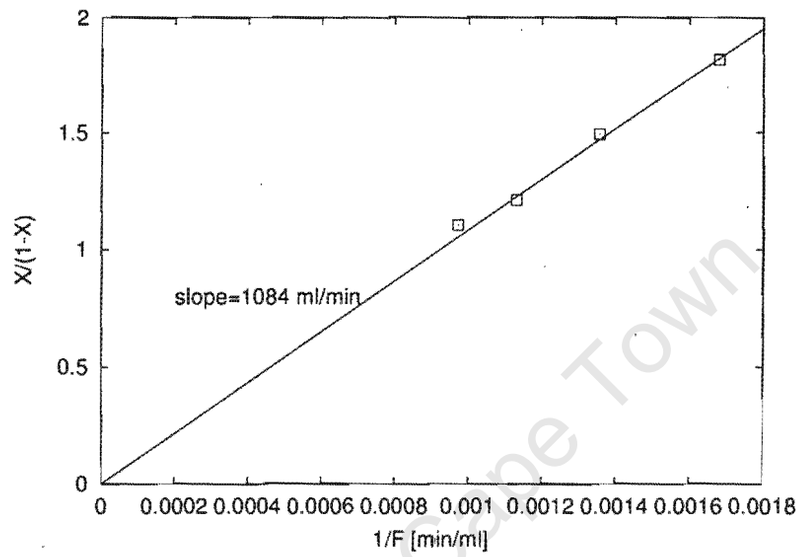

Figure 6.42: Evaluation of the pellet first order rate constant k_{obs}

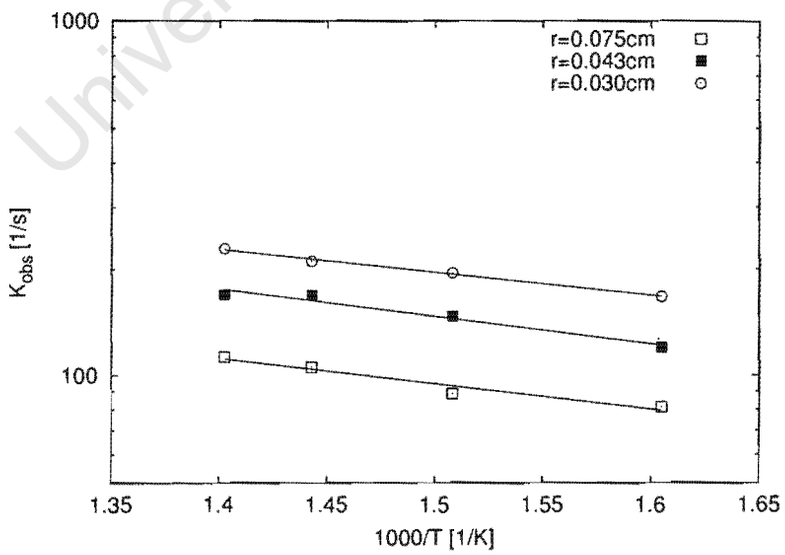

Figure 6.43: Arrhenius plot of pellet first order rate constant k_{obs}

6.3.2.3 Thiele modulus and diffusivity

The Thiele modulus φ can be directly calculated from the effectiveness factor $\eta = \frac{k_{obs}}{k_{eff}}$ eq. 2.10. The Thiele modulus has to account for the macropore voidage and solid volume fraction of the active zeolite and is defined as in the transient model (see eq. 5.36).

Macropore diffusivities can be directly calculated from the Thiele modulus, which is shown in the spreadsheet in Figure J.2 (see Appendix J).

The estimated values for the cumene macropore diffusivity are shown in Table 6.7. Slightly higher diffusivities are observed for the uncrushed pellet samples compared to the two crushed samples, while diffusivities decreased with temperature. For both trends deviations are smaller than 50% from the estimated values, which is within the experimental error. The average value for D_y is $0.01 cm^2/s$.

Table 6.7: Macropore diffusivities $D_y[cm^2/s]$ measured from steady state experiments at four different temperatures and three particle sizes.

R_y[cm]	350°C	390°C	420°C	440°C
0.075	0.014	0.010	0.012	0.011
0.043	0.011	0.010	0.009	0.008
0.033	0.011	0.009	0.008	0.008

6.3.2.4 Steady state vs. Transient

A direct comparison of the rate constant k_{eff} and the diffusivity for cumene D_y obtained from the transient and the steady state experiments is not possible, since additional assumptions had to be made for a unique parameter estimation from transient experiments. In a comparative study the following conclusions can however be drawn:

The steady state diffusivity for cumene is in excellent agreement to the diffusivity calculated from the benzene diffusivity using the Knudsen relation with an average value of $D_y = 0.012 cm^2/s$. This value had been used in Section 6.2.2 for the estimation of the rate constant k_{eff} and the benzene adsorption K_{Be} from a single pulse experiment. The analysis of pulse experiments using the same mass of catalyst as in the steady state experiments yielded 3 to 20 times smaller values of k_{eff} than it was observed by Henry (1998) for the case of steady state.

Conversions during pulse experiments were two to three times lower than those measured under steady state at the same run conditions. It has to be emphasised that the lower conversion can only be explained by a lower transient value of k_{eff}, if a transient cumene diffusivity of $D_y = 0.012cm^2/s$ is assumed. In contrast, assuming the same value of k_{eff} in the transient model as in the steady state and estimating for the unknown cumene diffusivity, would have led to an equally good model fit but with a lower value of the diffusivity.

Chapter 7

Conclusion

The jetloop reactor system fulfilled the requirements set by the continuum model, e.g. CSTR reactor, "ideal" pulse. It was proven by RTD studies that the jetloop reactor could always achieve a minimum needed recycle ratio of 20, which guarantees a good approximation to CSTR behaviour for the chosen reaction system. For reactions with a high reaction enthalpy and undiluted reactant feed streams this may however not hold true, so that even the maximum achievable recycle ratio of 70 in an empty reactor may be insufficient. Furthermore, a high momentum from the jet stream is needed, if the flow resistance in the catalyst bed is high, which may lead to an extremely small residence time. Small residence times, as 2s in this work, require a rapid sampling technique of the effluent stream. The semi-automated Multi-Ampoule-Sample (MAS) proved to be an excellent sampling technique for transient experiments. The fastest sampling rates were 1 sample per second. Pulse response curves could be monitored successfully, even if concentration levels decreased three orders of magnitude in 15 seconds. A disadvantage of this technique is (compared to a commercial multi-port valve) the time consuming gas chromatographic analysis, which has as yet not been automated.

The model description of the pulse sorption system without reaction is similar to that of the zero-length-column (ZLC) technique, where a step function is used as input function. The parameter estimation from the pulse response is as straightforward by calculating the adsorption coefficient from the first moment and the diffusion coefficient from the slope of the long time solution. An advantage of this analysis is that the validity of the model fit can be verified by comparing "as a third term" the intercept of the long time solution to

the experimental data. It has been shown that intercrystalline and intracrystalline diffusion cannot be simultaneously measured without varying particle sizes of the adsorbent. Experimental data of propane and butane on commercial zeolite 5A could be well described by this linear model. Parameters of intracrystalline diffusion and adsorption compare to those found in literature. Estimated values of propane adsorption on commercial ZSM-5 extrudates were in excellent agreement to values found in literature. Macropore diffusivities of propane in ZSM-5 extrudates were ten times larger than expected theoretically from Knudsen diffusion, while diffusivities of benzene were three to four times larger than theory. This enhancement of diffusional transport was ascribed to an additional parallel transport, the surface diffusion. This mechanism appears reasonable regarding the observed large extra-crystalline area of the small and intergrown ZSM-5 crystals. The small increase of diffusion with temperature and the relatively large influence of this mechanism are nevertheless unexpected. The variance of the estimated macropore diffusion coefficients was a factor two.

Adsorption coefficients and the adsorption enthalpy of benzene on the ZSM-5 extrudate were larger than any values found in literature. This phenomena is explained by the heterogeneity of the adsorption sites, which at very low sorbate concentrations, lead to a strong interaction with sorbate molecules like olefins and aromatics, as can be found in literature. This effect is furthermore enhanced by impurities and irregularities in the crystallite structure usually found in commercial zeolite samples. Estimated parameters from pulse experiments hence differ substantially from those found by alternative methods. The usefulness of the pulse technique for such systems is thus questionable.

The first order parameter sensitivity analysis proved to be a simple and useful tool in order to clarify the question of parameter uniqueness and measurability for pulse experiments with reaction. It was conclusively shown that the model parameters, e.g. diffusion, adsorption and reaction rate constant, are in general highly correlated to each other resulting in a high inaccuracy of the parameter estimates. This makes a thorough error analysis of the parameter estimates indispensable. For large values of the Thiele modulus φ it has been shown that there is an infinite number of different parameter sets with the same reactant response curve. For low values of the Thiele modulus, it was shown that the reactant curve may become relatively insensitive to changes of the Thiele modulus. The measurability of the adsorption coefficient is indirectly proportional to φ^3. If the reversible adsorption dynamics of the reactant become insignificant, the reactant response curve degenerates. The only information that can then be extracted from the reactant curve is the conversion.

A simultaneous parameter estimation from pulse response curves using a simple moment analysis will thus lead to erroneous results, which explains the discrepancies between transient diffusion measurements with and without reaction.

Pulse response curves of cumene on ZSM-5 extrudates showed no measurable effect of reversible adsorption with the system being at the same time diffusion limited, while the product curves of benzene and propene were clearly influenced by adsorption. It could be shown that two parameter estimation procedures are possible in such a case using a least square method to fit the model to the experimental data:

Using the diffusivity estimated from benzene pulse experiments and calculating the ratio of the diffusivities from the Knudsen relation, it should have been theoretically possible to accurately determine the two unknown parameters, reaction rate constant and the benzene adsorption coefficient. But results for both parameters had a scatter of more than an order of magnitude. The reaction rate constant was also found to be dependent on conversion, which could be qualitatively explained by a Langmuir-Hinshelwood model.

In an alternative procedure for the parameter estimation, experiments with different mass of catalyst, particle size and flow rate were fitted simultaneously. The diffusivity of benzene was again taken from benzene pulse experiments. Although good model fits could be achieved, a high degree of uncertainty in the parameter estimates was observed with a physically inconsistent temperature dependency. Moreover, conversions measured under transient conditions were two to three times lower than those measured for steady state.

An accurate and consistent parameter estimation from cumene pulse experiments was thus not possible.

Steady state experiments for the measurement of cumene diffusion using a Thiele modulus approach proved to be more accurate. The results were consistent with the diffusivity calculated by the Knudsen relation using the measured benzene diffusion coefficient. However, no adsorption properties can be measured with this method and a change of particle size is necessary.

Bibliography

Anderson, B., de Gauw, F., Noordhoek, N., van Ijzendoorn, L., van Santen, R., and de Voigt, M. (1998). *Ind. Eng. Chem. Res.*, 37:815–824.

Anderson, B., van Santen, R., and van Ijzendoorn, L. (1997). *App. Catal. A*, 160:125–138.

Aris, R. (1957). *Chem. Eng. Sci.*, 6:265.

Aris, R. (1975). *The Mathematical Theory of Diffusion and Reaction in Permeable Catalysts.* Oxford University Press, London.

Baiker, A., New, M., and Richarz, W. (1982). *Chem. Eng. Sci.*, 37(4):643.

Barrer, R. (1990). *J. Chem. Soc. Farad. Trans.*, 86(7):1123.

Berty, J. (1974). *Chem. Eng. Prog.*, 70:78.

Beschmann, K., Kokotailo, G. T., and Riekert, L. (1987). *Chem. Eng. Proc.*, 27:223.

Bird, R., Stewart, W., and Lightfood, E. (1960). *Transport Phenomena*, chapter 16, page 512. Wiley and Sons.

Blenke, H., Bohner, K., and Schuster, S. (1965). *Chem.-Ing.-Tech.*, 35:289.

Bülow, M., Schlodder, H., Rees, L., and Richards, R. (1986). In *7th Internat. Conf. on Zeolites, Tokyo.*

Brandani, S. (1996). *Chem. Eng. Sci.*, 51(12):3283–3288.

Brandani, S., Jama, M., and Ruthven, D. (2000). *Micr. and Mes. Mat.*, 35-36:283.

Brigham, E. (1988). *The Fast Fourier Transform and its Application.* Prentice Hall, New Jersey,.

Burghardt, A., Rogut, J., and Gotkowski, J. (1988). *Chem. Eng. Sci.*, 43:2463.

Caracotsios, M. and Stewart, W. (1985). *Comp. Chem. Eng.*, 9(4):359.

Caracotsios, M. and Stewart, W. (1995). *Comp. Chem. Eng.*, 19(9):1019.

Carberry, J. (1964). *Ind. Eng. Chem.*, 56(11):39.

Caro, J., Bülow, M., Schirmer, W., Kärger, J., Heink, W., and Pfeifer, H. (1985). *J. Chem. Soc. Faraday Trans. I.*, 81:2541.

Chen, N., T.F., D., and Smith, C. (1994). *Molecular Diffusion and Reaction in Zeolites.* VCH.

Chiang, A., Dixon, A., and Ma, Y. (1984). *Chem. Eng. Sci.*, 39(10):1461–1468.

Corrigan, T., Garver, J., Rase, H., and Kirk, R. (1953). *Chem. Eng. Prog.*, 49(11):603.

Costa, E., Calleja, G., and Domingo, F. (1985). *AIChE J.*, 31:982.

Cussler, E. (1984). *Diffusion.* Cambridge University Press.

Datka, J., Boczar, M., and Gil, P. (1995). *Coll. Suf. A*, 105:1.

Datka, J., Boczar, M., and Rymarowicz, P. (1988). *J. Catal.*, 114:368.

Dietz, W. (1967). *J. of G.C*, 68.

Do, D. (1998). *Adsorption Analysis: Equilibria and Kinetics.* Imperial College Press, 1 edition.

Do, D. and Smith, J. (1984). *Chem. Eng. Sci.*, 39(12).

Doelle, H.-J., Heering, J., and Riekert, L. (1981). *J. Catal.*, 71:22.

Dogu, G. and Smith, J. (1975). *AIChE J.*, 21(1):58.

Dogu, G. and Smith, J. (1976). *Chem. Eng. Sci.*, 31:123.

Dreyer, D. and Luft, G. (1982). *Chemie-Technik*, 9:1061.

Dreyer, D. and Luft, G. (1984). *Chemie-Technik*, 4:123.

Duncan, W. and Möller, K. (2000). *Chem. Eng. Sci.*, 55(22):5413–5418.

Eic, M. and Ruthven, D. (1989). In Jacobs, P. and van Santen, editors, *8th Internat. Conf. on Zeolites, Amsterdam*, page 897. Elsevier.

Eic, M. and Ruthven, D. M. (1988). *Zeolites*, 8:40–45.

Finlayson, B. (1973). *Method of Weighted Residuals and Variational Priniciples.* Academic Press, New York.

Fogler, H. (1999). *Elements of chemical reaction engineering*, pages 817–819. Prentice Hall, 3 rd ed edition.

Forni, L., Viscardi, C., and Oliva, C. (1986a). *J. Catal.*, 97:469.

Forni, L., Viscardi, C., and Oliva, C. (1986b). *J. Catal.*, 97:480.

Fukase, S. and Wojciechowski (1986). *J. Catal.*, 102(452).

Fuller, Schettler, and Giddings (1966). *Ind. Eng. Chem.*, 58:18.

Garcia, S. and Weisz, P. (1993). *J. Catal.*, 142:691.

Gleaves, J. and Ebner, J. (1986). *Method and apparatus for carrying out the catalyzed chemical reactions and for studying catalysts.* U.S. Patent 4,626,412 assigned to Monsanto Company.

Gleaves, J., Ebner, J., and Kuechler, T. (1988). *Catal. Rev. Sci. Eng.*, 30:49–116.

Haag, W., Lago, R., and Weisz, P. (1982). *Farad. Disc.*, 72:317.

Hampson, J. and Rees, L. (1993). *J. Chem. Soc. Farad. Trans.*, 86:3169.

Hayhurst, D. and Paravar, A. (1988). *Zeolites*, 8:27.

Heink, W., Kärger, J., Pfeifer, H., Salverda, P., Datema, K., and Nowak, A. (1992). *J. Chem. Soc. Farad. Trans.*, 88(3):515.

Henry, P. (1998). Cumene cracking over zsm-5 - a diffusional atudy. Master's thesis, University of Cape Town.

Hill, C. (1977). *An Introduction to Chemical Engineering Kinetics and Reactor Design*, chapter 12. John Wiley and Sons, New York.

Hindmarsh, A. (1980). *ACM-SIGNUM Newsl.*, 15(4):10.

Hong, U., Kärger, J., Hunger, B., N.N., F., and Zhdanov, S. (1992). *J. Catal.*, 137:243.

HSU, L.-K. and Haynes, Jr., H. W. (1981). *AIChE J.*, 27(1):81–91.

Hufton, J. and Danner, R. (1993). *AIChE J.*, 39(6):954–961.

Hufton, J., Ruthven, D., and Danner, R. (1995). *Mic. Mat.*, 5:39.

Iauw-Bieng, T. and Biegler, L. (1991). *Ind. Eng. Chem. Res.*, 30:376.

IZA Structure Comission (2001). Internet: http://www.iza-online.org.

Kania, W. (1981). *Bull. Acad. Pol. Sci. Ser. Sci. Chim*, 29(7-8):365.

Karge, H. and Niessen, W. (1991). *Catalysis Today*, 9:451.

Kärger, J. and Ruthven, D. (1992a). *Diffusion in Zeolites and Other Microporous Solids*, chapter 8.2.5, page 228. Wiley, New York.

Kärger, J. and Ruthven, D. (1992b). *Diffusion in Zeolites and Other Microporous Solids*. Wiley, New York.

Kärger, J. and Ruthven, D. (1992c). *Diffusion in Zeolites and Other Microporous Solids*, chapter 9.4, page 272. Wiley, New York.

Kärger, J. and Ruthven, D. (1992d). *Diffusion in Zeolites and Other Microporous Solids*, chapter 9.2, page 240. Wiley, New York.

Kelly, J. and Fuller, O. (1972). *Can. J. Chem. Eng.*, 50:534.

Klemm, E. and Emig, G. (1997a). *Mic. Mat.*, 12:281.

Klemm, E. and Emig, G. (1997b). *Chem. Eng. Sci*, 52(23):4329.

Knudsen, M. (1909). *Annal. der Physik (Leipzig)*, 28:75.

Kärger, J., Pfeifer, H., and Haberlandt, R. (1980). *J.Chem.Soc.Farad. Trans. I.*, 76:1569.

Lechert, H. and Schweitzer, W. (1984). In Olson, D. and Bisio, A., editors, *Proc. of 6th Internat. Zeolite Conf., Reno, 1983*, page 210.

Levenspiel, O. (1972). *Chemical Reaction Engineering.* John Wiley and Sons, 2 edition.

Luft, G. and Herbertz, H.-A. (1969). *Chem. Ing. Tech.*, 41(11):667.

Magalhaes, F., Laurence, R., and Conner, W. (1996). *AIChE J.*, 42(1):68.

Malecka, A., Bielanski, A., Berak, J., and Datka, J. (1987). *Bull. Pol. Acad. Sci. Chem.*, 35(3-4):133.

McGreavy, C. and Siddiqui, M. (1980). *Chem. Eng. Sci.*, 35:3.

Meier, W. and Olson, D. (1996). *Atlas of Zeolite Structure Types.* Butterworth-Heinemann, Boston, MA, 4 edition.

Micke, A., Bülow, M., and Kocirik, M. (1994). *J. Phys. Chem.*, 98:924.

Mills, P. and Lerou, J. (1993). *Rev. Chem. Eng.*, 9(1-2):1–96.

Miro, E., Ardiles, D., Lombardo, E., and Petunchi, J. (1986). *J. Catal.*, 97:43.

Miro, E., Lombardo, E., and Petunchi, J. (1987). *J. Catal.*, 103:204.

Möller, K. (1989). PhD thesis, University of Cape Town.

Möller, K., Fletcher, J., O'Connor, C., and Becker, R. (1995). *Chem. Eng. Comm.*, 137:111–118.

Möller, K. and O'Connor, C. (1994). In J. Weitkamp, H.G. Karge, H. P. and Hölderich, W., editors, *Zeolites and related microporous materials: state of the art*, volume 84B of *Studies in Surface Science and Catalysis*, pages 1201–1208. Elsevier, Amsterdam.

Möller, K. and O'Connor, C. (1996). *AIChE J.*, 42(4):1187.

Niessen, W. and Karge, H. (1993). *Mic. Mat.*, 1(1).

Nijhuis, T., Van den Broeke, L., Van De Graaf, J., Kapteijn, F., Makkee, M., and Moulijn, J. (1997). *Chem. Eng. Sci.*, 52(19):3401–3404.

Nijhuis, T. A. (1998). *Towards a new propene epoxidation process - Transient adsorption and kinetics measurements applied in catalysis.* PhD thesis, Delft University of Technology (in English).

Niwa, M., Itoh, H., Kato, S., Hattori, T., and Murakami, Y. (1982). *J. Chem. Soc. , Chem. Commun.,*, 15:819.

Paravar, A. and Hayhurst, D. (1984). In Olson, D. and Bisio, A., editors, *Proc. 6th Int. Zeolites Conf.*, page 217. Butterworths, Guildford, England.

Park, S. and Kim, Y. (1984a). *Chem. Eng. Sci.*, 39(3):523–531.

Park, S. and Kim, Y. (1984b). *Chem. Eng. Sci.*, 39(3):533–549.

Perry, R., Green, D., and Maloney, J., editors (1997). *Perry's Chemical Engineers' Handbook*, chapter 2, page 95. MacGraw-Hill, 7 edition.

Pichler, H. and Gärtner, R. (1962). *Brennstoff-Chem.*, 43:336.

Pope, C. (1984). *J. Phys. Chem.*, 88:6312.

Pope, C. (1986). *J. Phys. Chem.*, 90:837.

Post, M. (1991). In van Bekkum, H., Flamingen, E., and Jansen, J., editors, *Introduction ot Zeolite Science and Practise*, page 391. Studies in Surface Science and catalysis 58, Elsevier.

Post, M., van Amstel, J., and Kouwenhoven, H. (1983). In Olson, D. and Bisio, A., editors, *Proc. of the 6th Zeolite Conference*, page 517. Butterworths, Guildford, England.

Prater, C. and Lago, R. (1956). *Adv. in Catal.*, 8:293.

Press, W., Teukolsky, S., Vetterling, W., and Flannery, B. (1988). *Numerical Recipes in C-The Art of Scientific Computing*, page 657. Cambridge University Press, 2 edition.

Qureshi, W. R. and Wei, J. (1990). *J. Catal.*, 126:147.

Rabitz, H., Kramer, M., and Dacol, D. (1983). *Ann. Rev. Phys. Chem.*, 34:419.

Randal, E., Moon, P., and Garvin, A. (1993). *Journal of Microcomputer Applications*, 16:385–393.

Rippin, D. (1967). *I and EC Fund.*, 6(4):488.

Rivarola, J. and Smith, J. (1964). *Ind. Eng. Chem. Fund.*, 3:308.

Ruckenstein, E., Vaidyanathan, A., and Youngquist, G. (1971). *Chem. Eng. Sci.*, 26:1305–1318.

Ruthven, D. (1984). *Principles of Adsorption and Adsorption Processes.* Wiley, New York.

Ruthven, D. and Derrah, R. (1972). *J. Chem. Soc. Farad. Trans. I*, 68:2332.

Ruthven, D. and Xu, Z. (1993). Diffusion of oxygen and nitrogen in 5a zeolite crystals and commercial 5a pellets. *Chem. Eng. Sci.*, 48(18):3307.

Sandler, S. (1989). *Chemical and Engineering Thermodynamics.* Wiley and Sons, 2 edition.

Satterfield, C. and Cadle, P. (1968). *Ind. Eng. Chem. Proc. Des. Develop.*, 7(2):256–265.

Schermuly, O. and Luft, G. (1978). *Ger. Chem. Eng.*, 1(4):222.

Schnitzler, A. (1997). *Studies of the Methanol to Hydrocarbon Reaction in the Jetloop Reactor.* PhD thesis, University of Cape Town.

Schobert, M. and Ma, Y. (1981a). *J. Catal.*, 70:102.

Schobert, M. and Ma, Y. (1981b). *J. Catal.*, 70:111.

Schulz, H., Boehringer, W., Kohl, C. P., Rahman, N., and Will, A. (1984). Development and application of the capillary gc total sample technique for gas/vapour multi-component mixtures. In *DGMK-Forschungsbericht 320.* DGMK.

Shah, D., Hayhurst, D., Evanina, G., and Guo, C. (1988). *AIChE J.*, 34:1713.

Shah, D. and Ruthven, D. (1977). *AIChE J.*, 23(6):804–809.

Silva, J. and Rodrigues, A. (1996). *Gas. Sep. Purif.*, 10(4):207–224.

Sommers, H. (1971). *Chem.-Ing.-Tech.*, 43:1177.

Song, L. and Rees, L. (2000). *Micr. and Mes. Mat.*, 35-36:301.

Stach, H., Thamm, H., Jänchen, J., Fiedler, K., and Schirmer, W. (1984). In Olson, D. and Bisio, A., editors, *Proc. of 6th Internat. Zeolite Conf., Reno, 1983*, page 225.

Stewart and Associates Engineering Software Inc Madison Wisconsin, U. (1996). Gregpak96.

Sun, M., O., T., and Shah, D. (1996). *AIChE J.*, 42(11):3001.

Suzuki, M. and Smith, J. (1971). *Chem. Eng. Sci.*, 26:221.

Swabb, E. and Gates, B. (1972). *Ind. Eng. Chem. Fund.*, 11(4):540.

Szostak, R. (1992). *Handbook of Molecular Sieves.* van Nostrand, Reinhold, New York.

Thamm, H. (1987). *J. Phys. Chem.*, 91:8.

Thamm, H., Jerschkewitz, H.-G., and Stach, H. (1988). *Zeolites*, 8:151.

Thiele, E. (1939). *Ind. Eng. Chem.*, 31:916.

van den Begin, N., Rees, L., Caro, J., and Bülow, M. (1989). *Zeolites*, 9:287.

van Santen, R., Anderson, B., Cunninghan, R., Mangnus, A., Ijzendoorn, L., and de Voigt, M. (1996). *Angew. Chem. Int. Ed. Engl.*, 35(23/24):2785.

Villadsen, J. and Michelsen, M. (1978). *Solution of Differential Equation Models by Polynomial Approximation.* Prentice Hall, New Jersey.

Voogd, P. and van Bekkum, H. (1990). *Appl. Catal.*, 59:311.

Wei, J. (1996). *Chem. Eng. Sci.*, 51(11):2995.

Weisz, P. and Goodwin, R. (1963). *J. Catal.*, 2:397.

Weisz, P. and Goodwin, R. (1966). *J. Catal.*, 6:227.

Weisz, P. and Hicks, J. (1962). *Chem. Eng. Sci.*, 17:265.

Weisz, P. and Prater, C. (1954). *Adv. Catal.*, 6:143.

Weitkamp, J. (1988). In Grobet, P., Mortier, W., Vansant, E., and Schulz-Ekloff, G., editors, *Innovation in Zeolite Materials Science*, volume 37, page 515. Studies in Surface Science and Catalysis.

Wernick, D. and Osterhuber, E. (1985). *J. Membrane Sci.*, 22:137.

Wicke, E. and Kallenbach, R. (1941). *Kolloid Z.*, 97:135.

Yang, R. (1987a). *Gas Separation by Adsorption Processes.* Butterworth.

Yang, R. (1987b). *Gas Separation by Adsorption Processes*, chapter 5, page 155. Butterworth.

Yang, R. (1987c). *Gas Separation by Adsorption Processes*, chapter 4, pages 120–121. Butterworth.

Yasuda, Y. (1994). *Heterogenous Chemistry Reviews*, 1:103.

Zdenek, V. (1985). *Coll. Czeck. Chem. Comm.*, 50:1268.

Appendix A

X-ray diffraction

A.1 ZSM-5 T4480

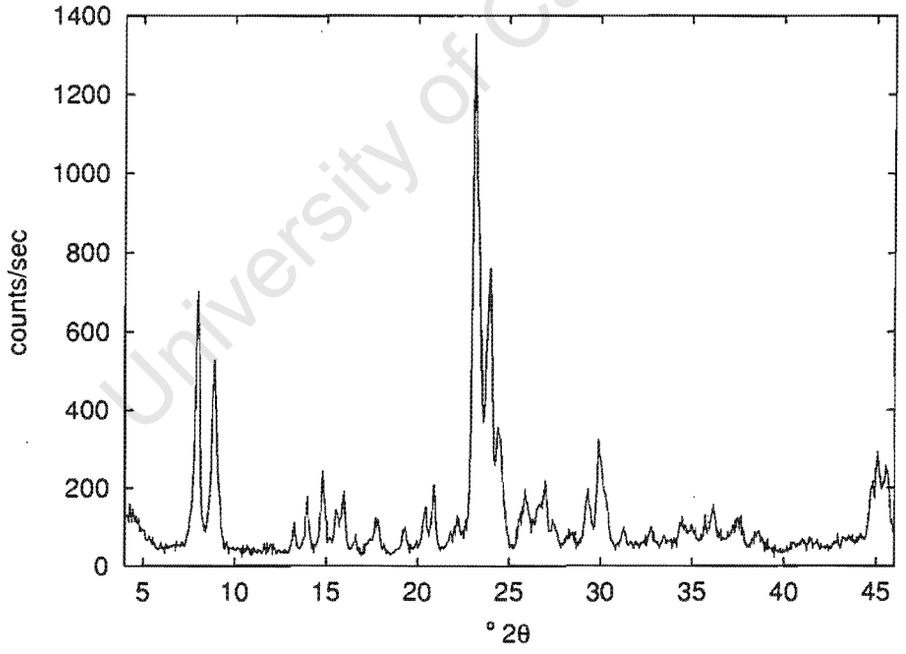

Figure A.1: XRD ZSM-5 T4480

A.2 ZSM-5 P1

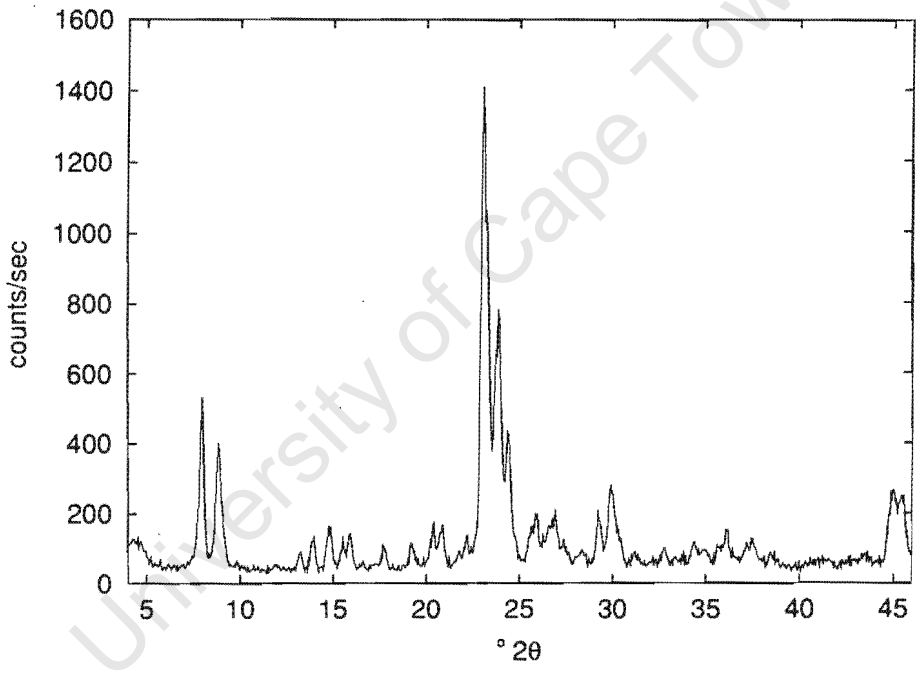

Figure A.2: XRD ZSM-5 P1

Appendix B

BET-Analysis

B.1 Extrudate T4480

B.1.1 BET-Isotherm

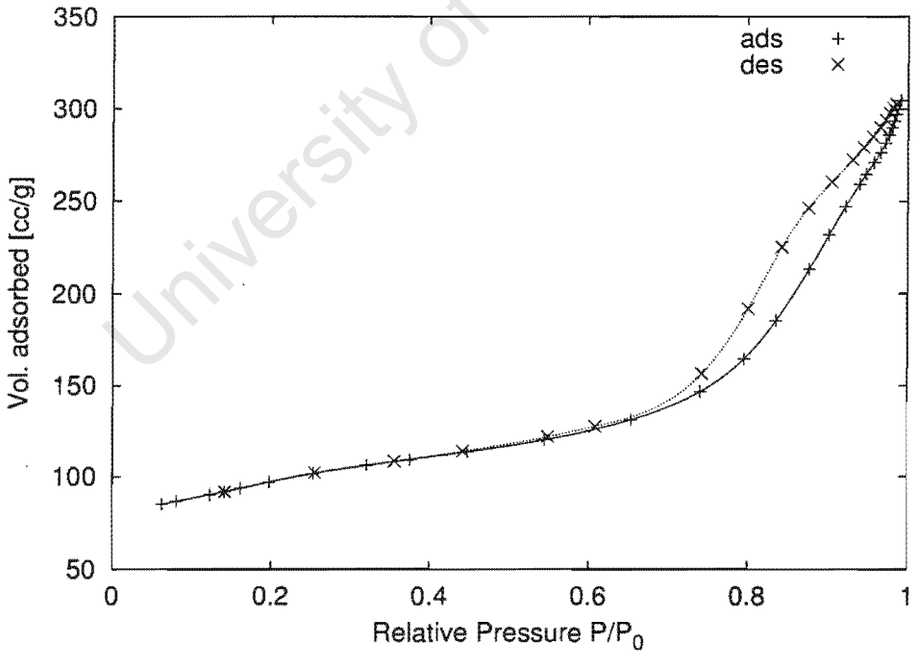

Figure B.1: BET-Isotherm for T4480 extrudates

B.1.2 Desorption pore volume plot

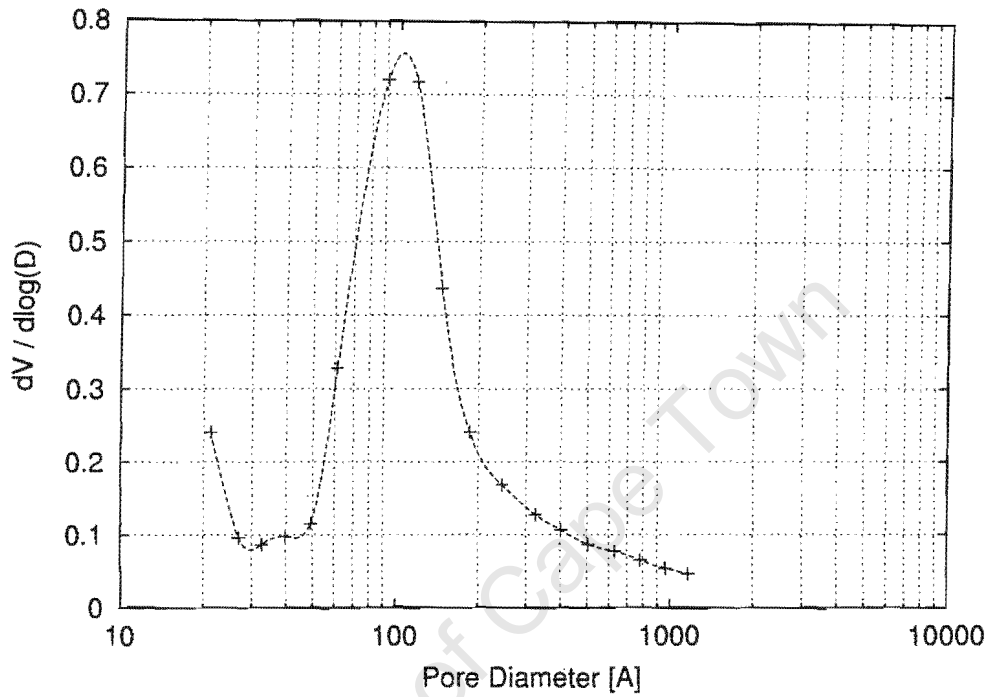

Figure B.2: BET: Desorption Pore volume plot T4480 extrudates

BJH Desorption average pore diameter: 78.9 Å

B.2 Extrudates E1-E3

B.2.1 BET-Isotherm

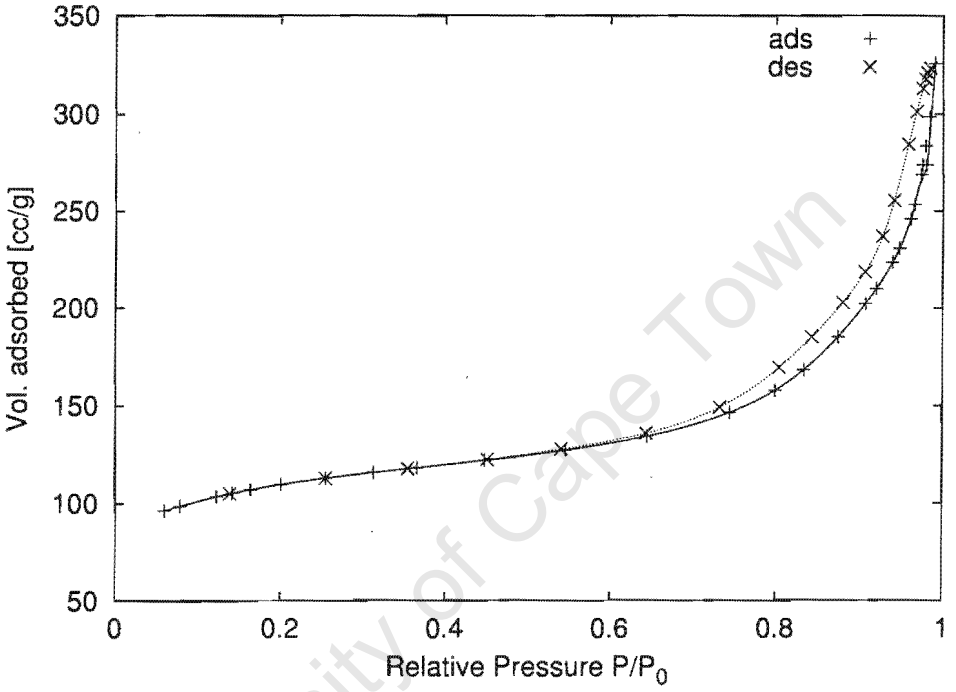

Figure B.3: BET-Isotherm for E1 extrudates

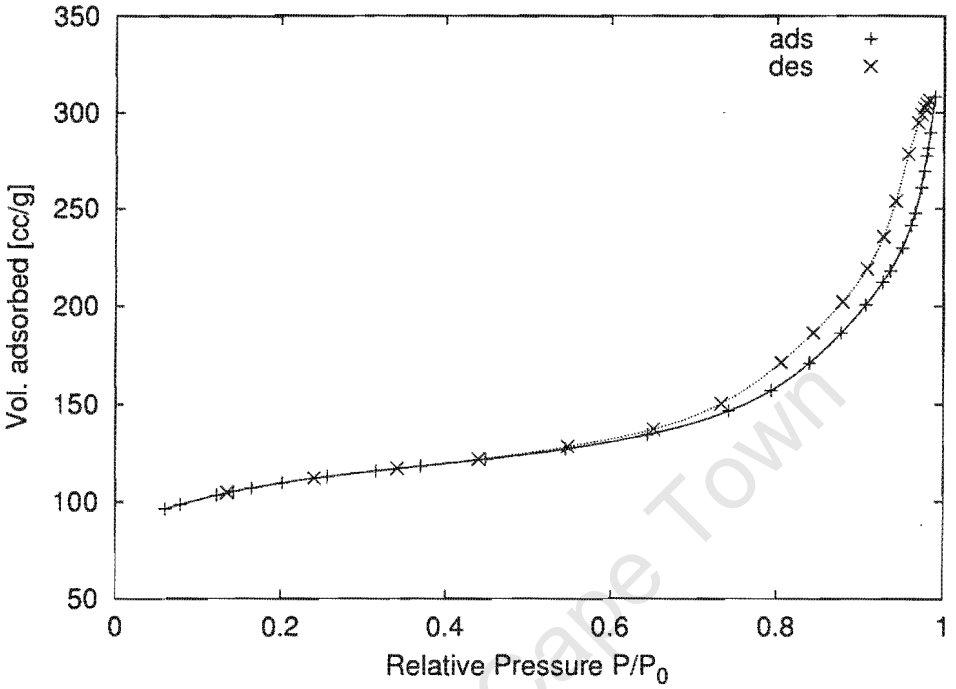

Figure B.4: BET-Isotherm for E2 extrudates

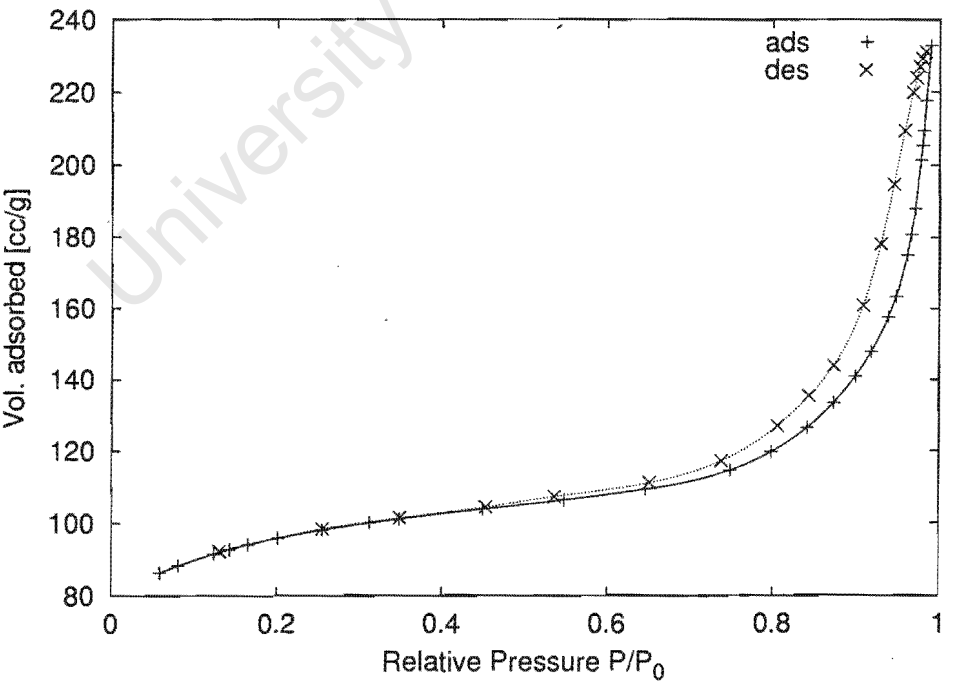

Figure B.5: BET-Isotherm for E3 extrudates

B.2.2 Desorption pore volume plot

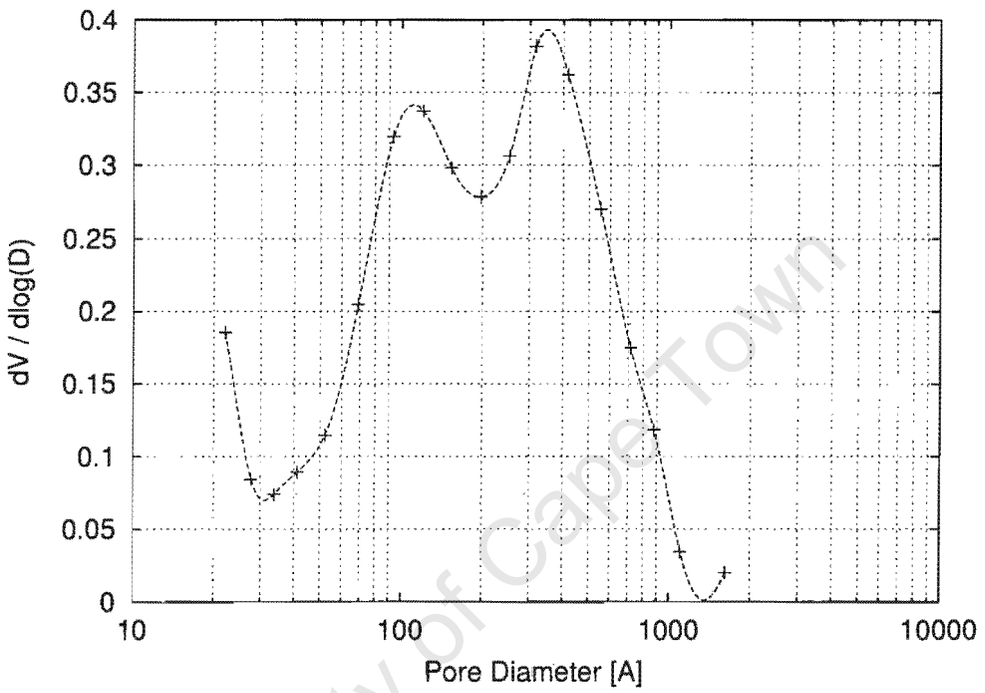

Figure B.6: BET: Desorption Pore volume plot for E1 extrudates

BJH Desorption average pore diameter: 105 Å
BJH Desorption average pore diameter: 96 Å
BJH Desorption average pore diameter: 98 Å

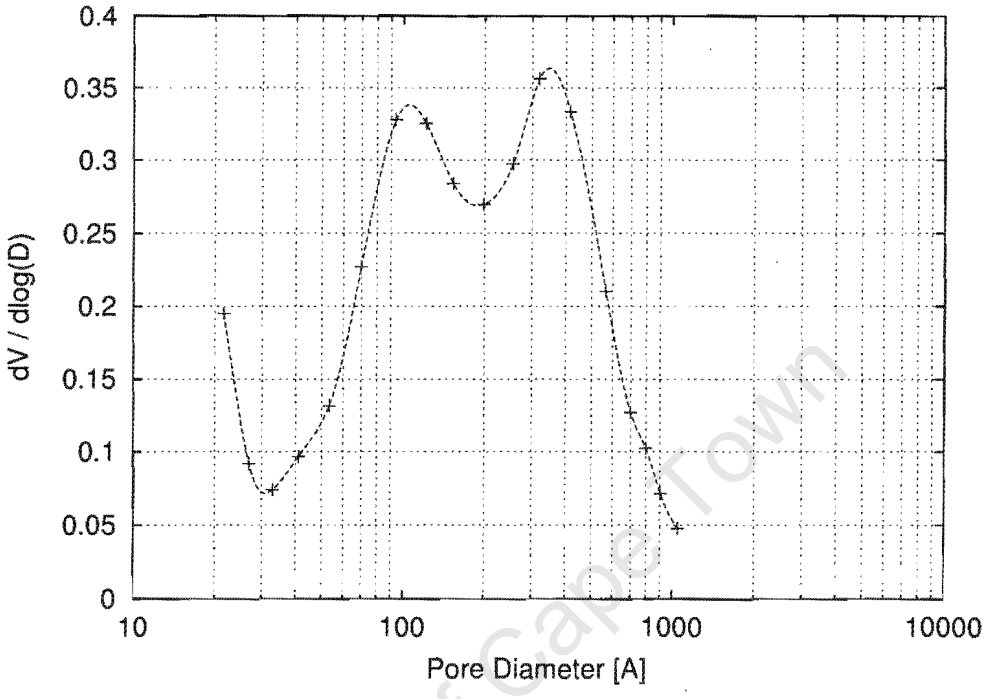

Figure B.7: BET: Desorption Pore volume plot for E2 extrudates

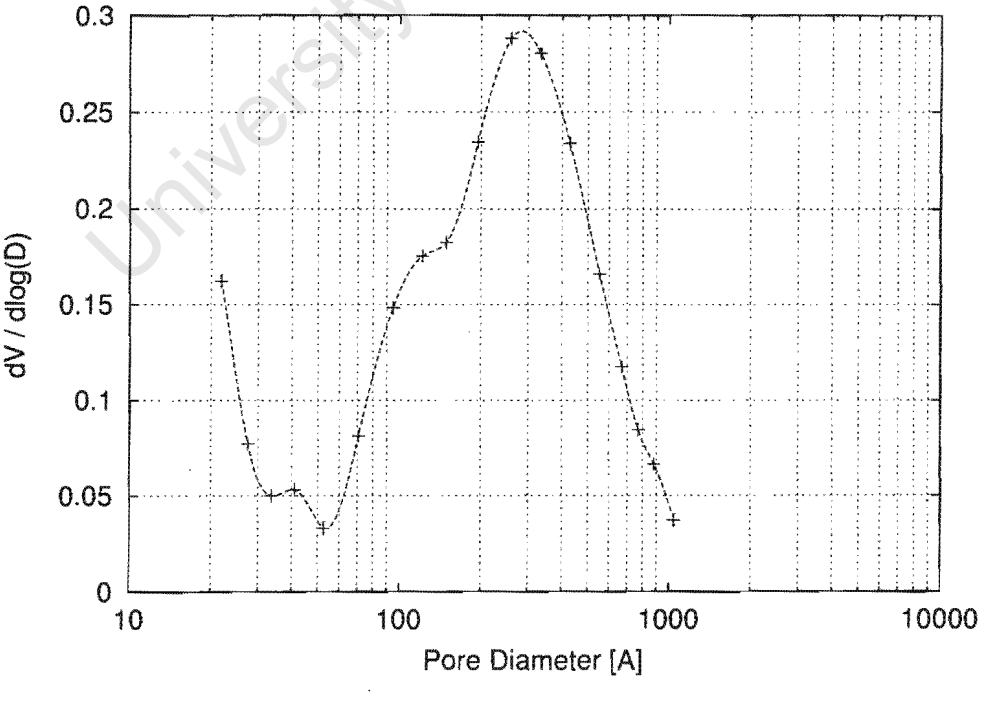

Figure B.8: BET: Desorption Pore volume plot for E3 extrudates

Appendix C

Gas chromatographic analysis

Program Gas Chromatogram:

Chromatograph Hewlett-Packard HP 5890A

column OV1 (15m x 0.32 mm, film-thickness 0.5 μm)

FID H_2 (30ml/min); Air (350 ml/min); He (20 ml/min) as make-up gas
Temperature 270°C

Carrier gas helium, column flow 2ml/min

Split 1:50

Temperature 50°C (2min); Ramping 10°/min; 120°C

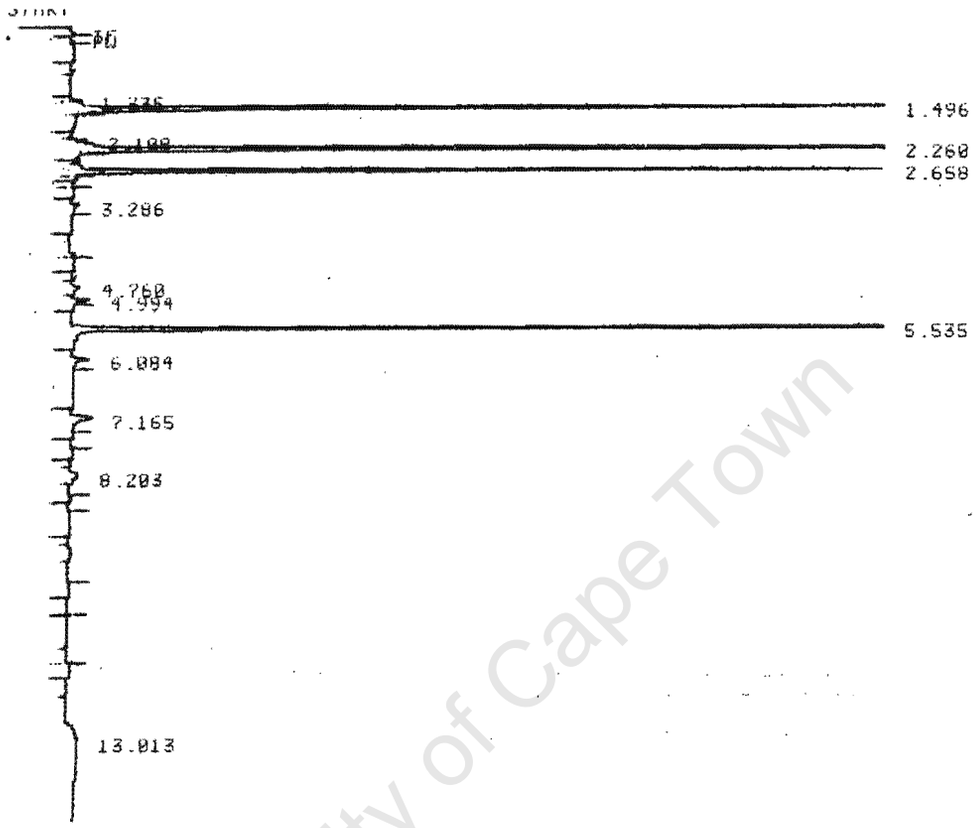

Retention time [min]	Area	
1.335	1251	
1.496	187860	propene
2.108	2114	
2.260	319407	benzene
2.658	138750	n-heptane
3.286	1709	
4.760	2358	
4.994	2899	
5.535	237821	cumene
6.084	4143	
7.165	10027	
8.203	4641	

Appendix D

RTD studies of Multi-Ampoule-Sampler

D.1 Pulse of propane or benzene in empty JLR

Table D.1: Pulse: Propane #1, τ =3.5 s, Flow (@STP)= 490 ml/min, T= 473 K, Relative area for normalisation $\int Area_{C_3}/Area_{ISTD}dt$ =31.8 s

Amp No	t [s]	Area C-3	Area ISTD	C/Co	FID	error %	log error %
1	0	1980	133718	0.0016	0.0012	27.0	-3.6
2	0.5	1408791	170517	0.8658	0.7300	18.6	-54.2
3	1.5	1059587	140938	0.7879	0.6720	17.2	-40.0
4	2.5	794109	140689	0.5915	0.5020	17.8	-23.8
6	6.5	271860	127315	0.2238	0.1660	34.8	-16.6
7	8.5	165546	138064	0.1257	0.0960	30.9	-11.5
8	10.5	419001	765027	0.0574	0.0560	2.5	-0.9
9	12.5	252661	754082	0.0351	0.0340	3.3	-1.0
10	14.5	209189	887308	0.0247	0.0200	23.5	-5.4
11	16.5	97473	839610	0.0122	0.0120	1.4	-0.3
12	18.5	53804	802786	0.0070	0.0070	0.3	-0.1
13	20.5	31607	591922	0.0056	0.0040	39.9	-6.1
14	22.5	16878	666754	0.0027	0.0022	20.6	-3.1
16	26.5	8914	599348	0.0016	0.0007	122.7	-11.0
18	30.5	4317	540735	0.0008	0.0002	318.3	-16.8
19	32.5	3315	587487	0.0006	0.0001	491.3	-19.3

Table D.2: Pulse: Benzene #2, τ =3.5 s, Flow (@STP)= 490 ml/min, T= 473 K, Relative area for normalisation $\int Area_{C_6}/Area_{ISTD}dt$ =8.6 s

Amp No	t [s]	Area C-6	Area ISTD	C/Co	FID	error %	log error %
1	0.5	347625	174161	0.7704	0.7300	+5.5	-17.1
4	4	181648	186236	0.3765	0.3340	+12.7	-10.9
5	5	118034	181331	0.2512	0.2530	-0.7	+0.5
6	6	102381	169018	0.2338	0.1970	+18.7	-10.5
7	7	33906	78511	0.1667	0.1450	+15.0	-7.2
8	8	521572	1929425	0.1043	0.1090	-4.3	+2.0
9	9	1463303	6656922	0.0848	0.0840	+1.0	-0.4
10	10	231687	1556572	0.0575	0.0650	-11.6	+4.5
13	14	327079	5179098	0.0244	0.0220	+10.8	-2.7
14	15	293400	5673930	0.0200	0.0170	+17.4	-3.9
15	16	262581	6347392	0.0160	0.0130	+22.8	-4.7
16	17	43221	1439590	0.0116	0.0100	+15.9	-3.2
18	21	42182	3822030	0.0043	0.0030	+42.0	-6.0
19	23	14654	1676956	0.0034	0.0020	+68.6	-8.4
20	25	10025	2138685	0.0018	0.0010	80.9	-8.6

Table D.3: Pulse: Propane #1, τ =2.2 s, Flow (@STP)= 510 ml/min, T= 713 K, Relative area for normalisation $\int Area_{C_3}/Area_{ISTD}dt$ =45.6 s

Amp No	t [s]	Area C-3	Area ISTD	C/Co	FID	error %	log error %
1	0	713499	42304	0.8117	1.0000	-18.8	—
2	1	1480007	123778	0.5754	0.6357	-9.5	+22.0
4	3	245123	79293	0.1488	0.2569	-42.1	+40.2
5	4	327996	112640	0.1401	0.1633	-14.2	+8.4
7	6	284718	354540	0.0386	0.0660	-41.4	+19.7
8	7	359548	620953	0.0279	0.0419	-33.6	+12.9
10	9	130094	509205	0.0123	0.0170	-27.5	+7.9
11	10	64965	356164	0.0088	0.0108	-18.5	+4.5
13	12	41655	496766	0.0040	0.0044	-7.3	+1.4
14	13	23623	417122	0.0027	0.0028	-1.5	+0.3
15	14	22316	405343	0.0026	0.0018	+50.6	-6.5
16	15	29977	625402	0.0023	0.0011	+106.2	-10.7
17	16	21219	714950	0.0014	0.0007	+100.9	-9.6

Table D.4: Pulse: Propane #2, τ =2.2 s, Flow (@STP)= 510 ml/min, T= 713 K, Relative area for normalisation $\int Area_{C_3}/Area_{ISTD}dt$ =7.3 s

Amp No	t [s]	Area C-3	Area ISTD	C/Co	FID	error %	log error %
1	0.5	1315866	497329	0.8012	0.7973	+0.5	-2.1
2	1.5	880683	528617	0.5045	0.5068	-0.5	+0.7
3	3	313259	322490	0.2941	0.2569	+14.5	-10.0
4	4	412130	708846	0.1760	0.1633	+7.8	-4.2
5	5	160503	425411	0.1142	0.1038	+10.1	-4.2
6	6	240127	986590	0.0737	0.0660	+11.7	-4.1
7	7	99479	829315	0.0363	0.0419	-13.4	+4.5
8	8	58869	730942	0.0244	0.0267	-8.5	+2.5
9	9	31286	772031	0.0123	0.0170	-27.6	+7.9
10	10	39642	1346681	0.0089	0.0108	-17.3	+4.2
11	12	22680	1249448	0.0055	0.0044	+26.2	-4.3
12	13	14253	1078778	0.0040	0.0028	+44.5	-6.3
13	14	13394	1147096	0.0035	0.0018	+100.9	-11.0
14	15	11343	1162500	0.0030	0.0011	+164.2	-14.3
15	16	26152	5667539	0.0014	0.0007	+96.5	-9.3

Table D.5: Pulse: Propane #1, τ =5.9 s, Flow (@STP)= 290 ml/min, T= 473 K, Relative area for normalisation $\int Area_{C_3}/Area_{ISTD}dt$ =12.9 s

Amp No	t [s]	Area C-3	Area ISTD	C/Co	FID	error %	log error %
1	0.5	2822	637949	0.0020	0.7650	-99.7	2220.9
3	2	836720	513315	0.7351	0.7120	3.2	-9.4
4	3	1377410	1012184	0.6137	0.6100	0.6	-1.2
5	5	1159381	1106915	0.4724	0.4360	8.3	-9.7
6	7	1209111	1151564	0.4735	0.3140	50.8	-35.5
7	9	2217153	4687971	0.2133	0.2267	-5.9	4.1
8	11	2157541	3862117	0.2519	0.1639	53.7	-23.8
9	13	2077621	6547018	0.1431	0.1188	20.5	-8.7
10	15	1115011	4703875	0.1069	0.0860	24.3	-8.9
11	18	213163	1975908	0.0487	0.0526	-7.5	2.6
12	22	599751	7879731	0.0343	0.0270	27.1	-6.6
13	26	100887	3034568	0.0150	0.0140	7.1	-1.6
14	30	149082	9861850	0.0068	0.0071	-4.2	0.9
15	33	37748	3546338	0.0048	0.0043	11.6	-2.0
16	36	36973	5457965	0.0031	0.0026	19.3	-3.0
19	46	13627	10049640	0.0006	0.0005	32.4	-3.7

Table D.6: Pulse: Propane #2, τ =5.9 s, Flow (@STP)= 290 ml/min, T= 473 K, Relative area for normalisation $\int Area_{C_3}/Area_{ISTD}dt$ =29.2 s

Amp No	t [s]	Area C-3	Area ISTD	C/Co	FID	error %	log error %
1	0.5	1117056	251348	0.8831	0.7650	15.4	-53.6
3	2	1299361	345840	0.7466	0.7120	4.9	-14.0
4	3	959732	314817	0.6058	0.6100	-0.7	1.4
5	5	778294	362699	0.4264	0.4360	-2.2	2.7
6	7	146734	97909	0.2978	0.3140	-5.2	4.6
7	9	565771	573987	0.1959	0.2267	-13.6	9.9
8	11	404335	577339	0.1392	0.1639	-15.1	9.0
9	13	261143	481919	0.1077	0.1188	-9.4	4.6
10	15	191437	502615	0.0757	0.0860	-12.0	5.2
11	18	466968	2185018	0.0425	0.0526	-19.3	7.3
12	22	239784	1990537	0.0239	0.0270	-11.3	3.3
14	30	62719	1990295	0.0063	0.0071	-12.1	2.6
15	33	43676	2076322	0.0042	0.0043	-2.8	0.5
16	36	26997	2102902	0.0026	0.0026	-0.4	0.1
17	40	19382	2029303	0.0019	0.0013	46.0	-5.7
19	46	14329	1813238	0.0016	0.0005	239.9	-15.9
20	50	5816	1789899	0.0006	0.0001	545.7	-20.3

D.2 Pulse of cumene in empty JLR

Table D.7: Pulse: Cumene #1, τ =2.2 s, Flow (@STP)= 510 ml/min, T= 717 K, Relative area for normalisation $\int Area_{C_9}/Area_{ISTD}dt$ =30.2 s

Amp No	t [s]	Area C-9	Area ISTD	C/Co	FID	error %	log error %
1	0.5	1193045	110126	0.7864	0.7963	-1.2	5.5
2	1	1301634	164078	0.5759	0.6341	-9.2	21.1
3	3	470075	130088	0.2623	0.2549	2.9	-2.1
4	4	443502	177244	0.1816	0.1616	12.4	-6.4
5	5	364938	211531	0.1252	0.1025	22.2	-8.8
6	6	181364	159514	0.0825	0.0650	27.0	-8.7
7	7	127412	181482	0.0510	0.0412	23.7	-6.7
8	8	284437	760666	0.0271	0.0261	3.9	-1.0
9	9	110299	437811	0.0183	0.0166	10.4	-2.4
10	10	164223	828098	0.0144	0.0105	37.0	-6.9
11	11	73218	557945	0.0095	0.0067	43.0	-7.1
12	12	72158	625587	0.0084	0.0042	98.3	-12.5
14	14	49653	662598	0.0054	0.0017	220.4	-18.3
16	16	22645	649035	0.0025	0.0007	271.0	-18.0
17	17	19895	591630	0.0024	0.0004	464.0	-22.3
18	18	15598	765670		0.0003	438.8	-20.5

Table D.8: Pulse: Cumene #1, τ =2.7 s, Flow (@STP)= 410 ml/min, T= 717 K, Relative area for normalisation $\int Area_{C_9}/Area_{ISTD}dt$ =38.0 s

Amp No	t [s]	Area C-9	Area ISTD	C/Co	FID	error %	log error %
1	0.5	2068261	204623	0.7240	0.8327	-13.1	76.4
2	1.5	1065258	130801	0.5833	0.5773	1.0	-1.9
3	3	747791	148402	0.3609	0.3333	8.3	-7.3
4	4	316130	94391	0.2399	0.2321	3.8	-2.6
5	5.5	214182	106841	0.1436	0.1334	7.6	-3.7
6	7	189627	145286	0.0935	0.0770	21.4	-7.6
7	8.5	391932	626707	0.0448	0.0445	0.8	-0.2
8	10	282027	602747	0.0335	0.0257	30.6	-7.3
9	11.5	132326	519505	0.0182	0.0148	23.1	-4.9
10	13	104721	730321	0.0102	0.0086	20.1	-3.8
11	14.5	70476	659583	0.0077	0.0049	55.0	-8.3
12	16	46027	740436	0.0045	0.0029	56.2	-7.6
13	17.5	35849	660316	0.0039	0.0016	136.3	-13.4
14	19	18814	451510	0.0030	0.0010	214.1	-16.4
15	20.5	22122	705141	0.0022	0.0005	309.7	-18.8
16	22	20149	632305	0.0023	0.0003	620.8	-24.5
17	23.5	16791	719243	0.0017	0.0002	814.8	-25.7
18	25	15598	765670	0.0015	0.0001	1282.7	-28.7

Table D.9: Pulse: Cumene #1, τ =3.6 s, Flow (@STP)= 310 ml/min, T= 717 K, Relative area for normalisation $\int Area_{C_9}/Area_{ISTD}dt$ =39.7 s

Amp No	t [s]	Area C-9	Area ISTD	C/Co	FID	error %	log error %
1	0	866091	119851	0.6572	1.000	-34.3	—
3	2.5	516645	101779	0.4616	0.5004	-7.8	11.7
4	4.5	702540	227654	0.2806	0.2876	-2.4	2.0
5	6.5	314792	161024	0.1778	0.1653	7.6	-4.0
7	10.5	574430	926777	0.0564	0.0546	3.2	-1.1
8	12.5	352869	844982	0.0380	0.0314	21.0	-5.5
9	14.5	165396	716442	0.0210	0.0180	16.4	-3.8
10	16.5	116113	791863	0.0133	0.0104	28.7	-5.5
11	18.5	51958	552979	0.0085	0.0060	43.4	-7.0
12	20.5	64796	881422	0.0067	0.0034	95.3	-11.8
14	24.5	36960	1028478	0.0033	0.0011	189.0	-15.6
15	26.5	14680	608395	0.0022	0.0006	237.6	-16.6
16	28.5	19289	822299	0.0021	0.0004	471.1	-22.1
17	30.5	14295	723744	0.0018	0.0002	736.7	-25.2
18	32.5	8531	608383	0.0013	0.0001	933.5	-26.0
19	34.5	11768	898008	0.0012	0.0001	1580.6	-29.5

Table D.10: Pulse: Cumene #2, τ =3.6 s, Flow (@STP)= 310 ml/min, T= 717 K, Relative area for normalisation $\int Area_{C_9}/Area_{ISTD}dt$ =36.3 s

Amp No	t [s]	Area C-9	Area ISTD	C/Co	FID	error %	log error %
1	0	2589352	367440	0.7401	1.000	-26.0	—
2	1	1364180	191151	0.7495	0.7581	-1.1	4.1
3	2.5	1089123	262090	0.4364	0.5004	-12.8	19.8
4	4.5	737678	313804	0.2469	0.2876	-14.2	12.3
5	6.5	401419	269040	0.1567	0.1653	-5.2	3.0
6	8.5	180235	194113	0.0975	0.0950	2.6	-1.1
7	10.5	536271	1021317	0.0551	0.0546	1.0	-0.3
8	12.5	344351	935186	0.0387	0.0314	23.2	-6.0
9	14.5	124010	535344	0.0243	0.0180	34.9	-7.5
10	16.5	95059	617853	0.0162	0.0104	55.9	-9.7
11	18.5	47818	431001	0.0117	0.0060	95.6	-13.1
12	20.5	77071	1011648	0.0080	0.0034	133.7	-15.0
13	22.5	74294	1166803	0.0067	0.0020	239.8	-19.6
14	24.5	46104	901318	0.0054	0.0011	375.0	-23.0
16	28.5	28028	1017887	0.0029	0.0004	674.2	-25.9
17	30.5	21017	794931	0.0028	0.0002	1193.4	-30.3
18	32.5	17044	800229	0.0022	0.0001	1712.9	-32.2
19	34.5	13958	807549	0.00186	0.0001	2459.8	-33.9

Appendix E

Solution of bipore sorption model

By introducing the following dimensionless numbers

$$\begin{aligned} \zeta &= \frac{r}{r_c} \quad & \psi &= \frac{y}{R_y} \quad & \tau_c &= \frac{D_c}{r_c^2} t \\ N_c &= \zeta q \quad & N_y &= \psi C_y \end{aligned} \tag{E.1}$$

eq.(5.1) to (5.9) can be written in dimensionless form

Micropores:

$$\frac{\partial N_c}{\partial \tau_c} = \frac{\partial^2 N_c}{\partial \zeta^2} \tag{E.2}$$

Macropores:

$$\kappa \left(1 + K_y\right) \frac{\partial N_y}{\partial \tau_c} + 3 \frac{\left(1 - \varepsilon_y\right)}{\varepsilon_y} \kappa \psi \left(\frac{\partial N_c}{\partial \zeta} - N_c \right)_{\zeta = 1} = \frac{\partial^2 N_y}{\partial \psi^2} \tag{E.3}$$

with the boundary condition eq.(5.9) to

$$N_c|_{\zeta = 1} = \frac{K_c N_y}{\psi} \tag{E.4}$$

the symmetry and the initial condition of eq.(5.5) can be solved in the Laplace Transform to

$$\widetilde{N}_c\left(\psi\right) = \frac{K_c \widetilde{N}_y\left(\psi\right)}{\psi} \frac{e^{\sqrt{s}\zeta} - e^{-\sqrt{s}\zeta}}{e^{\sqrt{s}} - e^{-\sqrt{s}}} \tag{E.5}$$

and the Laplace solution for the macropore balance

$$k\left(1+K_y\right)\left(\widetilde{N}_y\left(\psi\right)s-0\right)+3\frac{\left(1-\varepsilon_y\right)}{\varepsilon_y}\kappa K_c\widetilde{N}_y\left(\psi\right)\left(\sqrt{s}\coth\sqrt{s}-1\right)=\frac{\partial^2\widetilde{N}_y\left(\psi\right)}{\partial\psi^2} \tag{E.6}$$

Reactor Mass Balance

$$\widetilde{N}_y\left(\psi=1\right)\left(1-L\right)-\left(\frac{\partial\widetilde{N}_y}{\partial\psi}\right)=\gamma\left(\widetilde{N}_y s-1\right)_{\psi=1} \tag{E.7}$$

eq.E.6 may be solved using the symmetry condition and combined with eq.E.7 this yields the Laplace solution for the reactor response

$$\frac{\widetilde{C}}{C_0}=\widetilde{N}_y\left(\psi=1\right)=\frac{\gamma}{f(s)}=\frac{\gamma}{\sqrt{x}\coth\sqrt{x}+L-1+\gamma s} \tag{E.8}$$

with

$$x=\left(1+K_y\right)\kappa s+\lambda\left(\sqrt{s}\coth\sqrt{s}-1\right) \tag{E.9}$$

for the solution to be finite one substitutes

$$\sqrt{s}=i\phi \tag{E.10}$$

where roots of eq.E.9 ϕ_n are positive real number. The time solution to eq.E.8 can then be found by the means of the Heaviside theorem

$$\frac{C_z\left(t\right)}{C_0}=\sum_{n=1}^{\infty}\left.\frac{\gamma}{\frac{\partial f}{\partial s}}\right|_{s_n}\exp(s_n\tau_c) \tag{E.11}$$

Appendix F

Index of CD-ROM

Sensitivity Analysis:

Directory on CD: Sensana (for run number, #, see Appendix I)

- Files parasens#.mab: text file of simulated data from sensitivity analysis with 9 columns
  (1) time (2) C_R (3) C_P (4) $s_{R,\alpha}$ (5) $s_{R,\beta}$ (6) s_{R,φ^2} (7) $s_{P,\alpha}$ (8) $s_{P,\beta}$ (9) s_{P,φ^2}
- Files parasens#a.eps: figure in eps format with $s_{R,i}$ vs. τ
- File parasens#b.eps: figure in eps format with $\frac{s_{R,\varphi^2}}{s_{R,\beta}}$ vs. $\frac{s_{R,\alpha}}{s_{R,\beta}}$

Pulse Experiments without reaction:

Directory on CD: pulsworea

- Files propan#.xls: Excel spreadsheet with raw propane pulse response data and evaluation for diffusion and adsorption (for run number, #, see Appendix G)
- Files be#.xls: Excel spreadsheet with raw benzene pulse response data and evaluation for diffusion and adsorption (for run number, #, see Appendix G)

Cumene Cracking Transient:

- Files react#.xls: Excel spreadsheet with raw cumene pulse response data and normalisation of response (for run number, #, see Appendix K and L)

Cumene Cracking Steady State:

- Files cumss#.xls: Excel spreadsheet with steady state cumene cracking and bypass data

Appendix G

Propane pulse measurements over T4480

Table G.1: List of pulse experiments of propane on T4480 ZSM-5 extrudates. Diffusion and adsorption coefficients estimated from first moment and long time solution. see Appendix cdrom for file information.

File Name	T [°C]	Flow [ml/min]	Radius [cm]	Vcat [ml]	Dy [cm^2/s]	Kc [/]	dilution
propan1	98	275	0.055	0.5	3.08E-2	411	1: 100
propan2	99	190	0.055	0.5	3.67E-2	416	1: 100
propan3	99	360	0.055	0.5	3.01E-2	418	1: 100
propan5	75	415	0.055	0.5	4.70E-2	932	1: 100
propan6	75	180	0.055	0.5	3.91E-2	881	1: 100
propan7	75	260	0.055	0.5	3.51E-2	874	1: 100
propan8	75	335	0.055	0.5	4.90E-2	843	1: 100
propan9	55	425	0.055	0.5	4.93E-2	2022	1: 100
propan10	55	390	0.055	0.5	4.63E-2	1864	1: 100
propan11	55	350	0.055	0.5	5.05E-2	1970	1: 100
propan12	54	315	0.055	0.5	3.99E-2	1890	1: 100
propan13	123	380	0.055	0.5	4.21E-2	220	1: 100
propan14	123	470	0.055	0.5	4.84E-2	206	1: 100
propan15	123	425	0.055	0.5	2.32E-2	197	1: 100
propan16	123	335	0.055	0.5	8.95E-2	209	1: 100
propan17	151	310	0.055	0.5	6.12E-2	99	1: 100

propan18	150	215	0.055	0.5	5.30E-2	94	1: 100
propan19	151	360	0.055	0.5	4.85E-2	87	1: 100
propan20	152	505	0.055	0.5	3.19E-2	93	1: 100
propan21	198	345	0.055	0.5	2.17E-2	33	1: 100
propan22	198	400	0.055	0.5	1.11E-1	39	1: 100
propan23	197	450	0.055	0.5	1.11E-1	42	1: 100
propan24	197	505	0.055	0.5	1.11E-1	35	1: 100
propan29	55	240	0.055	0.5	3.95E-2	1906	-
propan30	55	280	0.055	0.5	4.41E-2	1912	-
propan31	55	350	0.055	0.5	4.33E-2	1908	-
propan32	55	425	0.055	0.5	4.05E-2	1648	-
propan42	150	405	0.055	2.4	4.41E-2	97	-
propan43	150	455	0.055	2.4	6.46E-2	102	-
propan44	150	360	0.055	2.4	6.47E-2	101	-
propan45	200	405	0.055	2.4	1.11E-1	33	-
propan46	200	540	0.055	2.4	1.11E-1	36	-
propan47	200	355	0.055	2.4	1.11E-1	41	-
propan48	55	260	0.03	0.5	8.15E-3	1987	1: 100
propan49	55	315	0.03	0.5	3.55E-2	1965	1: 100
propan50	55	365	0.03	0.5	1.10E-2	2211	1: 100
propan51	75	280	0.03	0.5	1.64E-2	811	1: 100
propan52	75	335	0.03	0.5	4.41E-2	870	1: 100
propan54	101	360	0.03	0.5	1.55E-2	393	1: 100
propan55	101	420	0.03	0.5	2.90E-2	419	1: 100
propan56	101	315	0.03	0.5	3.10E-2	375	1: 100
propan57	127	340	0.03	0.5	2.01E-2	171	1: 100
propan58	127	385	0.03	0.5	4.90E-2	177	1: 100
propan59	127	450	0.03	0.5	1.8E-2	187	1: 100
propan60	150	440	0.03	0.5	1.29E-2	135	1: 100
propan61	150	385	0.03	0.5	1.30E-2	102	1: 100
propan62	150	335	0.03	0.5	1.91E-2	90	1: 100
propan63	200	375	0.03	0.5	1.11E-1	37	1: 100
propan64	200	455	0.03	0.5	1.11E-1	35	1: 100

Appendix H

Benzene pulse measurements over T4480

Table H.1: List of pulse experiments of benzene on T4480 ZSM-5 extrudates. Diffusion and adsorption coefficients estimated from first moment and long time solution. see Appendix CD-ROM for file information.

File Name	T_R [°C]	F $[ml/min]$	R_y $[cm]$	D_y $[cm^2/s]$	K_c [/]
bes40a5	390	755	0.033	6.5E-3	8610
bes40b5	390	995	0.033	7.7E-3	8570
bem40a5	390	755	0.055	1.6E-2	8150
bem40b5	390	995	0.055	1.3E-2	6650
bes42a5	420	785	0.033	8.4E-3	3600
bes42b5	420	1040	0.033	8.5E-3	3440
bem42a5	420	785	0.055	1.5E-2	3755
bem42b5	420	1040	0.055	1.6E-2	3045
bes45a5	440	810	0.033	1.3E-2	1980
bes45b5	440	1070	0.033	1.7E-2	1620
bem45a5	440	810	0.055	1.8E-2	1820
bes48a5	470	845	0.033	1.3E-2	765
bes48b5	470	1115	0.033	1.8E-2	725
bem48a5	470	845	0.055	2.3E-2	750
bem48b5	470	1115	0.055	2.6E-2	670

Appendix I

Sensitivity analysis

Table I.1: Sensitivity Analysis, Model Parameters μ_0 =0.1, α=0.01, Filename=parasens{No.} with extension (.eps, .mab) Appendix CDROM

File No.	ϕ	β	b_1	a_1	rel.err	R^2	b_2	a_2	rel.err	R^2
30	50	0.1837	1.024	0.497	1.e-6	0.9999	1.0	0.497	1.8e-6	1.0
31	25	0.375	1.02	0.51	8.7e-6	0.9999	1.	0.55	1.0e-5	1.0
32	10	1.0	1.05	0.56	8.3e-5	0.9999	0.998	0.556	1.0e-4	1.0
33	5	2.25	1.121	0.65	3.16e-4	0.9996	0.991	0.622	1.8e-4	1.0
34	3	4.467	1.42	0.82	4.0e-4	0.9950	0.994	0.674	4e-4	1.0
35	2	8.375	2.75	1.6	1.6e-3	0.8960	0.996	0.7	0.003	1.0
36b	1.414	15.249	-2.03	-1.14	0.001	0.7110	0.9998	0.605	3.9e-8	1.0
36	1	28.751	-0.4	-0.22	1.8e-5	0.9420	0.9988	0.72	9.0e-5	1.0
37	0.7	56.877	-0.067	-0.034	7.9e-8	0.9600	0.9998	0.605	3.9e-8	1.0

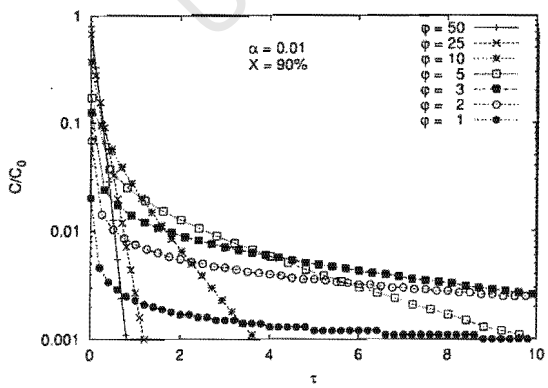

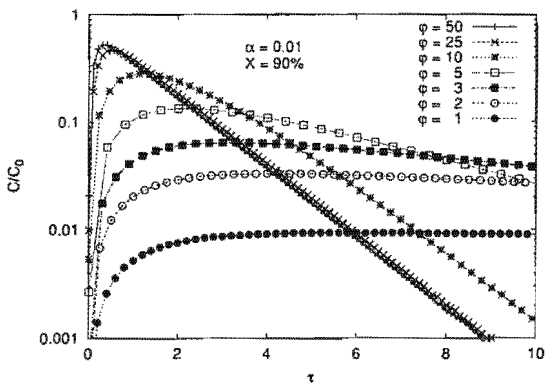

Table I.2: Sensitivity Analysis, Model Parameters μ_0 =0.1, α=0.0001, Filename=parasens{No.} with extension (.eps, .mab) Appendix CDROM

File No.	ϕ	β	b_1	a_1	rel.err	R^2	b_2	a_2	rel.err	R^2
parasens38	50	0.1837	1.011	0.513	4.1e-5	0.9999	0.998	0.497	1.6e-4	1.0
parasens39	25	0.375	1.038	0.528	5.5e-6	0.9998	0.999	0.512	1.5e-4	1.0
parasens40	10	1.0	1.256	0.641	9.18e-6	0.99	0.999	0.525	5.75e-5	1.0
parasens41	5	2.25	0.076	0.047	a	a	a	a	a	a
parasens42	3	4.467	0.004	0.003	a	a	a	a	a	a
parasens43	2	8.375	0.0019	0.001	a	a	a	a	a	a

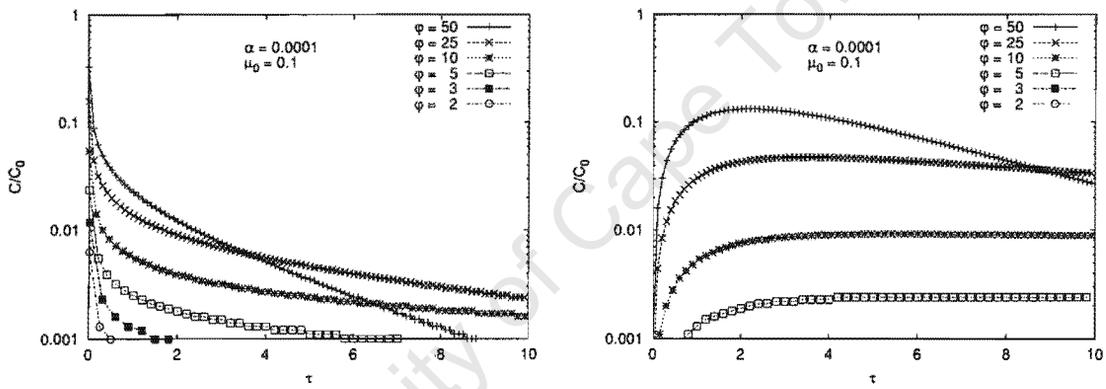

Table I.3: Sensitivity Analysis, Model Parameters μ_0 =0.1, α=1.0, Filename=parasens{No.} with extension (.eps, .mab) Appendix CDROM

File No.	ϕ	β	b_1	a_1	rel.err	R^2	b_2	a_2	rel.err	R^2
44	50	0.1837	1.022	0.498	6.3e-4	1.0	1.08	0.498	1.53e-9	0.9999
45	25	0.375	1.027	0.515	3.9e-15	1.0	1.03	0.514	7.0e-10	1.0
46	10	1.0	1.06	0.553	4.0e-8	0.9999	1.01	0.55	6.8e-7	0.9999
47	5	2.25	1.12	0.622	1.0e-5	0.9997	1.0	0.624	3.8e-5	0.9997
48	3	4.467	1.13	0.727	5.0e-4	0.997	0.998	0.731	3.7e-4	0.9996
49	2	8.375	1.065	0.8489	2.4e-3	0.9956	0.9967	0.827	0.001	0.9999
50	1	28.751	1.011	0.975	0.0021	0.998	0.996	0.93	1.8e-3	0.9999

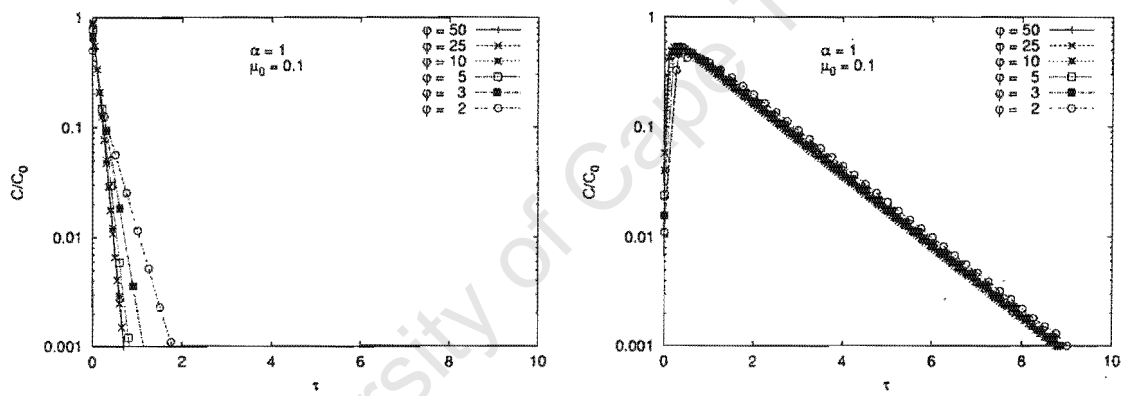

Table I.4: Sensitivity Analysis, Model Parameters μ_0 =0.9, α=0.0001, Filename=parasens{No.} with extension (.eps, .mab) Appendix CDROM

File No.	ϕ	β	b_1	a_1	rel.err	R^2	b_2	a_2	rel.err	R^2
51	50	0.0027	1.057	0.550	9.5e-4	1.0	0.973	.497	1.0e-4	.9996
52	25	0.0047	1.251	0.681	0.0022	1.0	0.941	0.528	7.8e-5	0.9980
53	10	0.0124	4.685	2.54	0.023	0.99	0.949	0.547	3.1e-5	0.9990
54	5	0.0278	-2.62	-1.463	0.0055	1.0	0.978	0.534	0.0055	1.0
55	3	0.055	-1.03	-0.6	2.5e-4	0.979	a	a	a	a
56	2	0.104	-0.03	-0.014	7.5e-7	0.29	a	a	a	a
57	1	0.355	-0.0076	-0.004	2.8e-8	0.24	a	a	a	a
58	0.7	0.705	-0.004	-0.002	6.9e-9	0.25	a	a	a	a

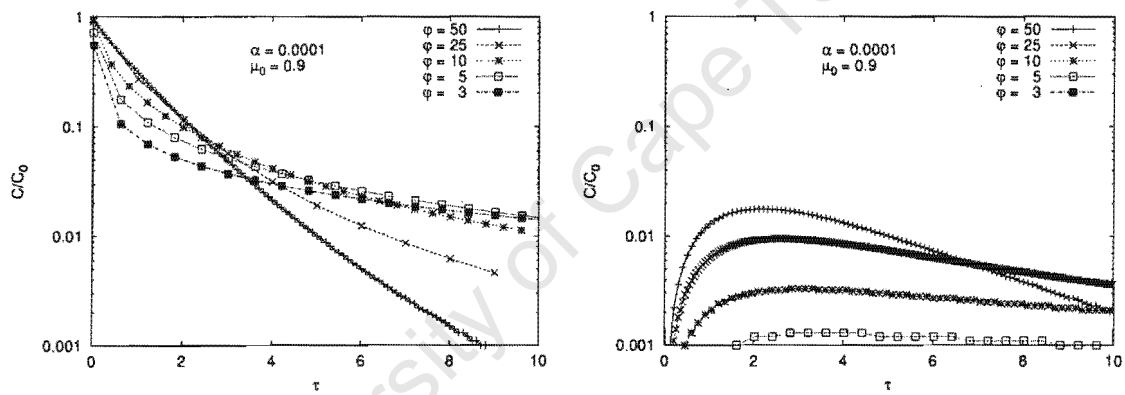

Table I.5: Sensitivity Analysis, Model Parameters μ_0 =0.9, α=0.01, Filename=parasens{No.} with extension (.eps, .mab) Appendix CDROM

File No.	ϕ	β	b_1	a_1	rel.err	R^2	b_2	a_2	rel.err	R^2
59	50	0.0027	1.027	0.498	3.63e-8	1.0	0.976	0.498	3.6e-8	1.0
60	25	0.0047	1.032	0.514	6.4e-7	1.0	0.969	0.514	8.4e-7	1.0
61	10	0.0124	1.045	0.556	6.5e-5	0.9999	0.944	0.5515	2.18e-5	0.9999
62	5	0.0278	1.228	0.773	0.0074	1.0	0.852	.62	4.e-5	0.9999
63	3	0.055	2.055	1.566	0.122	0.983	0.739	0.712	3.0e-4	0.998
64	2	0.104	-3.763	-3.544	2.593	0.27	0.69	0.797	0.001	.993
65	1	0.355	-0.6123	-0.508	0.0112	0.9997	0.857	0.83	7.6e-4	.998

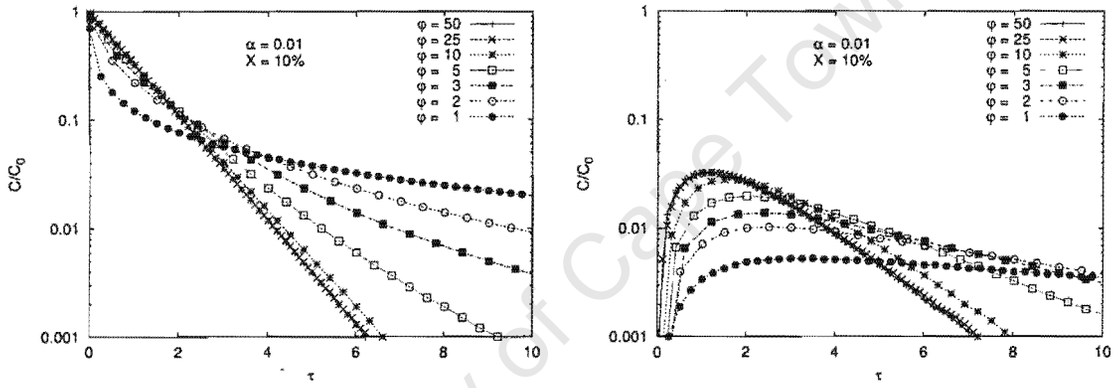

Table I.6: Sensitivity Analysis, Model Parameters μ_0 =0.9, α=1.0, Filename=parasens{No.} with extension (.eps, .mab) Appendix CDROM

File No.	ϕ	β	b_1	a_1	rel.err	R^2	b_2	a_2	rel.err	R^2
66	50	0.0027	1.023	0.498	1.5e-17	1.0	1.12	0.498	3.e-12	1.0
67	25	0.0047	1.027	0.514	4.0e-16	1.0	1.04	0.514	1.3e-7	1.0
68	10	0.0124	1.059	0.553	2.9e-10	1.0	0.954	0.553	2.3e-9	1.0
69	5	0.0278	1.135	0.623	4.09e-7	0.9998	0.882	0.623	3.3e-7	0.9994
70	3	0.055	1.201	0.723	2.5e-5	0.998	0.631	0.723	9.5e-6	0.99
71	2	0.104	1.17	0.82	3.0e-4	0.9937	0.507	0.817	8.9e-5	0.943
72	1	0.355	1.009	0.967	0.0025	0.999	0.601	0.924	9.0e-4	0.884
73	0.7	0.705	1.026	1.074	0.00393	1.0	0.073	0.951	0.0015	0.937

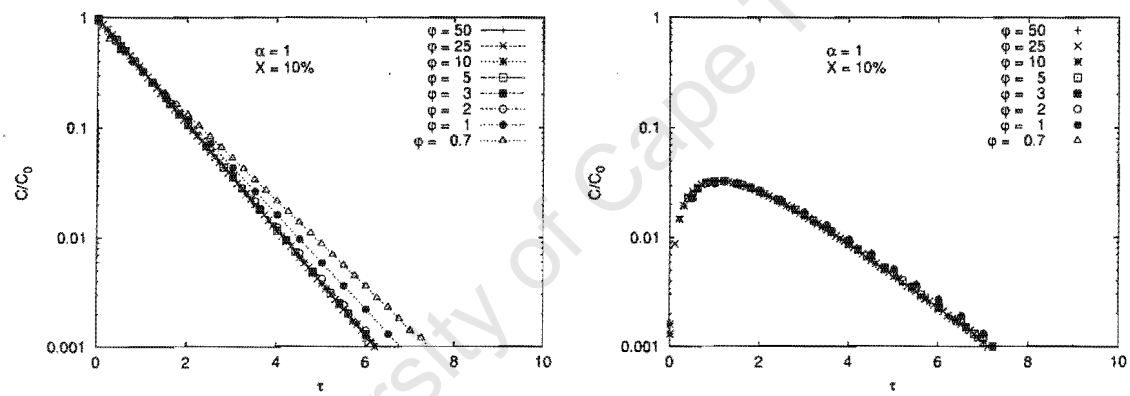

Table I.7: Sensitivity Analysis, Model Parameters μ_0 =0.5, α=0.0001, Filename=parasens{No.} with extension (.eps, .mab) Appendix CDROM

File No.	ϕ	β	b_1	a_1	rel.err	R^2	b_2	a_2	rel.err	R^2
74	50	0.0204	1.01	0.537	0.00053	1.0	0.989	.497	1.8e-4	0.999
75	25	0.0416	1.05	0.540	2.1e-4	0.9998	0.99	0.52	1.6e-4	.9997
76	10	0.111	1.284	0.658	1.3e-4	0.948	0.993	0.528	6.0e-5	1.0
77	5	0.25	.15	0.91	8.13e-5	0.006	0.997	0.53	4.5e-6	1.0
78	3	0.496	-0.004	-0.002	2.4e-6	0.149	a	a	a	a
79	2	0.931	-0.035	-0.017	4.0e-7	0.21	a	a	a	a
80	1	3.194	-0.002	6.2e-4	8.7e-9	0.03	a	a	a	a
81	0.7	6.320	-1.3e-4	8.93-5	1e-10	0.038	a	a	a	a

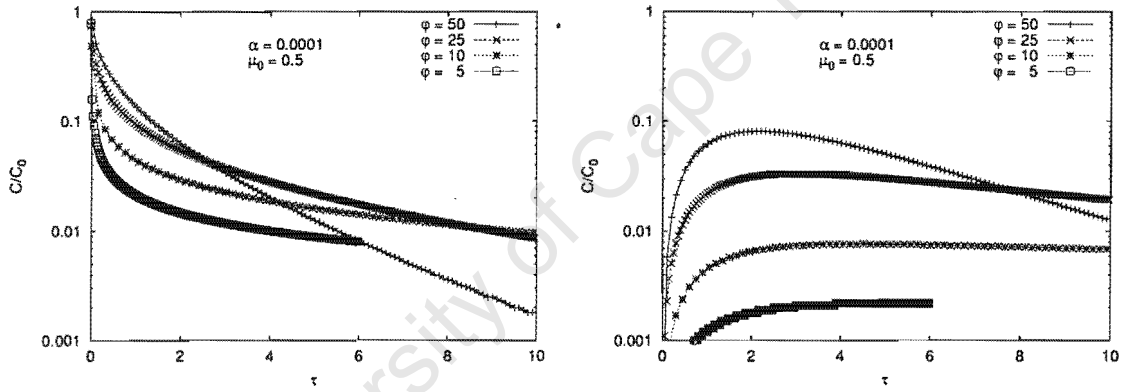

Table I.8: Sensitivity Analysis, Model Parameters μ_0 =0.5, α=0.01, Filename=parasens{No.} with extension (.eps, .mab) Appendix CDROM

File No.	ϕ	β	b_1	a_1	rel.err	R^2	b_2	a_2	rel.err	R^2
82	50	0.0204	1.03	0.498	2.16e-17 1.0	0.988	.497	1.17e-6	0.9998	
83	25	0.0416	1.03	0.514	1.9e-6	0.9999	0.9923	0.514	7.55e-6	.9999
84	10	0.111	1.04	0.56	9.3e-5	0.9999	0.988	0.5524	8.96e-5	1.0
85	5	0.25	1.12	0.754	7.2e-3	1.0	0.952	0.617	1.4e-4	0.9998
86	3	0.496	1.385	0.851	0.0022	.998	0.951	0.681	0.00026	0.9917
87	2	0.931	2.66	1.59	0.0036	0.94	0.966	0.71	0.0003	0.9998
88	1	3.194	-0.994	-0.603	0.0011	0.83	0.983	0.788	0.0003	1.0
89	0.7	6.320	-0.328	-0.199	8.1e-5	0.93	0.991	0.792	2.8e-4	1.0

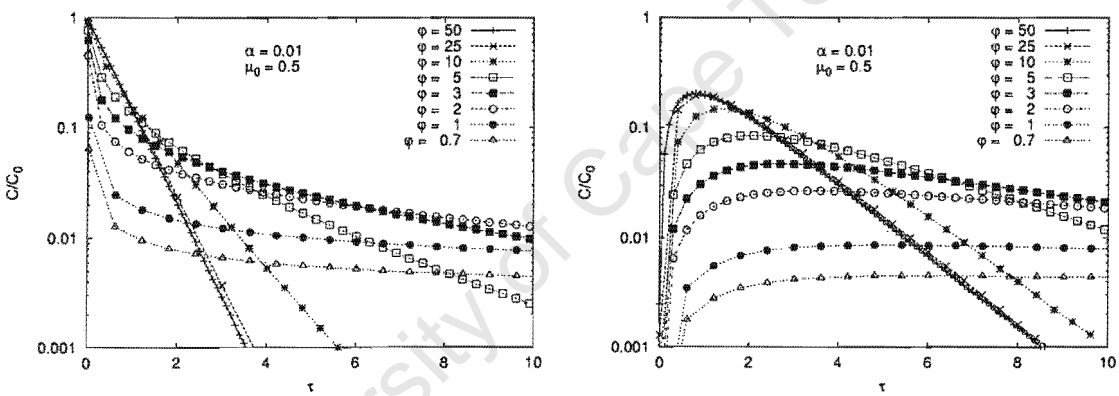

Table I.9: Sensitivity Analysis, Model Parameters μ_0 =0.5, α=1.0, Filename=parasens{No.} with extension (.eps, .mab) Appendix CDROM

File No.	ϕ	β	b_1	a_1	rel.err	R^2	b_2	a_2	rel.err	R^2
parasens90	50	0.0204	1.02	0.498	1.6e-16	1.0	1.11	.498	4.7e-10	1.0
parasens91	25	0.0416	1.03	0.515	4.8e-16	1.0	1.04	0.515	1.9e-10	1.0
parasens92	10	0.111	1.05	0.553	7.3e-9	1.0	0.977	0.552	2.5e-7	0.9995
parasens93	5	0.25	1.138	0.62	1.5e-6	1.0	0.939	0.619	2.0e-5	0.9956
parasens94	3	0.496	1.19	0.721	6.1e-5	.997	0.930	0.716	2.5e-4	0.990
parasens95	2	0.931	1.14	0.816	6.0e-4	.993	0.940	0.811	9.0e-4	0.992
parasens96	1	3.194	1.009	0.971	0.0024	1.0	0.962	0.925	0.002	0.997
parasens97	0.7	6.320	1.004	1.019	0.0019	1.0	0.964	0.953	0.0019	0.998

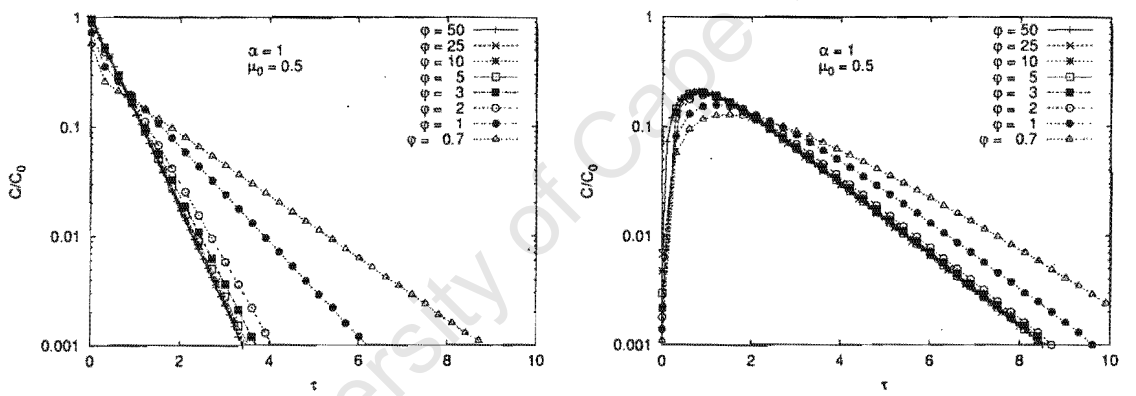

Appendix J

Steady state experiments

Table J.1: Steady state run data and results

Runid	d[mm]	T[C]	FSTP[ml/min]	X	kobs[1/s]	C-bal.[]
2	0.9	441	177	0.638	161	98.2
3	0.9	441	291	0.566	189	100.2
4	0.9	441	406	0.482	192	96.3
5	0.9	441	406	0.481	192	100.7
6	0.9	441	349	0.509	184	100.4
7	0.9	441	235	0.576	162	101.8
8	0.9	390	177	0.614	133	99.0
9	0.9	390	406	0.481	178	103.0
10	0.9	390	235	0.570	147	101.6
11	0.9	390	349	0.500	165	99.1
12	0.9	390	291	0.540	162	101.3
13	0.9	350	177	0.607	121	103.6
14	0.9	350	406	0.447	158	98.1
15	0.9	350	235	0.554	129	99.2
16	0.9	350	349	0.506	159	98.0
17	0.9	350	291	0.537	160	101.0
18	0.9	419	291	0.581	198	97.46

19	0.9	419	348	0.536	198	101.1
20	0.9	419	235	0.574	172	96.2
21	0.9	419	177	0.645	130	96.2
22	1.5	441	235	0.517	128	101.0
23	1.5	441	291	0.427	110	102.1
24	1.5	441	176	0.532	102	102.5
25	1.5	441	349	0.416	126	102.9
26	1.5	441	406	0.382	128	99.9
27	1.5	421	176	0.544	142	98.7
28	1.5	421	235	0.488	110	103.4
29	1.5	421	291	0.421	104	95.3
30	1.5	421	349	0.367	100	97.7
31	1.5	421	406	0.364	113	104.4
32	1.5	391	235	0.441	88	104.3
34	1.5	391	176	0.497	82	104.0
35	1.5	391	406	0.334	96	98.6
36	1.5	391	291	0.389	88	101.5
37	1.5	348	291	0.417	92	101.4
38	1.5	348	235	0.421	76	97.4
39	1.5	348	406	0.297	167	95.9
40	1.5	348	349	0.401	103	103.9
41	1.5	348	176	0.492	76	98.8
42	0.7	441	235	0.603	181	95.1
43	0.7	441	349	0.555	221	99.4
44	0.7	441	291	0.560	219	97.1
45	0.7	441	406	0.539	241	101.6
46	0.7	441	176	0.611	151	96.0
48	0.7	450	291	0.597	222	95.6
49	0.7	450	409	0.571	245	95.8
50	0.7	450	349	0.577	245	95.9
51	0.7	450	235	0.637	212	96.0
52	0.7	450	465	0.528	267	102.7

53	0.7	419	291	0.599	206	102.6
54	0.7	419	465	0.530	238	98.5
55	0.7	419	406	0.525	221	103.8
56	0.7	419	235	0.645	212	102.4
57	0.7	419	349	0.548	208	103.3
58	0.7	391	465	0.518	236	102.1
59	0.7	391	406	0.533	219	103.8
60	0.7	391	349	0.541	194	98.1
61	0.7	391	291	0.578	187	97.8
62	0.7	391	235	0.623	184	102.9
63	0.7	346	465	0.483	191	98.9
64	0.7	346	291	0.558	162	95.9
65	0.7	346	406	0.535	206	101.0
66	0.7	346	235	0.597	153	101.1
67	0.7	346	349	0.518	165	94.9

J.1 Sample spreadsheet

			CumSS2			ml/min	
Catalyst	T4480	d=-1.18 +1.(	mass [g]	0.2	Flow [STF	176.5	
Calcined	12h @ 480C	in Air	mass glass	2.1 g	Flow [@T	461	
			d=1.5mm				
T=441							
Bypass							
t [min]	Area Decan	Area Cume	Ratio Cum/Dec				
0	229571	1231429	5.364				
10	321107	1673301	5.211				
33	322084	1755062	5.449				
47	339936	1823083	5.363				
75	373108	2025360	5.428				
average			5.363				
Reaction							
t [min]	Area Propene	Area Benzene	Area Decane	Area Cumene	Ratio Prod/I	C-bal.	X
10	429933	894858	390133	711966	5.221	0.973	0.650
25	487624	1022840	467193	910880	5.183	0.966	0.624
40	460466	975091	427234	834514	5.313	0.991	0.632
55	452615	909511	401348	816320	5.428	1.012	0.625
70	501734	1011307	476617	891383	5.045	0.941	0.629
85	537607	1087968	510873	945459	5.033	0.938	0.632
110	529270	1053358	468621	891009	5.279	0.984	0.640
180	392080	789253	306142	561889	5.694	1.062	0.678
210	537072	1054643	484349	976450	5.302	0.989	0.620
235	521512	1071424	486421	915072	5.156	0.961	0.635
250	522913	1078441	467659	874946	5.295	0.987	0.647
average					5.268		0.638
average mass balance		98.23					

Figure J.1: Sample spreadsheet for the analysis of steady state conversion and carbon balance from GC analysis data.

350°C									
	Ry [cm]	slope [ml/min]	Vzeol [ml]	kobs[1/s]	keff[1/s]	φ	Dy ε cm²/s	η	solve
	0.075	419	0.086	81	505	18	0.0046	0.16	0.000
	0.043	699	0.086	120	505	12	0.0035	0.24	0.000
	0.030	861	0.086	167	505	8	0.0036	0.33	0.000
						Dy cm²/s	0.0123		
390°C									
	Ry [cm]	slope [ml/min]	Vzeol [ml]	kobs[1/s]	keff[1/s]	φ	Dy ε cm²/s	η	solve
	0.075	457	0.086	89	818	27	0.0033	0.11	0.000
	0.043	758	0.086	147	818	16	0.0031	0.18	0.000
	0.030	1007	0.086	196	818	11	0.0028	0.24	0.000
						Dy cm²/s	0.0096		
420°C									
	Ry [cm]	slope [ml/min]	Vzeol [ml]	kobs[1/s]	keff[1/s]	φ	Dy ε cm²/s	η	solve
	0.075	544	0.086	106	1021	28	0.0038	0.10	-0.001
	0.043	869	0.086	169	1021	18	0.0030	0.17	0.007
	0.030	1084	0.086	211	1021	13	0.0026	0.21	0.000
						Dy cm²/s	0.0097		
440°C									
	Ry [cm]	slope [ml/min]	Vzeol [ml]	kobs[1/s]	keff[1/s]	φ	Dy ε cm²/s	η	solve
	0.075	581	0.086	113	1252	32	0.0034	0.09	0.000
	0.043	873	0.086	170	1252	21	0.0027	0.14	-0.002
	0.030	1179	0.086	229	1252	15	0.0024	0.18	0.000
						Dy cm²/s	0.0088		

Figure J.2: Spreadsheet for kinetic evaluation of steady state experiments. Data used: Pellet density 1.167 g/ml; fraction of zeolite volume in total solid volume ε_c 0.735; macropore voidage $\varepsilon_y = 0.32$. mass of catalyst=0.2g

Appendix K

Cumene pulse experiments over T4480

Appendix K. Cumene pulse experiments over T4480

Run Conditions react1

T_R [°C]	F(STP) [ml/min]	R_y [cm]	V_{cat} [ml]	τ [s]
441	311	0.075	0.173	3.62

Errors of C(t)

	Cumene	Propene	Benzene
Least Err	0.15E+00	0.13E+00	0.63E-01
R^2	0.984	0.963	0.979
Min Err% (@ time)	0.73(1.5)	1.49(8.0)	0.15(37.0)
Max Err% (@ time)	42.97(0.5)	61.24(33.0)	12.65(0.5)

Parameter Estimates

	Low Estimate	Estimate	High Estimate
$K_c(Benzene)$	158	252	400
$k_{eff}[1/s]$	108	197	359
$\alpha(Benzene)$	0.15E-01	0.24E-01	0.39E-01
ϕ	8	11	16

Model Parameters

	Cumene	Propene	Benzene
$D_y[cm^2/s]$	0.12E-01	0.20E-01	0.15E-01
$K_c[/]$	0	0	252
α	0.78E+01	0.13E+02	0.24E-01
β	0.26E-01	0.43E-01	0.33E-01

Experiment versus Model

	CUMENE		PROPENE		BENZENE	
t[s]	Exp	Mod	Exp	Mod	Exp	Mod
0.50	0.73E+00	0.84E+00	0.18E-01	0.11E-01	0.15E-01	0.85E-02
1.50	0.58E+00	0.59E+00	0.29E-01	0.25E-01	0.31E-01	0.26E-01
3.50	0.34E+00	0.29E+00	0.29E-01	0.31E-01	0.41E-01	0.42E-01
6.00	0.17E+00	0.12E+00	0.26E-01	0.24E-01	0.41E-01	0.40E-01
8.00	0.99E-01	0.58E-01	0.18E-01	0.17E-01	0.31E-01	0.33E-01
13.00	0.28E-01	0.98E-02	0.81E-02	0.60E-02	0.16E-01	0.17E-01
16.00	0.15E-01	0.34E-02	0.48E-02	0.29E-02	0.11E-01	0.11E-01
22.00	0.35E-02	0.40E-03	0.10E-02	0.64E-03	0.37E-02	0.52E-02
24.00	0.26E-02	0.20E-03	0.72E-03	0.38E-03	0.29E-02	0.42E-02
29.00	0.18E-02	0.34E-04	0.58E-03	0.10E-03	0.20E-02	0.26E-02
33.00	0.19E-02	0.87E-05	0.17E-02	0.35E-04	0.26E-02	0.19E-02
37.00	0.12E-02	0.23E-05	0.40E-03	0.12E-04	0.14E-02	0.14E-02
41.00	0.90E-03	0.60E-06	0.27E-03	0.41E-05	0.10E-02	0.11E-02
46.00	0.12E-02	0.25E-06	0.70E-03	0.12E-05	0.13E-02	0.78E-03

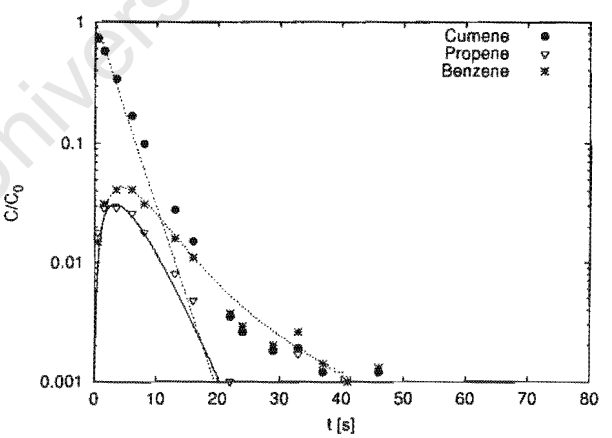

Appendix K. Cumene pulse experiments over T4480

Run Conditions react2

T_R [°C]	F(STP) [ml/min]	R_y [cm]	V_{cat} [ml]	τ [s]
441	411	0.075	0.173	2.74

Errors of C(t)

	Cumene	Propene	Benzene
Least Err	0.10E+00	0.75E-01	0.73E-01
R^2	0.990	0.919	0.890
Min Err% (@ time)	9.48(0.5)	1.05(11.0)	0.02(22.0)
Max Err% (@ time)	36.14(5.0)	15.78(1.0)	16.45(1.0)

Parameter Estimates

	Low Estimate	Estimate	High Estimate
$K_c(Benzene)$	111	204	373
$k_{eff}[1/s]$	117	185	292
$\alpha(Benzene)$	0.13E-01	0.23E-01	0.42E-01
ϕ	9	11	14

Model Parameters

	Cumene	Propene	Benzene
$D_y[cm^2/s]$	0.12E-01	0.20E-01	0.15E-01
$K_c[/]$	0	0	204
α	0.59E+01	0.97E+01	0.23E-01
β	0.20E-01	0.33E-01	0.25E-01

Experiment versus Model

	CUMENE		PROPENE		BENZENE	
t[s]	Exp	Mod	Exp	Mod	Exp	Mod
0.50	0.78E+00	0.80E+00	0.15E-01	0.10E-01	0.12E-01	0.84E-02
1.00	0.67E+00	0.64E+00	0.30E-01	0.17E-01	0.31E-01	0.17E-01
2.00	0.46E+00	0.41E+00	0.28E-01	0.23E-01	0.36E-01	0.28E-01
3.00	0.31E+00	0.27E+00	0.27E-01	0.23E-01	0.37E-01	0.32E-01
5.00	0.20E+00	0.11E+00	0.22E-01	0.17E-01	0.34E-01	0.30E-01
7.00	0.66E-01	0.45E-01	0.99E-02	0.11E-01	0.16E-01	0.22E-01
9.00	0.32E-01	0.19E-01	0.59E-02	0.63E-02	0.11E-01	0.16E-01
11.00	0.19E-01	0.78E-02	0.37E-02	0.35E-02	0.78E-02	0.11E-01
15.00	0.77E-02	0.13E-02	0.16E-02	0.97E-03	0.43E-02	0.53E-02
18.00	0.36E-02	0.35E-03	0.86E-03	0.35E-03	0.25E-02	0.34E-02
22.00	0.28E-02	0.61E-04	0.51E-03	0.90E-04	0.20E-02	0.20E-02
26.00	0.19E-02	0.11E-04	0.46E-03	0.22E-04	0.14E-02	0.13E-02
30.00	0.17E-02	0.21E-05	0.55E-03	0.55E-05	0.12E-02	0.93E-03

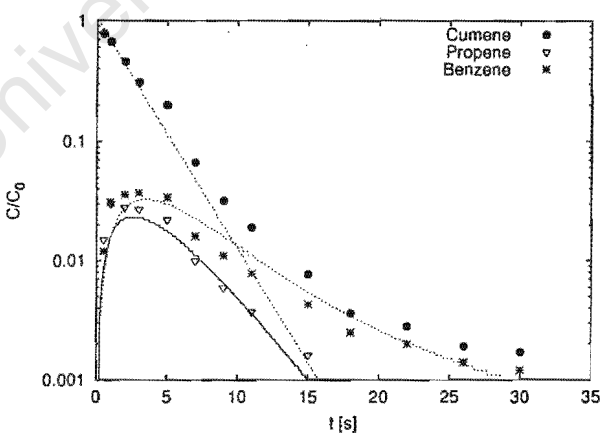

Appendix K. Cumene pulse experiments over T4480

Run Conditions react3

T_R [°C]	F(STP) [ml/min]	R_y [cm]	V_{cat} [ml]	τ [s]
444	511	0.075	0.173	2.20

Errors of C(t)

	Cumene	Propene	Benzene
Least Err	0.18E+00	0.11E+00	0.66E-01
R^2	0.997	0.878	0.940
Min Err% (@ time)	3.75(2.0)	0.99(3.0)	0.63(2.0)
Max Err% (@ time)	43.97(9.0)	18.02(0.5)	13.16(0.5)

Parameter Estimates

	Low Estimate	Estimate	High Estimate
$K_c(Benzene)$	71	173	422
$k_{eff}[1/s]$	143	288	580
$\alpha(Benzene)$	0.89E-02	0.22E-01	0.52E-01
ϕ	10	14	20

Model Parameters

	Cumene	Propene	Benzene
$D_y[cm^2/s]$	0.12E-01	0.20E-01	0.15E-01
$K_c[/]$	0	0	173
α	0.47E+01	0.78E+01	0.22E-01
β	0.16E-01	0.26E-01	0.20E-01

Experiment versus Model

	CUMENE		PROPENE		BENZENE	
t[s]	Exp	Mod	Exp	Mod	Exp	Mod
0.50	0.74E+00	0.76E+00	0.24E-01	0.13E-01	0.20E-01	0.12E-01
2.00	0.34E+00	0.33E+00	0.25E-01	0.24E-01	0.33E-01	0.34E-01
3.00	0.23E+00	0.19E+00	0.22E-01	0.22E-01	0.31E-01	0.35E-01
7.00	0.49E-01	0.21E-01	0.72E-02	0.68E-02	0.14E-01	0.16E-01
9.00	0.31E-01	0.69E-02	0.57E-02	0.33E-02	0.12E-01	0.10E-01
11.00	0.13E-01	0.23E-02	0.21E-02	0.15E-02	0.45E-02	0.62E-02
13.00	0.76E-02	0.75E-03	0.12E-02	0.65E-03	0.33E-02	0.40E-02
15.00	0.58E-02	0.25E-03	0.96E-03	0.28E-03	0.26E-02	0.27E-02
18.00	0.27E-02	0.48E-04	0.59E-03	0.77E-04	0.13E-02	0.17E-02
22.00	0.24E-02	0.51E-05	0.55E-03	0.13E-04	0.13E-02	0.99E-03

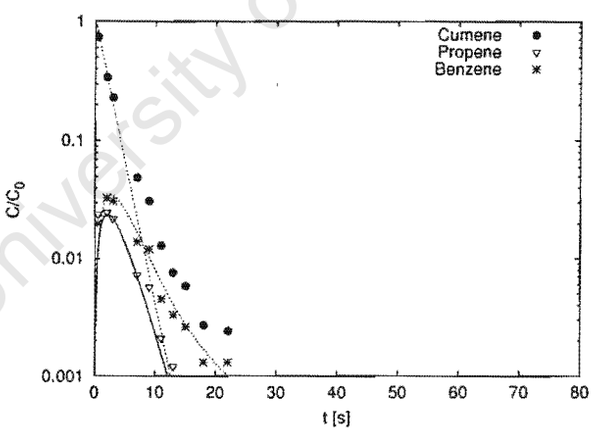

Appendix K. Cumene pulse experiments over T4480

Run Conditions react4

T_R [°C]	F(STP) [ml/min]	R_y [cm]	V_{cat} [ml]	τ [s]
419	311	0.075	0.173	3.74

Errors of C(t)

	Cumene	Propene	Benzene
Least Err	0.15E+00	0.14E+00	0.58E-01
R^2	0.981	0.891	0.944
Min Err% (@ time)	7.41(1.5)	1.48(1.5)	0.53(27.0)
Max Err% (@ time)	38.63(7.0)	26.32(27.0)	9.51(7.0)

Parameter Estimates

	Low Estimate	Estimate	High Estimate
$K_c(Benzene)$	169	274	444
$k_{eff}[1/s]$	53	90	153
$\alpha(Benzene)$	0.14E-01	0.23E-01	0.37E-01
ϕ	6	8	10

Model Parameters

	Cumene	Propene	Benzene
$D_y[cm^2/s]$	0.12E-01	0.20E-01	0.15E-01
$K_c[/]$	0	0	274
α	0.80E+01	0.13E+02	0.23E-01
β	0.27E-01	0.45E-01	0.34E-01

Experiment versus Model

	CUMENE		PROPENE		BENZENE	
t[s]	Exp	Mod	Exp	Mod	Exp	Mod
1.50	0.64E+00	0.62E+00	0.16E-01	0.17E-01	0.11E-01	0.14E-01
2.50	0.53E+00	0.45E+00	0.23E-01	0.21E-01	0.22E-01	0.21E-01
7.00	0.20E+00	0.11E+00	0.24E-01	0.16E-01	0.34E-01	0.25E-01
9.00	0.12E+00	0.57E-01	0.19E-01	0.11E-01	0.29E-01	0.21E-01
11.00	0.57E-01	0.30E-01	0.13E-01	0.76E-02	0.23E-01	0.17E-01
14.00	0.25E-01	0.11E-01	0.56E-02	0.41E-02	0.11E-01	0.12E-01
20.00	0.56E-02	0.17E-02	0.22E-02	0.10E-02	0.55E-02	0.61E-02
23.00	0.52E-02	0.65E-03	0.17E-02	0.50E-03	0.47E-02	0.45E-02
27.00	0.38E-02	0.18E-03	0.11E-02	0.18E-03	0.32E-02	0.31E-02
30.00	0.15E-02	0.71E-04	0.51E-03	0.87E-04	0.17E-02	0.25E-02
34.00	0.18E-02	0.20E-04	0.57E-03	0.31E-04	0.16E-02	0.18E-02
42.00	0.83E-03	0.21E-05	0.33E-03	0.41E-05	0.91E-03	0.11E-02
47.00	0.96E-03	0.42E-06	0.38E-03	0.12E-05	0.10E-02	0.82E-03

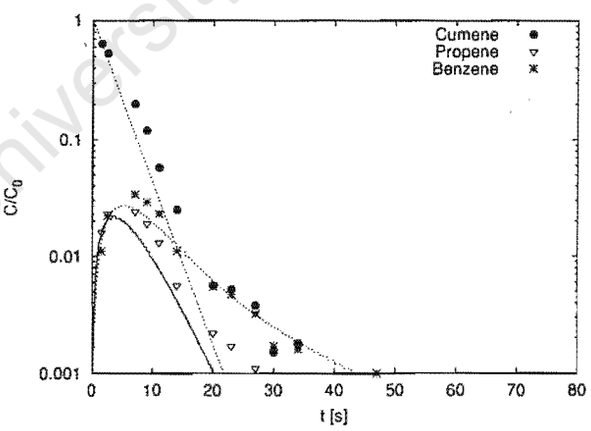

Appendix K. Cumene pulse experiments over T4480

Run Conditions react5

T_R [°C]	F(STP) [ml/min]	R_y [cm]	V_{cat} [ml]	τ [s]
419	411	0.075	0.173	2.83

Errors of C(t)

	Cumene	Propene	Benzene
Least Err.	0.79E-01	0.10E+00	0.70E-01
R^2	0.987	0.927	0.947
Min Err% (@ time)	2.04(1.0)	0.67(3.0)	1.49(3.0)
Max Err% (@ time)	37.61(0.5)	29.79(18.0)	9.84(18.0)

Parameter Estimates

	Low Estimate	Estimate	High Estimate
$K_c(Benzene)$	117	208	368
$k_{eff}[1/s]$	80	122	186
$\alpha(Benzene)$	0.13E-01	0.23E-01	0.41E-01
ϕ	7	9	11

Model Parameters

	Cumene	Propene	Benzene
$D_y[cm^2/s]$	0.12E-01	0.20E-01	0.15E-01
$K_c[/]$	0	0	208
α	0.61E+01	0.10E+02	0.23E-01
β	0.21E-01	0.34E-01	0.25E-01

Experiment versus Model

	CUMENE		PROPENE		BENZENE	
t[s]	Exp	Mod	Exp	Mod	Exp	Mod
0.50	0.72E+00	0.81E+00	0.10E-01	0.83E-02	0.47E-02	0.60E-02
1.00	0.65E+00	0.66E+00	0.21E-01	0.14E-01	0.18E-01	0.13E-01
2.00	0.45E+00	0.44E+00	0.21E-01	0.19E-01	0.25E-01	0.22E-01
3.00	0.31E+00	0.29E+00	0.19E-01	0.19E-01	0.27E-01	0.25E-01
5.00	0.19E+00	0.13E+00	0.19E-01	0.15E-01	0.27E-01	0.25E-01
7.00	0.68E-01	0.55E-01	0.11E-01	0.98E-02	0.17E-01	0.19E-01
9.00	0.34E-01	0.24E-01	0.67E-02	0.59E-02	0.11E-01	0.14E-01
11.00	0.20E-01	0.10E-01	0.45E-02	0.34E-02	0.86E-02	0.10E-01
18.00	0.90E-02	0.57E-03	0.23E-02	0.39E-03	0.57E-02	0.35E-02
22.00	0.17E-02	0.11E-03	0.57E-03	0.10E-03	0.16E-02	0.21E-02
26.00	0.92E-03	0.22E-04	0.28E-03	0.27E-04	0.10E-02	0.14E-02
30.00	0.19E-02	0.44E-05	0.47E-03	0.72E-05	0.15E-02	0.98E-03

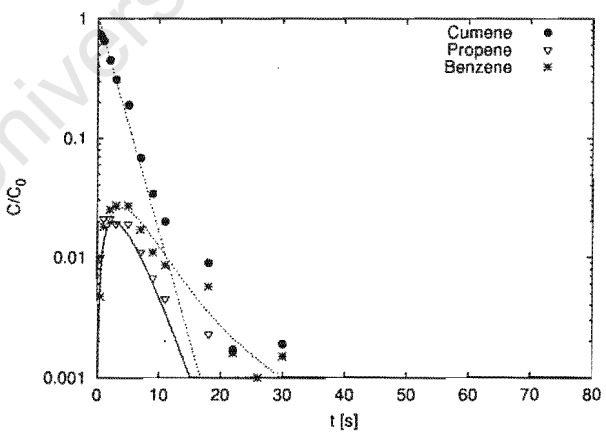

Appendix K. Cumene pulse experiments over T4480

Run Conditions react6

T_R [°C]	F(STP) [ml/min]	R_y [cm]	V_{cat} [ml]	τ [s]
419	511	0.075	0.173	2.28

Errors of C(t)

	Cumene	Propene	Benzene
Least Err	0.90E-01	0.13E+00	0.10E+00
R^2	0.941	0.968	0.965
Min Err% (@ time)	4.71(9.0)	3.23(0.5)	0.06(18.0)
Max Err% (@ time)	51.39(0.5)	16.86(7.0)	10.01(2.0)

Parameter Estimates

	Low Estimate	Estimate	High Estimate
$K_c(Benzene)$	75	199	531
$k_{eff}[1/s]$	39	61	96
$\alpha(Benzene)$	0.73E-02	0.19E-01	0.51E-01
ϕ	5	6	8

Model Parameters

	Cumene	Propene	Benzene
$D_y[cm^2/s]$	0.12E-01	0.20E-01	0.15E-01
$K_c[/]$	0	0	199
α	0.49E+01	0.81E+01	0.19E-01
β	0.17E-01	0.27E-01	0.21E-01

Experiment versus Model

	CUMENE		PROPENE		BENZENE	
t[s]	Exp	Mod	Exp	Mod	Exp	Mod
0.50	0.61E+00	0.79E+00	0.63E-02	0.53E-02	0.19E-02	0.32E-02
1.00	0.57E+00	0.62E+00	0.15E-01	0.86E-02	0.94E-02	0.68E-02
2.00	0.47E+00	0.38E+00	0.19E-01	0.11E-01	0.17E-01	0.11E-01
3.00	0.29E+00	0.24E+00	0.17E-01	0.10E-01	0.19E-01	0.13E-01
5.00	0.15E+00	0.90E-01	0.13E-01	0.69E-02	0.17E-01	0.12E-01
7.00	0.60E-01	0.35E-01	0.86E-02	0.39E-02	0.13E-01	0.88E-02
9.00	0.16E-01	0.13E-01	0.33E-02	0.20E-02	0.51E-02	0.62E-02
11.00	0.75E-02	0.51E-02	0.15E-02	0.97E-03	0.31E-02	0.43E-02
13.00	0.56E-02	0.19E-02	0.12E-02	0.46E-03	0.25E-02	0.31E-02
15.00	0.30E-02	0.74E-03	0.60E-03	0.21E-03	0.16E-02	0.23E-02
18.00	0.29E-02	0.18E-03	0.79E-03	0.65E-04	0.15E-02	0.15E-02

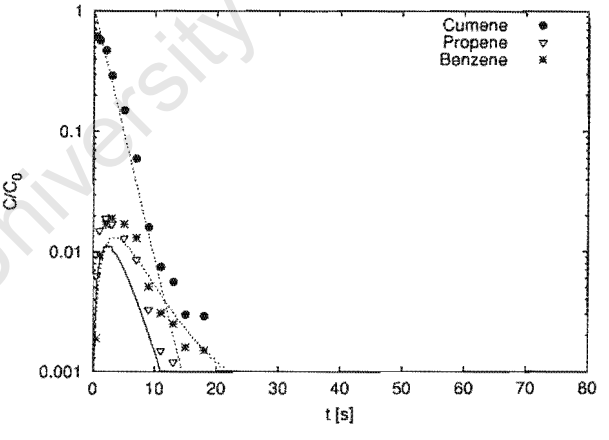

Appendix K. Cumene pulse experiments over T4480

Run Conditions react7				
T_R [°C]	F(STP) [ml/min]	R_y [cm]	V_{cat} [ml]	τ [s]
419	461	0.075	0.173	2.52

	Errors of C(t)		
	Cumene	Propene	Benzene
Least Err	0.10E+00	0.90E-01	0.82E-01
R^2	0.984	0.900	0.953
Min Err% (@ time)	3.59(1.0)	0.16(9.0)	0.25(7.0)
Max Err% (@ time)	35.14(0.5)	16.73(0.5)	12.96(26.0)

Parameter Estimates			
	Low Estimate	Estimate	High Estimate
$K_c(Benzene)$	70	113	182
$k_{eff}[1/s]$	92	148	237
$\alpha(Benzene)$	0.23E-01	0.38E-01	0.60E-01
ϕ	8	10	13

Model Parameters			
	Cumene	Propene	Benzene
$D_y[cm^2/s]$	0.12E-01	0.20E-01	0.15E-01
$K_c[/]$	0	0	113
α	0.54E+01	0.90E+01	0.38E-01
β	0.18E-01	0.30E-01	0.23E-01

Experiment versus Model

	CUMENE		PROPENE		BENZENE	
t[s]	Exp	Mod	Exp	Mod	Exp	Mod
0.50	0.84E+00	0.79E+00	0.18E-01	0.90E-02	0.11E-01	0.84E-02
1.00	0.64E+00	0.63E+00	0.24E-01	0.15E-01	0.22E-01	0.17E-01
2.00	0.35E+00	0.39E+00	0.20E-01	0.19E-01	0.23E-01	0.27E-01
3.00	0.31E+00	0.25E+00	0.22E-01	0.19E-01	0.29E-01	0.29E-01
5.00	0.17E+00	0.98E-01	0.18E-01	0.13E-01	0.26E-01	0.25E-01
7.00	0.80E-01	0.39E-01	0.10E-01	0.79E-02	0.18E-01	0.18E-01
9.00	0.25E-01	0.15E-01	0.43E-02	0.43E-02	0.73E-02	0.12E-01
13.00	0.69E-02	0.24E-02	0.14E-02	0.11E-02	0.37E-02	0.50E-02
15.00	0.55E-02	0.94E-03	0.11E-02	0.56E-03	0.29E-02	0.34E-02
18.00	0.21E-02	0.23E-03	0.61E-03	0.19E-03	0.17E-02	0.19E-02
22.00	0.65E-03	0.37E-04	0.27E-03	0.43E-04	0.73E-03	0.10E-02
26.00	0.17E-02	0.60E-05	0.59E-03	0.94E-05	0.13E-02	0.55E-03

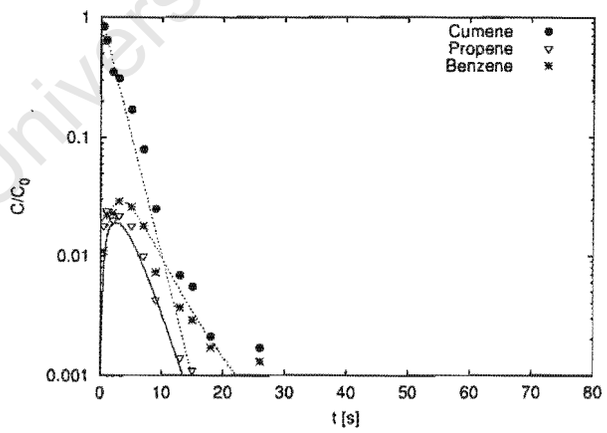

Appendix K. Cumene pulse experiments over T4480

Run Conditions react8

T_R [°C]	F(STP) [ml/min]	R_y [cm]	V_{cat} [ml]	τ [s]
392	311	0.075	0.173	3.89

Errors of C(t)

	Cumene	Propene	Benzene
Least Err	0.12E+00	0.17E+00	0.11E+00
R^2	0.927	0.893	0.886
Min Err% (@ time)	5.99(3.5)	4.68(1.5)	0.64(37.0)
Max Err% (@ time)	78.44(0.5)	26.26(26.0)	32.19(3.5)

Parameter Estimates

	Low Estimate	Estimate	High Estimate
$K_c(Benzene)$	157	839	4463
$k_{eff}[1/s]$	17	31	58
$\alpha(Benzene)$	0.15E-02	0.79E-02	0.42E-01
ϕ	3	4	6

Model Parameters

	Cumene	Propene	Benzene
$D_y[cm^2/s]$	0.12E-01	0.20E-01	0.15E-01
$K_c[/]$	0	0	839
α	0.84E+01	0.14E+02	0.79E-02
β	0.28E-01	0.47E-01	0.35E-01

Experiment versus Model

	CUMENE		PROPENE		BENZENE	
t[s]	Exp	Mod	Exp	Mod	Exp	Mod
0.50	0.52E+00	0.87E+00	0.23E-02	0.39E-02	0.57E-03	0.10E-02
1.50	0.53E+00	0.65E+00	0.11E-01	0.92E-02	0.84E-02	0.37E-02
3.50	0.39E+00	0.37E+00	0.21E-01	0.13E-01	0.25E-01	0.76E-02
8.00	0.14E+00	0.10E+00	0.18E-01	0.85E-02	0.28E-01	0.91E-02
10.00	0.79E-01	0.58E-01	0.13E-01	0.62E-02	0.24E-01	0.84E-02
13.00	0.31E-01	0.25E-01	0.71E-02	0.36E-02	0.13E-01	0.70E-02
16.00	0.18E-01	0.11E-01	0.48E-02	0.20E-02	0.92E-02	0.57E-02
19.00	0.12E-01	0.45E-02	0.37E-02	0.10E-02	0.75E-02	0.46E-02
22.00	0.60E-02	0.19E-02	0.19E-02	0.54E-03	0.46E-02	0.38E-02
24.00	0.43E-02	0.11E-02	0.15E-02	0.34E-03	0.38E-02	0.34E-02
26.00	0.37E-02	0.61E-03	0.13E-02	0.22E-03	0.34E-02	0.30E-02
29.00	0.23E-02	0.26E-03	0.74E-03	0.11E-03	0.24E-02	0.26E-02
33.00	0.21E-02	0.84E-04	0.64E-03	0.42E-04	0.22E-02	0.21E-02
37.00	0.16E-02	0.27E-04	0.55E-03	0.16E-04	0.17E-02	0.18E-02

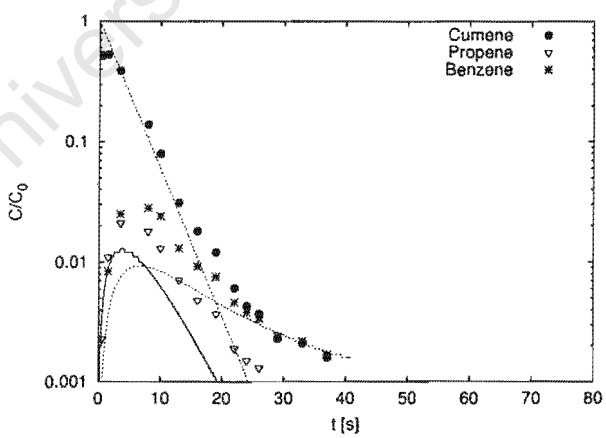

Appendix K. Cumene pulse experiments over T4480

Run Conditions react9

T_R [°C]	F(STP) [ml/min]	R_y [cm]	V_{cat} [ml]	τ [s]
392	411	0.075	0.173	2.94

Errors of C(t)

	Cumene	Propene	Benzene
Least Err	0.17E+00	0.11E+00	0.49E-01
R^2	0.973	0.901	0.949
Min Err% (@ time)	19.00(2.0)	1.81(2.0)	0.55(18.0)
Max Err% (@ time)	559.18(46.0)	30.14(22.0)	10.63(1.0)

Parameter Estimates

	Low Estimate	Estimate	High Estimate
$K_c(Benzene)$	141	304	657
$k_{eff}[1/s]$	122	228	423
$\alpha(Benzene)$	0.76E-02	0.16E-01	0.35E-01
ϕ	9	12	17

Model Parameters

	Cumene	Propene	Benzene
$D_y[cm^2/s]$	0.12E-01	0.20E-01	0.15E-01
$K_c[/]$	0	0	304
α	0.63E+01	0.10E+02	0.16E-01
β	0.21E-01	0.35E-01	0.27E-01

Experiment versus Model

	CUMENE		PROPENE		BENZENE	
t[s]	Exp	Mod	Exp	Mod	Exp	Mod
0.50	0.87E+00	0.81E+00	0.19E-01	0.12E-01	0.12E-01	0.88E-02
1.00	0.88E+00	0.65E+00	0.30E-01	0.19E-01	0.27E-01	0.18E-01
2.00	0.49E+00	0.43E+00	0.29E-01	0.27E-01	0.32E-01	0.31E-01
3.00	0.37E+00	0.28E+00	0.25E-01	0.27E-01	0.33E-01	0.36E-01
5.00	0.26E+00	0.12E+00	0.29E-01	0.21E-01	0.37E-01	0.34E-01
7.00	0.13E+00	0.51E-01	0.21E-01	0.14E-01	0.30E-01	0.27E-01
9.00	0.50E-01	0.22E-01	0.10E-01	0.85E-02	0.16E-01	0.20E-01
11.00	0.23E-01	0.92E-02	0.60E-02	0.49E-02	0.11E-01	0.14E-01
13.00	0.12E-01	0.39E-02	0.38E-02	0.27E-02	0.72E-02	0.10E-01
18.00	0.66E-02	0.47E-03	0.22E-02	0.58E-03	0.49E-02	0.48E-02
22.00	0.40E-02	0.86E-04	0.12E-02	0.16E-03	0.34E-02	0.30E-02
26.00	0.19E-02	0.17E-04	0.53E-03	0.44E-04	0.18E-02	0.20E-02
30.00	0.13E-02	0.31E-05	0.56E-03	0.12E-04	0.13E-02	0.15E-02
36.00	0.11E-02	0.46E-06	0.67E-03	0.18E-05	0.11E-02	0.10E-02
40.00	0.11E-02	0.72E-07	0.49E-03	0.48E-06	0.10E-02	0.80E-03
43.00	0.83E-03	0.11E-06	0.32E-03	0.23E-06	0.75E-03	0.67E-03
46.00	0.78E-01	0.50E-07	0.00E+00	0.16E-06	0.46E-03	0.57E-03

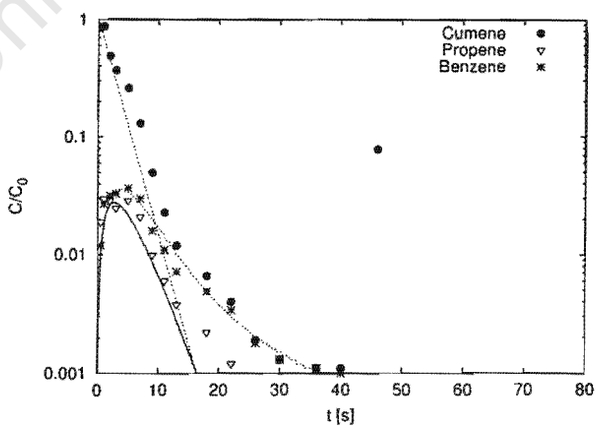

Appendix K. Cumene pulse experiments over T4480

Run Conditions react10

T_R [°C]	F(STP) [ml/min]	R_y [cm]	V_{cat} [ml]	τ [s]
392	511	0.075	0.173	2.37

Errors of C(t)

	Cumene	Propene	Benzene
Least Err	0.12E+00	0.11E+00	0.55E-01
R^2	0.988	0.960	0.945
Min Err% (@ time)	8.96(2.0)	1.18(7.0)	0.06(2.0)
Max Err% (@ time)	36.93(11.0)	19.73(15.0)	7.49(7.0)

Parameter Estimates

	Low Estimate	Estimate	High Estimate
$K_c(Benzene)$	84	187	418
$k_{eff}[1/s]$	86	136	214
$\alpha(Benzene)$	0.96E-02	0.21E-01	0.48E-01
ϕ	7	9	12

Model Parameters

	Cumene	Propene	Benzene
$D_y[cm^2/s]$	0.12E-01	0.20E-01	0.15E-01
$K_c[/]$	0	0	187
α	0.51E+01	0.84E+01	0.21E-01
β	0.17E-01	0.28E-01	0.21E-01

Experiment versus Model

	CUMENE		PROPENE		BENZENE	
t[s]	Exp	Mod	Exp	Mod	Exp	Mod
0.50	0.74E+00	0.78E+00	0.14E-01	0.85E-02	0.72E-02	0.66E-02
1.00	0.57E+00	0.61E+00	0.20E-01	0.14E-01	0.17E-01	0.13E-01
2.00	0.41E+00	0.38E+00	0.21E-01	0.17E-01	0.21E-01	0.21E-01
3.00	0.31E+00	0.23E+00	0.22E-01	0.17E-01	0.24E-01	0.24E-01
5.00	0.12E+00	0.87E-01	0.12E-01	0.11E-01	0.17E-01	0.20E-01
7.00	0.54E-01	0.33E-01	0.67E-02	0.64E-02	0.10E-01	0.14E-01
9.00	0.27E-01	0.12E-01	0.40E-02	0.33E-02	0.69E-02	0.96E-02
11.00	0.20E-01	0.47E-02	0.30E-02	0.16E-02	0.57E-02	0.64E-02
13.00	0.99E-02	0.18E-02	0.17E-02	0.79E-03	0.34E-02	0.44E-02
15.00	0.87E-02	0.67E-03	0.14E-02	0.37E-03	0.31E-02	0.31E-02
18.00	0.47E-02	0.16E-03	0.79E-03	0.12E-03	0.21E-02	0.20E-02
22.00	0.26E-02	0.22E-04	0.44E-03	0.24E-04	0.12E-02	0.12E-02

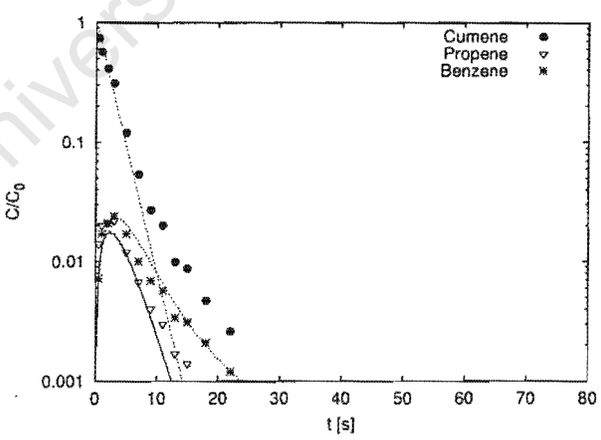

Appendix K. Cumene pulse experiments over T4480

Run Conditions react11				
T_R [°C]	F(STP) [ml/min]	R_y [cm]	V_{cat} [ml]	τ [s]
392	461	0.075	0.173	2.62

	Errors of C(t)		
	Cumene	Propene	Benzene
Least Err	0.10E+00	NAN	NAN
R^2	0.984	0.864	0.945
Min Err% (@ time)	6.56(0.5)	2.86(7.0)	0.06(18.0)
Max Err% (@ time)	28.95(5.0)	23.61(18.0)	6.21(11.0)

Parameter Estimates			
	Low Estimate	Estimate	High Estimate
$K_c(Benzene)$	90	186	386
$k_{eff}[1/s]$	87	147	249
$\alpha(Benzene)$	0.12E-01	0.24E-01	0.49E-01
ϕ	7	10	13

Model Parameters			
	Cumene	Propene	Benzene
$D_y[cm^2/s]$	0.12E-01	0.20E-01	0.15E-01
$K_c[/]$	0	0	186
α	0.56E+01	0.93E+01	0.24E-01
β	0.19E-01	0.31E-01	0.24E-01

Experiment versus Model

	CUMENE		PROPENE		BENZENE	
t[s]	Exp	Mod	Exp	Mod	Exp	Mod
0.50	0.79E+00	0.80E+00	0.00E+00	0.91E-02	0.00E+00	0.72E-02
1.00	0.57E+00	0.64E+00	0.22E-01	0.15E-01	0.19E-01	0.15E-01
2.00	0.45E+00	0.41E+00	0.24E-01	0.20E-01	0.26E-01	0.24E-01
3.00	0.30E+00	0.26E+00	0.22E-01	0.20E-01	0.27E-01	0.28E-01
5.00	0.18E+00	0.11E+00	0.18E-01	0.14E-01	0.25E-01	0.25E-01
7.00	0.65E-01	0.43E-01	0.10E-01	0.88E-02	0.16E-01	0.19E-01
9.00	0.36E-01	0.18E-01	0.68E-02	0.50E-02	0.11E-01	0.13E-01
11.00	0.16E-01	0.72E-02	0.35E-02	0.27E-02	0.65E-02	0.89E-02
13.00	0.93E-02	0.29E-02	0.22E-02	0.14E-02	0.47E-02	0.61E-02
15.00	0.59E-02	0.12E-02	0.14E-02	0.71E-03	0.35E-02	0.44E-02
18.00	0.44E-02	0.31E-03	0.12E-02	0.25E-03	0.27E-02	0.27E-02
22.00	0.22E-02	0.52E-04	0.59E-03	0.60E-04	0.16E-02	0.16E-02
26.00	0.19E-02	0.93E-05	0.50E-03	0.14E-04	0.12E-02	0.11E-02

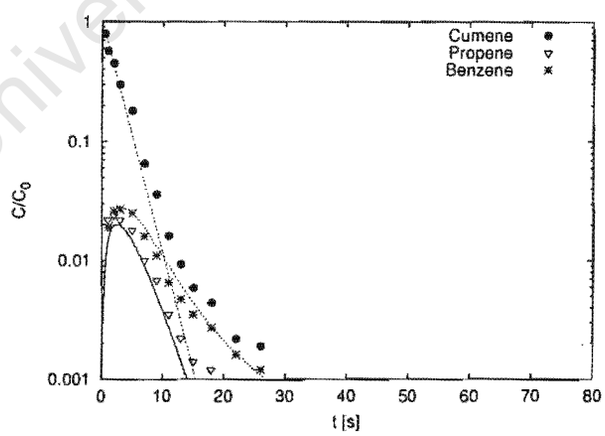

Appendix K. Cumene pulse experiments over T4480

Run Conditions react12

T_R [°C]	F(STP) [ml/min]	R_y [cm]	V_{cat} [ml]	τ [s]
441	511	0.075	2.593	2.07

Errors of C(t)

	Cumene	Propene	Benzene
Least Err	0.27E+00	0.49E-01	0.77E-01
R^2	0.958	0.997	0.980
Min Err% (@ time)	14.94(0.5)	0.63(9.0)	0.14(115.0)
Max Err% (@ time)	44.51(1.5)	8.91(0.5)	20.20(0.5)

Parameter Estimates

	Low Estimate	Estimate	High Estimate
$K_c(Propene)$	24	33	45
$K_c(Benzene)$	340	493	714
$k_{eff}[1/s]$	294	727	1793
$\alpha(Propene)$	0.10E+00	0.14E+00	0.19E+00
$\alpha(Benzene)$	0.49E-02	0.72E-02	0.10E-01
ϕ	14	22	36

Model Parameters

	Cumene	Propene	Benzene
$D_y[cm^2/s]$	0.12E-01	0.20E-01	0.15E-01
$K_c[/]$	0	33	493
α	0.45E+01	0.14E+00	0.72E-02
β	0.24E+00	0.40E+00	0.30E+00

Experiment versus Model

	CUMENE		PROPENE		BENZENE	
t[s]	Exp	Mod	Exp	Mod	Exp	Mod
0.50	0.17E+00	0.22E+00	0.14E+00	0.12E+00	0.13E+00	0.84E-01
1.50	0.43E-01	0.11E-01	0.13E+00	0.11E+00	0.11E+00	0.80E-01
6.00	0.45E-02	0.22E-06	0.29E-01	0.33E-01	0.34E-01	0.35E-01
9.00	0.31E-02	0.20E-07	0.17E-01	0.17E-01	0.26E-01	0.26E-01
15.00	0.11E-02	-0.79E-08	0.45E-02	0.48E-02	0.16E-01	0.17E-01
21.00	0.23E-03	-0.12E-07	0.11E-02	0.13E-02	0.92E-02	0.13E-01
28.00	0.19E-03	-0.37E-10	0.46E-03	0.29E-03	0.60E-02	0.98E-02
45.00	0.87E-12	-0.17E-06	0.39E-03	0.80E-05	0.51E-02	0.60E-02
55.00	0.74E-12	-0.94E-07	0.22E-03	0.97E-06	0.34E-02	0.48E-02
65.00	0.77E-12	-0.20E-09	0.43E-03	0.13E-06	0.27E-02	0.39E-02
75.00	0.59E-12	0.31E-08	0.19E-03	0.16E-07	0.26E-02	0.32E-02
100.00	0.28E-12	0.53E-09	0.21E-03	0.53E-08	0.17E-02	0.20E-02
115.00	0.58E-12	-0.16E-10	0.27E-03	0.13E-08	0.15E-02	0.15E-02
145.00	0.74E-12	-0.11E-12	0.20E-03	-0.51E-10	0.12E-02	0.85E-03

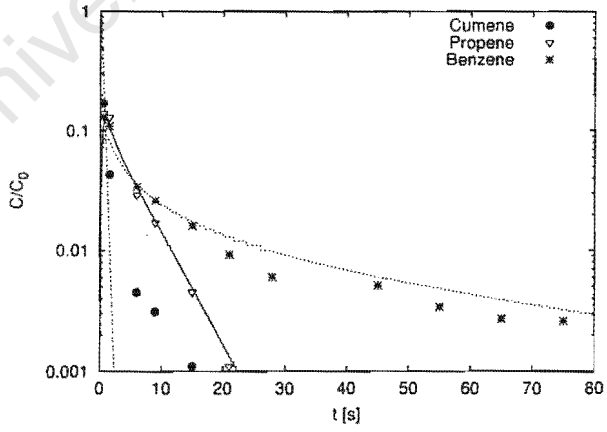

Appendix K. Cumene pulse experiments over T4480

Run Conditions react13

T_R [°C]	F(STP) [ml/min]	R_y [cm]	V_{cat} [ml]	τ [s]
441	467	0.075	2.593	2.27

Errors of C(t)

	Cumene	Propene	Benzene
Least Err	0.32E+00	0.10E+00	0.82E-01
R^2	0.792	0.967	0.945
Min Err% (@ time)	16.76(0.5)	1.62(1.5)	0.57(145.0)
Max Err% (@ time)	81.75(1.5)	11.01(0.5)	22.57(1.5)

Parameter Estimates

	Low Estimate	Estimate	High Estimate
$K_c(Propene)$	19	29	44
$K_c(Benzene)$	448	765	1307
$k_{eff}[1/s]$	345	843	2062
$\alpha(Propene)$	0.11E+00	0.17E+00	0.25E+00
$\alpha(Benzene)$	0.30E-02	0.50E-02	0.86E-02
ϕ	15	24	38

Model Parameters

	Cumene	Propene	Benzene
$D_y[cm^2/s]$	0.12E-01	0.20E-01	0.15E-01
$K_c[/]$	0	29	765
α	0.49E+01	0.17E+00	0.50E-02
β	0.26E+00	0.43E+00	0.33E+00

Experiment versus Model

	CUMENE		PROPENE		BENZENE	
t[s]	Exp	Mod	Exp	Mod	Exp	Mod
0.50	0.15E+00	0.20E+00	0.10E+00	0.13E+00	0.78E-01	0.71E-01
1.50	0.71E-01	0.83E-02	0.11E+00	0.12E+00	0.11E+00	0.67E-01
6.00	0.63E-02	0.12E-06	0.48E-01	0.38E-01	0.48E-01	0.32E-01
9.00	0.29E-02	0.28E-07	0.22E-01	0.20E-01	0.30E-01	0.24E-01
15.00	0.36E-03	0.33E-07	0.34E-02	0.55E-02	0.14E-01	0.17E-01
21.00	0.44E-03	0.22E-08	0.19E-02	0.15E-02	0.10E-01	0.13E-01
28.00	0.17E-03	-0.46E-08	0.72E-03	0.35E-03	0.79E-02	0.10E-01
36.00	0.11E-03	0.11E-07	0.31E-03	0.64E-04	0.55E-02	0.83E-02
45.00	0.82E-12	-0.17E-07	0.25E-03	0.96E-05	0.42E-02	0.67E-02
55.00	0.70E-12	0.14E-08	0.00E+00	0.12E-05	0.39E-02	0.56E-02
65.00	0.87E-12	0.11E-09	0.65E-03	0.30E-06	0.51E-02	0.47E-02
75.00	0.48E-11	0.12E-09	0.48E-05	0.13E-07	0.25E-02	0.41E-02
100.00	0.96E-12	-0.40E-12	0.20E-03	0.34E-09	0.21E-02	0.29E-02
115.00	0.63E-12	0.34E-12	0.17E-03	-0.20E-08	0.18E-02	0.24E-02
130.00	0.68E-11	-0.96E-13	0.18E-03	0.12E-08	0.15E-02	0.20E-02
145.00	0.92E-12	0.44E-13	0.24E-03	-0.56E-09	0.16E-02	0.17E-02
180.00	0.90E-12	0.70E-15	0.31E-03	0.21E-09	0.14E-02	0.11E-02

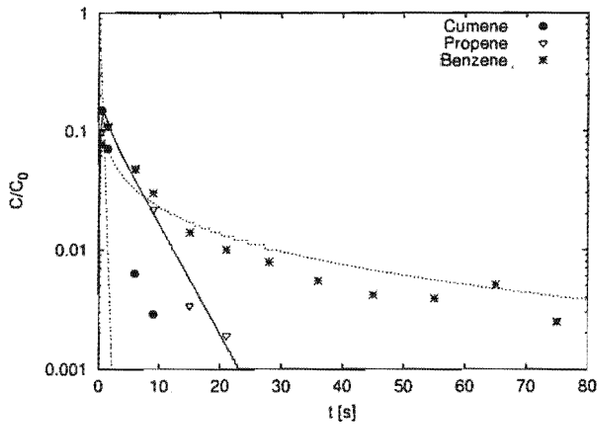

Appendix K. Cumene pulse experiments over T4480

Run Conditions react14

T_R [°C]	F(STP) [ml/min]	R_y [cm]	V_{cat} [ml]	τ [s]
441	411	0.075	2.593	2.57

Errors of C(t)

	Cumene	Propene	Benzene
Least Err	0.29E+00	0.40E-01	0.64E-01
R^2	0.930	0.993	0.980
Min Err% (@ time)	7.93(0.5)	0.07(20.0)	0.42(150.0)
Max Err% (@ time)	64.58(1.5)	9.22(4.5)	29.12(0.5)

Parameter Estimates

	Low Estimate	Estimate	High Estimate
$K_c(Propene)$	16	23	33
$K_c(Benzene)$	417	670	1078
$k_{eff}[1/s]$	349	892	2282
$\alpha(Propene)$	0.17E+00	0.24E+00	0.34E+00
$\alpha(Benzene)$	0.41E-02	0.65E-02	0.11E-01
ϕ	15	25	40

Model Parameters

	Cumene	Propene	Benzene
$D_y[cm^2/s]$	0.12E-01	0.20E-01	0.15E-01
$K_c[/]$	0	23	670
α	0.55E+01	0.24E+00	0.65E-02
β	0.30E+00	0.49E+00	0.37E+00

Experiment versus Model

	CUMENE		PROPENE		BENZENE	
t[s]	Exp	Mod	Exp	Mod	Exp	Mod
0.50	0.17E+00	0.20E+00	0.16E+00	0.14E+00	0.14E+00	0.80E-01
1.50	0.53E-01	0.79E-02	0.15E+00	0.13E+00	0.13E+00	0.75E-01
4.50	0.92E-02	0.89E-06	0.79E-01	0.63E-01	0.74E-01	0.43E-01
6.00	0.50E-02	-0.23E-07	0.41E-01	0.45E-01	0.43E-01	0.36E-01
14.00	0.82E-03	-0.56E-08	0.82E-02	0.81E-02	0.21E-01	0.21E-01
20.00	0.22E-03	0.66E-08	0.22E-02	0.23E-02	0.14E-01	0.16E-01
26.00	0.94E-12	0.41E-08	0.64E-03	0.62E-03	0.94E-02	0.13E-01
35.00	0.33E-12	0.34E-08	0.43E-03	0.91E-04	0.73E-02	0.10E-01
45.00	0.92E-12	-0.65E-08	0.49E-03	0.11E-04	0.61E-02	0.81E-02
55.00	0.10E-11	-0.17E-08	0.30E-03	0.14E-05	0.53E-02	0.67E-02
65.00	0.11E-11	0.59E-09	0.31E-03	0.50E-06	0.42E-02	0.57E-02
75.00	0.87E-12	0.38E-10	0.41E-03	0.21E-07	0.43E-02	0.49E-02
90.00	0.66E-12	-0.10E-09	0.21E-03	0.13E-06	0.30E-02	0.40E-02
105.00	0.86E-11	-0.28E-11	0.59E-03	-0.46E-07	0.28E-02	0.33E-02
135.00	0.94E-12	-0.62E-11	0.18E-03	-0.63E-07	0.23E-02	0.23E-02
150.00	0.73E-12	0.27E-11	0.19E-03	0.16E-07	0.18E-02	0.19E-02
165.00	0.64E-12	-0.36E-12	0.64E-06	-0.51E-09	0.19E-02	0.16E-02

Appendix K. Cumene pulse experiments over T4480

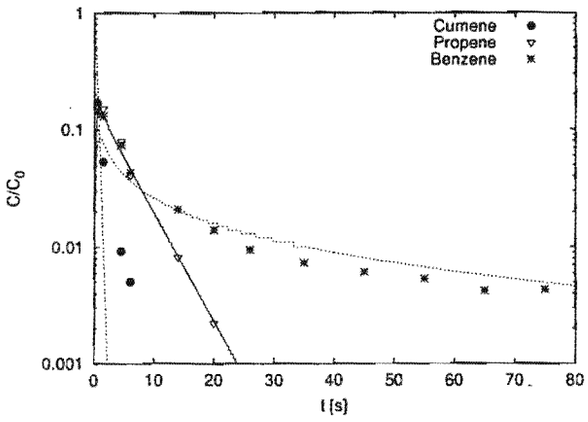

Appendix K. Cumene pulse experiments over T4480

Run Conditions react15

T_R [°C]	F(STP) [ml/min]	R_y [cm]	V_{cat} [ml]	τ [s]
419	311	0.075	2.593	3.51

Errors of C(t)

	Cumene	Propene	Benzene
Least Err	0.34E+00	0.61E-01	0.79E-01
R^2	0.808	0.915	0.925
Min Err% (@ time)	2.36(0.5)	1.38(35.0)	0.20(20.0)
Max Err% (@ time)	258.31(4.5)	18.12(3.0)	24.80(3.0)

Parameter Estimates

	Low Estimate	Estimate	High Estimate
$K_c(Propene)$	26	37	54
$K_c(Benzene)$	322	589	1077
$k_{eff}[1/s]$	760	1869	4595
$\alpha(Propene)$	0.15E+00	0.21E+00	0.30E+00
$\alpha(Benzene)$	0.56E-02	0.10E-01	0.19E-01
ϕ	23	36	57

Model Parameters

	Cumene	Propene	Benzene
$D_y[cm^2/s]$	0.12E-01	0.20E-01	0.15E-01
$K_c[/]$	0	37	589
α	0.75E+01	0.21E+00	0.10E-01
β	0.41E+00	0.67E+00	0.51E+00

Experiment versus Model

	CUMENE		PROPENE		BENZENE	
t[s]	Exp	Mod	Exp	Mod	Exp	Mod
0.50	0.10E+00	0.11E+00	0.14E+00	0.16E+00	0.13E+00	0.12E+00
1.50	0.49E-01	0.13E-02	0.16E+00	0.13E+00	0.13E+00	0.94E-01
3.00	0.24E-01	0.22E-05	0.14E+00	0.96E-01	0.11E+00	0.67E-01
4.50	0.12E-01	0.14E-06	0.11E+00	0.76E-01	0.88E-01	0.54E-01
6.00	0.74E-02	-0.48E-07	0.84E-01	0.62E-01	0.70E-01	0.45E-01
8.00	0.57E-02	-0.28E-07	0.63E-01	0.48E-01	0.57E-01	0.38E-01
11.00	0.25E-02	0.12E-08	0.28E-01	0.33E-01	0.30E-01	0.32E-01
14.00	0.15E-02	-0.41E-08	0.18E-01	0.23E-01	0.25E-01	0.27E-01
20.00	0.15E-05	0.18E-08	0.99E-02	0.11E-01	0.22E-01	0.21E-01
35.00	0.23E-05	-0.25E-08	0.15E-02	0.16E-02	0.10E-01	0.14E-01
45.00	0.13E-05	-0.79E-10	0.69E-03	0.46E-03	0.76E-02	0.12E-01
65.00	0.12E-05	0.39E-07	0.31E-03	0.38E-04	0.62E-02	0.88E-02
75.00	0.15E-05	0.18E-07	0.68E-03	0.11E-04	0.57E-02	0.77E-02
165.00	0.21E-05	-0.11E-10	0.13E-03	-0.33E-08	0.26E-02	0.27E-02

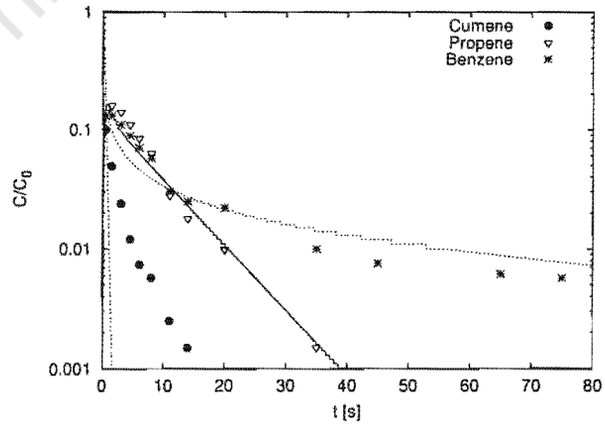

Appendix K. Cumene pulse experiments over T4480

Run Conditions react16

T_R [°C]	F(STP) [ml/min]	R_y [cm]	V_{cat} [ml]	τ [s]
419	411	0.075	2.593	2.66

Errors of C(t)

	Cumene	Propene	Benzene
Least Err	0.34E+00	0.11E+00	0.78E-01
R^2	0.892	0.963	0.978
Min Err% (@ time)	0.06(0.5)	1.32(20.0)	2.94(65.0)
Max Err% (@ time)	166.51(3.0)	42.63(3.0)	22.99(1.5)

Parameter Estimates

	Low Estimate	Estimate	High Estimate
$K_c(Propene)$	17	29	52
$K_c(Benzene)$	199	598	1791
$k_{eff}[1/s]$	419	1367	4458
$\alpha(Propene)$	0.11E+00	0.20E+00	0.34E+00
$\alpha(Benzene)$	0.25E-02	0.76E-02	0.23E-01
ϕ	17	31	56

Model Parameters

	Cumene	Propene	Benzene
$D_y[cm^2/s]$	0.12E-01	0.20E-01	0.15E-01
$K_c[/]$	0	29	598
α	0.57E+01	0.20E+00	0.76E-02
β	0.31E+00	0.51E+00	0.38E+00

Experiment versus Model

	CUMENE		PROPENE		BENZENE	
t[s]	Exp	Mod	Exp	Mod	Exp	Mod
0.50	0.14E+00	0.14E+00	0.22E+00	0.15E+00	0.14E+00	0.10E+00
1.50	0.52E-01	0.28E-02	0.23E+00	0.13E+00	0.14E+00	0.85E-01
3.00	0.12E-01	0.84E-05	0.18E+00	0.85E-01	0.99E-01	0.60E-01
4.50	0.25E-02	0.35E-06	0.11E+00	0.63E-01	0.60E-01	0.47E-01
6.00	0.14E-02	0.40E-07	0.77E-01	0.47E-01	0.48E-01	0.39E-01
8.00	0.77E-05	-0.98E-08	0.49E-01	0.33E-01	0.38E-01	0.33E-01
14.00	0.14E-05	-0.13E-07	0.92E-02	0.11E-01	0.16E-01	0.22E-01
20.00	0.34E-05	0.51E-08	0.33E-02	0.36E-02	0.13E-01	0.17E-01
26.00	0.16E-05	0.61E-08	0.21E-02	0.12E-02	0.10E-01	0.14E-01
35.00	0.23E-05	-0.33E-08	0.47E-04	0.23E-03	0.76E-02	0.11E-01
45.00	0.13E-05	-0.44E-07	0.26E-04	0.37E-04	0.64E-02	0.86E-02
55.00	0.12E-05	0.13E-07	0.24E-04	0.59E-05	0.57E-02	0.71E-02
65.00	0.56E-05	-0.14E-08	0.11E-03	0.99E-06	0.52E-02	0.60E-02

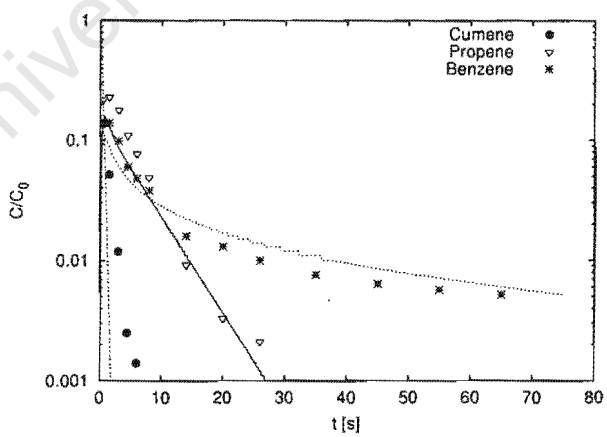

Appendix K. Cumene pulse experiments over T4480

Run Conditions react17

T_R [°C]	F(STP) [ml/min]	R_y [cm]	V_{cat} [ml]	τ [s]
419	511	0.075	2.593	2.14

Errors of C(t)

	Cumene	Propene	Benzene
Least Err	0.32E+00	0.11E+00	0.18E-01
R^2	0.875	0.982	0.999
Min Err% (@ time)	0.75(0.5)	0.97(20.0)	0.09(4.5)
Max Err% (@ time)	110.10(1.5)	41.37(0.5)	3.02(11.0)

Parameter Estimates

	Low Estimate	Estimate	High Estimate
$K_c(Propene)$	109	161	239
$K_c(Benzene)$	278	695	1733
$k_{eff}[1/s]$	739	1865	4705
$\alpha(Propene)$	0.20E-01	0.30E-01	0.44E-01
$\alpha(Benzene)$	0.21E-02	0.52E-02	0.13E-01
ϕ	23	36	58

Model Parameters

	Cumene	Propene	Benzene
$D_y[cm^2/s]$	0.12E-01	0.20E-01	0.15E-01
$K_c[/]$	0	161	695
α	0.46E+01	0.30E-01	0.52E-02
β	0.25E+00	0.41E+00	0.31E+00

Experiment versus Model

	CUMENE		PROPENE		BENZENE	
t[s]	Exp	Mod	Exp	Mod	Exp	Mod
0.50	0.10E+00	0.99E-01	0.19E+00	0.98E-01	0.11E+00	0.10E+00
1.50	0.37E-01	0.98E-03	0.15E+00	0.67E-01	0.77E-01	0.77E-01
3.00	0.29E-02	0.21E-05	0.10E+00	0.43E-01	0.52E-01	0.52E-01
4.50	0.39E-05	0.30E-06	0.78E-01	0.33E-01	0.41E-01	0.41E-01
6.00	0.22E-05	-0.83E-07	0.61E-01	0.26E-01	0.35E-01	0.34E-01
8.00	0.33E-05	-0.35E-07	0.43E-01	0.21E-01	0.29E-01	0.27E-01
11.00	0.21E-05	-0.19E-07	0.22E-01	0.16E-01	0.19E-01	0.22E-01
14.00	0.24E-05	-0.23E-07	0.14E-01	0.12E-01	0.17E-01	0.18E-01
20.00	0.21E-05	0.43E-08	0.87E-02	0.84E-02	0.14E-01	0.13E-01
26.00	0.21E-05	0.10E-07	0.51E-02	0.58E-02	0.12E-01	0.11E-01
45.00	0.53E-06	-0.46E-09	0.17E-02	0.18E-02	0.70E-02	0.64E-02
55.00	0.15E-05	0.33E-09	0.11E-02	0.10E-02	0.57E-02	0.52E-02

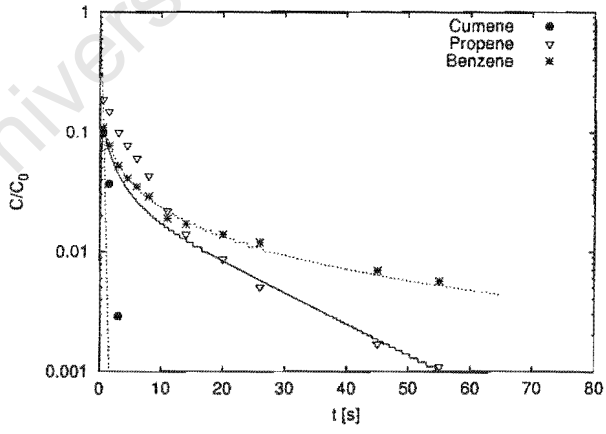

Appendix K. Cumene pulse experiments over T4480

Run Conditions react18

T_R [°C]	F(STP) [ml/min]	R_y [cm]	V_{cat} [ml]	τ [s]
391	311	0.075	2.593	3.66

Errors of C(t)

	Cumene	Propene	Benzene
Least Err	0.47E-01	0.13E+00	0.10E+00
R^2	0.999	0.940	0.732
Min Err% (@ time)	0.08(2.5)	1.55(20.0)	0.11(11.0)
Max Err% (@ time)	16.90(0.5)	75.09(0.5)	54.96(0.5)

Parameter Estimates

	Low Estimate	Estimate	High Estimate
$K_c(Propene)$	41	62	94
$K_c(Benzene)$	691	1352	2645
$k_{eff}[1/s]$	155	235	354
$\alpha(Propene)$	0.88E-01	0.13E+00	0.20E+00
$\alpha(Benzene)$	0.24E-02	0.46E-02	0.90E-02
ϕ	10	13	16

Model Parameters

	Cumene	Propene	Benzene
$D_y[cm^2/s]$	0.12E-01	0.20E-01	0.15E-01
$K_c[/]$	0	62	1352
α	0.79E+01	0.13E+00	0.46E-02
β	0.42E+00	0.70E+00	0.53E+00

Experiment versus Model

	CUMENE		PROPENE		BENZENE	
t[s]	Exp	Mod	Exp	Mod	Exp	Mod
0.50	0.37E+00	0.43E+00	0.21E+00	0.66E-01	0.86E-01	0.22E-01
1.50	0.79E-01	0.81E-01	0.22E+00	0.94E-01	0.96E-01	0.34E-01
2.50	0.15E-01	0.15E-01	0.18E+00	0.84E-01	0.71E-01	0.33E-01
3.50	0.55E-02	0.29E-02	0.15E+00	0.72E-01	0.55E-01	0.30E-01
4.50	0.40E-02	0.54E-03	0.12E+00	0.63E-01	0.37E-01	0.28E-01
7.00	0.56E-06	0.93E-05	0.91E-01	0.48E-01	0.30E-01	0.23E-01
11.00	0.15E-06	0.12E-07	0.48E-01	0.33E-01	0.19E-01	0.19E-01
20.00	0.60E-06	-0.15E-06	0.14E-01	0.15E-01	0.12E-01	0.14E-01
26.00	0.63E-06	-0.32E-07	0.72E-02	0.90E-02	0.10E-01	0.12E-01
35.00	0.11E-05	-0.11E-07	0.37E-02	0.41E-02	0.77E-02	0.10E-01
45.00	0.21E-06	-0.45E-08	0.21E-02	0.17E-02	0.68E-02	0.89E-02
55.00	0.21E-06	-0.21E-08	0.20E-02	0.73E-03	0.59E-02	0.78E-02
70.00	0.16E-06	-0.10E-08	0.34E-02	0.20E-03	0.51E-02	0.67E-02

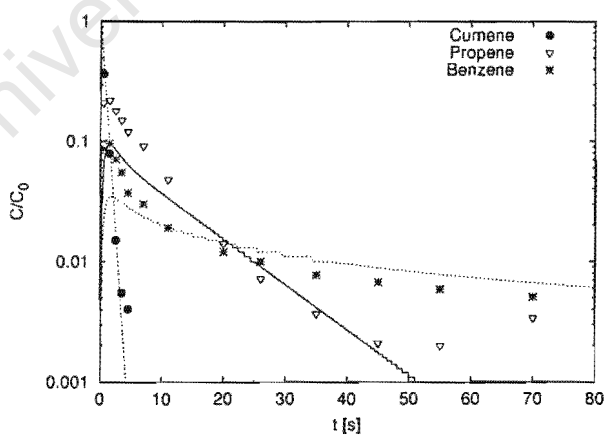

Appendix K. Cumene pulse experiments over T4480

Run Conditions react19

T_R [°C]	F(STP) [ml/min]	R_y [cm]	V_{cat} [ml]	τ [s]
391	411	0.075	2.593	2.77

Errors of C(t)

	Cumene	Propene	Benzene
Least Err	0.33E+00	0.15E+00	0.45E-01
R^2	0.645	0.979	0.974
Min Err% (@ time)	6.57(0.5)	0.73(14.0)	0.45(90.0)
Max Err% (@ time)	151.89(1.5)	119.04(110.0)	12.03(1.5)

Parameter Estimates

	Low Estimate	Estimate	High Estimate
$K_c(Propene)$	32	74	171
$K_c(Benzene)$	889	2001	4501
$k_{eff}[1/s]$	343	1320	5078
$\alpha(Propene)$	0.36E-01	0.83E-01	0.19E+00
$\alpha(Benzene)$	0.10E-02	0.24E-02	0.53E-02
ϕ	15	30	60

Model Parameters

	Cumene	Propene	Benzene
$D_y[cm^2/s]$	0.12E-01	0.20E-01	0.15E-01
$K_c[/]$	0	74	2001
α	0.60E+01	0.83E-01	0.24E-02
β	0.32E+00	0.53E+00	0.40E+00

Experiment versus Model

	CUMENE		PROPENE		BENZENE	
t[s]	Exp	Mod	Exp	Mod	Exp	Mod
0.50	0.17E+00	0.15E+00	0.20E+00	0.12E+00	0.63E-01	0.48E-01
1.50	0.10E+00	0.32E-02	0.19E+00	0.97E-01	0.61E-01	0.43E-01
2.50	0.86E-02	0.70E-04	0.15E+00	0.74E-01	0.43E-01	0.35E-01
3.50	0.38E-02	0.26E-05	0.12E+00	0.60E-01	0.34E-01	0.30E-01
6.00	0.61E-06	0.30E-07	0.76E-01	0.41E-01	0.25E-01	0.23E-01
7.00	0.76E-06	-0.17E-06	0.68E-01	0.37E-01	0.23E-01	0.22E-01
9.00	0.75E-06	-0.41E-07	0.39E-01	0.29E-01	0.15E-01	0.19E-01
14.00	0.14E-05	0.42E-07	0.17E-01	0.18E-01	0.12E-01	0.15E-01
20.00	0.61E-06	-0.25E-07	0.11E-01	0.10E-01	0.10E-01	0.12E-01
35.00	0.87E-06	0.13E-08	0.33E-02	0.24E-02	0.66E-02	0.81E-02
70.00	0.27E-06	-0.13E-10	0.57E-02	0.85E-04	0.46E-02	0.49E-02
90.00	0.74E-06	0.13E-10	0.14E-02	0.13E-04	0.39E-02	0.40E-02
110.00	0.67E-06	0.28E-11	0.25E-02	0.20E-05	0.29E-02	0.34E-02

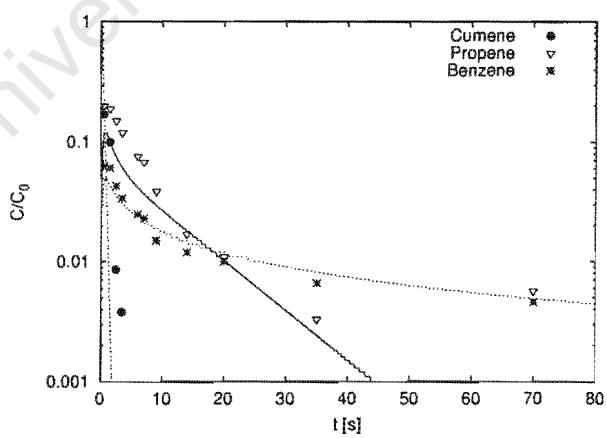

Appendix K. Cumene pulse experiments over T4480

Run Conditions react20

T_R [°C]	F(STP) [ml/min]	R_y [cm]	V_{cat} [ml]	τ [s]
391	511	0.075	2.593	2.23

Errors of C(t)

	Cumene	Propene	Benzene
Least Err	0.10E+00	0.14E+00	0.76E-01
R^2	0.997	0.936	0.774
Min Err% (@ time)	3.37(1.5)	0.00(26.0)	2.54(45.0)
Max Err% (@ time)	19.70(0.5)	85.43(0.5)	39.04(0.5)

Parameter Estimates

	Low Estimate	Estimate	High Estimate
$K_c(Propene)$	37	65	115
$K_c(Benzene)$	434	942	2041
$k_{eff}[1/s]$	185	318	549
$\alpha(Propene)$	0.44E-01	0.76E-01	0.13E+00
$\alpha(Benzene)$	0.19E-02	0.40E-02	0.87E-02
ϕ	11	15	19

Model Parameters

	Cumene	Propene	Benzene
$D_y[cm^2/s]$	0.12E-01	0.20E-01	0.15E-01
$K_c[/]$	0	65	942
α	0.48E+01	0.76E-01	0.40E-02
β	0.26E+00	0.43E+00	0.32E+00

Experiment versus Model

	CUMENE		PROPENE		BENZENE	
t[s]	Exp	Mod	Exp	Mod	Exp	Mod
0.50	0.27E+00	0.35E+00	0.24E+00	0.71E-01	0.88E-01	0.34E-01
1.50	0.48E-01	0.43E-01	0.22E+00	0.82E-01	0.77E-01	0.44E-01
2.50	0.79E-02	0.53E-02	0.13E+00	0.64E-01	0.50E-01	0.39E-01
3.50	0.14E-05	0.65E-03	0.13E+00	0.51E-01	0.41E-01	0.34E-01
4.50	0.44E-05	0.81E-04	0.98E-01	0.42E-01	0.33E-01	0.30E-01
6.00	0.16E-05	0.41E-05	0.74E-01	0.33E-01	0.29E-01	0.26E-01
9.00	0.30E-06	-0.28E-07	0.30E-01	0.21E-01	0.16E-01	0.20E-01
11.00	0.39E-06	-0.66E-08	0.20E-01	0.17E-01	0.14E-01	0.18E-01
14.00	0.36E-06	-0.78E-07	0.16E-01	0.11E-01	0.12E-01	0.15E-01
20.00	0.35E-06	-0.20E-07	0.58E-02	0.53E-02	0.98E-02	0.12E-01
26.00	0.29E-06	-0.17E-07	0.25E-02	0.25E-02	0.81E-02	0.97E-02
45.00	0.27E-06	-0.29E-08	0.27E-02	0.23E-03	0.54E-02	0.62E-02

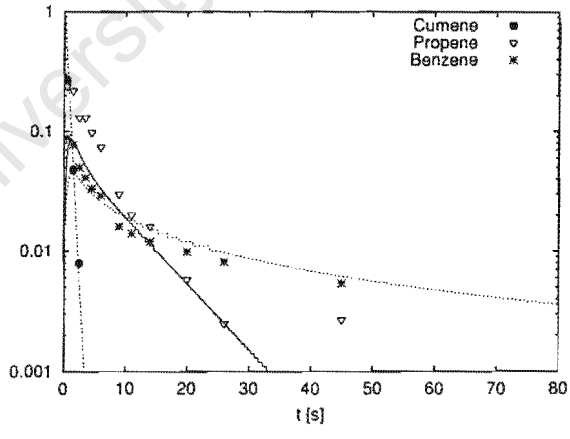

Appendix K. Cumene pulse experiments over T4480

Run Conditions react21

T_R [°C]	F(STP) [ml/min]	R_y [cm]	V_{cat} [ml]	τ [s]
419	511	0.033	0.432	2.26

Errors of C(t)

	Cumene	Propene	Benzene
Least Err	0.99E-01	0.17E+02	0.10E+00
R^2	1.000	0.993	0.975
Min Err% (@ time)	7.32(3.0)	25.76(12.0)	0.93(12.0)
Max Err% (@ time)	9.30(2.0)	111.28(23.0)	48.87(2.0)

Parameter Estimates

	Low Estimate	Estimate	High Estimate
$K_c(Benzene)$	308	1228	4898
$k_{eff}[1/s]$	345	655	1245
$\alpha(Benzene)$	0.41E-02	0.16E-01	0.65E-01
ϕ	6	9	13

Model Parameters

	Cumene	Propene	Benzene
$D_y[cm^2/s]$	0.12E-01	0.20E-01	0.15E-01
$K_c[/]$	0	0	1228
α	0.25E+02	0.41E+02	0.16E-01
β	0.21E+00	0.35E+00	0.26E+00

Experiment versus Model

	CUMENE		PROPENE		BENZENE	
t[s]	Exp	Mod	Exp	Mod	Exp	Mod
2.00	0.10E+00	0.81E-01	0.23E+00	0.11E+00	0.17E+00	0.72E-01
3.00	0.30E-01	0.23E-01	0.17E+00	0.81E-01	0.14E+00	0.65E-01
4.00	0.79E-02	0.66E-02	0.13E+00	0.55E-01	0.11E+00	0.56E-01
6.00	0.68E-05	0.54E-03	0.53E-01	0.23E-01	0.88E-01	0.42E-01
8.00	0.19E-05	0.44E-04	0.42E-01	0.97E-02	0.65E-01	0.34E-01
12.00	0.21E-05	0.35E-06	0.62E-02	0.17E-02	0.22E-01	0.23E-01
14.00	0.11E-05	0.47E-07	0.63E-02	0.69E-03	0.29E-01	0.20E-01
16.00	0.15E-05	0.18E-07	0.15E-05	0.29E-03	0.30E-01	0.17E-01
19.00	0.13E-05	0.15E-07	0.41E-02	0.77E-04	0.21E-01	0.15E-01
23.00	0.10E-05	0.63E-08	0.49E-02	0.13E-04	0.18E-01	0.12E-01
27.00	0.13E-05	-0.61E-08	0.13E-05	0.27E-05	0.17E-01	0.97E-02
31.00	0.11E-05	0.32E-08	0.11E-05	0.49E-06	0.14E-01	0.81E-02
34.00	0.37E-05	-0.77E-08	0.37E-05	0.36E-06	0.11E-01	0.71E-02
37.00	0.10E-05	-0.42E-08	0.10E-05	0.29E-06	0.11E-01	0.63E-02
41.00	0.11E-05	0.30E-08	0.11E-05	-0.15E-07	0.99E-02	0.53E-02

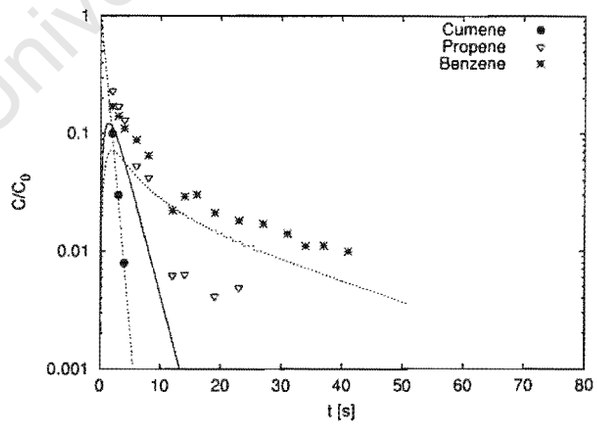

Appendix K. Cumene pulse experiments over T4480

Run Conditions react22

T_R [°C]	F(STP) [ml/min]	R_y [cm]	V_{cat} [ml]	τ [s]
419	411	0.033	0.432	2.81

Errors of C(t)

	Cumene	Propene	Benzene
Least Err	0.10E+00	0.17E+00	0.66E-01
R^2	0.947	0.984	0.966
Min Err% (@ time)	0.99(2.0)	4.22(8.0)	0.11(26.0)
Max Err% (@ time)	41.76(0.5)	158.88(43.0)	16.15(0.5)

Parameter Estimates

	Low Estimate	Estimate	High Estimate
$K_c(Benzene)$	412	557	755
$k_{eff}[1/s]$	544	919	1553
$\alpha(Benzene)$	0.33E-01	0.44E-01	0.60E-01
ϕ	8	11	14

Model Parameters

	Cumene	Propene	Benzene
$D_y[cm^2/s]$	0.12E-01	0.20E-01	0.15E-01
$K_c[/]$	0	0	557
α	0.31E+02	0.52E+02	0.44E-01
β	0.27E+00	0.44E+00	0.33E+00

Experiment versus Model

	CUMENE		PROPENE		BENZENE	
t[s]	Exp	Mod	Exp	Mod	Exp	Mod
0.50	0.62E+00	0.51E+00	0.20E+00	0.11E+00	0.11E+00	0.78E-01
1.00	0.18E+00	0.26E+00	0.21E+00	0.15E+00	0.15E+00	0.12E+00
2.00	0.71E-01	0.69E-01	0.20E+00	0.14E+00	0.15E+00	0.13E+00
3.00	0.22E-01	0.18E-01	0.15E+00	0.11E+00	0.13E+00	0.11E+00
4.00	0.99E-02	0.48E-02	0.11E+00	0.79E-01	0.10E+00	0.97E-01
8.00	0.67E-03	0.24E-04	0.23E-01	0.19E-01	0.38E-01	0.55E-01
10.00	0.11E-02	0.22E-05	0.16E-01	0.96E-02	0.40E-01	0.45E-01
15.00	0.39E-06	-0.27E-07	0.38E-02	0.16E-02	0.22E-01	0.29E-01
18.00	0.19E-06	-0.22E-08	0.41E-02	0.56E-03	0.22E-01	0.23E-01
22.00	0.22E-06	0.27E-07	0.13E-02	0.14E-03	0.16E-01	0.17E-01
26.00	0.15E-06	-0.30E-08	0.12E-02	0.34E-04	0.12E-01	0.12E-01
30.00	0.18E-06	-0.63E-08	0.23E-03	0.82E-05	0.12E-01	0.92E-02
33.00	0.14E-06	-0.29E-08	0.19E-02	0.33E-05	0.97E-02	0.74E-02
36.00	0.40E-06	0.62E-08	0.12E-02	0.13E-05	0.78E-02	0.60E-02
40.00	0.14E-05	-0.35E-08	0.14E-05	0.30E-06	0.70E-02	0.44E-02
43.00	0.36E-06	0.81E-08	0.27E-02	0.23E-06	0.77E-02	0.36E-02
46.00	0.50E-06	0.11E-07	0.50E-06	0.31E-06	0.64E-02	0.29E-02

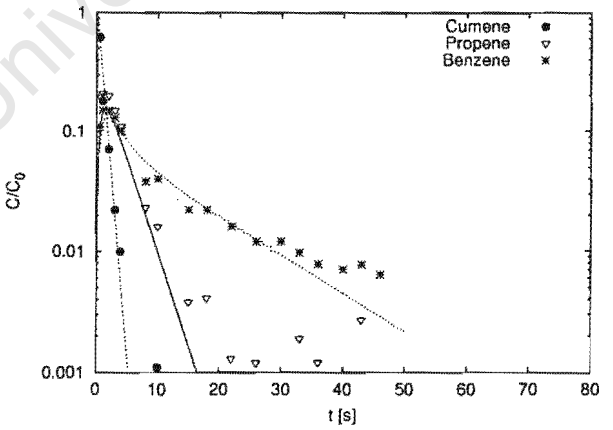

Appendix K. Cumene pulse experiments over T4480

Run Conditions react23

T_R [°C]	F(STP) [ml/min]	R_y [cm]	V_{cat} [ml]	τ [s]
419	311	0.033	0.432	3.72

Errors of C(t)

	Cumene	Propene	Benzene
Least Err	0.59E-01	0.14E+00	0.51E-01
R^2	0.990	0.980	0.949
Min Err% (@ time)	0.24(0.5)	4.55(6.0)	0.30(6.0)
Max Err% (@ time)	13.55(1.0)	67.90(33.0)	32.10(1.0)

Parameter Estimates

	Low Estimate	Estimate	High Estimate
$K_c(Benzene)$	306	433	613
$k_{eff}[1/s]$	507	857	1450
$\alpha(Benzene)$	0.53E-01	0.75E-01	0.11E+00
ϕ	8	10	14

Model Parameters

	Cumene	Propene	Benzene
$D_y[cm^2/s]$	0.12E-01	0.20E-01	0.15E-01
$K_c[/]$	0	0	433
α	0.41E+02	0.68E+02	0.75E-01
β	0.35E+00	0.58E+00	0.44E+00

Experiment versus Model

	CUMENE		PROPENE		BENZENE	
t[s]	Exp	Mod	Exp	Mod	Exp	Mod
0.50	0.54E+00	0.55E+00	0.15E+00	0.11E+00	0.14E+00	0.85E-01
1.00	0.25E+00	0.30E+00	0.22E+00	0.15E+00	0.22E+00	0.13E+00
2.00	0.87E-01	0.89E-01	0.21E+00	0.16E+00	0.23E+00	0.16E+00
3.00	0.33E-01	0.26E-01	0.16E+00	0.14E+00	0.20E+00	0.15E+00
6.00	0.42E-02	0.70E-03	0.74E-01	0.66E-01	0.10E+00	0.99E-01
8.00	0.32E-06	0.63E-04	0.25E-01	0.39E-01	0.87E-01	0.80E-01
10.00	0.13E-06	0.61E-05	0.34E-01	0.23E-01	0.63E-01	0.66E-01
12.00	0.31E-06	0.10E-05	0.20E-01	0.13E-01	0.47E-01	0.56E-01
15.00	0.10E-06	0.45E-08	0.12E-01	0.59E-02	0.39E-01	0.44E-01
18.00	0.87E-07	0.10E-06	0.52E-02	0.27E-02	0.24E-01	0.35E-01
22.00	0.10E-06	0.46E-07	0.41E-02	0.91E-03	0.23E-01	0.26E-01
26.00	0.93E-06	-0.37E-08	0.25E-02	0.31E-03	0.17E-01	0.19E-01
30.00	0.17E-06	-0.40E-07	0.12E-02	0.11E-03	0.12E-01	0.14E-01
33.00	0.14E-05	-0.48E-08	0.27E-02	0.48E-04	0.11E-01	0.11E-01
36.00	0.27E-06	0.83E-08	0.70E-03	0.22E-04	0.87E-02	0.92E-02
40.00	0.16E-06	-0.32E-10	0.78E-03	0.75E-05	0.79E-02	0.68E-02
43.00	0.46E-06	0.20E-07	0.86E-03	0.37E-05	0.65E-02	0.55E-02

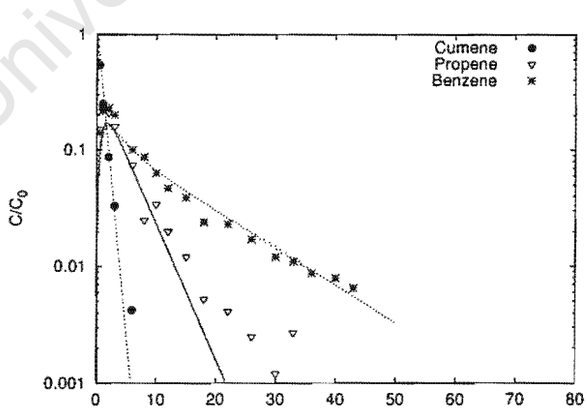

Appendix K. Cumene pulse experiments over T4480

Run Conditions react24

T_R [°C]	F(STP) [ml/min]	R_y [cm]	V_{cat} [ml]	τ [s]
441	311	0.033	0.432	3.60

Errors of C(t)

	Cumene	Propene	Benzene
Least Err	0.16E+00	0.14E+00	0.55E-01
R^2	0.960	0.990	0.970
Min Err% (@ time)	3.31(3.0)	0.12(8.0)	0.45(30.0)
Max Err% (@ time)	23.91(4.0)	53.44(33.0)	23.22(1.0)

Parameter Estimates

	Low Estimate	Estimate	High Estimate
$K_c(Benzene)$	319	512	823
$k_{eff}[1/s]$	533	913	1563
$\alpha(Benzene)$	0.39E-01	0.62E-01	0.99E-01
ϕ	8	11	14

Model Parameters

	Cumene	Propene	Benzene
$D_y[cm^2/s]$	0.12E-01	0.20E-01	0.15E-01
$K_c[/]$	0	0	512
α	0.40E+02	0.66E+02	0.62E-01
β	0.34E+00	0.56E+00	0.42E+00

Experiment versus Model

	CUMENE		PROPENE		BENZENE	
t[s]	Exp	Mod	Exp	Mod	Exp	Mod
0.50	0.56E+00	0.53E+00	0.16E+00	0.11E+00	0.12E+00	0.83E-01
1.00	0.19E+00	0.29E+00	0.20E+00	0.16E+00	0.19E+00	0.13E+00
3.00	0.26E-01	0.23E-01	0.15E+00	0.14E+00	0.19E+00	0.14E+00
4.00	0.18E-01	0.67E-02	0.13E+00	0.11E+00	0.17E+00	0.12E+00
8.00	0.14E-02	0.45E-04	0.36E-01	0.36E-01	0.72E-01	0.74E-01
10.00	0.88E-03	0.43E-05	0.29E-01	0.21E-01	0.63E-01	0.61E-01
12.00	0.35E-06	0.72E-06	0.16E-01	0.12E-01	0.46E-01	0.52E-01
15.00	0.38E-06	-0.35E-07	0.93E-02	0.52E-02	0.38E-01	0.42E-01
18.00	0.83E-06	0.13E-06	0.43E-02	0.23E-02	0.27E-01	0.34E-01
22.00	0.77E-06	0.26E-07	0.22E-02	0.75E-03	0.23E-01	0.26E-01
26.00	0.34E-06	-0.26E-07	0.15E-02	0.25E-03	0.16E-01	0.20E-01
30.00	0.39E-06	-0.31E-08	0.11E-02	0.82E-04	0.15E-01	0.15E-01
33.00	0.29E-06	-0.22E-07	0.13E-02	0.36E-04	0.10E-01	0.12E-01
46.00	0.12E-06	0.18E-07	0.73E-03	0.14E-05	0.86E-02	0.52E-02

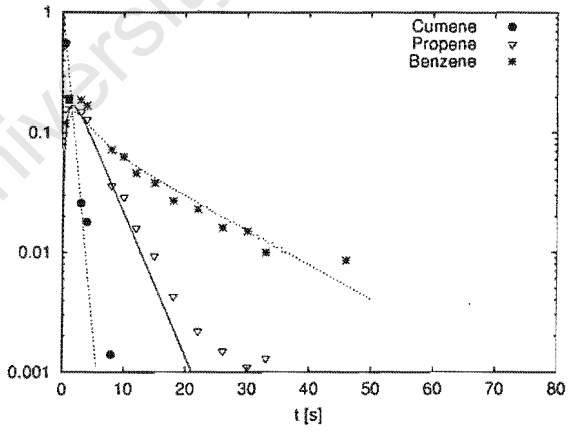

Appendix K. Cumene pulse experiments over T4480

Run Conditions react25

T_R [°C]	F(STP) [ml/min]	R_y [cm]	V_{cat} [ml]	τ [s]
441	411	0.033	0.432	2.72

Errors of C(t)

	Cumene	Propene	Benzene
Least Err	0.19E+00	0.19E+00	0.86E-01
R^2	0.973	0.988	0.986
Min Err% (@ time)	14.57(1.0)	17.57(1.0)	1.45(33.0)
Max Err% (@ time)	39.06(4.0)	96.36(33.0)	39.80(4.0)

Parameter Estimates

	Low Estimate	Estimate	High Estimate
$K_c(Benzene)$	351	857	2089
$k_{eff}[1/s]$	421	1026	2499
$\alpha(Benzene)$	0.11E-01	0.28E-01	0.68E-01
ϕ	7	12	18

Model Parameters

	Cumene	Propene	Benzene
$D_y[cm^2/s]$	0.12E-01	0.20E-01	0.15E-01
$K_c[/]$	0	0	857
α	0.30E+02	0.50E+02	0.28E-01
β	0.26E+00	0.42E+00	0.32E+00

Experiment versus Model

	CUMENE		PROPENE		BENZENE	
t[s]	Exp	Mod	Exp	Mod	Exp	Mod
0.50	0.56E+00	0.49E+00	0.16E+00	0.11E+00	0.12E+00	0.68E-01
1.00	0.19E+00	0.24E+00	0.20E+00	0.15E+00	0.19E+00	0.10E+00
3.00	0.26E-01	0.15E-01	0.15E+00	0.11E+00	0.19E+00	0.96E-01
4.00	0.18E-01	0.36E-02	0.13E+00	0.76E-01	0.17E+00	0.82E-01
8.00	0.14E-02	0.14E-04	0.36E-01	0.18E-01	0.72E-01	0.48E-01
10.00	0.88E-03	0.10E-05	0.29E-01	0.86E-02	0.63E-01	0.39E-01
12.00	0.35E-06	0.24E-06	0.16E-01	0.41E-02	0.46E-01	0.33E-01
15.00	0.38E-06	0.17E-06	0.93E-02	0.14E-02	0.38E-01	0.27E-01
18.00	0.83E-06	-0.59E-07	0.43E-02	0.46E-03	0.27E-01	0.22E-01
22.00	0.77E-06	-0.27E-07	0.22E-02	0.11E-03	0.23E-01	0.17E-01
26.00	0.34E-06	-0.20E-08	0.15E-02	0.25E-04	0.16E-01	0.14E-01
30.00	0.39E-06	0.46E-08	0.11E-02	0.62E-05	0.15E-01	0.11E-01
33.00	0.29E-06	-0.13E-08	0.13E-02	0.21E-05	0.10E-01	0.96E-02
46.00	0.12E-06	-0.15E-08	0.73E-03	0.18E-07	0.86E-02	0.50E-02

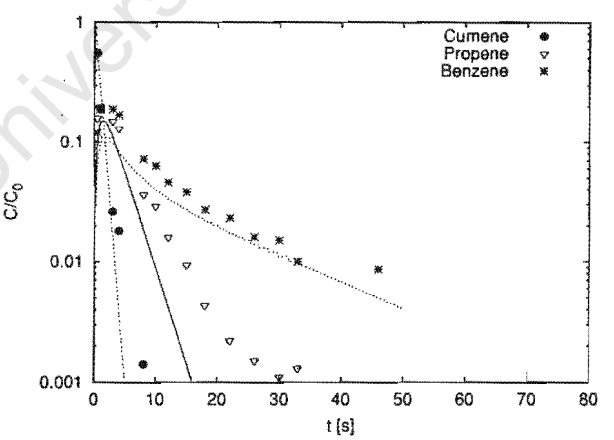

Appendix K. Cumene pulse experiments over T4480

Run Conditions react26

T_R [°C]	F(STP) [ml/min]	R_y [cm]	V_{cat} [ml]	τ [s]
441	511	0.033	0.432	2.19

Errors of C(t)

	Cumene	Propene	Benzene
Least Err	0.21E-01	0.13E+00	0.56E-01
R^2	1.000	0.914	0.958
Min Err% (@ time)	1.39(2.0)	1.45(8.0)	0.22(40.0)
Max Err% (@ time)	5.42(0.5)	35.60(18.0)	31.97(0.5)

Parameter Estimates

	Low Estimate	Estimate	High Estimate
$K_c(Benzene)$	539	696	899
$k_{eff}[1/s]$	851	1332	2085
$\alpha(Benzene)$	0.21E-01	0.28E-01	0.36E-01
ϕ	10	13	17

Model Parameters

	Cumene	Propene	Benzene
$D_y[cm^2/s]$	0.12E-01	0.20E-01	0.15E-01
$K_c[/]$	0	0	696
α	0.24E+02	0.40E+02	0.28E-01
β	0.21E+00	0.34E+00	0.26E+00

Experiment versus Model

	CUMENE		PROPENE		BENZENE	
t[s]	Exp	Mod	Exp	Mod	Exp	Mod
0.50	0.46E+00	0.44E+00	0.20E+00	0.12E+00	0.16E+00	0.86E-01
2.00	0.35E-01	0.37E-01	0.13E+00	0.12E+00	0.15E+00	0.11E+00
3.00	0.94E-02	0.70E-02	0.93E-01	0.83E-01	0.12E+00	0.93E-01
4.00	0.27E-02	0.13E-02	0.63E-01	0.53E-01	0.10E+00	0.75E-01
6.00	0.24E-02	0.50E-04	0.41E-01	0.22E-01	0.79E-01	0.53E-01
8.00	0.00E+00	0.22E-05	0.93E-02	0.87E-02	0.33E-01	0.40E-01
12.00	0.00E+00	0.62E-07	0.21E-02	0.14E-02	0.19E-01	0.25E-01
18.00	0.00E+00	-0.44E-07	0.11E-02	0.93E-04	0.13E-01	0.15E-01
22.00	0.00E+00	-0.11E-07	0.00E+00	0.15E-04	0.97E-02	0.11E-01
26.00	0.00E+00	0.99E-08	0.00E+00	0.28E-05	0.86E-02	0.84E-02
33.00	0.00E+00	0.55E-08	0.72E-03	0.29E-06	0.46E-02	0.52E-02
36.00	0.00E+00	-0.48E-08	0.66E-03	0.17E-06	0.37E-02	0.42E-02
40.00	0.00E+00	0.23E-08	0.34E-03	-0.12E-07	0.31E-02	0.32E-02
43.00	0.00E+00	-0.11E-08	0.70E-03	0.28E-07	0.27E-02	0.26E-02
46.00	0.00E+00	-0.66E-08	0.62E-03	0.62E-07	0.25E-02	0.21E-02

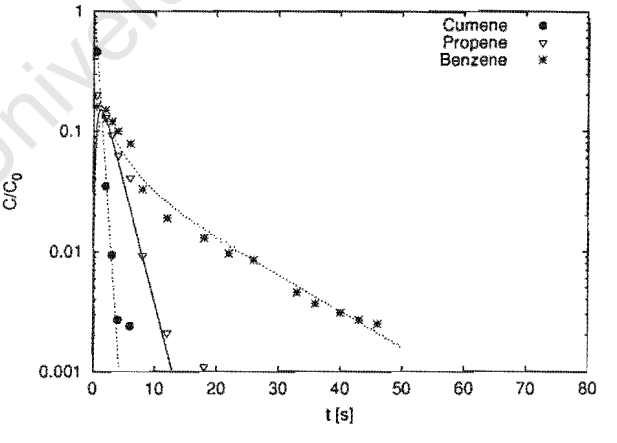

Appendix K. Cumene pulse experiments over T4480

Run Conditions react27

T_R [°C]	F(STP) [ml/min]	R_y [cm]	V_{cat} [ml]	τ [s]
472	311	0.033	0.432	3.45

Errors of C(t)

	Cumene	Propene	Benzene
Least Err	0.11E+00	0.12E+00	0.65E-01
R^2	0.990	0.961	0.957
Min Err% (@ time)	3.77(2.0)	0.39(3.0)	1.90(12.0)
Max Err% (@ time)	18.51(1.0)	21.42(6.0)	27.71(0.5)

Parameter Estimates

	Low Estimate	Estimate	High Estimate
$K_c(Benzene)$	216	359	596
$k_{eff}[1/s]$	643	986	1510
$\alpha(Benzene)$	0.51E-01	0.85E-01	0.14E+00
ϕ	9	11	14

Model Parameters

	Cumene	Propene	Benzene
$D_y[cm^2/s]$	0.12E-01	0.20E-01	0.15E-01
$K_c[/]$	0	0	359
α	0.38E+02	0.63E+02	0.85E-01
β	0.33E+00	0.54E+00	0.40E+00

Experiment versus Model

	CUMENE		PROPENE		BENZENE	
t[s]	Exp	Mod	Exp	Mod	Exp	Mod
0.50	0.47E+00	0.52E+00	0.15E+00	0.11E+00	0.16E+00	0.10E+00
1.00	0.20E+00	0.27E+00	0.19E+00	0.16E+00	0.23E+00	0.15E+00
2.00	0.66E-01	0.73E-01	0.17E+00	0.16E+00	0.23E+00	0.17E+00
3.00	0.25E-01	0.20E-01	0.13E+00	0.13E+00	0.20E+00	0.15E+00
4.00	0.10E-01	0.54E-02	0.11E+00	0.10E+00	0.18E+00	0.13E+00
6.00	0.00E+00	0.40E-03	0.27E-01	0.59E-01	0.86E-01	0.10E+00
10.00	0.00E+00	0.27E-05	0.19E-01	0.18E-01	0.58E-01	0.63E-01
12.00	0.00E+00	0.28E-06	0.15E-01	0.10E-01	0.55E-01	0.52E-01
15.00	0.00E+00	0.21E-06	0.53E-02	0.44E-02	0.32E-01	0.39E-01
18.00	0.00E+00	0.99E-08	0.28E-02	0.18E-02	0.23E-01	0.30E-01
22.00	0.00E+00	-0.20E-07	0.12E-02	0.58E-03	0.16E-01	0.21E-01
26.00	0.00E+00	-0.32E-07	0.96E-03	0.18E-03	0.13E-01	0.14E-01
30.00	0.00E+00	0.17E-07	0.93E-03	0.58E-04	0.12E-01	0.10E-01
45.00	0.00E+00	0.28E-08	0.00E+00	0.87E-06	0.50E-02	0.26E-02

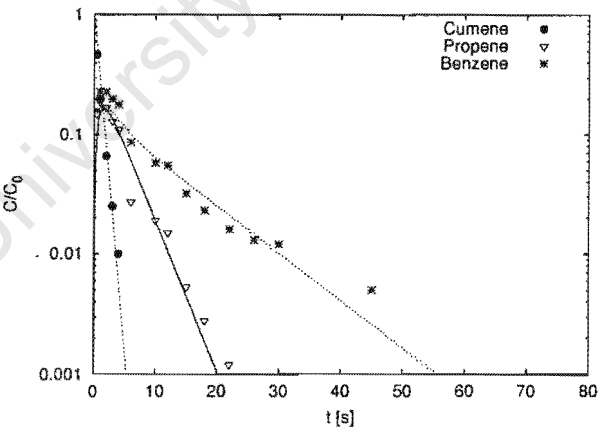

Appendix K. Cumene pulse experiments over T4480

Run Conditions react28

T_R [°C]	F(STP) [ml/min]	R_y [cm]	V_{cat} [ml]	τ [s]
472	411	0.033	0.432	2.61

Errors of C(t)

	Cumene	Propene	Benzene
Least Err	0.12E+00	0.24E+00	0.44E-01
R^2	0.969	0.980	0.978
Min Err% (@ time)	2.11(2.0)	0.48(2.0)	0.29(10.0)
Max Err% (@ time)	20.68(1.0)	117.22(40.0)	25.78(1.0)

Parameter Estimates

	Low Estimate	Estimate	High Estimate
$K_c(Benzene)$	435	542	675
$k_{eff}[1/s]$	861	1242	1791
$\alpha(Benzene)$	0.34E-01	0.42E-01	0.53E-01
ϕ	11	13	15

Model Parameters

	Cumene	Propene	Benzene
$D_y[cm^2/s]$	0.12E-01	0.20E-01	0.15E-01
$K_c[/]$	0	0	542
α	0.29E+02	0.48E+02	0.42E-01
β	0.25E+00	0.41E+00	0.31E+00

Experiment versus Model

	CUMENE		PROPENE		BENZENE	
t[s]	Exp	Mod	Exp	Mod	Exp	Mod
0.50	0.48E+00	0.46E+00	0.14E+00	0.12E+00	0.13E+00	0.94E-01
1.00	0.14E+00	0.22E+00	0.19E+00	0.16E+00	0.20E+00	0.14E+00
2.00	0.43E-01	0.46E-01	0.14E+00	0.14E+00	0.17E+00	0.14E+00
3.00	0.15E-01	0.10E-01	0.12E+00	0.10E+00	0.16E+00	0.11E+00
4.00	0.30E-02	0.21E-02	0.65E-01	0.71E-01	0.11E+00	0.95E-01
6.00	0.00E+00	0.10E-03	0.53E-01	0.34E-01	0.11E+00	0.68E-01
10.00	0.00E+00	0.29E-06	0.94E-02	0.73E-02	0.42E-01	0.41E-01
12.00	0.00E+00	0.20E-06	0.46E-02	0.34E-02	0.33E-01	0.34E-01
15.00	0.00E+00	0.45E-07	0.21E-02	0.11E-02	0.22E-01	0.26E-01
18.00	0.00E+00	-0.54E-07	0.13E-02	0.35E-03	0.16E-01	0.20E-01
22.00	0.00E+00	-0.28E-07	0.95E-03	0.75E-04	0.15E-01	0.14E-01
26.00	0.00E+00	-0.13E-08	0.10E-02	0.17E-04	0.92E-02	0.10E-01
30.00	0.00E+00	0.12E-07	0.14E-02	0.40E-05	0.67E-02	0.77E-02
35.00	0.00E+00	-0.51E-08	0.16E-06	0.66E-06	0.58E-02	0.52E-02
40.00	0.00E+00	0.98E-08	0.10E-02	0.31E-06	0.32E-02	0.35E-02
45.00	0.00E+00	-0.40E-08	0.99E-03	0.22E-06	0.21E-02	0.24E-02
55.00	0.00E+00	-0.13E-08	0.94E-03	0.47E-07	0.12E-02	0.11E-02

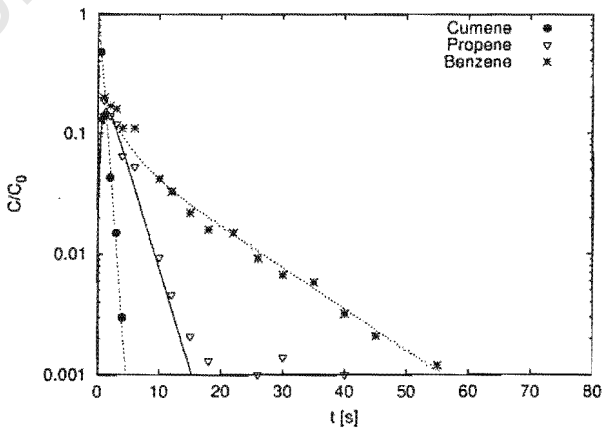

Appendix K. Cumene pulse experiments over T4480

Run Conditions react29

T_R [°C]	F(STP) [ml/min]	R_y [cm]	V_{cat} [ml]	τ [s]
472	511	0.033	0.432	2.10

Errors of C(t)

	Cumene	Propene	Benzene
Least Err	0.10E+00	0.11E+00	0.46E-01
R^2	0.999	0.974	0.981
Min Err% (@ time)	3.97(1.0)	0.56(8.0)	0.09(15.0)
Max Err% (@ time)	12.32(2.0)	25.90(15.0)	24.10(6.0)

Parameter Estimates

	Low Estimate	Estimate	High Estimate
$K_c(Benzene)$	472	586	728
$k_{eff}[1/s]$	1421	2493	4373
$\alpha(Benzene)$	0.25E-01	0.32E-01	0.39E-01
ϕ	14	18	24

Model Parameters

	Cumene	Propene	Benzene
$D_y[cm^2/s]$	0.12E-01	0.20E-01	0.15E-01
$K_c[/]$	0	0	586
α	0.23E+02	0.39E+02	0.32E-01
β	0.20E+00	0.33E+00	0.25E+00

Experiment versus Model

	CUMENE		PROPENE		BENZENE	
t[s]	Exp	Mod	Exp	Mod	Exp	Mod
0.50	0.31E+00	0.34E+00	0.21E+00	0.15E+00	0.18E+00	0.13E+00
1.00	0.11E+00	0.12E+00	0.20E+00	0.17E+00	0.20E+00	0.16E+00
2.00	0.22E-01	0.14E-01	0.13E+00	0.12E+00	0.16E+00	0.13E+00
3.00	0.00E+00	0.16E-02	0.87E-01	0.79E-01	0.14E+00	0.10E+00
4.00	0.00E+00	0.19E-03	0.57E-01	0.50E-01	0.12E+00	0.80E-01
6.00	0.00E+00	0.37E-05	0.35E-01	0.19E-01	0.95E-01	0.54E-01
8.00	0.00E+00	0.35E-06	0.77E-02	0.74E-02	0.32E-01	0.40E-01
10.00	0.00E+00	0.24E-07	0.42E-02	0.29E-02	0.26E-01	0.31E-01
12.00	0.00E+00	-0.75E-07	0.31E-02	0.11E-02	0.21E-01	0.24E-01
15.00	0.00E+00	-0.59E-07	0.15E-02	0.27E-03	0.18E-01	0.18E-01
18.00	0.00E+00	0.50E-07	0.00E+00	0.65E-04	0.12E-01	0.14E-01
22.00	0.00E+00	0.33E-08	0.00E+00	0.10E-04	0.86E-02	0.97E-02
26.00	0.00E+00	-0.39E-09	0.18E-02	0.16E-05	0.65E-02	0.70E-02
30.00	0.00E+00	0.32E-08	0.14E-02	0.49E-06	0.44E-02	0.50E-02
35.00	0.00E+00	0.24E-08	0.11E-02	0.27E-07	0.31E-02	0.33E-02
40.00	0.00E+00	-0.51E-08	0.10E-02	0.15E-06	0.20E-02	0.22E-02
45.00	0.00E+00	0.24E-08	0.17E-02	-0.37E-08	0.18E-02	0.14E-02

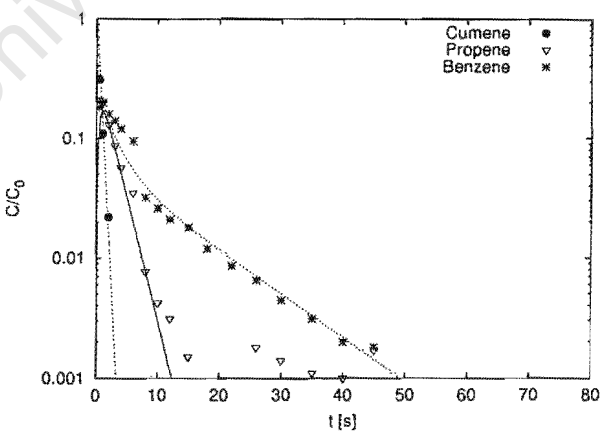

Appendix K. Cumene pulse experiments over T4480

Run Conditions react30

T_R [°C]	F(STP) [ml/min]	R_y [cm]	V_{cat} [ml]	τ [s]
391	311	0.033	0.432	3.87

Errors of C(t)

	Cumene	Propene	Benzene
Least Err	0.50E-01	NAN	0.94E-01
R^2	0.998	0.992	0.797
Min Err% (@ time)	0.17(4.0)	0.23(10.0)	3.03(6.0)
Max Err% (@ time)	16.42(0.5)	165.46(65.0)	44.04(30.0)

Parameter Estimates

	Low Estimate	Estimate	High Estimate
$K_c(Benzene)$	974	1998	4097
$k_{eff}[1/s]$	402	611	929
$\alpha(Benzene)$	0.83E-02	0.17E-01	0.35E-01
ϕ	7	9	11

Model Parameters

	Cumene	Propene	Benzene
$D_y[cm^2/s]$	0.12E-01	0.20E-01	0.15E-01
$K_c[/]$	0	0	1998
α	0.43E+02	0.71E+02	0.17E-01
β	0.37E+00	0.60E+00	0.45E+00

Experiment versus Model

	CUMENE		PROPENE		BENZENE	
t[s]	Exp	Mod	Exp	Mod	Exp	Mod
0.50	0.64E+00	0.59E+00	0.12E+00	0.94E-01	0.43E-01	0.30E-01
2.00	0.11E+00	0.13E+00	0.21E+00	0.16E+00	0.10E+00	0.66E-01
3.00	0.38E-01	0.44E-01	0.18E+00	0.14E+00	0.92E-01	0.65E-01
4.00	0.16E-01	0.16E-01	0.16E+00	0.11E+00	0.86E-01	0.61E-01
6.00	0.42E-02	0.20E-02	0.88E-01	0.70E-01	0.47E-01	0.51E-01
8.00	0.00E+00	0.25E-03	0.76E-01	0.42E-01	0.39E-01	0.44E-01
10.00	0.00E+00	0.32E-04	0.25E-01	0.25E-01	0.30E-01	0.39E-01
26.00	0.00E+00	0.34E-07	0.26E-02	0.41E-03	0.14E-01	0.20E-01
30.00	0.00E+00	-0.41E-07	0.00E+00	0.15E-03	0.62E-01	0.18E-01
35.00	0.00E+00	0.51E-08	0.20E-02	0.41E-04	0.12E-01	0.16E-01
40.00	0.00E+00	-0.23E-07	0.35E-02	0.12E-04	0.90E-02	0.14E-01
50.00	0.00E+00	0.63E-08	0.17E-02	0.11E-05	0.88E-02	0.12E-01
65.00	0.00E+00	0.36E-08	0.12E-02	0.20E-07	0.68E-02	0.87E-02
80.00	0.00E+00	-0.38E-08	0.11E-02	0.38E-07	0.51E-02	0.66E-02

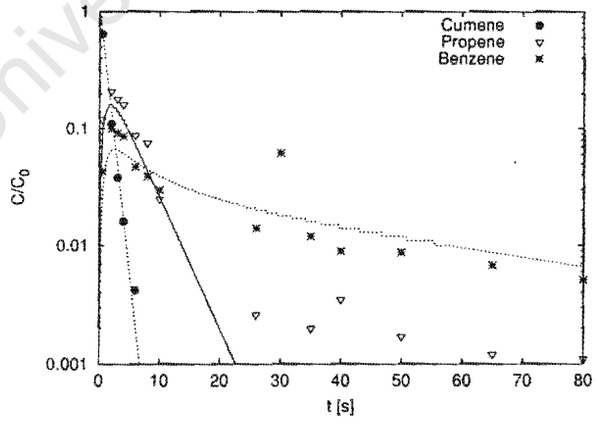

Appendix K. Cumene pulse experiments over T4480

Run Conditions react31

T_R [°C]	F(STP) [ml/min]	R_y [cm]	V_{cat} [ml]	τ [s]
391	411	0.033	0.432	2.93

Errors of C(t)

	Cumene	Propene	Benzene
Least Err	0.13E+00	0.18E+00	0.93E-01
R^2	0.953	0.991	0.886
Min Err% (@ time)	2.02(2.0)	7.33(8.0)	0.24(15.0)
Max Err% (@ time)	101.13(0.5)	116.85(40.0)	39.17(1.0)

Parameter Estimates

	Low Estimate	Estimate	High Estimate
$K_c(Benzene)$	1312	3758	10757
$k_{eff}[1/s]$	483	1034	2212
$\alpha(Benzene)$	0.24E-02	0.69E-02	0.20E-01
ϕ	8	12	17

Model Parameters

	Cumene	Propene	Benzene
$D_y[cm^2/s]$	0.12E-01	0.20E-01	0.15E-01
$K_c[/]$	0	0	3758
α	0.33E+02	0.54E+02	0.69E-02
β	0.28E+00	0.46E+00	0.34E+00

Experiment versus Model

	CUMENE		PROPENE		BENZENE	
t[s]	Exp	Mod	Exp	Mod	Exp	Mod
0.50	0.71E+00	0.50E+00	0.16E+00	0.11E+00	0.57E-01	0.29E-01
1.00	0.21E+00	0.25E+00	0.22E+00	0.15E+00	0.11E+00	0.45E-01
2.00	0.66E-01	0.63E-01	0.18E+00	0.15E+00	0.96E-01	0.51E-01
3.00	0.34E-01	0.16E-01	0.17E+00	0.11E+00	0.89E-01	0.47E-01
8.00	0.27E-02	0.16E-04	0.28E-01	0.22E-01	0.25E-01	0.30E-01
10.00	0.00E+00	0.20E-05	0.17E-01	0.11E-01	0.23E-01	0.26E-01
15.00	0.00E+00	-0.83E-07	0.63E-02	0.20E-02	0.20E-01	0.20E-01
22.00	0.00E+00	0.65E-08	0.20E-02	0.19E-03	0.11E-01	0.15E-01
30.00	0.00E+00	-0.23E-08	0.17E-02	0.13E-04	0.92E-02	0.12E-01
35.00	0.00E+00	0.21E-07	0.18E-02	0.28E-05	0.75E-02	0.10E-01
40.00	0.00E+00	-0.97E-08	0.13E-02	0.59E-06	0.65E-02	0.93E-02
50.00	0.00E+00	-0.23E-08	0.00E+00	0.33E-06	0.89E-02	0.77E-02
65.00	0.00E+00	-0.16E-08	0.16E-02	0.53E-07	0.58E-02	0.60E-02

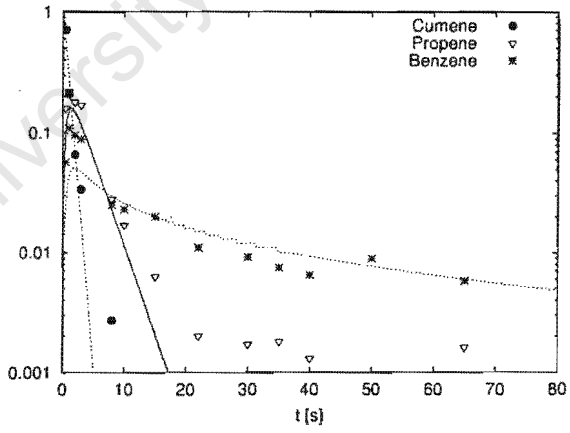

Appendix K. Cumene pulse experiments over T4480

Run Conditions react33

T_R [°C]	F(STP) [ml/min]	R_y [cm]	V_{cat} [ml]	τ [s]
391	311	0.055	0.432	3.87

Errors of C(t)

	Cumene	Propene	Benzene
Least Err	0.13E+00	0.16E+00	0.73E-01
R^2	0.987	0.989	0.927
Min Err% (@ time)	4.45(3.0)	1.78(10.0)	1.50(50.0)
Max Err% (@ time)	35.48(0.5)	85.76(35.0)	28.60(1.0)

Parameter Estimates

	Low Estimate	Estimate	High Estimate
$K_c(Benzene)$	1122	3433	10504
$k_{eff}[1/s]$	1046	1840	3234
$\alpha(Benzene)$	0.12E-02	0.36E-02	0.11E-01
ϕ	20	26	35

Model Parameters

	Cumene	Propene	Benzene
$D_y[cm^2/s]$	0.12E-01	0.20E-01	0.15E-01
$K_c[/]$	0	0	3433
α	0.15E+02	0.26E+02	0.36E-02
β	0.13E+00	0.22E+00	0.16E+00

Experiment versus Model

	CUMENE		PROPENE		BENZENE	
t[s]	Exp	Mod	Exp	Mod	Exp	Mod
0.50	0.66E+00	0.57E+00	0.13E+00	0.10E+00	0.51E-01	0.42E-01
1.00	0.30E+00	0.32E+00	0.21E+00	0.15E+00	0.12E+00	0.68E-01
3.00	0.28E-01	0.33E-01	0.19E+00	0.14E+00	0.12E+00	0.78E-01
4.00	0.28E-01	0.11E-01	0.17E+00	0.12E+00	0.11E+00	0.70E-01
8.00	0.18E-02	0.12E-03	0.67E-01	0.42E-01	0.51E-01	0.46E-01
10.00	0.00E+00	0.13E-04	0.24E-01	0.25E-01	0.29E-01	0.38E-01
12.00	0.00E+00	0.15E-05	0.27E-01	0.15E-01	0.29E-01	0.33E-01
18.00	0.00E+00	0.19E-06	0.81E-02	0.32E-02	0.16E-01	0.24E-01
22.00	0.00E+00	-0.11E-06	0.60E-02	0.12E-02	0.17E-01	0.20E-01
30.00	0.00E+00	0.51E-08	0.25E-02	0.15E-03	0.11E-01	0.14E-01
35.00	0.00E+00	-0.60E-07	0.44E-02	0.41E-04	0.94E-02	0.12E-01
40.00	0.00E+00	0.21E-07	0.00E+00	0.12E-04	0.89E-02	0.11E-01
50.00	0.00E+00	0.32E-07	0.16E-02	0.13E-05	0.78E-02	0.84E-02
65.00	0.00E+00	0.48E-09	0.28E-02	0.10E-06	0.74E-02	0.63E-02

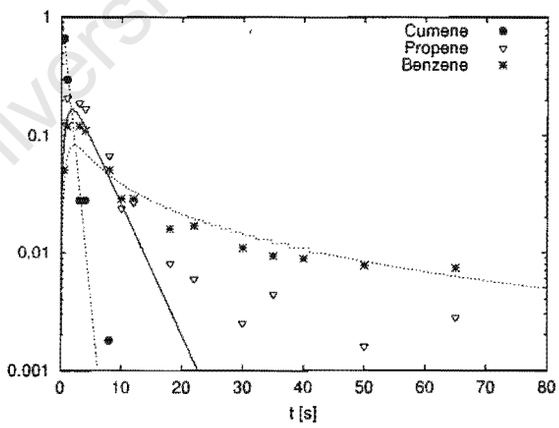

Appendix K. Cumene pulse experiments over T4480

Run Conditions react34

T_R [°C]	F(STP) [ml/min]	R_y [cm]	V_{cat} [ml]	τ [s]
391	411	0.055	0.432	2.93

Errors of C(t)

	Cumene	Propene	Benzene
Least Err	0.12E+00	0.14E+00	0.91E-01
R^2	0.957	0.983	0.951
Min Err% (@ time)	1.97(2.0)	1.93(6.0)	2.13(35.0)
Max Err% (@ time)	29.00(1.0)	90.74(35.0)	31.27(1.0)

Parameter Estimates

	Low Estimate	Estimate	High Estimate
$K_c(Benzene)$	147	258	454
$k_{eff}[1/s]$	623	1157	2147
$\alpha(Benzene)$	0.20E-01	0.36E-01	0.63E-01
ϕ	15	21	28

Model Parameters

	Cumene	Propene	Benzene
$D_y[cm^2/s]$	0.12E-01	0.20E-01	0.15E-01
$K_c[/]$	0	0	258
α	0.12E+02	0.19E+02	0.36E-01
β	0.10E+00	0.16E+00	0.12E+00

Experiment versus Model

	CUMENE		PROPENE		BENZENE	
t[s]	Exp	Mod	Exp	Mod	Exp	Mod
0.50	0.59E+00	0.60E+00	0.13E+00	0.81E-01	0.14E+00	0.87E-01
1.00	0.23E+00	0.36E+00	0.17E+00	0.12E+00	0.22E+00	0.14E+00
2.00	0.12E+00	0.13E+00	0.17E+00	0.13E+00	0.23E+00	0.16E+00
3.00	0.53E-01	0.46E-01	0.14E+00	0.10E+00	0.19E+00	0.15E+00
4.00	0.28E-01	0.16E-01	0.10E+00	0.80E-01	0.15E+00	0.12E+00
6.00	0.84E-02	0.21E-02	0.40E-01	0.42E-01	0.65E-01	0.81E-01
10.00	0.32E-02	0.35E-04	0.13E-01	0.11E-01	0.29E-01	0.40E-01
12.00	0.21E-02	0.47E-05	0.86E-02	0.56E-02	0.22E-01	0.29E-01
15.00	0.15E-02	0.42E-06	0.47E-02	0.20E-02	0.16E-01	0.20E-01
26.00	0.00E+00	-0.34E-07	0.77E-03	0.48E-04	0.45E-02	0.66E-02
35.00	0.00E+00	0.99E-08	0.12E-02	0.25E-05	0.34E-02	0.30E-02
50.00	0.00E+00	0.17E-08	0.69E-03	0.16E-06	0.21E-02	0.82E-03

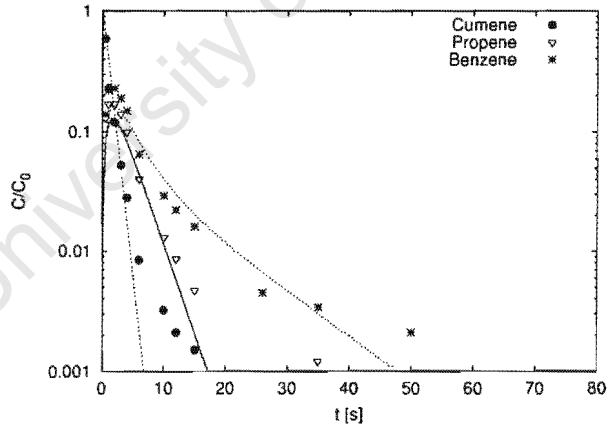

Appendix K. Cumene pulse experiments over T4480

Run Conditions react35

T_R [°C]	F(STP) [ml/min]	R_y [cm]	V_{cat} [ml]	τ [s]
391	511	0.055	0.432	2.36

Errors of C(t)

	Cumene	Propene	Benzene
Least Err	0.81E-01	0.91E-01	0.10E+00
R^2	0.965	0.989	0.962
Min Err% (@ time)	0.35(3.0)	1.24(8.0)	1.24(26.0)
Max Err% (@ time)	40.70(0.5)	23.94(0.5)	29.76(0.5)

Parameter Estimates

	Low Estimate	Estimate	High Estimate
$K_c(Benzene)$	132	205	319
$k_{eff}[1/s]$	500	824	1358
$\alpha(Benzene)$	0.23E-01	0.36E-01	0.56E-01
ϕ	13	17	23

Model Parameters

	Cumene	Propene	Benzene
$D_y[cm^2/s]$	0.12E-01	0.20E-01	0.15E-01
$K_c[/]$	0	0	205
α	0.94E+01	0.16E+02	0.36E-01
β	0.80E-01	0.13E+00	0.99E-01

Experiment versus Model

	CUMENE		PROPENE		BENZENE	
t[s]	Exp	Mod	Exp	Mod	Exp	Mod
0.50	0.43E+00	0.61E+00	0.11E+00	0.67E-01	0.13E+00	0.72E-01
1.00	0.34E+00	0.37E+00	0.14E+00	0.95E-01	0.19E+00	0.12E+00
2.00	0.16E+00	0.14E+00	0.14E+00	0.97E-01	0.21E+00	0.13E+00
3.00	0.49E-01	0.50E-01	0.11E+00	0.77E-01	0.16E+00	0.12E+00
4.00	0.23E-01	0.18E-01	0.86E-01	0.55E-01	0.14E+00	0.94E-01
6.00	0.42E-02	0.25E-02	0.29E-01	0.25E-01	0.52E-01	0.58E-01
8.00	0.13E-02	0.34E-03	0.12E-01	0.11E-01	0.25E-01	0.37E-01
10.00	0.68E-03	0.47E-04	0.57E-02	0.48E-02	0.15E-01	0.25E-01
12.00	0.46E-03	0.65E-05	0.29E-02	0.21E-02	0.11E-01	0.17E-01
15.00	0.28E-03	0.44E-06	0.13E-02	0.58E-03	0.66E-02	0.11E-01
18.00	0.44E-03	0.21E-06	0.88E-03	0.16E-03	0.63E-02	0.74E-02
22.00	0.20E-03	0.12E-07	0.58E-03	0.31E-04	0.63E-02	0.45E-02
26.00	0.13E-03	-0.94E-08	0.32E-03	0.57E-05	0.26E-02	0.28E-02
30.00	0.00E+00	-0.17E-07	0.00E+00	0.11E-05	0.29E-02	0.18E-02

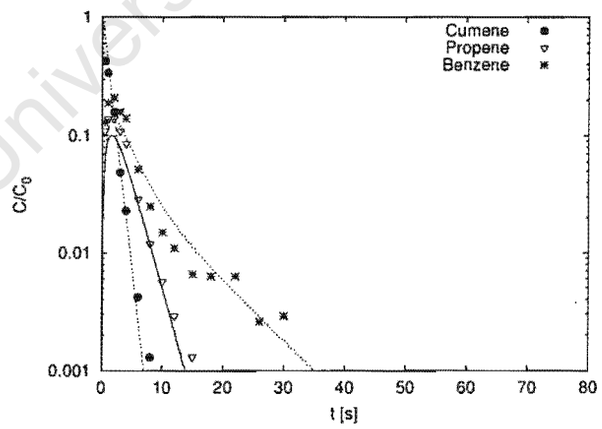

Appendix K. Cumene pulse experiments over T4480

Run Conditions react36				
T_R [°C]	F(STP) [ml/min]	R_y [cm]	V_{cat} [ml]	τ [s]
419	311	0.055	0.432	3.72

	Errors of C(t)		
	Cumene	Propene	Benzene
Least Err	0.13E+00	0.66E-01	0.77E-01
R^2	0.991	0.954	0.979
Min Err% (@ time)	4.73(2.0)	0.74(4.0)	1.93(35.0)
Max Err% (@ time)	25.78(0.5)	19.03(0.5)	20.46(0.5)

Parameter Estimates			
	Low Estimate	Estimate	High Estimate
$K_c(Benzene)$	100	140	196
$k_{eff}[1/s]$	1218	1989	3249
$\alpha(Benzene)$	0.60E-01	0.84E-01	0.12E+00
ϕ	21	27	35

Model Parameters			
	Cumene	Propene	Benzene
$D_y[cm^2/s]$	0.12E-01	0.20E-01	0.15E-01
$K_c[/]$	0	0	140
α	0.15E+02	0.25E+02	0.84E-01
β	0.13E+00	0.21E+00	0.16E+00

Experiment versus Model

	CUMENE		PROPENE		BENZENE	
t[s]	Exp	Mod	Exp	Mod	Exp	Mod
0.50	0.45E+00	0.55E+00	0.15E+00	0.11E+00	0.20E+00	0.14E+00
1.00	0.22E+00	0.31E+00	0.19E+00	0.15E+00	0.28E+00	0.22E+00
2.00	0.84E-01	0.94E-01	0.17E+00	0.16E+00	0.27E+00	0.24E+00
3.00	0.42E-01	0.29E-01	0.14E+00	0.14E+00	0.23E+00	0.22E+00
4.00	0.17E-01	0.88E-02	0.11E+00	0.11E+00	0.20E+00	0.18E+00
12.00	0.56E-03	0.11E-05	0.12E-01	0.13E-01	0.33E-01	0.47E-01
15.00	0.29E-03	0.33E-07	0.62E-02	0.59E-02	0.20E-01	0.31E-01
22.00	0.27E-03	0.11E-07	0.17E-02	0.91E-03	0.92E-02	0.12E-01
26.00	0.14E-03	0.69E-08	0.89E-03	0.31E-03	0.59E-02	0.74E-02
30.00	0.00E+00	-0.14E-07	0.51E-03	0.11E-03	0.59E-02	0.45E-02
35.00	0.00E+00	0.18E-08	0.26E-03	0.28E-04	0.27E-02	0.24E-02
40.00	0.00E+00	0.71E-08	0.51E-03	0.76E-05	0.21E-02	0.13E-02

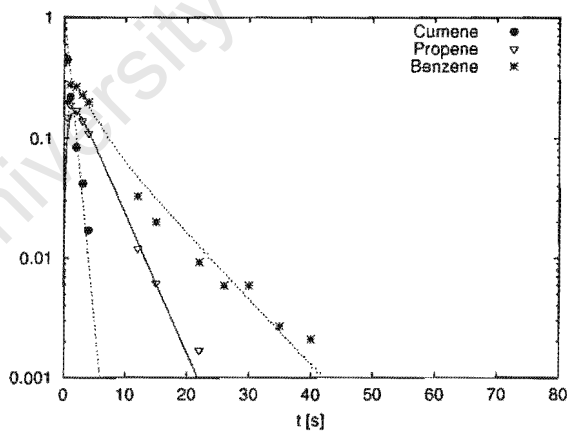

Appendix K. Cumene pulse experiments over T4480

Run Conditions react37

T_R [°C]	F(STP) [ml/min]	R_y [cm]	V_{cat} [ml]	τ [s]
419	411	0.055	0.432	2.81

Errors of C(t)

	Cumene	Propene	Benzene
Least Err	0.11E+00	0.11E+00	0.13E+00
R^2	0.966	0.986	0.975
Min Err% (@ time)	0.78(0.5)	0.32(12.0)	1.68(22.0)
Max Err% (@ time)	24.96(1.0)	34.17(22.0)	36.30(65.0)

Parameter Estimates

	Low Estimate	Estimate	High Estimate
$K_c(Benzene)$	139	211	321
$k_{eff}[1/s]$	730	1396	2671
$\alpha(Benzene)$	0.28E-01	0.42E-01	0.64E-01
ϕ	16	23	32

Model Parameters

	Cumene	Propene	Benzene
$D_y[cm^2/s]$	0.12E-01	0.20E-01	0.15E-01
$K_c[/]$	0	0	211
α	0.11E+02	0.19E+02	0.42E-01
β	0.96E-01	0.16E+00	0.12E+00

Experiment versus Model

	CUMENE		PROPENE		BENZENE	
t[s]	Exp	Mod	Exp	Mod	Exp	Mod
0.50	0.57E+00	0.57E+00	0.11E+00	0.88E-01	0.13E+00	0.10E+00
1.00	0.23E+00	0.33E+00	0.16E+00	0.12E+00	0.24E+00	0.16E+00
2.00	0.97E-01	0.11E+00	0.15E+00	0.13E+00	0.22E+00	0.18E+00
4.00	0.16E-01	0.12E-01	0.87E-01	0.77E-01	0.14E+00	0.12E+00
6.00	0.86E-02	0.12E-02	0.65E-01	0.39E-01	0.11E+00	0.79E-01
10.00	0.95E-03	0.15E-04	0.94E-02	0.96E-02	0.24E-01	0.37E-01
12.00	0.62E-03	0.18E-05	0.46E-02	0.47E-02	0.14E-01	0.27E-01
15.00	0.46E-03	0.71E-07	0.20E-02	0.16E-02	0.95E-02	0.18E-01
18.00	0.33E-03	0.67E-07	0.12E-02	0.56E-03	0.70E-02	0.12E-01
22.00	0.44E-03	0.18E-07	0.13E-02	0.14E-03	0.83E-02	0.77E-02
26.00	0.19E-03	-0.82E-08	0.38E-03	0.33E-04	0.38E-02	0.50E-02
30.00	0.14E-03	-0.11E-07	0.30E-03	0.82E-05	0.27E-02	0.32E-02
35.00	0.22E-03	0.60E-08	0.51E-03	0.17E-05	0.44E-02	0.19E-02
40.00	0.25E-03	-0.54E-08	0.29E-03	0.30E-06	0.28E-02	0.11E-02
50.00	0.00E+00	-0.32E-08	0.17E-03	0.39E-07	0.19E-02	0.39E-03
65.00	0.00E+00	-0.27E-08	0.17E-03	-0.65E-08	0.10E-02	0.82E-04

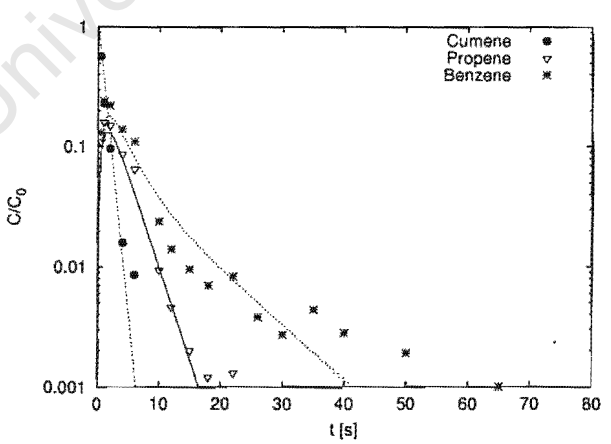

Appendix K. Cumene pulse experiments over T4480

Run Conditions react38

T_R [°C]	F(STP) [ml/min]	R_y [cm]	V_{cat} [ml]	τ [s]
419	511	0.055	0.432	2.26

Errors of C(t)

	Cumene	Propene	Benzene
Least Err	0.92E-01	NAN	NAN
R^2	0.998	0.214	0.441
Min Err% (@ time)	1.48(3.0)	0.56(12.0)	1.28(8.0)
Max Err% (@ time)	32.39(0.5)	11.97(8.0)	61.85(40.0)

Parameter Estimates

	Low Estimate	Estimate	High Estimate
$K_c(Benzene)$	109	162	243
$k_{eff}[1/s]$	946	1679	2980
$\alpha(Benzene)$	0.29E-01	0.44E-01	0.65E-01
ϕ	19	25	34

Model Parameters

	Cumene	Propene	Benzene
$D_y[cm^2/s]$	0.12E-01	0.20E-01	0.15E-01
$K_c[/]$	0	0	162
α	0.90E+01	0.15E+02	0.44E-01
β	0.77E-01	0.13E+00	0.95E-01

Experiment versus Model

	CUMENE		PROPENE		BENZENE	
t[s]	Exp	Mod	Exp	Mod	Exp	Mod
0.50	0.39E+00	0.53E+00	0.00E+00	0.91E-01	0.00E+00	0.12E+00
1.00	0.22E+00	0.28E+00	0.00E+00	0.12E+00	0.00E+00	0.17E+00
2.00	0.69E-01	0.78E-01	0.12E+00	0.11E+00	0.18E+00	0.17E+00
3.00	0.20E-01	0.22E-01	0.84E-01	0.81E-01	0.14E+00	0.13E+00
4.00	0.82E-02	0.60E-02	0.71E-01	0.55E-01	0.11E+00	0.10E+00
6.00	0.26E-02	0.47E-03	0.15E-01	0.23E-01	0.38E-01	0.57E-01
8.00	0.11E-02	0.37E-04	0.52E-02	0.97E-02	0.36E-01	0.35E-01
12.00	0.26E-03	0.53E-06	0.16E-02	0.17E-02	0.80E-02	0.15E-01
15.00	0.14E-03	0.53E-07	0.73E-03	0.45E-03	0.58E-02	0.92E-02
18.00	0.87E-04	-0.25E-07	0.35E-03	0.12E-03	0.37E-02	0.58E-02
22.00	0.11E-03	-0.20E-07	0.25E-03	0.21E-04	0.27E-02	0.32E-02
26.00	0.00E+00	0.61E-09	0.16E-03	0.37E-05	0.21E-02	0.18E-02
30.00	0.00E+00	-0.67E-08	0.19E-03	0.98E-06	0.19E-02	0.10E-02
35.00	0.00E+00	-0.31E-08	0.18E-03	0.11E-06	0.13E-02	0.49E-03
40.00	0.00E+00	0.77E-08	0.39E-03	0.11E-06	0.58E-02	0.24E-03

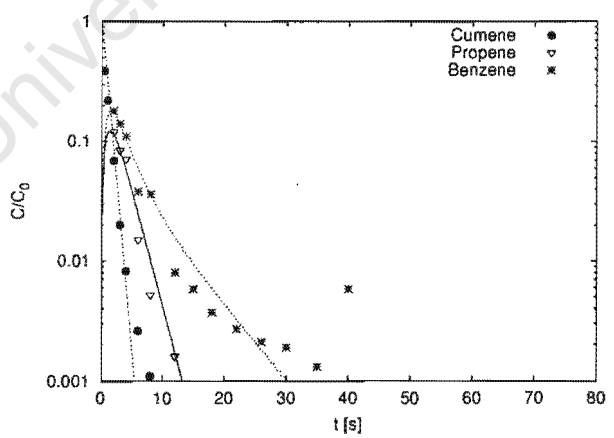

Appendix K. Cumene pulse experiments over T4480

Run Conditions react39

T_R [°C]	F(STP) [ml/min]	R_y [cm]	V_{cat} [ml]	τ [s]
441	311	0.055	0.432	3.60

Errors of C(t)

	Cumene	Propene	Benzene
Least Err	0.65E-01	NAN	NAN
R^2	0.959	0.818	0.880
Min Err% (@ time)	0.94(4.0)	1.61(4.0)	0.30(30.0)
Max Err% (@ time)	24.51(1.0)	12.85(1.0)	114.42(65.0)

Parameter Estimates

	Low Estimate	Estimate	High Estimate
$K_c(Benzene)$	97	140	201
$k_{eff}[1/s]$	734	1158	1827
$\alpha(Benzene)$	0.57E-01	0.81E-01	0.12E+00
ϕ	16	21	26

Model Parameters

	Cumene	Propene	Benzene
$D_y[cm^2/s]$	0.12E-01	0.20E-01	0.15E-01
$K_c[/]$	0	0	140
α	0.14E+02	0.24E+02	0.81E-01
β	0.12E+00	0.20E+00	0.15E+00

Experiment versus Model

	CUMENE		PROPENE		BENZENE	
t[s]	Exp	Mod	Exp	Mod	Exp	Mod
0.50	0.68E+00	0.62E+00	0.00E+00	0.84E-01	0.00E+00	0.11E+00
1.00	0.28E+00	0.38E+00	0.16E+00	0.13E+00	0.22E+00	0.17E+00
2.00	0.14E+00	0.14E+00	0.17E+00	0.14E+00	0.27E+00	0.21E+00
3.00	0.51E-01	0.55E-01	0.14E+00	0.13E+00	0.23E+00	0.19E+00
4.00	0.20E-01	0.21E-01	0.99E-01	0.10E+00	0.17E+00	0.17E+00
8.00	0.17E-02	0.44E-03	0.30E-01	0.36E-01	0.84E-01	0.81E-01
10.00	0.80E-03	0.65E-04	0.16E-01	0.21E-01	0.39E-01	0.59E-01
12.00	0.81E-03	0.99E-05	0.14E-01	0.12E-01	0.38E-01	0.43E-01
18.00	0.30E-03	0.19E-06	0.28E-02	0.23E-02	0.13E-01	0.19E-01
22.00	0.22E-03	0.53E-07	0.12E-02	0.75E-03	0.87E-02	0.11E-01
26.00	0.20E-03	0.59E-08	0.62E-03	0.25E-03	0.53E-02	0.66E-02
30.00	0.00E+00	-0.36E-07	0.29E-06	0.83E-04	0.40E-02	0.39E-02
35.00	0.00E+00	0.83E-08	0.12E-06	0.21E-04	0.28E-02	0.21E-02
40.00	0.00E+00	-0.79E-08	0.50E-03	0.55E-05	0.30E-02	0.11E-02
65.00	0.00E+00	0.16E-08	0.53E-03	0.78E-09	0.93E-02	0.44E-04

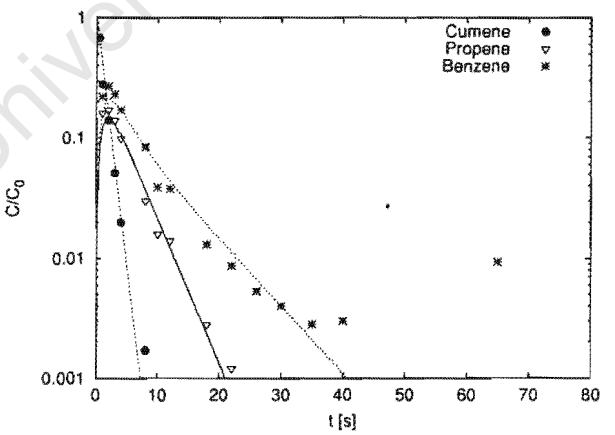

Appendix K. Cumene pulse experiments over T4480

Run Conditions react40

T_R [°C]	F(STP) [ml/min]	R_y [cm]	V_{cat} [ml]	τ [s]
441	411	0.055	0.432	2.72

Errors of C(t)

	Cumene	Propene	Benzene
Least Err	0.93E-01	0.67E-01	0.13E+00
R^2	0.996	0.932	0.955
Min Err% (@ time)	0.52(3.0)	0.53(12.0)	2.85(30.0)
Max Err% (@ time)	37.96(0.5)	26.56(0.5)	33.26(0.5)

Parameter Estimates

	Low Estimate	Estimate	High Estimate
$K_c(Benzene)$	125	194	301
$k_{eff}[1/s]$	625	1162	2160
$\alpha(Benzene)$	0.29E-01	0.44E-01	0.68E-01
ϕ	15	21	29

Model Parameters

	Cumene	Propene	Benzene
$D_y[cm^2/s]$	0.12E-01	0.20E-01	0.15E-01
$K_c[/]$	0	0	194
α	0.11E+02	0.18E+02	0.44E-01
β	0.93E-01	0.15E+00	0.11E+00

Experiment versus Model

	CUMENE		PROPENE		BENZENE	
t[s]	Exp	Mod	Exp	Mod	Exp	Mod
0.50	0.43E+00	0.59E+00	0.14E+00	0.81E-01	0.17E+00	0.93E-01
2.00	0.11E+00	0.12E+00	0.13E+00	0.12E+00	0.21E+00	0.17E+00
3.00	0.43E-01	0.42E-01	0.11E+00	0.97E-01	0.18E+00	0.15E+00
4.00	0.20E-01	0.15E-01	0.81E-01	0.72E-01	0.14E+00	0.12E+00
10.00	0.10E-02	0.27E-04	0.78E-02	0.85E-02	0.22E-01	0.34E-01
12.00	0.54E-03	0.34E-05	0.40E-02	0.41E-02	0.14E-01	0.25E-01
15.00	0.66E-03	0.21E-06	0.19E-02	0.14E-02	0.11E-01	0.16E-01
18.00	0.28E-03	0.12E-06	0.88E-03	0.46E-03	0.60E-02	0.11E-01
22.00	0.00E+00	0.17E-07	0.47E-03	0.11E-03	0.48E-02	0.66E-02
26.00	0.00E+00	-0.16E-07	0.68E-03	0.25E-04	0.15E-01	0.41E-02
30.00	0.00E+00	-0.45E-08	0.39E-03	0.59E-05	0.31E-02	0.26E-02
35.00	0.00E+00	0.13E-08	0.33E-03	0.13E-05	0.22E-02	0.15E-02
50.00	0.00E+00	-0.33E-09	0.32E-03	0.27E-07	0.18E-02	0.26E-03

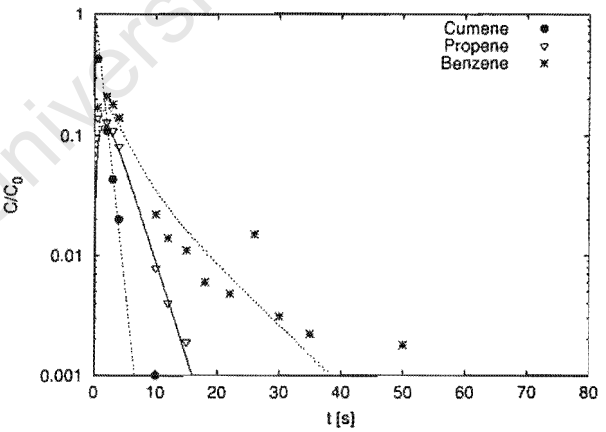

Appendix K. Cumene pulse experiments over T4480

Run Conditions react41

T_R [°C]	F(STP) [ml/min]	R_y [cm]	V_{cat} [ml]	τ [s]
441	511	0.055	0.432	2.19

Errors of C(t)

	Cumene	Propene	Benzene
Least Err	0.75E-01	NAN	NAN
R^2	0.948	0.710	0.809
Min Err% (@ time)	0.40(3.0)	1.30(8.0)	2.27(30.0)
Max Err% (@ time)	102.64(0.5)	29.97(1.0)	50.53(1.0)

Parameter Estimates

	Low Estimate	Estimate	High Estimate
$K_c(Benzene)$	154	224	326
$k_{eff}[1/s]$	695	1132	1845
$\alpha(Benzene)$	0.21E-01	0.31E-01	0.45E-01
ϕ	16	21	26

Model Parameters

	Cumene	Propene	Benzene
$D_y[cm^2/s]$	0.12E-01	0.20E-01	0.15E-01
$K_c[/]$	0	0	224
α	0.88E+01	0.14E+02	0.31E-01
β	0.74E-01	0.12E+00	0.92E-01

Experiment versus Model

	CUMENE		PROPENE		BENZENE	
t[s]	Exp	Mod	Exp	Mod	Exp	Mod
0.50	0.76E+00	0.57E+00	0.00E+00	0.76E-01	0.00E+00	0.85E-01
1.00	0.25E+00	0.32E+00	0.18E+00	0.10E+00	0.26E+00	0.13E+00
2.00	0.82E-01	0.10E+00	0.14E+00	0.99E-01	0.22E+00	0.14E+00
3.00	0.33E-01	0.33E-01	0.11E+00	0.74E-01	0.18E+00	0.12E+00
4.00	0.11E-01	0.11E-01	0.70E-01	0.50E-01	0.13E+00	0.89E-01
6.00	0.22E-02	0.11E-02	0.17E-01	0.21E-01	0.36E-01	0.52E-01
8.00	0.91E-03	0.11E-03	0.92E-02	0.87E-02	0.25E-01	0.32E-01
12.00	0.00E+00	0.14E-05	0.16E-02	0.14E-02	0.85E-02	0.15E-01
15.00	0.00E+00	0.17E-06	0.12E-02	0.36E-03	0.12E-01	0.97E-02
22.00	0.80E-04	-0.27E-07	0.25E-03	0.16E-04	0.29E-02	0.41E-02
26.00	0.71E-04	-0.85E-08	0.26E-03	0.27E-05	0.21E-02	0.26E-02
30.00	0.43E-04	0.10E-07	0.21E-03	0.52E-06	0.19E-02	0.17E-02
35.00	0.00E+00	-0.13E-07	0.22E-03	0.23E-06	0.14E-02	0.97E-03

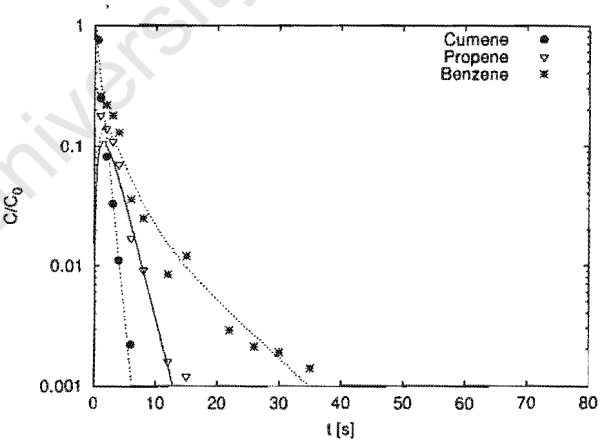

Appendix K. Cumene pulse experiments over T4480

Run Conditions react42

T_R [°C]	F(STP) [ml/min]	R_y [cm]	V_{cat} [ml]	τ [s]
471	311	0.055	0.432	3.46

Errors of C(t)

	Cumene	Propene	Benzene
Least Err	0.11E+00	0.79E-01	0.11E+00
R^2	0.999	0.968	0.961
Min Err% (@ time)	2.49(0.5)	0.15(3.0)	0.71(35.0)
Max Err% (@ time)	8.91(3.0)	14.34(0.5)	36.67(65.0)

Parameter Estimates

	Low Estimate	Estimate	High Estimate
$K_c(Benzene)$	129	177	242
$k_{eff}[1/s]$	864	1406	2289
$\alpha(Benzene)$	0.45E-01	0.62E-01	0.84E-01
ϕ	18	23	29

Model Parameters

	Cumene	Propene	Benzene
$D_y[cm^2/s]$	0.12E-01	0.20E-01	0.15E-01
$K_c[/]$	0	0	177
α	0.14E+02	0.23E+02	0.62E-01
β	0.12E+00	0.19E+00	0.15E+00

Experiment versus Model

	CUMENE		PROPENE		BENZENE	
t[s]	Exp	Mod	Exp	Mod	Exp	Mod
0.50	0.58E+00	0.59E+00	0.12E+00	0.91E-01	0.16E+00	0.11E+00
3.00	0.31E-01	0.43E-01	0.13E+00	0.13E+00	0.22E+00	0.19E+00
4.00	0.19E-01	0.15E-01	0.12E+00	0.10E+00	0.22E+00	0.16E+00
8.00	0.12E-02	0.22E-03	0.26E-01	0.33E-01	0.58E-01	0.75E-01
10.00	0.80E-03	0.28E-04	0.18E-01	0.19E-01	0.44E-01	0.54E-01
15.00	0.20E-03	0.22E-06	0.49E-02	0.44E-02	0.19E-01	0.27E-01
18.00	0.24E-03	0.14E-06	0.21E-02	0.18E-02	0.11E-01	0.19E-01
22.00	0.29E-03	0.31E-07	0.14E-02	0.58E-03	0.79E-02	0.12E-01
26.00	0.13E-03	-0.96E-08	0.51E-03	0.18E-03	0.54E-02	0.75E-02
30.00	0.15E-03	-0.23E-07	0.50E-03	0.58E-04	0.42E-02	0.48E-02
35.00	0.86E-04	0.11E-07	0.26E-03	0.14E-04	0.29E-02	0.28E-02
40.00	0.44E-03	-0.43E-08	0.24E-03	0.35E-05	0.27E-02	0.16E-02
50.00	0.00E+00	-0.39E-08	0.23E-03	0.27E-06	0.13E-02	0.53E-03
65.00	0.00E+00	-0.11E-08	0.50E-03	0.37E-08	0.12E-02	0.10E-03

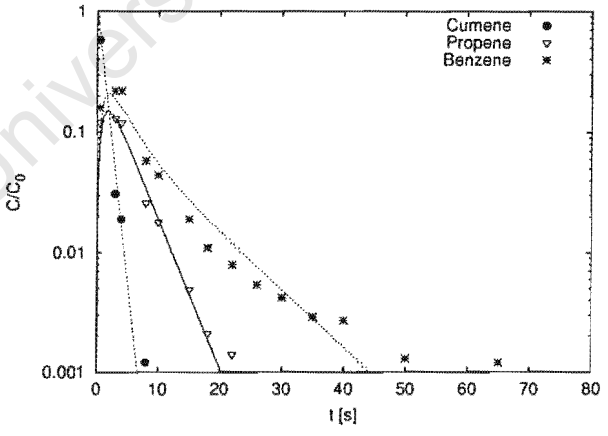

Appendix K. Cumene pulse experiments over T4480

Run Conditions react43

T_R [°C]	F(STP) [ml/min]	R_y [cm]	V_{cat} [ml]	τ [s]
471	411	0.055	0.432	2.61

Errors of C(t)

	Cumene	Propene	Benzene
Least Err	0.14E+00	0.76E-01	0.11E+00
R^2	0.959	0.948	0.957
Min Err% (@ time)	2.02(3.0)	2.49(6.0)	0.47(15.0)
Max Err% (@ time)	28.82(1.0)	35.31(0.5)	101.68(65.0)

Parameter Estimates

	Low Estimate	Estimate	High Estimate
$K_c(Benzene)$	116	167	241
$k_{eff}[1/s]$	1096	1789	2919
$\alpha(Benzene)$	0.34E-01	0.49E-01	0.71E-01
ϕ	20	26	33

Model Parameters

	Cumene	Propene	Benzene
$D_y[cm^2/s]$	0.12E-01	0.20E-01	0.15E-01
$K_c[/]$	0	0	167
α	0.10E+02	0.17E+02	0.49E-01
β	0.89E-01	0.15E+00	0.11E+00

Experiment versus Model

	CUMENE		PROPENE		BENZENE	
t[s]	Exp	Mod	Exp	Mod	Exp	Mod
0.50	0.51E+00	0.54E+00	0.18E+00	0.96E-01	0.25E+00	0.12E+00
1.00	0.17E+00	0.29E+00	0.18E+00	0.13E+00	0.29E+00	0.18E+00
2.00	0.75E-01	0.83E-01	0.16E+00	0.13E+00	0.28E+00	0.19E+00
3.00	0.26E-01	0.24E-01	0.12E+00	0.98E-01	0.22E+00	0.16E+00
4.00	0.15E-01	0.68E-02	0.85E-01	0.70E-01	0.17E+00	0.12E+00
6.00	0.23E-02	0.57E-03	0.31E-01	0.34E-01	0.70E-01	0.74E-01
8.00	0.87E-03	0.48E-04	0.12E-01	0.16E-01	0.31E-01	0.47E-01
10.00	0.51E-03	0.44E-05	0.64E-02	0.73E-02	0.21E-01	0.32E-01
12.00	0.19E-02	0.64E-06	0.27E-02	0.34E-02	0.13E-01	0.22E-01
15.00	0.26E-03	0.24E-07	0.18E-02	0.11E-02	0.14E-01	0.14E-01
18.00	0.00E+00	-0.34E-07	0.66E-03	0.35E-03	0.61E-02	0.89E-02
26.00	0.14E-03	0.84E-08	0.28E-03	0.17E-04	0.28E-02	0.30E-02
30.00	0.98E-04	-0.10E-07	0.18E-03	0.39E-05	0.20E-02	0.18E-02
40.00	0.00E+00	0.48E-08	0.66E-04	0.18E-06	0.11E-02	0.47E-03
65.00	0.00E+00	0.10E-08	0.18E-03	-0.19E-07	0.44E-02	0.18E-04

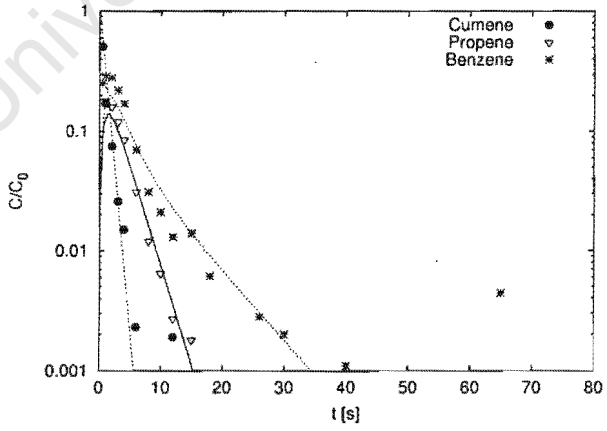

Appendix K. Cumene pulse experiments over T4480

Run Conditions react44

T_R [°C]	F(STP) [ml/min]	R_y [cm]	V_{cat} [ml]	τ [s]
471	511	0.055	0.432	2.10

Errors of C(t)

	Cumene	Propene	Benzene
Least Err	0.19E+00	0.11E+00	0.85E-01
R^2	0.985	0.920	0.918
Min Err% (@ time)	11.28(0.5)	0.71(10.0)	0.42(40.0)
Max Err% (@ time)	18.74(1.0)	52.02(0.5)	91.17(0.5)

Parameter Estimates

	Low Estimate	Estimate	High Estimate
$K_c(Benzene)$	245	322	424
$k_{eff}[1/s]$	1768	3579	7245
$\alpha(Benzene)$	0.16E-01	0.21E-01	0.27E-01
ϕ	26	37	53

Model Parameters

	Cumene	Propene	Benzene
$D_y[cm^2/s]$	0.12E-01	0.20E-01	0.15E-01
$K_c[/]$	0	0	322
α	0.84E+01	0.14E+02	0.21E-01
β	0.71E-01	0.12E+00	0.89E-01

Experiment versus Model

	CUMENE		PROPENE		BENZENE	
t[s]	Exp	Mod	Exp	Mod	Exp	Mod
0.50	0.38E+00	0.42E+00	0.25E+00	0.12E+00	0.37E+00	0.15E+00
1.00	0.12E+00	0.18E+00	0.20E+00	0.15E+00	0.32E+00	0.19E+00
3.00	0.13E-01	0.59E-02	0.88E-01	0.78E-01	0.17E+00	0.12E+00
4.00	0.74E-02	0.11E-02	0.59E-01	0.50E-01	0.13E+00	0.89E-01
6.00	0.14E-02	0.34E-04	0.12E-01	0.19E-01	0.36E-01	0.50E-01
8.00	0.62E-03	0.17E-05	0.65E-02	0.75E-02	0.23E-01	0.32E-01
10.00	0.54E-03	0.36E-06	0.28E-02	0.29E-02	0.15E-01	0.21E-01
12.00	0.10E-02	0.20E-06	0.23E-02	0.11E-02	0.15E-01	0.15E-01
15.00	0.33E-03	-0.81E-07	0.69E-03	0.27E-03	0.10E-01	0.10E-01
18.00	0.13E-03	-0.44E-07	0.42E-03	0.66E-04	0.47E-02	0.73E-02
22.00	0.00E+00	-0.41E-07	0.28E-06	0.10E-04	0.34E-02	0.49E-02
26.00	0.91E-04	0.28E-07	0.35E-03	0.16E-05	0.30E-02	0.35E-02
30.00	0.00E+00	0.56E-09	0.00E+00	0.35E-06	0.28E-02	0.25E-02
35.00	0.00E+00	-0.97E-08	0.42E-03	0.29E-07	0.13E-02	0.17E-02
40.00	0.00E+00	0.78E-08	0.00E+00	0.27E-07	0.12E-02	0.11E-02
50.00	0.00E+00	0.21E-08	0.00E+00	-0.11E-08	0.11E-02	0.52E-03

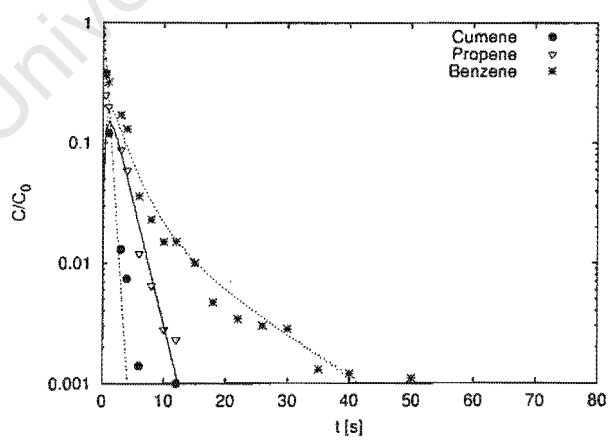

Appendix K. Cumene pulse experiments over T4480

Run Conditions react45

T_R [°C]	F(STP) [ml/min]	R_y [cm]	V_{cat} [ml]	τ [s]
391	311	0.075	0.432	3.87

Errors of C(t)

	Cumene	Propene	Benzene
Least Err	0.25E+00	0.14E+01	0.19E+00
R^2	0.967	0.653	0.000
Min Err% (@ time)	0.27(3.0)	8.69(1.0)	4.23(50.0)
Max Err% (@ time)	31.75(1.0)	46.72(0.5)	636.63(0.5)

Parameter Estimates

	Low Estimate	Estimate	High Estimate
$K_c(Benzene)$	0	2000000	*********
$k_{eff}[1/s]$	701	5916	49925
$\alpha(Benzene)$	0.00E+00	0.33E-05	0.10E+02
ϕ	22	65	190

Model Parameters

	Cumene	Propene	Benzene
$D_y[cm^2/s]$	0.12E-01	0.20E-01	0.15E-01
$K_c[/]$	0	0	2000000
α	0.83E+01	0.14E+02	0.33E-05
β	0.71E-01	0.12E+00	0.88E-01

Experiment versus Model

	CUMENE		PROPENE		BENZENE	
t[s]	Exp	Mod	Exp	Mod	Exp	Mod
0.50	0.38E+00	0.49E+00	0.25E+00	0.13E+00	0.37E+00	0.64E-03
1.00	0.12E+00	0.24E+00	0.20E+00	0.18E+00	0.32E+00	0.95E-03
3.00	0.13E-01	0.13E-01	0.88E-01	0.15E+00	0.17E+00	0.12E-02
4.00	0.74E-02	0.32E-02	0.59E-01	0.12E+00	0.13E+00	0.12E-02
6.00	0.14E-02	0.18E-03	0.12E-01	0.71E-01	0.36E-01	0.11E-02
8.00	0.62E-03	0.95E-05	0.65E-02	0.42E-01	0.23E-01	0.11E-02
10.00	0.54E-03	0.10E-06	0.28E-02	0.25E-01	0.15E-01	0.11E-02
12.00	0.10E-02	0.49E-07	0.23E-02	0.15E-01	0.15E-01	0.11E-02
15.00	0.33E-03	-0.45E-07	0.69E-03	0.70E-02	0.10E-01	0.10E-02
18.00	0.13E-03	0.24E-07	0.42E-03	0.32E-02	0.47E-02	0.10E-02
22.00	0.00E+00	0.17E-07	0.28E-06	0.12E-02	0.34E-02	0.97E-03
26.00	0.91E-04	0.75E-08	0.35E-03	0.41E-03	0.30E-02	0.94E-03
30.00	0.00E+00	0.30E-07	0.00E+00	0.15E-03	0.28E-02	0.92E-03
35.00	0.00E+00	-0.29E-08	0.42E-03	0.41E-04	0.13E-02	0.89E-03
40.00	0.00E+00	-0.24E-07	0.00E+00	0.12E-04	0.12E-02	0.87E-03
50.00	0.00E+00	-0.41E-08	0.00E+00	0.10E-05	0.11E-02	0.83E-03

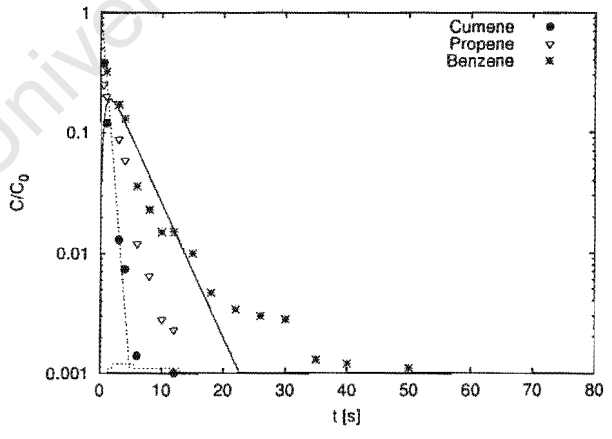

Appendix K. Cumene pulse experiments over T4480

Run Conditions react46

T_R [°C]	F(STP) [ml/min]	R_y [cm]	V_{cat} [ml]	τ [s]
391	411	0.075	0.432	2.93

Errors of C(t)

	Cumene	Propene	Benzene
Least Err	NAN	NAN	0.15E+00
R^2	0.998	0.924	0.868
Min Err% (@ time)	0.38(2.0)	1.68(12.0)	1.26(18.0)
Max Err% (@ time)	392.92(40.0)	127.92(40.0)	51.90(40.0)

Parameter Estimates

	Low Estimate	Estimate	High Estimate
$K_c(Benzene)$	33	65	129
$k_{eff}[1/s]$	188	303	489
$\alpha(Benzene)$	0.38E-01	0.75E-01	0.15E+00
ϕ	11	14	18

Model Parameters

	Cumene	Propene	Benzene
$D_y[cm^2/s]$	0.12E-01	0.20E-01	0.15E-01
$K_c[/]$	0	0	65
α	0.63E+01	0.10E+02	0.75E-01
β	0.54E-01	0.88E-01	0.66E-01

Experiment versus Model

	CUMENE		PROPENE		BENZENE	
t[s]	Exp	Mod	Exp	Mod	Exp	Mod
0.50	0.69E+00	0.74E+00	0.67E-01	0.33E-01	0.75E-01	0.40E-01
1.00	0.55E+00	0.55E+00	0.95E-01	0.53E-01	0.13E+00	0.73E-01
2.00	0.31E+00	0.30E+00	0.10E+00	0.67E-01	0.15E+00	0.10E+00
3.00	0.15E+00	0.17E+00	0.89E-01	0.64E-01	0.13E+00	0.11E+00
4.00	0.88E-01	0.93E-01	0.69E-01	0.54E-01	0.10E+00	0.97E-01
6.00	0.21E-01	0.28E-01	0.28E-01	0.34E-01	0.43E-01	0.69E-01
8.00	0.67E-02	0.86E-02	0.16E-01	0.19E-01	0.26E-01	0.45E-01
10.00	0.27E-02	0.26E-02	0.82E-02	0.10E-01	0.15E-01	0.29E-01
12.00	0.12E-02	0.80E-03	0.58E-02	0.53E-02	0.12E-01	0.19E-01
15.00	0.57E-03	0.14E-03	0.14E-01	0.20E-02	0.53E-02	0.10E-01
18.00	0.57E-03	0.23E-04	0.11E-01	0.72E-03	0.53E-02	0.56E-02
22.00	0.29E-03	0.23E-05	0.00E+00	0.19E-03	0.28E-02	0.26E-02
26.00	0.37E-03	0.36E-06	0.46E-03	0.48E-04	0.34E-02	0.12E-02
30.00	0.00E+00	0.23E-07	0.00E+00	0.13E-04	0.18E-02	0.56E-03
40.00	0.19E-01	-0.30E-08	0.17E-02	0.49E-06	0.21E-02	0.86E-04

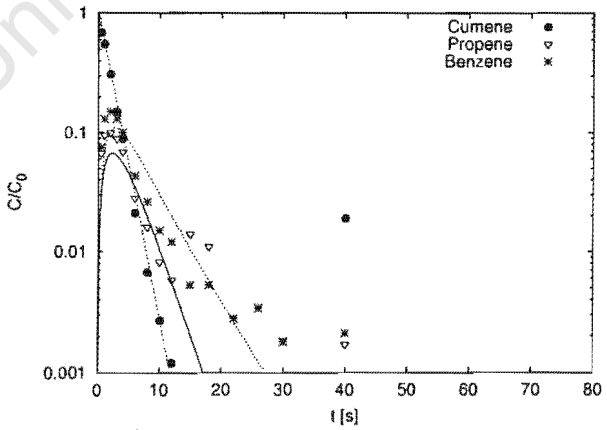

Appendix K. Cumene pulse experiments over T4480

Run Conditions react47

T_R [°C]	F(STP) [ml/min]	R_y [cm]	V_{cat} [ml]	τ [s]
391	511	0.075	0.432	2.36

Errors of C(t)

	Cumene	Propene	Benzene
Least Err	0.14E+00	0.14E+00	0.10E+00
R^2	0.928	0.868	0.839
Min Err% (@ time)	0.30(3.0)	1.61(8.0)	0.12(15.0)
Max Err% (@ time)	1197.41(0.5)	53.88(0.5)	69.07(0.5)

Parameter Estimates

	Low Estimate	Estimate	High Estimate
$K_c(Benzene)$	110	180	294
$k_{eff}[1/s]$	242	578	1377
$\alpha(Benzene)$	0.14E-01	0.22E-01	0.36E-01
ϕ	13	20	31

Model Parameters

	Cumene	Propene	Benzene
$D_y[cm^2/s]$	0.12E-01	0.20E-01	0.15E-01
$K_c[/]$	0	0	180
α	0.51E+01	0.84E+01	0.22E-01
β	0.43E-01	0.71E-01	0.53E-01

Experiment versus Model

	CUMENE		PROPENE		BENZENE	
t[s]	Exp	Mod	Exp	Mod	Exp	Mod
0.50	0.10E+01	0.68E+00	0.13E+00	0.44E-01	0.16E+00	0.46E-01
1.00	0.42E+00	0.46E+00	0.11E+00	0.65E-01	0.16E+00	0.79E-01
2.00	0.29E+00	0.21E+00	0.13E+00	0.73E-01	0.20E+00	0.10E+00
3.00	0.97E-01	0.96E-01	0.75E-01	0.61E-01	0.11E+00	0.95E-01
4.00	0.83E-01	0.44E-01	0.88E-01	0.46E-01	0.13E+00	0.79E-01
6.00	0.31E-01	0.93E-02	0.43E-01	0.23E-01	0.67E-01	0.50E-01
8.00	0.50E-02	0.19E-02	0.11E-01	0.11E-01	0.21E-01	0.30E-01
10.00	0.27E-02	0.41E-03	0.91E-02	0.47E-02	0.19E-01	0.19E-01
12.00	0.11E-02	0.87E-04	0.36E-02	0.20E-02	0.86E-02	0.13E-01
15.00	0.98E-03	0.87E-05	0.22E-02	0.58E-03	0.79E-02	0.80E-02
18.00	0.47E-03	0.11E-05	0.11E-02	0.16E-03	0.32E-02	0.53E-02
22.00	0.41E-03	0.15E-06	0.52E-03	0.30E-04	0.26E-02	0.34E-02
26.00	0.55E-03	0.31E-08	0.65E-03	0.58E-05	0.37E-02	0.23E-02
30.00	0.00E+00	-0.22E-07	0.43E-03	0.12E-05	0.15E-02	0.16E-02
40.00	0.00E+00	-0.25E-07	0.73E-03	0.11E-06	0.12E-02	0.72E-03

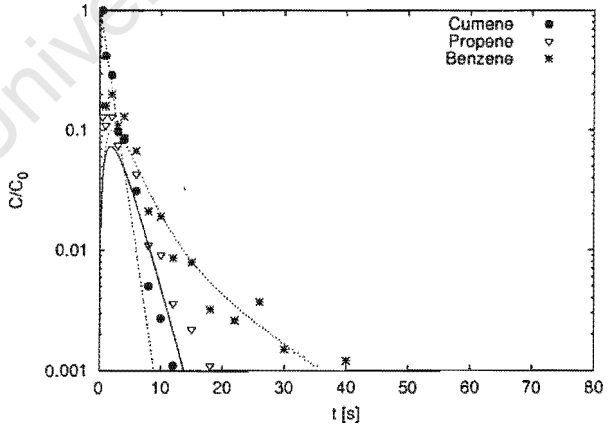

Appendix K. Cumene pulse experiments over T4480

Run Conditions react48

T_R [°C]	F(STP) [ml/min]	R_y [cm]	V_{cat} [ml]	τ [s]
419	311	0.075	0.432	3.72

Errors of C(t)

	Cumene	Propene	Benzene
Least Err	0.39E-01	0.77E-01	0.12E+00
R^2	0.979	0.946	0.877
Min Err% (@ time)	1.56(6.0)	0.19(12.0)	0.25(40.0)
Max Err% (@ time)	32.92(0.5)	21.40(1.0)	31.87(1.0)

Parameter Estimates

	Low Estimate	Estimate	High Estimate
$K_c(Benzene)$	102	151	222
$k_{eff}[1/s]$	211	334	529
$\alpha(Benzene)$	0.28E-01	0.42E-01	0.61E-01
ϕ	12	15	19

Model Parameters

	Cumene	Propene	Benzene
$D_y[cm^2/s]$	0.12E-01	0.20E-01	0.15E-01
$K_c[/]$	0	0	151
α	0.80E+01	0.13E+02	0.42E-01
β	0.68E-01	0.11E+00	0.84E-01

Experiment versus Model

	CUMENE		PROPENE		BENZENE	
t[s]	Exp	Mod	Exp	Mod	Exp	Mod
0.50	0.67E+00	0.76E+00	0.46E-01	0.36E-01	0.51E-01	0.35E-01
1.00	0.64E+00	0.59E+00	0.98E-01	0.59E-01	0.13E+00	0.67E-01
2.00	0.37E+00	0.34E+00	0.11E+00	0.80E-01	0.17E+00	0.10E+00
4.00	0.13E+00	0.12E+00	0.96E-01	0.74E-01	0.16E+00	0.11E+00
6.00	0.38E-01	0.40E-01	0.47E-01	0.53E-01	0.76E-01	0.91E-01
8.00	0.17E-01	0.14E-01	0.47E-01	0.34E-01	0.80E-01	0.68E-01
10.00	0.56E-02	0.47E-02	0.20E-01	0.21E-01	0.36E-01	0.50E-01
12.00	0.32E-02	0.16E-02	0.13E-01	0.13E-01	0.28E-01	0.37E-01
15.00	0.58E-03	0.32E-03	0.38E-02	0.58E-02	0.13E-01	0.24E-01
18.00	0.67E-03	0.66E-04	0.35E-02	0.26E-02	0.11E-01	0.17E-01
22.00	0.30E-03	0.82E-05	0.13E-02	0.90E-03	0.58E-02	0.11E-01
30.00	0.00E+00	0.36E-06	0.48E-03	0.11E-03	0.34E-02	0.49E-02
40.00	0.00E+00	0.11E-07	0.23E-03	0.75E-05	0.20E-02	0.20E-02
50.00	0.00E+00	-0.22E-08	0.34E-03	0.50E-06	0.16E-02	0.84E-03
65.00	0.00E+00	0.48E-09	0.21E-03	0.10E-07	0.12E-02	0.23E-03

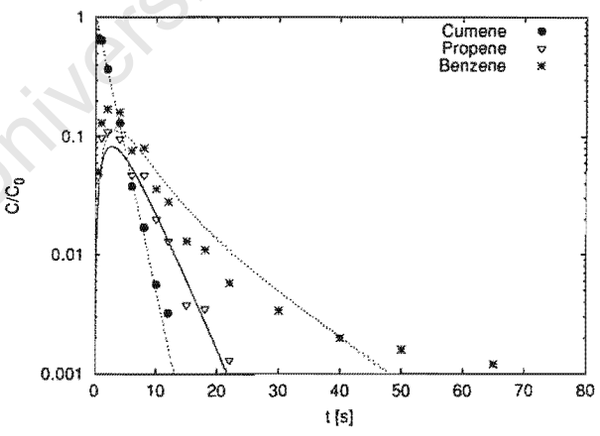

Appendix K. Cumene pulse experiments over T4480

Run Conditions react49

T_R [°C]	F(STP) [ml/min]	R_y [cm]	V_{cat} [ml]	τ [s]
419	411	0.075	0.432	2.81

Errors of C(t)

	Cumene	Propene	Benzene
Least Err	0.21E+00	0.13E+00	0.22E+00
R^2	0.814	0.768	0.690
Min Err% (@ time)	6.05(4.0)	1.15(15.0)	1.68(0.5)
Max Err% (@ time)	134.40(1.0)	39.76(1.0)	47.56(1.0)

Parameter Estimates

	Low Estimate	Estimate	High Estimate
$K_c(Benzene)$	46	84	153
$k_{eff}[1/s]$	168	287	489
$\alpha(Benzene)$	0.31E-01	0.57E-01	0.10E+00
ϕ	11	14	18

Model Parameters

	Cumene	Propene	Benzene
$D_y[cm^2/s]$	0.12E-01	0.20E-01	0.15E-01
$K_c[/]$	0	0	84
α	0.60E+01	0.10E+02	0.57E-01
β	0.51E-01	0.85E-01	0.64E-01

Experiment versus Model

	CUMENE		PROPENE		BENZENE	
t[s]	Exp	Mod	Exp	Mod	Exp	Mod
0.50	0.51E+00	0.74E+00	0.34E-01	0.32E-01	0.34E-01	0.36E-01
1.00	0.77E+00	0.55E+00	0.12E+00	0.51E-01	0.16E+00	0.66E-01
3.00	0.14E+00	0.16E+00	0.73E-01	0.60E-01	0.11E+00	0.96E-01
4.00	0.77E-01	0.90E-01	0.61E-01	0.50E-01	0.99E-01	0.87E-01
6.00	0.13E-01	0.27E-01	0.17E-01	0.31E-01	0.28E-01	0.62E-01
10.00	0.20E-01	0.24E-02	0.61E-02	0.88E-02	0.12E-01	0.27E-01
12.00	0.88E-03	0.74E-03	0.32E-02	0.45E-02	0.73E-02	0.18E-01
15.00	0.57E-03	0.12E-03	0.15E-02	0.16E-02	0.18E-01	0.99E-02
22.00	0.57E-03	0.22E-05	0.69E-03	0.14E-03	0.21E-02	0.30E-02
30.00	0.63E-04	0.53E-07	0.13E-03	0.83E-05	0.13E-02	0.82E-03

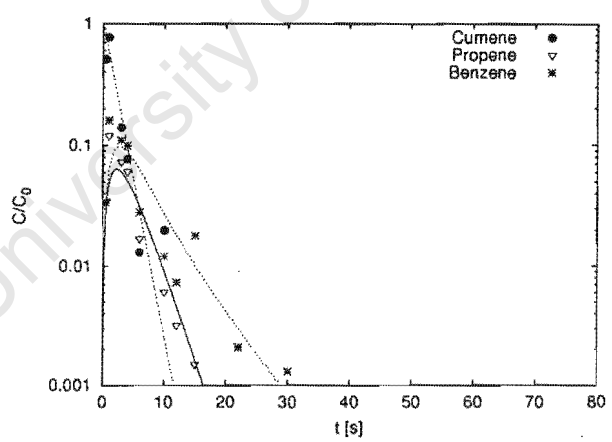

Appendix K. Cumene pulse experiments over T4480

Run Conditions react50

T_R [°C]	F(STP) [ml/min]	R_y [cm]	V_{cat} [ml]	τ [s]
419	511	0.075	0.432	2.26

Errors of C(t)

	Cumene	Propene	Benzene
Least Err	0.84E-01	0.95E-01	0.13E+00
R^2	0.997	0.876	0.835
Min Err% (@ time)	5.10(6.0)	0.77(8.0)	0.23(18.0)
Max Err% (@ time)	43.45(0.5)	27.58(0.5)	32.05(0.5)

Parameter Estimates

	Low Estimate	Estimate	High Estimate
$K_c(Benzene)$	93	155	259
$k_{eff}[1/s]$	182	314	542
$\alpha(Benzene)$	0.15E-01	0.25E-01	0.41E-01
ϕ	11	15	19

Model Parameters

	Cumene	Propene	Benzene
$D_y[cm^2/s]$	0.12E-01	0.20E-01	0.15E-01
$K_c[/]$	0	0	155
α	0.49E+01	0.80E+01	0.25E-01
β	0.41E-01	0.68E-01	0.51E-01

Experiment versus Model

	CUMENE		PROPENE		BENZENE	
t[s]	Exp	Mod	Exp	Mod	Exp	Mod
0.50	0.78E+00	0.70E+00	0.67E-01	0.32E-01	0.72E-01	0.31E-01
3.00	0.10E+00	0.12E+00	0.58E-01	0.48E-01	0.87E-01	0.73E-01
4.00	0.79E-01	0.61E-01	0.61E-01	0.37E-01	0.94E-01	0.62E-01
6.00	0.12E-01	0.15E-01	0.16E-01	0.19E-01	0.25E-01	0.40E-01
8.00	0.38E-02	0.37E-02	0.82E-02	0.85E-02	0.15E-01	0.25E-01
10.00	0.15E-02	0.91E-03	0.48E-02	0.37E-02	0.11E-01	0.16E-01
12.00	0.54E-03	0.23E-03	0.18E-02	0.16E-02	0.55E-02	0.11E-01
15.00	0.30E-03	0.27E-04	0.79E-03	0.44E-03	0.40E-02	0.65E-02
18.00	0.36E-03	0.32E-05	0.55E-03	0.12E-03	0.43E-02	0.43E-02
22.00	0.38E-03	0.31E-06	0.00E+00	0.20E-04	0.31E-02	0.27E-02
26.00	0.14E-03	0.61E-07	0.32E-03	0.37E-05	0.17E-02	0.18E-02
30.00	0.00E+00	-0.11E-07	0.00E+00	0.70E-06	0.14E-02	0.12E-02

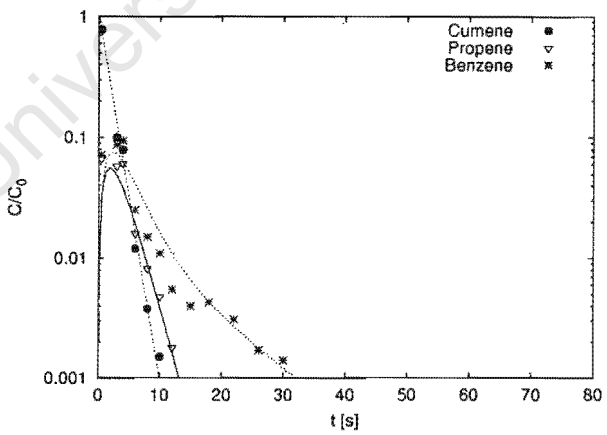

Appendix K. Cumene pulse experiments over T4480

Run Conditions react51

T_R [°C]	F(STP) [ml/min]	R_y [cm]	V_{cat} [ml]	τ [s]
441	311	0.075	0.432	3.60

Errors of C(t)

	Cumene	Propene	Benzene
Least Err	0.55E-01	0.73E-01	0.10E+00
R^2	0.980	0.911	0.813
Min Err% (@ time)	0.57(3.0)	0.28(10.0)	0.56(65.0)
Max Err% (@ time)	40.50(0.5)	24.11(4.0)	48.49(1.0)

Parameter Estimates

	Low Estimate	Estimate	High Estimate
$K_c(Benzene)$	238	344	497
$k_{eff}[1/s]$	233	364	570
$\alpha(Benzene)$	0.12E-01	0.18E-01	0.26E-01
ϕ	13	16	20

Model Parameters

	Cumene	Propene	Benzene
$D_y[cm^2/s]$	0.12E-01	0.20E-01	0.15E-01
$K_c[/]$	0	0	344
α	0.77E+01	0.13E+02	0.18E-01
β	0.66E-01	0.11E+00	0.82E-01

Experiment versus Model

	CUMENE		PROPENE		BENZENE	
t[s]	Exp	Mod	Exp	Mod	Exp	Mod
0.50	0.63E+00	0.76E+00	0.70E-01	0.37E-01	0.80E-01	0.28E-01
1.00	0.49E+00	0.57E+00	0.10E+00	0.61E-01	0.14E+00	0.55E-01
2.00	0.37E+00	0.33E+00	0.11E+00	0.82E-01	0.17E+00	0.86E-01
3.00	0.19E+00	0.19E+00	0.10E+00	0.82E-01	0.16E+00	0.95E-01
4.00	0.14E+00	0.11E+00	0.12E+00	0.74E-01	0.18E+00	0.93E-01
6.00	0.38E-01	0.35E-01	0.46E-01	0.51E-01	0.75E-01	0.77E-01
8.00	0.15E-01	0.12E-01	0.31E-01	0.32E-01	0.52E-01	0.59E-01
10.00	0.57E-02	0.38E-02	0.19E-01	0.20E-01	0.36E-01	0.45E-01
12.00	0.24E-02	0.13E-02	0.11E-01	0.12E-01	0.24E-01	0.34E-01
15.00	0.13E-02	0.24E-03	0.65E-02	0.51E-02	0.17E-01	0.24E-01
18.00	0.65E-03	0.45E-04	0.30E-02	0.23E-02	0.11E-01	0.17E-01
26.00	0.43E-03	0.81E-06	0.54E-03	0.25E-03	0.53E-02	0.90E-02
40.00	0.29E-03	-0.48E-07	0.00E+00	0.57E-05	0.33E-02	0.41E-02
50.00	0.00E+00	-0.40E-07	0.00E+00	0.53E-06	0.22E-02	0.26E-02
65.00	0.00E+00	-0.85E-08	0.00E+00	0.38E-07	0.13E-02	0.14E-02
80.00	0.00E+00	-0.63E-08	0.00E+00	-0.16E-07	0.11E-02	0.76E-03

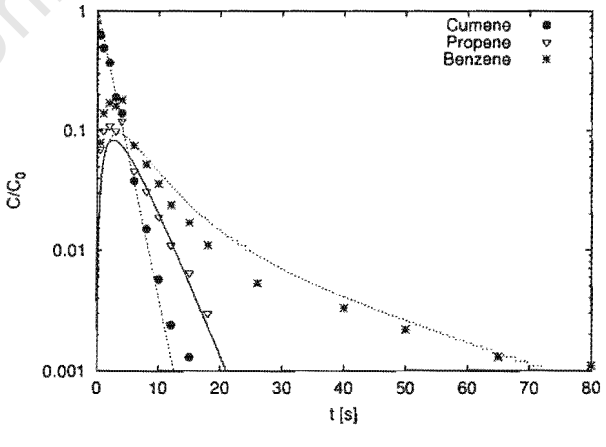

Appendix K. Cumene pulse experiments over T4480

Run Conditions react52

T_R [°C]	F(STP) [ml/min]	R_y [cm]	V_{cat} [ml]	τ [s]
441	411	0.075	0.432	2.72

Errors of C(t)

	Cumene	Propene	Benzene
Least Err	0.11E+00	0.11E+00	0.14E+00
R^2	0.980	0.866	0.865
Min Err% (@ time)	3.00(3.0)	1.70(12.0)	2.40(26.0)
Max Err% (@ time)	29.98(6.0)	31.05(0.5)	45.39(0.5)

Parameter Estimates

	Low Estimate	Estimate	High Estimate
$K_c(Benzene)$	75	120	190
$k_{eff}[1/s]$	258	505	988
$\alpha(Benzene)$	0.24E-01	0.39E-01	0.61E-01
ϕ	13	19	26

Model Parameters

	Cumene	Propene	Benzene
$D_y[cm^2/s]$	0.12E-01	0.20E-01	0.15E-01
$K_c[/]$	0	0	120
α	0.59E+01	0.97E+01	0.39E-01
β	0.50E-01	0.82E-01	0.62E-01

Experiment versus Model

	CUMENE		PROPENE		BENZENE	
t[s]	Exp	Mod	Exp	Mod	Exp	Mod
0.50	0.74E+00	0.70E+00	0.89E-01	0.42E-01	0.12E+00	0.48E-01
1.00	0.41E+00	0.50E+00	0.11E+00	0.65E-01	0.16E+00	0.85E-01
3.00	0.12E+00	0.12E+00	0.85E-01	0.70E-01	0.14E+00	0.11E+00
4.00	0.67E-01	0.61E-01	0.69E-01	0.56E-01	0.12E+00	0.97E-01
6.00	0.40E-01	0.15E-01	0.58E-01	0.32E-01	0.99E-01	0.65E-01
8.00	0.47E-02	0.37E-02	0.12E-01	0.17E-01	0.25E-01	0.41E-01
12.00	0.13E-02	0.23E-03	0.37E-02	0.40E-02	0.10E-01	0.18E-01
18.00	0.51E-03	0.35E-05	0.78E-03	0.46E-03	0.41E-02	0.67E-02
22.00	0.34E-03	0.21E-06	0.36E-03	0.11E-03	0.28E-02	0.39E-02
26.00	0.22E-03	0.13E-07	0.19E-03	0.24E-04	0.20E-02	0.24E-02
30.00	0.00E+00	0.74E-09	0.42E-03	0.56E-05	0.23E-02	0.15E-02
40.00	0.00E+00	-0.17E-11	0.24E-03	0.14E-06	0.13E-02	0.46E-03
50.00	0.00E+00	-0.11E-11	0.28E-03	-0.17E-08	0.15E-02	0.14E-03

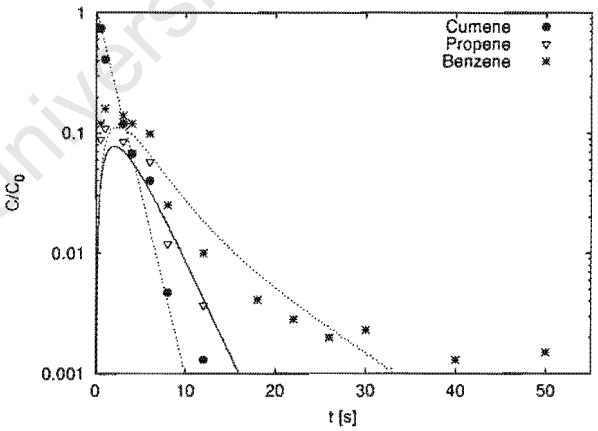

Appendix K. Cumene pulse experiments over T4480

Run Conditions react53

T_R [°C]	F(STP) [ml/min]	R_y [cm]	V_{cat} [ml]	τ [s]
441	511	0.075	0.432	2.19

Errors of C(t)

	Cumene	Propene	Benzene
Least Err	0.13E+00	0.17E+00	0.15E+00
R^2	0.905	0.705	0.840
Min Err% (@ time)	10.63(2.0)	4.15(8.0)	2.95(26.0)
Max Err% (@ time)	441.13(0.5)	58.72(0.5)	83.25(0.5)

Parameter Estimates

	Low Estimate	Estimate	High Estimate
$K_c(Benzene)$	91	176	341
$k_{eff}[1/s]$	213	463	1008
$\alpha(Benzene)$	0.11E-01	0.21E-01	0.41E-01
ϕ	12	18	27

Model Parameters

	Cumene	Propene	Benzene
$D_y[cm^2/s]$	0.12E-01	0.20E-01	0.15E-01
$K_c[/]$	0	0	176
α	0.47E+01	0.78E+01	0.21E-01
β	0.40E-01	0.66E-01	0.50E-01

Experiment versus Model

	CUMENE		PROPENE		BENZENE	
t[s]	Exp	Mod	Exp	Mod	Exp	Mod
0.50	0.11E+01	0.68E+00	0.13E+00	0.39E-01	0.17E+00	0.39E-01
1.00	0.41E+00	0.46E+00	0.48E-01	0.57E-01	0.13E+00	0.68E-01
2.00	0.25E+00	0.21E+00	0.11E+00	0.63E-01	0.18E+00	0.87E-01
3.00	0.13E+00	0.98E-01	0.10E+00	0.52E-01	0.17E+00	0.81E-01
6.00	0.24E-01	0.97E-02	0.36E-01	0.18E-01	0.68E-01	0.41E-01
8.00	0.24E-02	0.21E-02	0.65E-02	0.80E-02	0.14E-01	0.25E-01
15.00	0.29E-03	0.94E-05	0.71E-03	0.36E-03	0.40E-02	0.64E-02
18.00	0.64E-03	0.84E-06	0.12E-02	0.92E-04	0.75E-02	0.43E-02
26.00	0.15E-03	0.88E-08	0.24E-03	0.25E-05	0.15E-02	0.19E-02
30.00	0.15E-03	0.90E-08	0.28E-03	0.45E-06	0.22E-02	0.13E-02

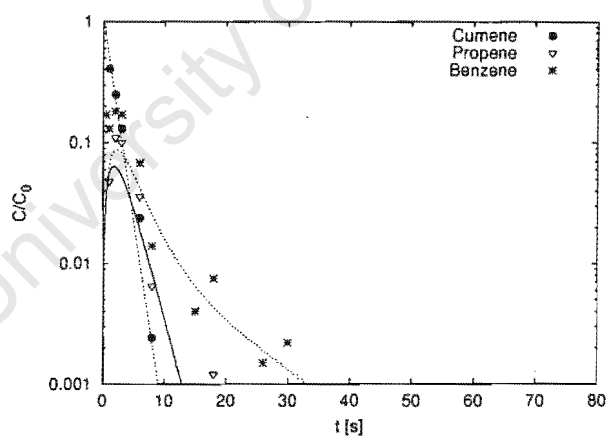

Appendix K. Cumene pulse experiments over T4480

Run Conditions react54

T_R [°C]	F(STP) [ml/min]	R_y [cm]	V_{cat} [ml]	τ [s]
471	311	0.075	0.432	3.46

Errors of C(t)

	Cumene	Propene	Benzene
Least Err	0.40E-01	0.71E-01	0.10E+00
R^2	0.987	0.953	0.913
Min Err% (@ time)	0.66(6.0)	2.00(10.0)	3.60(40.0)
Max Err% (@ time)	17.73(2.0)	20.60(1.0)	35.20(1.0)

Parameter Estimates

	Low Estimate	Estimate	High Estimate
$K_c(Benzene)$	92	140	212
$k_{eff}[1/s]$	275	452	741
$\alpha(Benzene)$	0.28E-01	0.42E-01	0.63E-01
ϕ	14	18	23

Model Parameters

	Cumene	Propene	Benzene
$D_y[cm^2/s]$	0.12E-01	0.20E-01	0.15E-01
$K_c[/]$	0	0	140
α	0.74E+01	0.12E+02	0.42E-01
β	0.63E-01	0.10E+00	0.78E-01

Experiment versus Model

	CUMENE		PROPENE		BENZENE	
t[s]	Exp	Mod	Exp	Mod	Exp	Mod
0.50	0.70E+00	0.74E+00	0.55E-01	0.41E-01	0.65E-01	0.44E-01
1.00	0.58E+00	0.55E+00	0.11E+00	0.67E-01	0.16E+00	0.82E-01
2.00	0.36E+00	0.30E+00	0.12E+00	0.87E-01	0.19E+00	0.12E+00
3.00	0.19E+00	0.16E+00	0.11E+00	0.85E-01	0.18E+00	0.13E+00
4.00	0.11E+00	0.90E-01	0.98E-01	0.75E-01	0.17E+00	0.12E+00
6.00	0.28E-01	0.27E-01	0.40E-01	0.50E-01	0.70E-01	0.90E-01
10.00	0.47E-02	0.24E-02	0.19E-01	0.18E-01	0.40E-01	0.45E-01
12.00	0.15E-02	0.73E-03	0.87E-02	0.10E-01	0.21E-01	0.32E-01
15.00	0.51E-03	0.12E-03	0.37E-02	0.43E-02	0.12E-01	0.21E-01
22.00	0.00E+00	0.20E-05	0.88E-03	0.58E-03	0.57E-02	0.86E-02
26.00	0.00E+00	0.48E-06	0.36E-03	0.18E-03	0.42E-02	0.56E-02
30.00	0.51E-03	0.32E-07	0.33E-03	0.58E-04	0.49E-02	0.37E-02
40.00	0.00E+00	0.22E-08	0.22E-03	0.32E-05	0.18E-02	0.14E-02

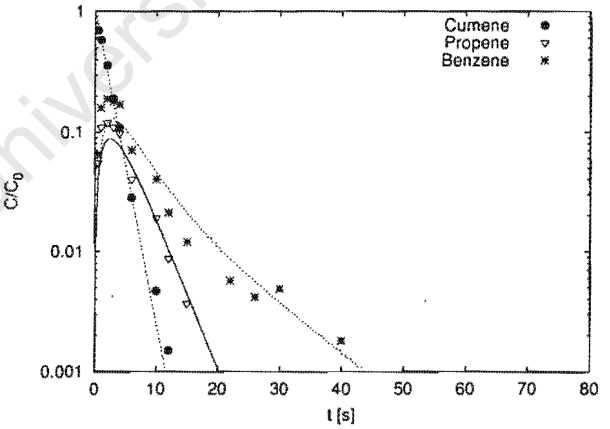

Appendix K. Cumene pulse experiments over T4480

Run Conditions react55

T_R [°C]	F(STP) [ml/min]	R_y [cm]	V_{cat} [ml]	τ [s]
471	411	0.075	0.432	2.61

Errors of C(t)

	Cumene	Propene	Benzene
Least Err	0.56E-01	0.85E-01	0.11E+00
R^2	0.965	0.926	0.903
Min Err% (@ time)	0.24(3.0)	1.26(15.0)	0.15(30.0)
Max Err% (@ time)	142.62(0.5)	28.81(0.5)	41.99(1.0)

Parameter Estimates

	Low Estimate	Estimate	High Estimate
$K_c(Benzene)$	103	149	214
$k_{eff}[1/s]$	335	568	964
$\alpha(Benzene)$	0.21E-01	0.30E-01	0.43E-01
ϕ	15	20	26

Model Parameters

	Cumene	Propene	Benzene
$D_y[cm^2/s]$	0.12E-01	0.20E-01	0.15E-01
$K_c[/]$	0	0	149
α	0.56E+01	0.93E+01	0.30E-01
β	0.48E-01	0.79E-01	0.59E-01

Experiment versus Model

	CUMENE		PROPENE		BENZENE	
t[s]	Exp	Mod	Exp	Mod	Exp	Mod
0.50	0.86E+00	0.69E+00	0.89E-01	0.44E-01	0.11E+00	0.49E-01
1.00	0.43E+00	0.48E+00	0.11E+00	0.67E-01	0.18E+00	0.85E-01
2.00	0.24E+00	0.23E+00	0.98E-01	0.78E-01	0.19E+00	0.11E+00
3.00	0.11E+00	0.11E+00	0.86E-01	0.69E-01	0.15E+00	0.11E+00
6.00	0.16E-01	0.12E-01	0.34E-01	0.30E-01	0.65E-01	0.60E-01
8.00	0.37E-02	0.28E-02	0.11E-01	0.15E-01	0.24E-01	0.38E-01
10.00	0.14E-02	0.64E-03	0.55E-02	0.71E-02	0.15E-01	0.25E-01
12.00	0.78E-03	0.15E-03	0.31E-02	0.34E-02	0.11E-01	0.17E-01
15.00	0.32E-03	0.17E-04	0.12E-02	0.11E-02	0.72E-02	0.10E-01
18.00	0.26E-03	0.22E-05	0.61E-03	0.35E-03	0.54E-02	0.66E-02
22.00	0.27E-03	0.14E-06	0.26E-03	0.76E-04	0.30E-02	0.41E-02
26.00	0.18E-03	0.70E-07	0.18E-03	0.17E-04	0.22E-02	0.27E-02
30.00	0.13E-03	0.35E-08	0.28E-03	0.38E-05	0.18E-02	0.18E-02
40.00	0.00E+00	0.91E-08	0.16E-03	0.96E-07	0.11E-02	0.67E-03

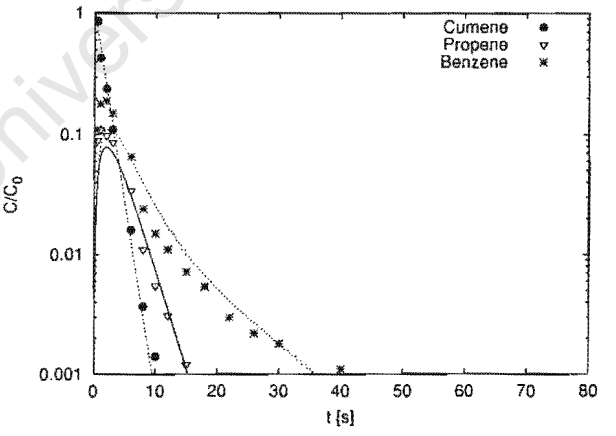

Appendix K. Cumene pulse experiments over T4480

Run Conditions react56

T_R [°C]	F(STP) [ml/min]	R_y [cm]	V_{cat} [ml]	τ [s]
391	411	0.043	0.432	2.93

Errors of C(t)

	Cumene	Propene	Benzene
Least Err	0.58E-01	0.12E+00	0.85E-01
R^2	0.996	0.893	0.870
Min Err% (@ time)	3.98(0.5)	2.21(6.0)	0.03(6.0)
Max Err% (@ time)	10.54(1.0)	31.85(1.0)	55.23(1.0)

Parameter Estimates

	Low Estimate	Estimate	High Estimate
$K_c(Benzene)$	171	235	324
$k_{eff}[1/s]$	457	839	1541
$\alpha(Benzene)$	0.47E-01	0.65E-01	0.90E-01
ϕ	10	14	19

Model Parameters

	Cumene	Propene	Benzene
$D_y[cm^2/s]$	0.12E-01	0.20E-01	0.15E-01
$K_c[/]$	0	0	235
α	0.19E+02	0.32E+02	0.65E-01
β	0.16E+00	0.27E+00	0.20E+00

Experiment versus Model

	CUMENE		PROPENE		BENZENE	
t[s]	Exp	Mod	Exp	Mod	Exp	Mod
0.50	0.57E+00	0.58E+00	0.14E+00	0.86E-01	0.16E+00	0.87E-01
1.00	0.30E+00	0.34E+00	0.20E+00	0.12E+00	0.28E+00	0.14E+00
2.00	0.10E+00	0.12E+00	0.14E+00	0.13E+00	0.24E+00	0.16E+00
4.00	0.18E-01	0.13E-01	0.61E-01	0.81E-01	0.11E+00	0.12E+00
6.00	0.98E-02	0.16E-02	0.46E-01	0.43E-01	0.85E-01	0.85E-01
8.00	0.59E-02	0.18E-03	0.34E-01	0.22E-01	0.74E-01	0.61E-01
10.00	0.28E-02	0.22E-04	0.15E-01	0.11E-01	0.39E-01	0.45E-01
12.00	0.16E-02	0.32E-05	0.76E-02	0.56E-02	0.24E-01	0.34E-01
15.00	0.90E-03	0.53E-06	0.36E-02	0.20E-02	0.15E-01	0.23E-01
18.00	0.11E-02	-0.14E-07	0.27E-02	0.73E-03	0.16E-01	0.16E-01
22.00	0.61E-03	-0.37E-07	0.13E-02	0.19E-03	0.75E-02	0.97E-02
26.00	0.58E-03	-0.21E-07	0.68E-03	0.48E-04	0.52E-02	0.60E-02
30.00	0.00E+00	0.88E-08	0.46E-03	0.13E-04	0.34E-02	0.37E-02
35.00	0.00E+00	-0.28E-07	0.44E-03	0.25E-05	0.25E-02	0.20E-02
50.00	0.00E+00	0.16E-07	0.38E-03	0.14E-06	0.14E-02	0.34E-03

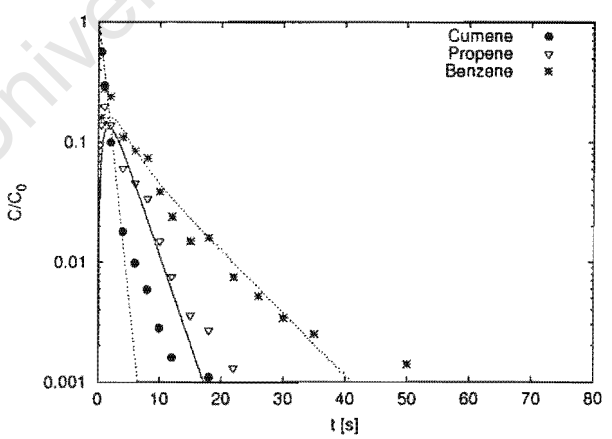

Appendix K. Cumene pulse experiments over T4480

Run Conditions react57

T_R [°C]	F(STP) [ml/min]	R_y [cm]	V_{cat} [ml]	τ [s]
441	411	0.043	0.432	2.72

Errors of C(t)

	Cumene	Propene	Benzene
Least Err	0.19E+00	0.62E-01	0.11E+00
R^2	0.954	0.897	0.939
Min Err% (@ time)	0.86(0.5)	0.61(2.0)	1.87(35.0)
Max Err% (@ time)	29.88(3.0)	36.29(0.5)	62.51(0.5)

Parameter Estimates

	Low Estimate	Estimate	High Estimate
$K_c(Benzene)$	221	293	388
$k_{eff}[1/s]$	968	1961	3975
$\alpha(Benzene)$	0.37E-01	0.49E-01	0.64E-01
ϕ	15	21	30

Model Parameters

	Cumene	Propene	Benzene
$D_y[cm^2/s]$	0.12E-01	0.20E-01	0.15E-01
$K_c[/]$	0	0	293
α '	0.18E+02	0.30E+02	0.49E-01
β	0.15E+00	0.25E+00	0.19E+00

Experiment versus Model

	CUMENE		PROPENE		BENZENE	
t[s]	Exp	Mod	Exp	Mod	Exp	Mod
0.50	0.46E+00	0.47E+00	0.21E+00	0.12E+00	0.29E+00	0.13E+00
1.00	0.14E+00	0.22E+00	0.17E+00	0.16E+00	0.28E+00	0.19E+00
2.00	0.74E-01	0.48E-01	0.15E+00	0.14E+00	0.30E+00	0.18E+00
3.00	0.30E-01	0.10E-01	0.13E+00	0.11E+00	0.23E+00	0.15E+00
6.00	0.31E-02	0.11E-03	0.31E-01	0.37E-01	0.67E-01	0.78E-01
8.00	0.13E-02	0.56E-05	0.15E-01	0.18E-01	0.39E-01	0.55E-01
10.00	0.83E-03	0.35E-06	0.82E-02	0.86E-02	0.26E-01	0.41E-01
12.00	0.73E-03	0.17E-06	0.49E-02	0.41E-02	0.19E-01	0.31E-01
18.00	0.34E-03	-0.54E-07	0.99E-03	0.46E-03	0.79E-02	0.15E-01
22.00	0.23E-03	-0.19E-07	0.61E-03	0.11E-03	0.81E-02	0.10E-01
26.00	0.84E-03	0.19E-08	0.39E-03	0.25E-04	0.44E-02	0.65E-02
30.00	0.34E-03	0.10E-07	0.67E-03	0.60E-05	0.61E-02	0.43E-02
35.00	0.11E-03	-0.55E-08	0.38E-03	0.11E-05	0.28E-02	0.25E-02
40.00	0.00E+00	0.25E-08	0.21E-03	0.32E-06	0.17E-02	0.15E-02
50.00	0.00E+00	0.16E-08	0.40E-03	-0.17E-07	0.11E-02	0.53E-03

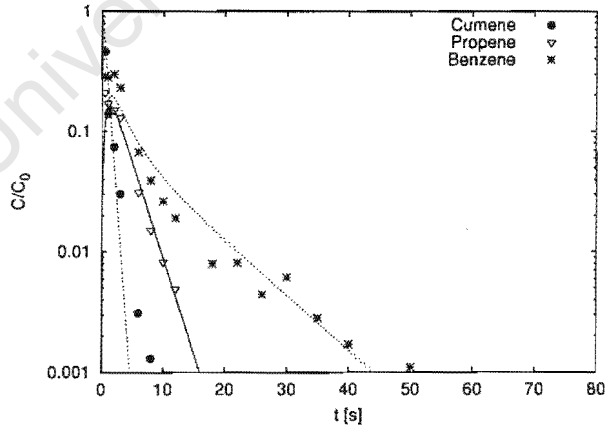

Appendix K. Cumene pulse experiments over T4480

Run Conditions react58

T_R [°C]	F(STP) [ml/min]	R_y [cm]	V_{cat} [ml]	τ [s]
471	411	0.043	0.432	2.61

Errors of C(t)

	Cumene	Propene	Benzene
Least Err	0.19E+00	0.58E-01	0.11E+00
R^2	0.983	0.986	0.991
Min Err% (@ time)	12.33(2.0)	0.27(8.0)	1.89(22.0)
Max Err% (@ time)	40.48(4.0)	14.67(6.0)	23.17(1.0)

Parameter Estimates

	Low Estimate	Estimate	High Estimate
$K_c(Benzene)$	92	133	191
$k_{eff}[1/s]$	802	1722	3695
$\alpha(Benzene)$	0.72E-01	0.10E+00	0.15E+00
ϕ	13	20	29

Model Parameters

	Cumene	Propene	Benzene
$D_y[cm^2/s]$	0.12E-01	0.20E-01	0.15E-01
$K_c[/]$	0	0	133
α	0.17E+02	0.29E+02	0.10E+00
β	0.15E+00	0.24E+00	0.18E+00

Experiment versus Model

	CUMENE		PROPENE		BENZENE	
t[s]	Exp	Mod	Exp	Mod	Exp	Mod
0.50	0.43E+00	0.48E+00	0.15E+00	0.11E+00	0.21E+00	0.15E+00
1.00	0.17E+00	0.23E+00	0.17E+00	0.15E+00	0.28E+00	0.21E+00
2.00	0.74E-01	0.54E-01	0.15E+00	0.14E+00	0.27E+00	0.21E+00
4.00	0.16E-01	0.29E-02	0.75E-01	0.71E-01	0.16E+00	0.13E+00
6.00	0.87E-02	0.16E-03	0.52E-01	0.34E-01	0.11E+00	0.81E-01
8.00	0.21E-02	0.94E-05	0.16E-01	0.16E-01	0.42E-01	0.52E-01
12.00	0.58E-03	0.33E-07	0.33E-02	0.34E-02	0.13E-01	0.23E-01
15.00	0.40E-03	-0.25E-07	0.15E-02	0.11E-02	0.89E-02	0.13E-01
18.00	0.22E-03	-0.30E-07	0.64E-03	0.35E-03	0.52E-02	0.72E-02
22.00	0.00E+00	-0.32E-08	0.00E+00	0.76E-04	0.37E-02	0.33E-02
30.00	0.00E+00	-0.29E-08	0.22E-03	0.38E-05	0.16E-02	0.70E-03
35.00	0.00E+00	-0.21E-08	0.21E-03	0.71E-06	0.12E-02	0.27E-03

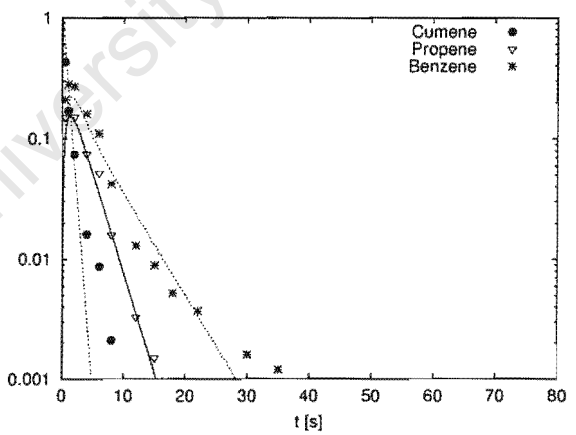

Appendix K. Cumene pulse experiments over T4480

Run Conditions react59

T_R [°C]	F(STP) [ml/min]	R_y [cm]	V_{cat} [ml]	τ [s]
391	311	0.055	0.432	3.87

Errors of C(t)

	Cumene	Propene	Benzene
Least Err	0.26E-01	0.10E+00	0.86E-01
R^2	0.996	0.923	0.898
Min Err% (@ time)	0.13(6.0)	1.72(8.0)	1.26(2.0)
Max Err% (@ time)	60.74(0.5)	19.94(3.0)	29.05(35.0)

Parameter Estimates

	Low Estimate	Estimate	High Estimate
$K_c(Benzene)$	72	93	121
$k_{eff}[1/s]$	58	85	125
$\alpha(Benzene)$	0.10E+00	0.13E+00	0.17E+00
ϕ	4	5	6

Model Parameters

	Cumene	Propene	Benzene
$D_y[cm^2/s]$	0.12E-01	0.20E-01	0.15E-01
$K_c[/]$	0	0	93
α	0.15E+02	0.26E+02	0.13E+00
β	0.13E+00	0.22E+00	0.16E+00

Experiment versus Model

	CUMENE		PROPENE		BENZENE	
t[s]	Exp	Mod	Exp	Mod	Exp	Mod
0.50	0.88E+00	0.81E+00	0.31E-01	0.22E-01	0.17E-01	0.19E-01
1.00	0.68E+00	0.66E+00	0.64E-01	0.38E-01	0.49E-01	0.39E-01
2.00	0.43E+00	0.43E+00	0.58E-01	0.55E-01	0.66E-01	0.68E-01
3.00	0.33E+00	0.28E+00	0.95E-01	0.59E-01	0.99E-01	0.82E-01
4.00	0.22E+00	0.19E+00	0.91E-01	0.57E-01	0.10E+00	0.86E-01
6.00	0.80E-01	0.80E-01	0.49E-01	0.44E-01	0.58E-01	0.79E-01
8.00	0.34E-01	0.35E-01	0.33E-01	0.31E-01	0.45E-01	0.64E-01
12.00	0.99E-02	0.65E-02	0.18E-01	0.13E-01	0.31E-01	0.38E-01
15.00	0.40E-02	0.18E-02	0.11E-01	0.64E-02	0.23E-01	0.24E-01
18.00	0.20E-02	0.52E-03	0.52E-02	0.30E-02	0.15E-01	0.15E-01
22.00	0.12E-02	0.98E-04	0.27E-02	0.11E-02	0.10E-01	0.83E-02
26.00	0.93E-03	0.18E-04	0.13E-02	0.40E-03	0.72E-02	0.45E-02
30.00	0.77E-03	0.40E-05	0.82E-03	0.15E-03	0.59E-02	0.24E-02
35.00	0.50E-03	0.51E-06	0.51E-03	0.41E-04	0.51E-02	0.11E-02

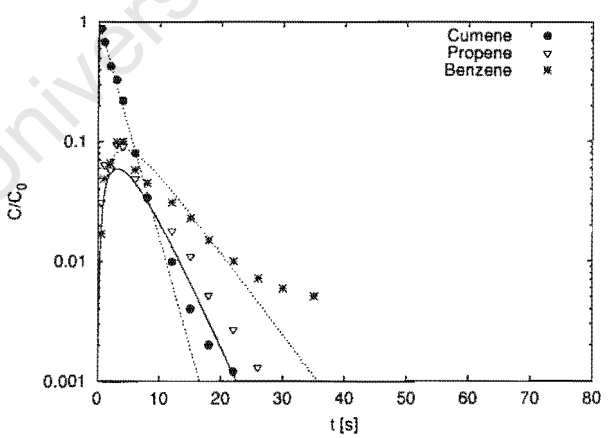

Appendix K. Cumene pulse experiments over T4480

Run Conditions react62

T_R [°C]	F(STP) [ml/min]	R_y [cm]	V_{cat} [ml]	τ [s]
441	411	0.055	0.432	2.72

Errors of C(t)

	Cumene	Propene	Benzene
Least Err	0.21E+00	0.11E+00	0.56E-01
R^2	0.960	0.923	0.937
Min Err% (@ time)	28.25(2.0)	2.44(8.0)	0.11(26.0)
Max Err% (@ time)	197.25(0.5)	18.94(18.0)	19.63(1.0)

Parameter Estimates

	Low Estimate	Estimate	High Estimate
$K_c(Benzene)$	223	347	539
$k_{eff}[1/s]$	134	259	503
$\alpha(Benzene)$	0.16E-01	0.25E-01	0.39E-01
ϕ	7	10	14

Model Parameters

	Cumene	Propene	Benzene
$D_y[cm^2/s]$	0.12E-01	0.20E-01	0.15E-01
$K_c[/]$	0	0	347
α	0.11E+02	0.18E+02	0.25E-01
β	0.93E-01	0.15E+00	0.11E+00

Experiment versus Model

	CUMENE		PROPENE		BENZENE	
t[s]	Exp	Mod	Exp	Mod	Exp	Mod
0.50	0.89E+00	0.71E+00	0.48E-01	0.39E-01	0.26E-01	0.27E-01
1.00	0.63E+00	0.51E+00	0.90E-01	0.61E-01	0.82E-01	0.50E-01
2.00	0.15E+00	0.26E+00	0.68E-01	0.74E-01	0.99E-01	0.73E-01
6.00	0.64E-01	0.17E-01	0.36E-01	0.31E-01	0.80E-01	0.54E-01
8.00	0.15E-01	0.45E-02	0.18E-01	0.16E-01	0.34E-01	0.40E-01
10.00	0.76E-02	0.12E-02	0.11E-01	0.82E-02	0.26E-01	0.30E-01
12.00	0.44E-02	0.30E-03	0.64E-02	0.40E-02	0.19E-01	0.23E-01
15.00	0.18E-02	0.41E-04	0.27E-02	0.14E-02	0.12E-01	0.16E-01
18.00	0.14E-02	0.60E-05	0.16E-02	0.46E-03	0.89E-02	0.12E-01
22.00	0.11E-02	0.70E-06	0.95E-03	0.11E-03	0.79E-02	0.83E-02
26.00	0.68E-03	0.18E-07	0.48E-03	0.25E-04	0.61E-02	0.60E-02
30.00	0.45E-03	0.58E-07	0.39E-03	0.60E-05	0.35E-02	0.45E-02
35.00	0.37E-03	-0.70E-08	0.00E+00	0.11E-05	0.35E-02	0.32E-02
40.00	0.00E+00	-0.45E-07	0.37E-03	0.33E-06	0.24E-02	0.22E-02
50.00	0.00E+00	0.10E-07	0.49E-03	-0.98E-08	0.16E-02	0.11E-02

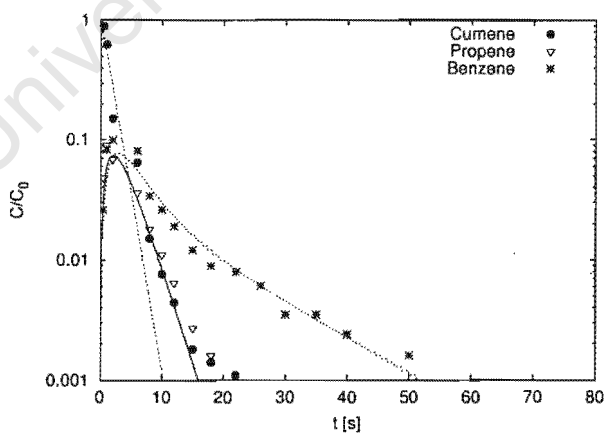

Appendix K. Cumene pulse experiments over T4480

Run Conditions react63				
T_R	F(STP)	R_y	V_{cat}	τ
$[°C]$	[ml/min]	[cm]	[ml]	[s]
391	411	0.055	0.432	2.93

Errors of C(t)			
	Cumene	Propene	Benzene
Least Err	0.74E-01	0.11E+00	0.10E+00
R^2	0.984	0.850	0.736
Min Err% (@ time)	2.83(3.0)	0.10(10.0)	1.54(40.0)
Max Err% (@ time)	23.58(1.0)	45.53(0.5)	64.62(0.5)

Parameter Estimates			
	Low Estimate	Estimate	High Estimate
$K_c(Benzene)$	354	622	1091
$k_{eff}[1/s]$	365	587	944
$\alpha(Benzene)$	0.85E-02	0.15E-01	0.26E-01
ϕ	11	15	19

Model Parameters			
	Cumene	Propene	Benzene
$D_y[cm^2/s]$	0.12E-01	0.20E-01	0.15E-01
$K_c[/]$	0	0	622
α	0.12E+02	0.19E+02	0.15E-01
β	0.10E+00	0.16E+00	0.12E+00

Experiment versus Model

	CUMENE		PROPENE		BENZENE	
t[s]	Exp	Mod	Exp	Mod	Exp	Mod
0.50	0.65E+00	0.66E+00	0.14E+00	0.60E-01	0.14E+00	0.40E-01
1.00	0.34E+00	0.44E+00	0.17E+00	0.90E-01	0.19E+00	0.70E-01
2.00	0.16E+00	0.19E+00	0.16E+00	0.10E+00	0.19E+00	0.95E-01
3.00	0.79E-01	0.85E-01	0.12E+00	0.91E-01	0.16E+00	0.94E-01
4.00	0.32E-01	0.37E-01	0.56E-01	0.73E-01	0.92E-01	0.85E-01
6.00	0.11E-01	0.72E-02	0.34E-01	0.41E-01	0.52E-01	0.63E-01
8.00	0.50E-02	0.14E-02	0.19E-01	0.21E-01	0.36E-01	0.47E-01
10.00	0.27E-02	0.27E-03	0.11E-01	0.11E-01	0.26E-01	0.36E-01
12.00	0.19E-02	0.53E-04	0.60E-02	0.56E-02	0.18E-01	0.28E-01
15.00	0.14E-02	0.51E-05	0.28E-02	0.20E-02	0.13E-01	0.21E-01
18.00	0.81E-03	0.77E-06	0.20E-02	0.73E-03	0.93E-02	0.16E-01
22.00	0.10E-02	0.37E-07	0.11E-02	0.19E-03	0.13E-01	0.12E-01
26.00	0.43E-03	-0.23E-07	0.55E-03	0.48E-04	0.60E-02	0.92E-02
35.00	0.00E+00	-0.60E-07	0.38E-03	0.28E-05	0.40E-02	0.58E-02
40.00	0.00E+00	0.15E-07	0.65E-03	0.53E-06	0.50E-02	0.46E-02
50.00	0.00E+00	0.14E-07	0.42E-03	0.10E-06	0.27E-02	0.31E-02
65.00	0.00E+00	0.87E-08	0.35E-03	0.70E-08	0.31E-02	0.17E-02

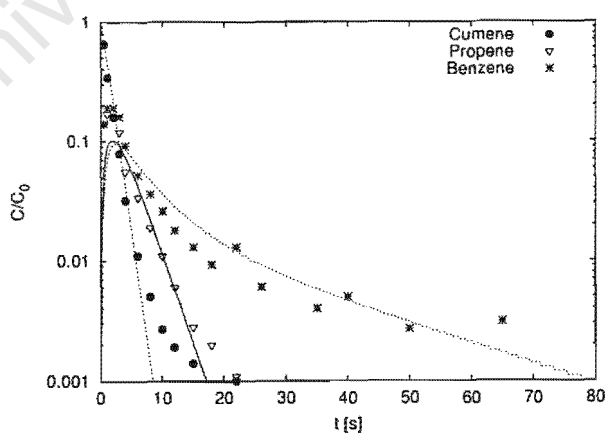

Appendix K. Cumene pulse experiments over T4480

Run Conditions react64

T_R [°C]	F(STP) [ml/min]	R_y [cm]	V_{cat} [ml]	τ [s]
441	411	0.055	0.432	2.72

Errors of C(t)

	Cumene	Propene	Benzene
Least Err	0.93E-01	0.67E-01	0.13E+00
R^2	0.996	0.932	0.955
Min Err% (@ time)	0.52(3.0)	0.53(12.0)	2.85(30.0)
Max Err% (@ time)	37.96(0.5)	26.56(0.5)	33.26(0.5)

Parameter Estimates

	Low Estimate	Estimate	High Estimate
$K_c(Benzene)$	125	194	301
$k_{eff}[1/s]$	625	1162	2160
$\alpha(Benzene)$	0.29E-01	0.44E-01	0.68E-01
ϕ	15	21	29

Model Parameters

	Cumene	Propene	Benzene
$D_y[cm^2/s]$	0.12E-01	0.20E-01	0.15E-01
$K_c[/]$	0	0	194
α	0.11E+02	0.18E+02	0.44E-01
β	0.93E-01	0.15E+00	0.11E+00

Experiment versus Model

	CUMENE		PROPENE		BENZENE	
t[s]	Exp	Mod	Exp	Mod	Exp	Mod
0.50	0.43E+00	0.59E+00	0.14E+00	0.81E-01	0.17E+00	0.93E-01
2.00	0.11E+00	0.12E+00	0.13E+00	0.12E+00	0.21E+00	0.17E+00
3.00	0.43E-01	0.42E-01	0.11E+00	0.97E-01	0.18E+00	0.15E+00
4.00	0.20E-01	0.15E-01	0.81E-01	0.72E-01	0.14E+00	0.12E+00
10.00	0.10E-02	0.27E-04	0.78E-02	0.85E-02	0.22E-01	0.34E-01
12.00	0.54E-03	0.34E-05	0.40E-02	0.41E-02	0.14E-01	0.25E-01
15.00	0.66E-03	0.21E-06	0.19E-02	0.14E-02	0.11E-01	0.16E-01
18.00	0.28E-03	0.12E-06	0.88E-03	0.46E-03	0.60E-02	0.11E-01
22.00	0.00E+00	0.17E-07	0.47E-03	0.11E-03	0.48E-02	0.66E-02
26.00	0.00E+00	-0.16E-07	0.68E-03	0.25E-04	0.15E-01	0.41E-02
30.00	0.00E+00	-0.45E-08	0.39E-03	0.59E-05	0.31E-02	0.26E-02
35.00	0.00E+00	0.13E-08	0.33E-03	0.13E-05	0.22E-02	0.15E-02
50.00	0.00E+00	-0.33E-09	0.32E-03	0.27E-07	0.18E-02	0.26E-03

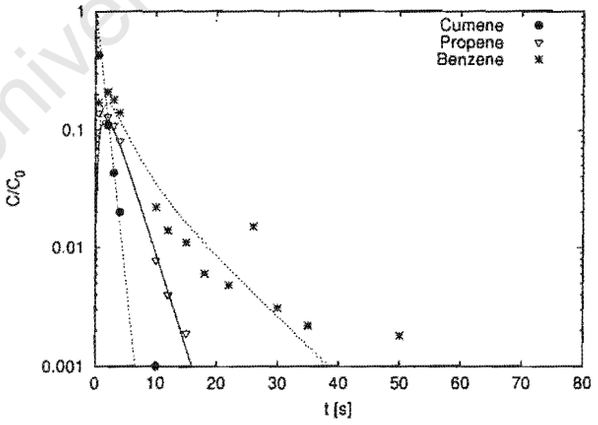

Appendix K. Cumene pulse experiments over T4480

Run Conditions react65

T_R [°C]	F(STP) [ml/min]	R_y [cm]	V_{cat} [ml]	τ [s]
471	411	0.055	0.432	2.61

Errors of C(t)

	Cumene	Propene	Benzene
Least Err	0.19E+00	NAN	NAN
R^2	0.940	0.785	0.878
Min Err% (@ time)	2.87(2.0)	2.77(8.0)	0.14(26.0)
Max Err% (@ time)	62.68(6.0)	47.06(22.0)	25.33(6.0)

Parameter Estimates

	Low Estimate	Estimate	High Estimate
$K_c(Benzene)$	148	275	512
$k_{eff}[1/s]$	328	768	1801
$\alpha(Benzene)$	0.16E-01	0.30E-01	0.56E-01
ϕ	11	17	26

Model Parameters

	Cumene	Propene	Benzene
$D_y[cm^2/s]$	0.12E-01	0.20E-01	0.15E-01
$K_c[/]$	0	0	275
α	0.10E+02	0.17E+02	0.30E-01
β	0.89E-01	0.15E+00	0.11E+00

Experiment versus Model

	CUMENE		PROPENE		BENZENE	
t[s]	Exp	Mod	Exp	Mod	Exp	Mod
0.50	0.54E+00	0.63E+00	0.00E+00	0.66E-01	0.00E+00	0.64E-01
1.00	0.22E+00	0.39E+00	0.11E+00	0.97E-01	0.15E+00	0.11E+00
2.00	0.16E+00	0.15E+00	0.12E+00	0.10E+00	0.19E+00	0.13E+00
3.00	0.86E-01	0.60E-01	0.10E+00	0.86E-01	0.17E+00	0.12E+00
4.00	0.50E-01	0.24E-01	0.72E-01	0.64E-01	0.13E+00	0.10E+00
6.00	0.32E-01	0.36E-02	0.57E-01	0.33E-01	0.11E+00	0.66E-01
8.00	0.81E-02	0.56E-03	0.14E-01	0.16E-01	0.33E-01	0.44E-01
10.00	0.66E-02	0.87E-04	0.10E-01	0.73E-02	0.29E-01	0.31E-01
12.00	0.43E-02	0.14E-04	0.50E-02	0.34E-02	0.18E-01	0.23E-01
15.00	0.33E-02	0.95E-06	0.29E-02	0.11E-02	0.13E-01	0.15E-01
18.00	0.26E-02	0.22E-06	0.22E-02	0.35E-03	0.10E-01	0.11E-01
22.00	0.23E-02	0.37E-07	0.16E-02	0.76E-04	0.80E-02	0.73E-02
26.00	0.14E-02	-0.16E-07	0.99E-03	0.17E-04	0.50E-02	0.51E-02
30.00	0.10E-02	-0.15E-07	0.72E-03	0.38E-05	0.38E-02	0.36E-02
35.00	0.78E-03	0.86E-08	0.54E-03	0.72E-06	0.28E-02	0.23E-02

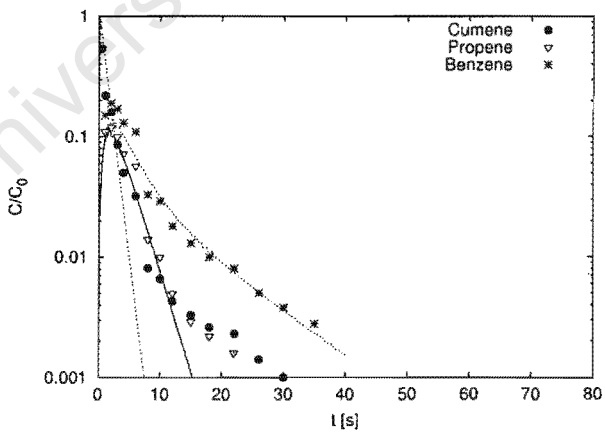

Appendix K. Cumene pulse experiments over T4480

Run Conditions react66

T_R [°C]	F(STP) [ml/min]	R_y [cm]	V_{cat} [ml]	τ [s]
391	411	0.055	0.432	2.93

Errors of C(t)

	Cumene	Propene	Benzene
Least Err	0.79E-01	0.10E+00	0.10E+00
R^2	0.998	0.980	0.933
Min Err% (@ time)	0.48(4.0)	0.41(8.0)	1.73(35.0)
Max Err% (@ time)	20.89(6.0)	26.91(1.0)	27.56(1.0)

Parameter Estimates

	Low Estimate	Estimate	High Estimate
$K_c(Benzene)$	172	245	349
$k_{eff}[1/s]$	212	353	587
$\alpha(Benzene)$	0.27E-01	0.38E-01	0.54E-01
ϕ	9	11	15

Model Parameters

	Cumene	Propene	Benzene
$D_y[cm^2/s]$	0.12E-01	0.20E-01	0.15E-01
$K_c[/]$	0	0	245
α	0.12E+02	0.19E+02	0.38E-01
β	0.10E+00	0.16E+00	0.12E+00

Experiment versus Model

	CUMENE		PROPENE		BENZENE	
t[s]	Exp	Mod	Exp	Mod	Exp	Mod
0.50	0.64E+00	0.70E+00	0.77E-01	0.46E-01	0.60E-01	0.39E-01
1.00	0.43E+00	0.49E+00	0.13E+00	0.72E-01	0.13E+00	0.71E-01
2.00	0.23E+00	0.24E+00	0.13E+00	0.87E-01	0.15E+00	0.10E+00
3.00	0.11E+00	0.12E+00	0.12E+00	0.80E-01	0.14E+00	0.10E+00
4.00	0.60E-01	0.59E-01	0.93E-01	0.65E-01	0.12E+00	0.94E-01
6.00	0.30E-01	0.14E-01	0.70E-01	0.38E-01	0.93E-01	0.69E-01
8.00	0.53E-02	0.35E-02	0.21E-01	0.21E-01	0.32E-01	0.50E-01
10.00	0.27E-02	0.86E-03	0.14E-01	0.11E-01	0.25E-01	0.36E-01
12.00	0.18E-02	0.21E-03	0.72E-02	0.55E-02	0.16E-01	0.27E-01
15.00	0.11E-02	0.26E-04	0.36E-02	0.20E-02	0.12E-01	0.19E-01
18.00	0.54E-03	0.35E-05	0.16E-02	0.73E-03	0.74E-02	0.13E-01
22.00	0.56E-03	0.24E-06	0.97E-03	0.19E-03	0.68E-02	0.88E-02
26.00	0.34E-03	0.58E-07	0.56E-03	0.48E-04	0.47E-02	0.60E-02
30.00	0.26E-03	0.17E-07	0.36E-03	0.12E-04	0.36E-02	0.41E-02
35.00	0.21E-03	-0.47E-07	0.35E-03	0.26E-05	0.29E-02	0.26E-02
40.00	0.00E+00	0.14E-07	0.42E-03	0.49E-06	0.24E-02	0.17E-02
50.00	0.00E+00	0.47E-08	0.54E-03	0.16E-06	0.20E-02	0.67E-03

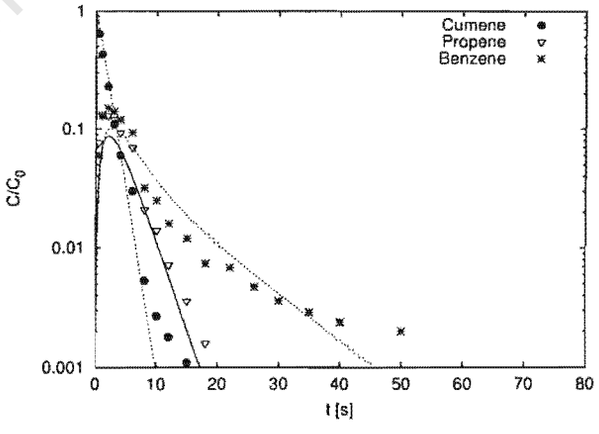

Appendix K. Cumene pulse experiments over T4480

Run Conditions react67

T_R [°C]	F(STP) [ml/min]	R_y [cm]	V_{cat} [ml]	τ [s]
391	411	0.075	0.432	2.93

Errors of C(t)

	Cumene	Propene	Benzene
Least Err	0.80E-01	0.12E+00	0.11E+00
R^2	0.989	0.924	0.881
Min Err% (@ time)	0.09(3.0)	3.76(10.0)	0.25(35.0)
Max Err% (@ time)	45.17(0.5)	28.00(1.0)	43.14(1.0)

Parameter Estimates

	Low Estimate	Estimate	High Estimate
$K_c(Benzene)$	107	157	230
$k_{eff}[1/s]$	184	339	625
$\alpha(Benzene)$	0.22E-01	0.32E-01	0.46E-01
ϕ	11	15	21

Model Parameters

	Cumene	Propene	Benzene
$D_y[cm^2/s]$	0.12E-01	0.20E-01	0.15E-01
$K_c[/]$	0	0	157
α	0.63E+01	0.10E+02	0.32E-01
β	0.54E-01	0.88E-01	0.66E-01

Experiment versus Model

	CUMENE		PROPENE		BENZENE	
t[s]	Exp	Mod	Exp	Mod	Exp	Mod
0.50	0.57E+00	0.74E+00	0.71E-01	0.35E-01	0.88E-01	0.34E-01
1.00	0.49E+00	0.54E+00	0.10E+00	0.56E-01	0.15E+00	0.63E-01
2.00	0.28E+00	0.30E+00	0.10E+00	0.70E-01	0.15E+00	0.92E-01
3.00	0.16E+00	0.16E+00	0.92E-01	0.66E-01	0.14E+00	0.96E-01
4.00	0.86E-01	0.87E-01	0.71E-01	0.56E-01	0.11E+00	0.88E-01
6.00	0.51E-01	0.26E-01	0.60E-01	0.35E-01	0.97E-01	0.65E-01
8.00	0.10E-01	0.76E-02	0.13E-01	0.19E-01	0.27E-01	0.45E-01
10.00	0.55E-02	0.22E-02	0.12E-01	0.10E-01	0.23E-01	0.31E-01
15.00	0.16E-02	0.11E-03	0.32E-02	0.20E-02	0.81E-02	0.13E-01
18.00	0.16E-02	0.18E-04	0.21E-02	0.72E-03	0.77E-02	0.90E-02
22.00	0.77E-03	0.19E-05	0.92E-03	0.19E-03	0.38E-02	0.56E-02
26.00	0.57E-03	0.17E-06	0.50E-03	0.48E-04	0.25E-02	0.37E-02
30.00	0.46E-03	0.84E-07	0.52E-03	0.13E-04	0.23E-02	0.25E-02
35.00	0.31E-03	0.27E-08	0.30E-03	0.24E-05	0.16E-02	0.16E-02
40.00	0.43E-03	-0.28E-07	0.61E-03	0.59E-06	0.24E-02	0.10E-02
50.00	0.00E+00	0.59E-08	0.22E-03	0.19E-07	0.10E-02	0.42E-03

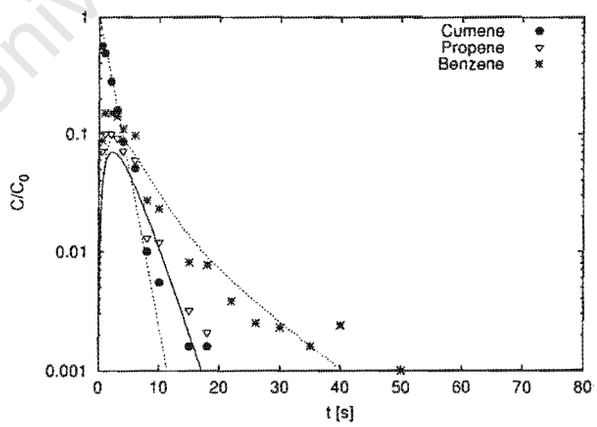

Appendix K. Cumene pulse experiments over T4480

Run Conditions react69

T_R [°C]	F(STP) [ml/min]	R_y [cm]	V_{cat} [ml]	τ [s]
441	411	0.075	0.432	2.72

Errors of C(t)

	Cumene	Propene	Benzene
Least Err	0.14E+00	0.10E+00	0.10E+00
R^2	0.995	0.892	0.897
Min Err% (@ time)	4.82(3.0)	1.80(4.0)	0.16(35.0)
Max Err% (@ time)	42.73(6.0)	24.46(0.5)	44.07(0.5)

Parameter Estimates

	Low Estimate	Estimate	High Estimate
$K_c(Benzene)$	163	276	467
$k_{eff}[1/s]$	293	628	1346
$\alpha(Benzene)$	0.99E-02	0.17E-01	0.28E-01
ϕ	14	21	31

Model Parameters

	Cumene	Propene	Benzene
$D_y[cm^2/s]$	0.12E-01	0.20E-01	0.15E-01
$K_c[/]$	0	0	276
α	0.59E+01	0.97E+01	0.17E-01
β	0.50E-01	0.82E-01	0.62E-01

Experiment versus Model

	CUMENE		PROPENE		BENZENE	
t[s]	Exp	Mod	Exp	Mod	Exp	Mod
0.50	0.59E+00	0.69E+00	0.85E-01	0.47E-01	0.11E+00	0.44E-01
2.00	0.18E+00	0.23E+00	0.91E-01	0.84E-01	0.15E+00	0.11E+00
3.00	0.97E-01	0.11E+00	0.70E-01	0.75E-01	0.12E+00	0.10E+00
4.00	0.65E-01	0.52E-01	0.63E-01	0.60E-01	0.11E+00	0.90E-01
6.00	0.45E-01	0.12E-01	0.51E-01	0.33E-01	0.90E-01	0.62E-01
10.00	0.64E-02	0.62E-03	0.92E-02	0.83E-02	0.21E-01	0.28E-01
12.00	0.38E-02	0.14E-03	0.51E-02	0.41E-02	0.13E-01	0.20E-01
15.00	0.25E-02	0.17E-04	0.24E-02	0.14E-02	0.83E-02	0.13E-01
18.00	0.19E-02	0.20E-05	0.14E-02	0.46E-03	0.58E-02	0.90E-02
22.00	0.14E-02	0.11E-06	0.84E-03	0.11E-03	0.41E-02	0.60E-02
26.00	0.12E-02	0.50E-07	0.56E-03	0.25E-04	0.34E-02	0.44E-02
35.00	0.80E-03	-0.38E-07	0.39E-03	0.11E-05	0.24E-02	0.24E-02
40.00	0.62E-03	0.95E-08	0.33E-03	0.25E-06	0.16E-02	0.18E-02
50.00	0.42E-03	0.15E-07	0.23E-03	0.54E-07	0.13E-02	0.10E-02
80.00	0.00E+00	-0.22E-08	0.00E+00	0.23E-08	0.10E-02	0.22E-03

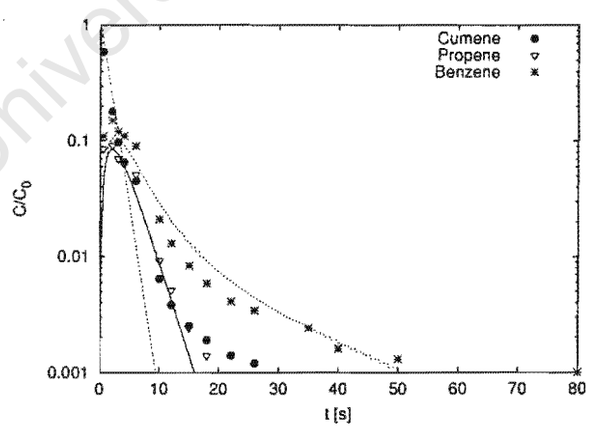

Appendix K. Cumene pulse experiments over T4480

Run Conditions react70

T_R [°C]	F(STP) [ml/min]	R_y [cm]	V_{cat} [ml]	τ [s]
471	411	0.075	0.432	2.61

Errors of C(t)

	Cumene	Propene	Benzene
Least Err	0.64E-01	NAN	NAN
R^2	0.981	0.646	0.637
Min Err% (@ time)	0.61(6.0)	1.31(15.0)	0.39(4.0)
Max Err% (@ time)	1011.91(0.5)	62.86(1.0)	106.33(1.0)

Parameter Estimates

	Low Estimate	Estimate	High Estimate
$K_c(Benzene)$	92	140	213
$k_{eff}[1/s]$	338	567	950
$\alpha(Benzene)$	0.21E-01	0.32E-01	0.48E-01
ϕ	15	20	26

Model Parameters

	Cumene	Propene	Benzene
$D_y[cm^2/s]$	0.12E-01	0.20E-01	0.15E-01
$K_c[/]$	0	0	140
α	0.56E+01	0.93E+01	0.32E-01
β	0.48E-01	0.79E-01	0.59E-01

Experiment versus Model

	CUMENE		PROPENE		BENZENE	
t[s]	Exp	Mod	Exp	Mod	Exp	Mod
0.50	0.97E+00	0.69E+00	0.00E+00	0.44E-01	0.00E+00	0.50E-01
1.00	0.57E+00	0.48E+00	0.19E+00	0.67E-01	0.31E+00	0.86E-01
2.00	0.19E+00	0.23E+00	0.11E+00	0.78E-01	0.18E+00	0.11E+00
3.00	0.10E+00	0.11E+00	0.90E-01	0.69E-01	0.16E+00	0.11E+00
4.00	0.43E-01	0.53E-01	0.51E-01	0.55E-01	0.94E-01	0.93E-01
6.00	0.12E-01	0.12E-01	0.23E-01	0.30E-01	0.43E-01	0.61E-01
8.00	0.44E-02	0.28E-02	0.12E-01	0.15E-01	0.27E-01	0.38E-01
10.00	0.18E-02	0.65E-03	0.57E-02	0.71E-02	0.16E-01	0.25E-01
12.00	0.85E-03	0.15E-03	0.30E-02	0.34E-02	0.10E-01	0.17E-01
15.00	0.94E-03	0.17E-04	0.12E-02	0.11E-02	0.64E-02	0.99E-02
22.00	0.20E-03	0.12E-06	0.32E-03	0.76E-04	0.27E-02	0.39E-02
30.00	0.12E-03	0.90E-08	0.15E-03	0.37E-05	0.17E-02	0.16E-02
35.00	0.00E+00	-0.45E-07	0.16E-03	0.76E-06	0.14E-02	0.98E-03

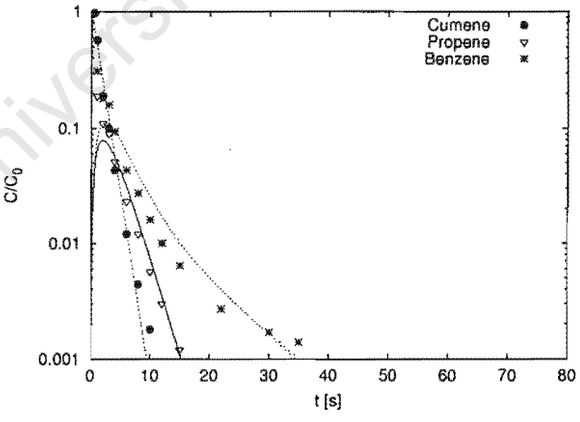

Appendix K. Cumene pulse experiments over T4480

Run Conditions react71

T_R [°C]	F(STP) [ml/min]	R_y [cm]	V_{cat} [ml]	τ [s]
391	411	0.033	0.432	2.93

Errors of C(t)

	Cumene	Propene	Benzene
Least Err	0.24E+00	0.10E+00	0.73E-01
R^2	0.964	0.983	0.980
Min Err% (@ time)	20.81(2.0)	0.74(6.0)	0.35(8.0)
Max Err% (@ time)	61.11(4.0)	26.80(22.0)	15.64(30.0)

Parameter Estimates

	Low Estimate	Estimate	High Estimate
$K_c(Benzene)$	112	146	190
$k_{eff}[1/s]$	540	1100	2242
$\alpha(Benzene)$	0.14E+00	0.18E+00	0.23E+00
ϕ	8	12	17

Model Parameters

	Cumene	Propene	Benzene
$D_y[cm^2/s]$	0.12E-01	0.20E-01	0.15E-01
$K_c[/]$	0	0	146
α	0.33E+02	0.54E+02	0.18E+00
β	0.28E+00	0.46E+00	0.34E+00

Experiment versus Model

	CUMENE		PROPENE		BENZENE	
t[s]	Exp	Mod	Exp	Mod	Exp	Mod
0.50	0.34E+00	0.49E+00	0.16E+00	0.12E+00	0.18E+00	0.14E+00
1.00	0.16E+00	0.24E+00	0.18E+00	0.16E+00	0.24E+00	0.20E+00
2.00	0.95E-01	0.58E-01	0.16E+00	0.15E+00	0.23E+00	0.21E+00
3.00	0.63E-01	0.14E-01	0.14E+00	0.12E+00	0.22E+00	0.18E+00
4.00	0.29E-01	0.34E-02	0.11E+00	0.84E-01	0.19E+00	0.15E+00
6.00	0.76E-02	0.20E-03	0.42E-01	0.43E-01	0.80E-01	0.10E+00
8.00	0.34E-02	0.12E-04	0.28E-01	0.22E-01	0.69E-01	0.69E-01
12.00	0.13E-02	0.13E-06	0.78E-02	0.56E-02	0.26E-01	0.33E-01
15.00	0.76E-03	0.23E-07	0.37E-02	0.20E-02	0.15E-01	0.19E-01
18.00	0.40E-03	0.73E-08	0.17E-02	0.73E-03	0.94E-02	0.11E-01
22.00	0.42E-03	-0.10E-07	0.11E-02	0.19E-03	0.77E-02	0.51E-02
26.00	0.00E+00	-0.58E-08	0.60E-03	0.48E-04	0.45E-02	0.24E-02
30.00	0.00E+00	0.57E-08	0.18E-03	0.13E-04	0.29E-02	0.12E-02

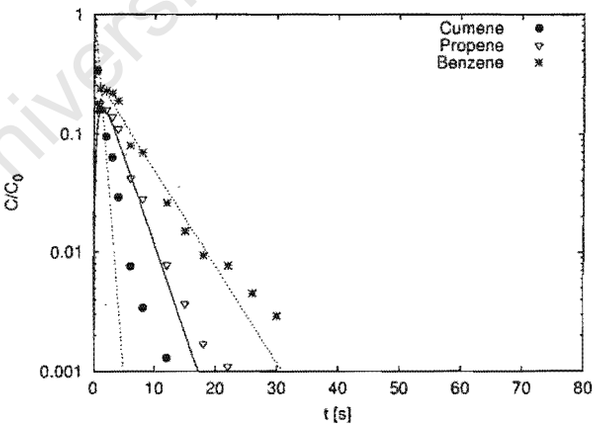

Appendix K. Cumene pulse experiments over T4480

Run Conditions react72

T_R [°C]	F(STP) [ml/min]	R_y [cm]	V_{cat} [ml]	τ [s]
419	411	0.033	0.432	2.81

Errors of C(t)

	Cumene	Propene	Benzene
Least Err	0.79E+00	0.74E+00	0.11E+00
R^2	0.898	0.445	0.248
Min Err% (@ time)	39.53(3.0)	7.45(6.0)	2.45(30.0)
Max Err% (@ time)	60.95(1.0)	140.36(0.5)	253.72(0.5)

Parameter Estimates

	Low Estimate	Estimate	High Estimate
$K_c(Benzene)$	129	372	1072
$k_{eff}[1/s]$	76	125	206
$\alpha(Benzene)$	0.23E-01	0.66E-01	0.19E+00
ϕ	3	4	5

Model Parameters

	Cumene	Propene	Benzene
$D_y[cm^2/s]$	0.12E-01	0.20E-01	0.15E-01
$K_c[/]$	0	0	372
α	0.31E+02	0.52E+02	0.66E-01
β	0.27E+00	0.44E+00	0.33E+00

Experiment versus Model

	CUMENE		PROPENE		BENZENE	
t[s]	Exp	Mod	Exp	Mod	Exp	Mod
0.50	0.45E+00	0.72E+00	0.26E+00	0.39E-01	0.34E+00	0.21E-01
1.00	0.18E+00	0.52E+00	0.26E+00	0.61E-01	0.39E+00	0.40E-01
2.00	0.82E-01	0.27E+00	0.22E+00	0.74E-01	0.37E+00	0.61E-01
3.00	0.38E-01	0.14E+00	0.77E-02	0.68E-01	0.60E-01	0.67E-01
6.00	0.43E-02	0.19E-01	0.42E-01	0.33E-01	0.86E-01	0.56E-01
8.00	0.23E-02	0.52E-02	0.24E-01	0.18E-01	0.56E-01	0.45E-01
10.00	0.22E-02	0.14E-02	0.18E-01	0.91E-02	0.53E-01	0.37E-01
12.00	0.85E-03	0.37E-03	0.76E-02	0.46E-02	0.27E-01	0.29E-01
15.00	0.52E-03	0.52E-04	0.32E-02	0.16E-02	0.15E-01	0.22E-01
18.00	0.45E-03	0.79E-05	0.18E-02	0.56E-03	0.12E-01	0.16E-01
22.00	0.29E-03	0.81E-06	0.81E-03	0.14E-03	0.73E-02	0.10E-01
26.00	0.23E-03	0.52E-07	0.58E-03	0.33E-04	0.60E-02	0.69E-02
30.00	0.00E+00	0.97E-07	0.46E-03	0.84E-05	0.40E-02	0.46E-02
35.00	0.00E+00	-0.33E-07	0.46E-03	0.18E-05	0.33E-02	0.28E-02
40.00	0.00E+00	0.17E-07	0.43E-03	0.33E-06	0.25E-02	0.17E-02
50.00	0.00E+00	0.79E-08	0.13E-03	0.57E-07	0.20E-02	0.60E-03

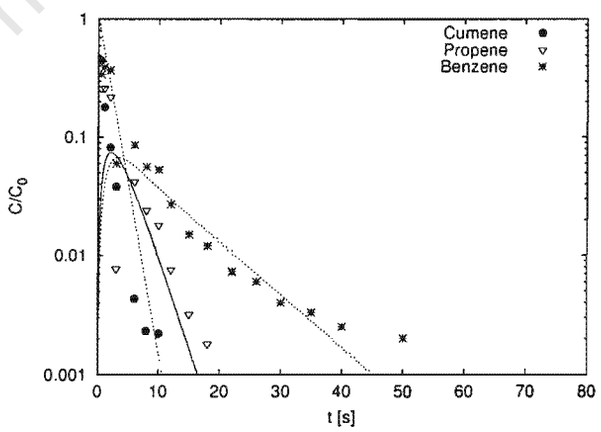

Appendix K. Cumene pulse experiments over T4480

Run Conditions react73

T_R [°C]	F(STP) [ml/min]	R_y [cm]	V_{cat} [ml]	τ [s]
441	411	0.033	0.432	2.72

Errors of C(t)

	Cumene	Propene	Benzene
Least Err	0.13E+00	0.23E+00	0.10E+00
R^2	0.984	0.834	0.809
Min Err% (@ time)	8.36(1.0)	6.27(6.0)	0.23(30.0)
Max Err% (@ time)	26.82(2.0)	36.13(0.5)	106.02(1.0)

Parameter Estimates

	Low Estimate	Estimate	High Estimate
$K_c(Benzene)$	233	336	486
$k_{eff}[1/s]$	899	1478	2430
$\alpha(Benzene)$	0.49E-01	0.71E-01	0.10E+00
ϕ	11	14	18

Model Parameters

	Cumene	Propene	Benzene
$D_y[cm^2/s]$	0.12E-01	0.20E-01	0.15E-01
$K_c[/]$	0	0	336
α	0.30E+02	0.50E+02	0.71E-01
β	0.26E+00	0.42E+00	0.32E+00

Experiment versus Model

	CUMENE		PROPENE		BENZENE	
t[s]	Exp	Mod	Exp	Mod	Exp	Mod
0.50	0.41E+00	0.44E+00	0.22E+00	0.13E+00	0.30E+00	0.13E+00
1.00	0.22E+00	0.20E+00	0.23E+00	0.17E+00	0.43E+00	0.17E+00
2.00	0.76E-01	0.38E-01	0.18E+00	0.15E+00	0.31E+00	0.17E+00
3.00	0.63E-02	0.74E-02	0.35E-01	0.11E+00	0.86E-01	0.14E+00
6.00	0.52E-02	0.57E-04	0.45E-01	0.37E-01	0.95E-01	0.81E-01
8.00	0.31E-02	0.27E-05	0.13E-01	0.18E-01	0.43E-01	0.60E-01
10.00	0.15E-02	0.47E-06	0.14E-01	0.86E-02	0.40E-01	0.46E-01
12.00	0.13E-02	0.18E-08	0.84E-02	0.41E-02	0.32E-01	0.36E-01
15.00	0.98E-03	-0.53E-07	0.39E-02	0.14E-02	0.20E-01	0.26E-01
18.00	0.61E-03	0.67E-08	0.22E-02	0.46E-03	0.12E-01	0.18E-01
22.00	0.40E-03	0.53E-08	0.91E-03	0.11E-03	0.80E-02	0.12E-01
26.00	0.36E-03	0.18E-08	0.72E-03	0.25E-04	0.63E-02	0.73E-02
30.00	0.25E-03	-0.44E-08	0.67E-03	0.59E-05	0.47E-02	0.47E-02
35.00	0.00E+00	0.11E-07	0.43E-03	0.14E-05	0.33E-02	0.26E-02
40.00	0.00E+00	-0.18E-08	0.27E-03	0.25E-06	0.24E-02	0.15E-02
65.00	0.00E+00	0.21E-08	0.53E-03	0.63E-08	0.12E-02	0.89E-04

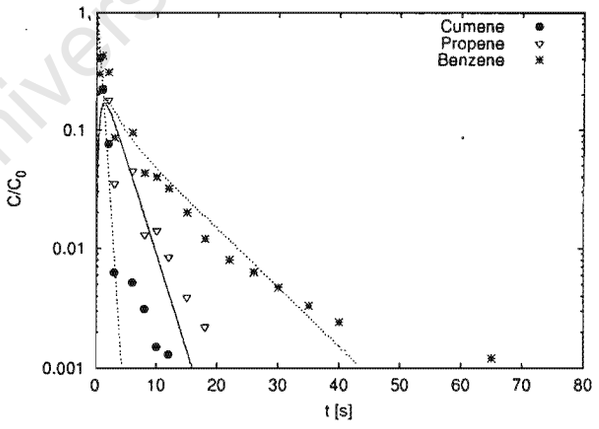

Appendix K. Cumene pulse experiments over T4480

Run Conditions react74

T_R [°C]	F(STP) [ml/min]	R_y [cm]	V_{cat} [ml]	τ [s]
471	411	0.033	0.432	2.61

Errors of C(t)

	Cumene	Propene	Benzene
Least Err	0.13E+00	0.94E-01	0.10E+00
R^2	0.999	0.913	0.902
Min Err% (@ time)	6.05(2.0)	1.12(6.0)	2.58(22.0)
Max Err% (@ time)	21.87(0.5)	31.69(0.5)	60.68(1.0)

Parameter Estimates

	Low Estimate	Estimate	High Estimate
$K_c(Benzene)$	133	186	261
$k_{eff}[1/s]$	817	1299	2066
$\alpha(Benzene)$	0.88E-01	0.12E+00	0.17E+00
ϕ	10	13	17

Model Parameters

	Cumene	Propene	Benzene
$D_y[cm^2/s]$	0.12E-01	0.20E-01	0.15E-01
$K_c[/]$	0	0	186
α	0.29E+02	0.48E+02	0.12E+00
β	0.25E+00	0.41E+00	0.31E+00

Experiment versus Model

	CUMENE		PROPENE		BENZENE	
t[s]	Exp	Mod	Exp	Mod	Exp	Mod
0.50	0.37E+00	0.46E+00	0.20E+00	0.12E+00	0.29E+00	0.14E+00
1.00	0.16E+00	0.21E+00	0.22E+00	0.16E+00	0.36E+00	0.20E+00
2.00	0.36E-01	0.44E-01	0.12E+00	0.14E+00	0.22E+00	0.19E+00
3.00	0.17E-01	0.92E-02	0.13E+00	0.10E+00	0.24E+00	0.16E+00
4.00	0.64E-02	0.19E-02	0.91E-01	0.72E-01	0.18E+00	0.13E+00
6.00	0.40E-02	0.85E-04	0.32E-01	0.34E-01	0.72E-01	0.84E-01
8.00	0.21E-02	0.40E-05	0.18E-01	0.16E-01	0.46E-01	0.58E-01
10.00	0.11E-02	0.25E-06	0.90E-02	0.73E-02	0.28E-01	0.40E-01
12.00	0.63E-03	0.71E-07	0.46E-02	0.34E-02	0.18E-01	0.28E-01
15.00	0.47E-03	0.14E-07	0.21E-02	0.11E-02	0.11E-01	0.17E-01
18.00	0.44E-03	0.49E-08	0.16E-02	0.35E-03	0.81E-02	0.97E-02
22.00	0.26E-03	-0.28E-08	0.49E-03	0.76E-04	0.42E-02	0.48E-02
26.00	0.20E-03	-0.51E-08	0.72E-03	0.17E-04	0.52E-02	0.24E-02
30.00	0.00E+00	0.79E-08	0.31E-03	0.39E-05	0.25E-02	0.12E-02
35.00	0.00E+00	-0.17E-09	0.36E-03	0.65E-06	0.19E-02	0.48E-03

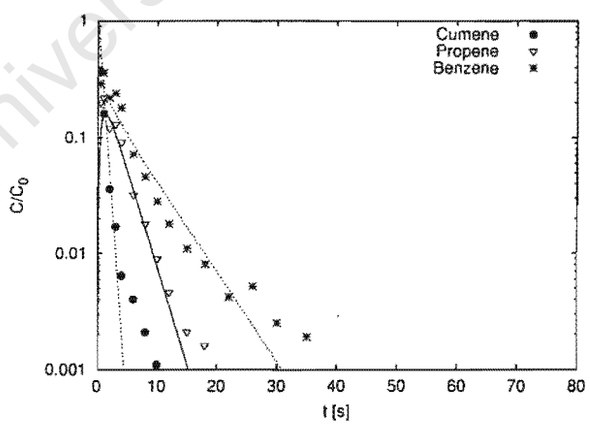

Appendix K. Cumene pulse experiments over T4480

Run Conditions react75

T_R [°C]	F(STP) [ml/min]	R_y [cm]	V_{cat} [ml]	τ [s]
471	411	0.033	0.432	2.61

Errors of C(t)

	Cumene	Propene	Benzene
Least Err	0.12E+00	0.66E-01	0.12E+00
R^2	0.989	0.961	0.907
Min Err% (@ time)	2.88(2.0)	1.00(10.0)	4.14(18.0)
Max Err% (@ time)	29.93(0.5)	29.82(0.5)	64.91(1.0)

Parameter Estimates

	Low Estimate	Estimate	High Estimate
$K_c(Benzene)$	104	146	204
$k_{eff}[1/s]$	436	697	1115
$\alpha(Benzene)$	0.11E+00	0.16E+00	0.22E+00
ϕ	7	9	12

Model Parameters

	Cumene	Propene	Benzene
$D_y[cm^2/s]$	0.12E-01	0.20E-01	0.15E-01
$K_c[/]$	0	0	146
α	0.29E+02	0.48E+02	0.16E+00
β	0.25E+00	0.41E+00	0.31E+00

Experiment versus Model

	CUMENE		PROPENE		BENZENE	
t[s]	Exp	Mod	Exp	Mod	Exp	Mod
0.50	0.42E+00	0.54E+00	0.16E+00	0.94E-01	0.25E+00	0.11E+00
1.00	0.19E+00	0.29E+00	0.19E+00	0.13E+00	0.33E+00	0.16E+00
2.00	0.81E-01	0.87E-01	0.17E+00	0.13E+00	0.32E+00	0.18E+00
3.00	0.30E-01	0.26E-01	0.11E+00	0.97E-01	0.23E+00	0.16E+00
4.00	0.11E-01	0.75E-02	0.80E-01	0.70E-01	0.17E+00	0.13E+00
6.00	0.32E-02	0.65E-03	0.27E-01	0.33E-01	0.62E-01	0.84E-01
8.00	0.19E-02	0.57E-04	0.17E-01	0.16E-01	0.44E-01	0.55E-01
10.00	0.92E-03	0.50E-05	0.70E-02	0.73E-02	0.23E-01	0.37E-01
12.00	0.67E-03	0.42E-06	0.39E-02	0.34E-02	0.15E-01	0.24E-01
15.00	0.38E-03	0.74E-08	0.15E-02	0.11E-02	0.85E-02	0.13E-01
18.00	0.31E-03	0.16E-08	0.83E-03	0.35E-03	0.58E-02	0.71E-02
22.00	0.00E+00	0.13E-10	0.74E-03	0.76E-04	0.40E-02	0.31E-02
26.00	0.00E+00	0.36E-10	0.52E-03	0.17E-04	0.22E-02	0.14E-02
30.00	0.00E+00	0.21E-09	0.33E-03	0.38E-05	0.17E-02	0.61E-03
35.00	0.00E+00	-0.10E-09	0.31E-03	0.76E-06	0.12E-02	0.22E-03
40.00	0.00E+00	0.31E-10	0.41E-03	0.12E-06	0.10E-02	0.79E-04

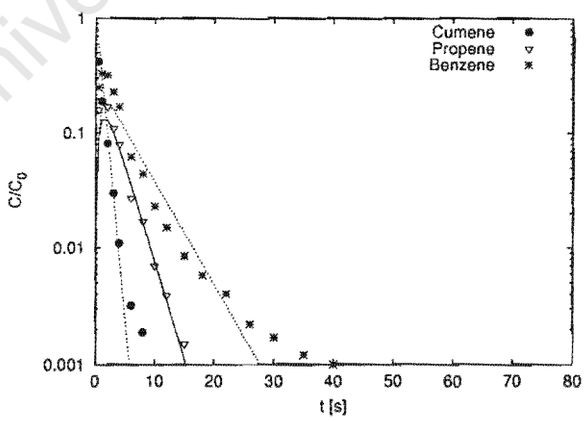

Appendix K. Cumene pulse experiments over T4480

Run Conditions react76

T_R [°C]	F(STP) [ml/min]	R_y [cm]	V_{cat} [ml]	τ [s]
471	511	0.033	0.432	2.10

Errors of C(t)

	Cumene	Propene	Benzene
Least Err	0.17E+00	0.90E+00	0.29E+00
R^2	0.974	0.944	0.987
Min Err% (@ time)	0.11(2.0)	1.63(8.0)	5.03(6.0)
Max Err% (@ time)	24.43(1.0)	36.77(0.5)	112.01(30.0)

Parameter Estimates

	Low Estimate	Estimate	High Estimate
$K_c(Benzene)$	0	0	*********
$k_{eff}[1/s]$	184	1088	6407
$\alpha(Benzene)$	0.00E+00	0.28E+02	0.29E+02
ϕ	5	12	30

Model Parameters

	Cumene	Propene	Benzene
$D_y[cm^2/s]$	0.12E-01	0.20E-01	0.15E-01
$K_c[/]$	0	0	0
α	0.23E+02	0.39E+02	0.28E+02
β	0.20E+00	0.33E+00	0.25E+00

Experiment versus Model

	CUMENE		PROPENE		BENZENE	
t[s]	Exp	Mod	Exp	Mod	Exp	Mod
0.50	0.40E+00	0.46E+00	0.20E+00	0.11E+00	0.31E+00	0.22E+00
1.00	0.13E+00	0.21E+00	0.18E+00	0.14E+00	0.33E+00	0.27E+00
2.00	0.45E-01	0.45E-01	0.13E+00	0.11E+00	0.26E+00	0.23E+00
3.00	0.21E-01	0.96E-02	0.10E+00	0.77E-01	0.21E+00	0.15E+00
4.00	0.79E-02	0.20E-02	0.61E-01	0.49E-01	0.14E+00	0.98E-01
6.00	0.22E-02	0.94E-04	0.17E-01	0.19E-01	0.45E-01	0.39E-01
8.00	0.11E-02	0.51E-05	0.69E-02	0.75E-02	0.23E-01	0.15E-01
10.00	0.58E-04	0.44E-06	0.29E-03	0.29E-02	0.13E-02	0.58E-02
12.00	0.68E-03	0.11E-07	0.36E-02	0.11E-02	0.94E-02	0.23E-02
15.00	0.30E-03	-0.22E-07	0.82E-03	0.27E-03	0.54E-02	0.54E-03
18.00	0.24E-03	-0.13E-07	0.42E-03	0.66E-04	0.32E-02	0.13E-03
22.00	0.00E+00	0.68E-09	0.31E-03	0.10E-04	0.21E-02	0.20E-04
26.00	0.00E+00	0.66E-08	0.27E-03	0.17E-05	0.14E-02	0.34E-05
30.00	0.00E+00	-0.25E-08	0.47E-03	0.27E-06	0.11E-02	0.54E-06

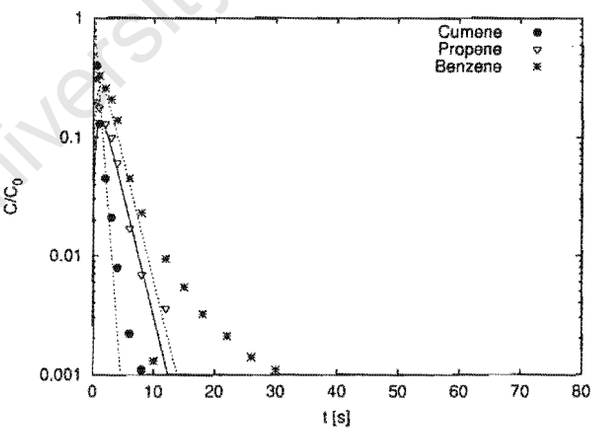

Appendix K. Cumene pulse experiments over T4480

Run Conditions react77

T_R [°C]	F(STP) [ml/min]	R_y [cm]	V_{cat} [ml]	τ [s]
441	511	0.033	0.432	2.19

Errors of C(t)

	Cumene	Propene	Benzene
Least Err	0.14E+00	0.81E-01	0.13E+00
R^2	0.993	0.880	0.779
Min Err% (@ time)	0.58(2.0)	1.61(10.0)	1.06(18.0)
Max Err% (@ time)	26.98(0.5)	48.50(0.5)	139.63(0.5)

Parameter Estimates

	Low Estimate	Estimate	High Estimate
$K_c(Benzene)$	108	157	228
$k_{eff}[1/s]$	579	1018	1790
$\alpha(Benzene)$	0.85E-01	0.12E+00	0.18E+00
ϕ	9	11	15

Model Parameters

	Cumene	Propene	Benzene
$D_y[cm^2/s]$	0.12E-01	0.20E-01	0.15E-01
$K_c[/]$	0	0	157
α	0.24E+02	0.40E+02	0.12E+00
β	0.21E+00	0.34E+00	0.26E+00

Experiment versus Model

	CUMENE		PROPENE		BENZENE	
t[s]	Exp	Mod	Exp	Mod	Exp	Mod
0.50	0.36E+00	0.47E+00	0.22E+00	0.11E+00	0.42E+00	0.13E+00
1.00	0.15E+00	0.23E+00	0.19E+00	0.14E+00	0.32E+00	0.18E+00
2.00	0.52E-01	0.51E-01	0.13E+00	0.12E+00	0.25E+00	0.17E+00
3.00	0.20E-01	0.11E-01	0.92E-01	0.81E-01	0.19E+00	0.14E+00
4.00	0.79E-02	0.26E-02	0.60E-01	0.53E-01	0.13E+00	0.11E+00
6.00	0.19E-02	0.13E-03	0.17E-01	0.22E-01	0.42E-01	0.65E-01
10.00	0.45E-03	0.41E-06	0.32E-02	0.35E-02	0.14E-01	0.26E-01
12.00	0.40E-03	0.81E-07	0.19E-02	0.14E-02	0.27E-01	0.16E-01
15.00	0.63E-03	0.65E-09	0.94E-03	0.36E-03	0.66E-02	0.82E-02
18.00	0.21E-03	0.98E-08	0.61E-03	0.93E-04	0.39E-02	0.42E-02
22.00	0.15E-03	-0.35E-08	0.42E-03	0.16E-04	0.27E-02	0.17E-02
26.00	0.11E-03	-0.42E-08	0.30E-03	0.26E-05	0.18E-02	0.68E-03

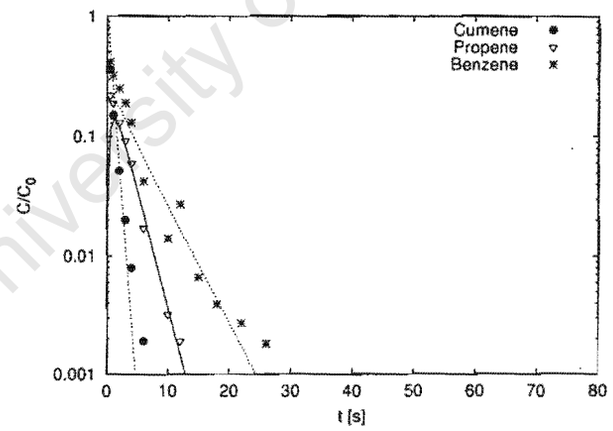

Appendix K. Cumene pulse experiments over T4480

Run Conditions react78

T_R [°C]	F(STP) [ml/min]	R_y [cm]	V_{cat} [ml]	τ [s]
441	411	0.033	0.432	2.72

Errors of C(t)

	Cumene	Propene	Benzene
Least Err	0.14E+00	0.12E+00	0.12E+00
R^2	0.977	0.926	0.887
Min Err% (@ time)	2.77(2.0)	0.01(8.0)	1.25(18.0)
Max Err% (@ time)	24.27(1.0)	40.72(22.0)	64.52(0.5)

Parameter Estimates

	Low Estimate	Estimate	High Estimate
$K_c(Benzene)$	130	181	252
$k_{eff}[1/s]$	552	899	1465
$\alpha(Benzene)$	0.95E-01	0.13E+00	0.18E+00
ϕ	8	11	14

Model Parameters

	Cumene	Propene	Benzene
$D_y[cm^2/s]$	0.12E-01	0.20E-01	0.15E-01
$K_c[/]$	0	0	181
α	0.30E+02	0.50E+02	0.13E+00
β	0.26E+00	0.42E+00	0.32E+00

Experiment versus Model

	CUMENE		PROPENE		BENZENE	
t[s]	Exp	Mod	Exp	Mod	Exp	Mod
0.50	0.44E+00	0.51E+00	0.19E+00	0.11E+00	0.27E+00	0.12E+00
1.00	0.17E+00	0.26E+00	0.18E+00	0.14E+00	0.31E+00	0.17E+00
2.00	0.75E-01	0.69E-01	0.17E+00	0.14E+00	0.31E+00	0.18E+00
3.00	0.31E-01	0.18E-01	0.13E+00	0.10E+00	0.25E+00	0.16E+00
4.00	0.62E-02	0.48E-02	0.46E-01	0.75E-01	0.93E-01	0.13E+00
6.00	0.63E-02	0.34E-03	0.54E-01	0.37E-01	0.12E+00	0.88E-01
8.00	0.15E-02	0.25E-04	0.18E-01	0.18E-01	0.46E-01	0.61E-01
10.00	0.62E-03	0.20E-05	0.79E-02	0.86E-02	0.31E-01	0.43E-01
12.00	0.44E-03	0.14E-06	0.41E-02	0.41E-02	0.16E-01	0.30E-01
15.00	0.35E-03	-0.18E-07	0.21E-02	0.14E-02	0.11E-01	0.18E-01
18.00	0.41E-03	-0.21E-08	0.15E-02	0.46E-03	0.10E-01	0.11E-01
22.00	0.57E-03	0.15E-07	0.15E-02	0.11E-03	0.45E-02	0.53E-02
26.00	0.15E-03	-0.15E-08	0.46E-03	0.25E-04	0.31E-02	0.26E-02
30.00	0.00E+00	-0.28E-08	0.51E-03	0.60E-05	0.26E-02	0.13E-02
35.00	0.00E+00	0.78E-08	0.40E-03	0.11E-05	0.17E-02	0.54E-03
40.00	0.00E+00	-0.23E-08	0.39E-03	0.21E-06	0.14E-02	0.23E-03
50.00	0.00E+00	-0.16E-08	0.53E-03	0.25E-07	0.12E-02	0.40E-04

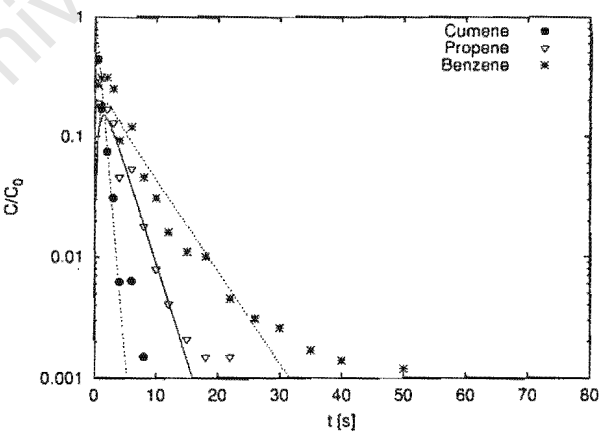

Appendix K. Cumene pulse experiments over T4480

Run Conditions react79

T_R [°C]	F(STP) [ml/min]	R_y [cm]	V_{cat} [ml]	τ [s]
419	411	0.033	0.432	2.81

Errors of C(t)

	Cumene	Propene	Benzene
Least Err	0.12E+00	0.61E-01	0.12E+00
R^2	0.973	0.986	0.969
Min Err% (@ time)	0.97(2.0)	0.03(12.0)	1.37(22.0)
Max Err% (@ time)	26.60(1.0)	15.58(0.5)	80.50(65.0)

Parameter Estimates

	Low Estimate	Estimate	High Estimate
$K_c(Benzene)$	122	178	260
$k_{eff}[1/s]$	424	701	1158
$\alpha(Benzene)$	0.95E-01	0.14E+00	0.20E+00
ϕ	7	9	12

Model Parameters

	Cumene	Propene	Benzene
$D_y[cm^2/s]$	0.12E-01	0.20E-01	0.15E-01
$K_c[/]$	0	0	178
α	0.31E+02	0.52E+02	0.14E+00
β	0.27E+00	0.44E+00	0.33E+00

Experiment versus Model

	CUMENE		PROPENE		BENZENE	
t[s]	Exp	Mod	Exp	Mod	Exp	Mod
0.50	0.50E+00	0.55E+00	0.13E+00	0.95E-01	0.15E+00	0.10E+00
1.00	0.20E+00	0.30E+00	0.17E+00	0.13E+00	0.25E+00	0.16E+00
2.00	0.89E-01	0.91E-01	0.16E+00	0.13E+00	0.26E+00	0.18E+00
3.00	0.32E-01	0.27E-01	0.12E+00	0.11E+00	0.22E+00	0.16E+00
4.00	0.14E-01	0.83E-02	0.83E-01	0.78E-01	0.16E+00	0.13E+00
6.00	0.72E-02	0.76E-03	0.58E-01	0.39E-01	0.12E+00	0.91E-01
8.00	0.15E-02	0.70E-04	0.19E-01	0.19E-01	0.46E-01	0.64E-01
10.00	0.13E-02	0.68E-05	0.14E-01	0.96E-02	0.39E-01	0.45E-01
12.00	0.44E-03	0.67E-06	0.47E-02	0.47E-02	0.17E-01	0.32E-01
15.00	0.40E-03	0.27E-07	0.24E-02	0.16E-02	0.11E-01	0.19E-01
22.00	0.27E-03	0.13E-07	0.61E-03	0.14E-03	0.53E-02	0.57E-02
26.00	0.22E-03	-0.14E-07	0.69E-03	0.34E-04	0.35E-02	0.29E-02
30.00	0.00E+00	-0.34E-08	0.81E-03	0.83E-05	0.30E-02	0.14E-02
35.00	0.00E+00	0.10E-07	0.36E-03	0.17E-05	0.22E-02	0.61E-03
40.00	0.00E+00	-0.25E-08	0.39E-03	0.29E-06	0.15E-02	0.26E-03
65.00	0.00E+00	0.52E-09	0.00E+00	-0.25E-07	0.10E-02	0.39E-05

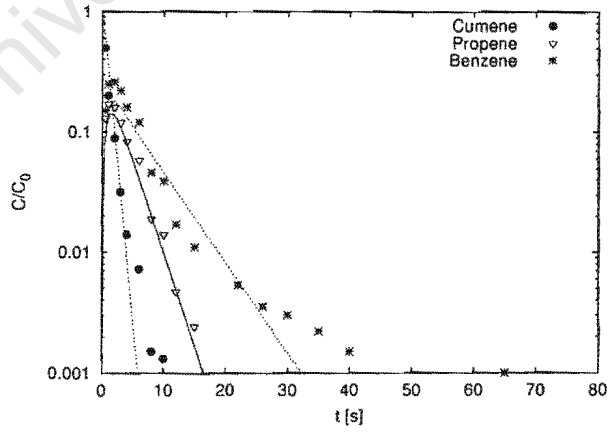

Appendix K. Cumene pulse experiments over T4480

Run Conditions react80

T_R [°C]	F(STP) [ml/min]	R_y [cm]	V_{cat} [ml]	τ [s]
419	511	0.033	0.432	2.26

Errors of C(t)

	Cumene	Propene	Benzene
Least Err	0.12E+00	0.67E-01	0.14E+00
R^2	0.981	0.959	0.969
Min Err% (@ time)	0.49(2.0)	0.31(8.0)	1.78(15.0)
Max Err% (@ time)	22.03(1.0)	27.91(0.5)	68.43(40.0)

Parameter Estimates

	Low Estimate	Estimate	High Estimate
$K_c(Benzene)$	72	115	185
$k_{eff}[1/s]$	495	828	1387
$\alpha(Benzene)$	0.11E+00	0.17E+00	0.27E+00
ϕ	8	10	13

Model Parameters

	Cumene	Propene	Benzene
$D_y[cm^2/s]$	0.12E-01	0.20E-01	0.15E-01
$K_c[/]$	0	0	115
α	0.25E+02	0.41E+02	0.17E+00
β	0.21E+00	0.35E+00	0.26E+00

Experiment versus Model

	CUMENE		PROPENE		BENZENE	
t[s]	Exp	Mod	Exp	Mod	Exp	Mod
0.50	0.45E+00	0.50E+00	0.16E+00	0.98E-01	0.21E+00	0.12E+00
1.00	0.17E+00	0.25E+00	0.17E+00	0.13E+00	0.26E+00	0.18E+00
2.00	0.66E-01	0.65E-01	0.14E+00	0.12E+00	0.23E+00	0.18E+00
3.00	0.26E-01	0.17E-01	0.11E+00	0.83E-01	0.20E+00	0.15E+00
4.00	0.65E-02	0.42E-02	0.58E-01	0.56E-01	0.12E+00	0.11E+00
6.00	0.28E-02	0.28E-03	0.37E-01	0.23E-01	0.87E-01	0.67E-01
8.00	0.79E-03	0.18E-04	0.99E-02	0.98E-02	0.28E-01	0.40E-01
10.00	0.42E-03	0.13E-05	0.39E-02	0.40E-02	0.15E-01	0.23E-01
12.00	0.31E-03	0.21E-06	0.20E-02	0.17E-02	0.98E-02	0.14E-01
15.00	0.23E-03	0.32E-07	0.87E-03	0.45E-03	0.58E-02	0.64E-02
18.00	0.14E-03	0.10E-07	0.83E-03	0.12E-03	0.48E-02	0.29E-02
22.00	0.86E-04	-0.79E-08	0.25E-03	0.21E-04	0.29E-02	0.10E-02
26.00	0.00E+00	-0.65E-08	0.00E+00	0.37E-05	0.21E-02	0.36E-03
30.00	0.00E+00	0.38E-08	0.38E-03	0.75E-06	0.24E-02	0.13E-03
35.00	0.00E+00	0.25E-08	0.37E-03	0.10E-06	0.16E-02	0.34E-04
40.00	0.00E+00	-0.20E-08	0.14E-03	0.23E-07	0.11E-02	0.96E-05

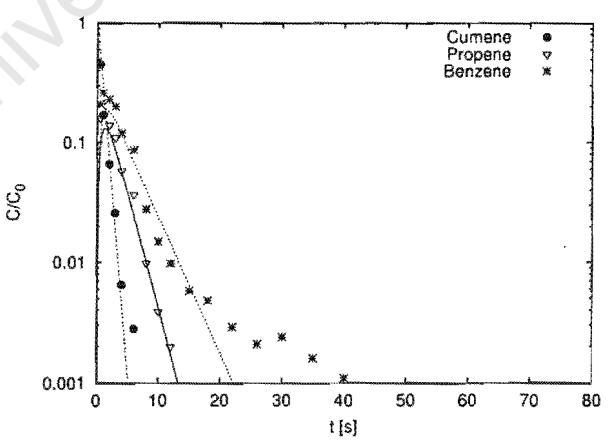

Appendix K. Cumene pulse experiments over T4480

Run Conditions react81				
T_R [°C]	F(STP) [ml/min]	R_y [cm]	V_{cat} [ml]	τ [s]
391	411	0.033	0.432	2.93

Errors of C(t)			
	Cumene	Propene	Benzene
Least Err	0.10E+00	0.78E-01	0.12E+00
R^2	0.987	0.964	0.938
Min Err% (@ time)	0.88(2.0)	1.94(10.0)	1.51(22.0)
Max Err% (@ time)	24.76(1.0)	29.97(0.5)	53.03(50.0)

Parameter Estimates			
	Low Estimate	Estimate	High Estimate
$K_c(Benzene)$	116	165	234
$k_{eff}[1/s]$	411	671	1096
$\alpha(Benzene)$	0.11E+00	0.16E+00	0.22E+00
ϕ	7	9	12

Model Parameters			
	Cumene	Propene	Benzene
$D_y[cm^2/s]$	0.12E-01	0.20E-01	0.15E-01
$K_c[/]$	0	0	165
α	0.33E+02	0.54E+02	0.16E+00
β	0.28E+00	0.46E+00	0.34E+00

Experiment versus Model

	CUMENE		PROPENE		BENZENE	
t[s]	Exp	Mod	Exp	Mod	Exp	Mod
0.50	0.46E+00	0.56E+00	0.16E+00	0.94E-01	0.20E+00	0.10E+00
1.00	0.21E+00	0.31E+00	0.19E+00	0.13E+00	0.27E+00	0.16E+00
2.00	0.95E-01	0.97E-01	0.17E+00	0.14E+00	0.27E+00	0.18E+00
3.00	0.40E-01	0.30E-01	0.14E+00	0.11E+00	0.23E+00	0.16E+00
4.00	0.13E-01	0.95E-02	0.86E-01	0.82E-01	0.16E+00	0.14E+00
6.00	0.77E-02	0.93E-03	0.59E-01	0.43E-01	0.12E+00	0.97E-01
8.00	0.11E-02	0.90E-04	0.18E-01	0.22E-01	0.43E-01	0.68E-01
10.00	0.50E-03	0.87E-05	0.10E-01	0.11E-01	0.29E-01	0.48E-01
12.00	0.40E-03	0.10E-05	0.66E-02	0.56E-02	0.22E-01	0.34E-01
15.00	0.34E-03	0.13E-06	0.32E-02	0.20E-02	0.15E-01	0.20E-01
18.00	0.17E-03	0.88E-07	0.15E-02	0.73E-03	0.84E-02	0.12E-01
22.00	0.00E+00	-0.62E-08	0.60E-03	0.19E-03	0.55E-02	0.59E-02
26.00	0.00E+00	-0.23E-07	0.52E-03	0.49E-04	0.38E-02	0.30E-02
30.00	0.00E+00	0.11E-07	0.31E-03	0.13E-04	0.29E-02	0.15E-02
35.00	0.00E+00	-0.99E-08	0.37E-03	0.26E-05	0.25E-02	0.62E-03
40.00	0.00E+00	0.85E-09	0.29E-03	0.50E-06	0.18E-02	0.26E-03
50.00	0.00E+00	0.17E-07	0.67E-03	0.10E-06	0.15E-02	0.47E-04

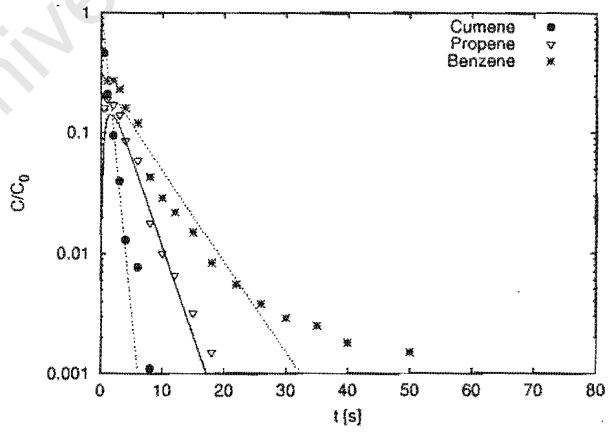

Appendix L

Cumene pulse experiments over E1-E3 extrudates

Appendix L. Cumene pulse experiments over E1-E3 extrudates

Run Conditions react83

T_R [°C]	F(STP) [ml/min]	R_y [cm]	V_{cat} [ml]	τ [s]
350	411	0.075	0.432	3.12

Errors of C(t)

	Cumene	Propene	Benzene
Least Err	0.12E+00	0.82E-01	0.10E+00
R^2	0.973	0.954	0.941
Min Err% (@ time)	0.04(0.5)	1.31(15.0)	0.14(4.0)
Max Err% (@ time)	30.18(6.0)	30.94(0.5)	76.12(26.0)

Parameter Estimates

	Low Estimate	Estimate	High Estimate
$K_c(Propene)$	26	74	205
$K_c(Benzene)$	66	254	971
$D_{Cumene}[cm^2/s]$	0.29E-2	0.70E-02	0.17E-01
$\alpha(Propene)$	0.88E-02	0.58E-01	0.39E+00
$\alpha(Benzene)$	0.13E-02	0.12E-01	0.11E+00
ϕ	35	55	87

Model Parameters

	Cumene	Propene	Benzene
$k_{eff}[1/s]$	0.25E+04		
$D_y[cm^2/s]$	0.70E-02	0.12E-01	0.87E-02
$K_c[/]$	0	74	254
α	0.39E+01	0.58E-01	0.12E-01
β	0.33E-01	0.58E-01	0.41E-01

Experiment versus Model

	CUMENE		PROPENE		BENZENE	
t[s]	Exp	Mod	Exp	Mod	Exp	Mod
0.50	0.64E+00	0.64E+00	0.11E+00	0.57E-01	0.13E+00	0.91E-01
1.00	0.30E+00	0.41E+00	0.15E+00	0.89E-01	0.20E+00	0.15E+00
2.00	0.13E+00	0.16E+00	0.14E+00	0.10E+00	0.20E+00	0.18E+00
3.00	0.63E-01	0.67E-01	0.13E+00	0.93E-01	0.17E+00	0.16E+00
4.00	0.31E-01	0.27E-01	0.99E-01	0.76E-01	0.14E+00	0.14E+00
6.00	0.16E-01	0.44E-02	0.73E-01	0.47E-01	0.10E+00	0.87E-01
8.00	0.23E-02	0.73E-03	0.22E-01	0.29E-01	0.32E-01	0.56E-01
10.00	0.14E-02	0.12E-03	0.15E-01	0.18E-01	0.23E-01	0.37E-01
12.00	0.87E-03	0.21E-04	0.92E-02	0.12E-01	0.15E-01	0.26E-01
15.00	0.71E-03	0.15E-05	0.69E-02	0.65E-02	0.13E-01	0.16E-01
18.00	0.75E-03	0.54E-06	0.42E-02	0.38E-02	0.97E-02	0.11E-01
22.00	0.00E+00	0.11E-06	0.22E-02	0.20E-02	0.59E-02	0.68E-02
26.00	0.00E+00	-0.50E-07	0.19E-02	0.10E-02	0.48E-01	0.47E-02
30.00	0.00E+00	-0.40E-08	0.13E-02	0.57E-03	0.44E-02	0.35E-02
35.00	0.00E+00	0.12E-07	0.94E-03	0.27E-03	0.46E-02	0.26E-02
50.00	0.00E+00	-0.41E-08	0.35E-03	0.29E-04	0.19E-02	0.13E-02
65.00	0.00E+00	-0.51E-08	0.47E-03	0.32E-05	0.18E-02	0.75E-03
80.00	0.00E+00	-0.77E-08	0.79E-03	0.39E-06	0.14E-02	0.44E-03

Appendix L. Cumene pulse experiments over E1-E3 extrudates

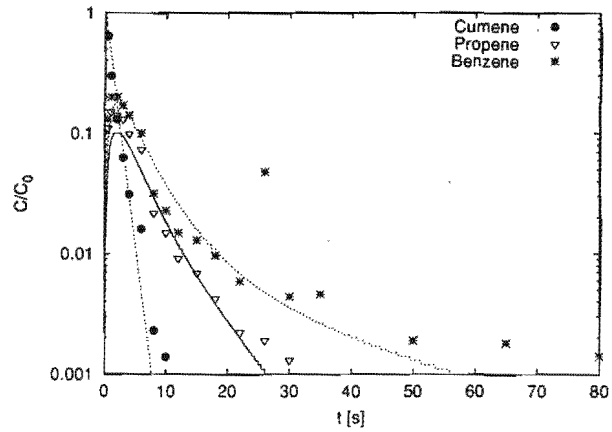

Appendix L. Cumene pulse experiments over E1-E3 extrudates

Run Conditions react84

T_R [°C]	F(STP) [ml/min]	R_y [cm]	V_{cat} [ml]	τ [s]
350	411	0.075	0.432	3.12

Errors of C(t)

	Cumene	Propene	Benzene
Least Err	0.68E-01	0.80E-01	0.75E-01
R^2	0.975	0.953	0.956
Min Err% (@ time)	8.55(3.0)	1.47(8.0)	1.09(35.0)
Max Err% (@ time)	45.52(0.5)	26.84(1.0)	28.53(1.0)

Parameter Estimates

	Low Estimate	Estimate	High Estimate
$K_c(Propene)$	39	80	166
$K_c(Benzene)$	161	408	1034
$D_{Cumene}[cm^2/s]$	0.42E-02	0.91E-02	0.19E-01
$\alpha(Propene)$	0.16E-01	0.69E-01	0.30E+00
$\alpha(Benzene)$	0.18E-02	0.97E-02	0.53E-01
ϕ	34	49	72

Model Parameters

	Cumene	Propene	Benzene
$k_{eff}[1/s]$	0.25E+04		
$D_y[cm^2/s]$	0.91E-02	0.16E-01	0.11E-01
$K_c[/]$	0	80	408
α	0.50E+01	0.69E-01	0.97E-02
β	0.43E-01	0.75E-01	0.53E-01

Experiment versus Model

	CUMENE		PROPENE		BENZENE	
t[s]	Exp	Mod	Exp	Mod	Exp	Mod
0.50	0.71E+00	0.61E+00	0.11E+00	0.63E-01	0.14E+00	0.90E-01
1.00	0.34E+00	0.38E+00	0.16E+00	0.96E-01	0.22E+00	0.15E+00
2.00	0.18E+00	0.14E+00	0.15E+00	0.11E+00	0.23E+00	0.17E+00
3.00	0.67E-01	0.53E-01	0.12E+00	0.96E-01	0.19E+00	0.16E+00
6.00	0.71E-02	0.28E-02	0.40E-01	0.48E-01	0.62E-01	0.84E-01
8.00	0.27E-02	0.40E-03	0.28E-01	0.30E-01	0.45E-01	0.56E-01
15.00	0.58E-03	0.11E-05	0.79E-02	0.71E-02	0.14E-01	0.18E-01
18.00	0.61E-03	0.14E-08	0.37E-02	0.41E-02	0.91E-02	0.13E-01
22.00	0.53E-03	-0.47E-08	0.25E-02	0.21E-02	0.72E-02	0.88E-02
26.00	0.53E-03	0.38E-07	0.18E-02	0.11E-02	0.58E-02	0.64E-02
30.00	0.46E-03	-0.69E-07	0.11E-02	0.57E-03	0.45E-02	0.49E-02
35.00	0.00E+00	-0.28E-08	0.91E-03	0.25E-03	0.35E-02	0.37E-02
45.00	0.00E+00	0.60E-07	0.80E-03	0.50E-04	0.31E-02	0.24E-02
60.00	0.00E+00	-0.23E-08	0.88E-03	0.46E-05	0.32E-02	0.14E-02
80.00	0.00E+00	0.13E-08	0.66E-04	0.22E-06	0.12E-02	0.78E-03
100.00	0.00E+00	0.11E-08	0.00E+00	0.35E-07	0.10E-02	0.45E-03

Appendix L. Cumene pulse experiments over E1-E3 extrudates

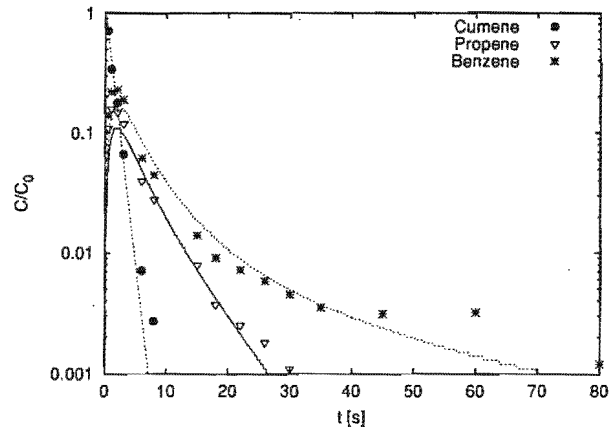

Appendix L. Cumene pulse experiments over E1-E3 extrudates

Run Conditions react85

T_R [°C]	F(STP) [ml/min]	R_y [cm]	V_{cat} [ml]	τ [s]
350	411	0.075	0.432	3.12

Errors of C(t)

	Cumene	Propene	Benzene
Least Err	0.12E+00	0.96E-01	0.82E-01
R^2	0.987	0.903	0.955
Min Err% (@ time)	5.98(3.0)	0.14(2.0)	0.33(22.0)
Max Err% (@ time)	51.01(0.5)	30.72(0.5)	20.66(0.5)

Parameter Estimates

	Low Estimate	Estimate	High Estimate
$K_c(Propene)$	10	38	132
$K_c(Benzene)$	41	126	386
$D_{Cumene}[cm^2/s]$	0.23E-02	0.53E-02	0.12E-01
$\alpha(Propene)$	0.11E-01	0.85E-01	0.64E+00
$\alpha(Benzene)$	0.27E-02	0.18E-01	0.13E+00
ϕ	43	64	96

Model Parameters

	Cumene	Propene	Benzene
$k_{eff}[1/s]$	0.25E+04		
$D_y[cm^2/s]$	0.53E-02	0.93E-02	0.66E-02
$K_c[/]$	0	38	126
α	0.29E+01	0.85E-01	0.18E-01
β	0.25E-01	0.44E-01	0.31E-01

Experiment versus Model

	CUMENE		PROPENE		BENZENE	
t[s]	Exp	Mod	Exp	Mod	Exp	Mod
0.50	0.76E+00	0.66E+00	0.11E+00	0.54E-01	0.14E+00	0.93E-01
1.00	0.41E+00	0.44E+00	0.14E+00	0.85E-01	0.20E+00	0.15E+00
2.00	0.22E+00	0.19E+00	0.10E+00	0.10E+00	0.20E+00	0.18E+00
3.00	0.96E-01	0.84E-01	0.11E+00	0.92E-01	0.17E+00	0.17E+00
4.00	0.53E-01	0.37E-01	0.91E-01	0.76E-01	0.14E+00	0.14E+00
6.00	0.26E-01	0.70E-02	0.70E-01	0.47E-01	0.11E+00	0.89E-01
8.00	0.42E-02	0.13E-02	0.21E-01	0.28E-01	0.34E-01	0.55E-01
10.00	0.18E-02	0.26E-03	0.14E-01	0.17E-01	0.23E-01	0.35E-01
12.00	0.12E-02	0.50E-04	0.92E-02	0.10E-01	0.16E-01	0.22E-01
15.00	0.83E-03	0.44E-05	0.52E-02	0.50E-02	0.95E-02	0.13E-01
18.00	0.53E-03	0.81E-06	0.30E-02	0.25E-02	0.63E-02	0.78E-02
22.00	0.50E-03	0.12E-06	0.20E-02	0.10E-02	0.47E-02	0.46E-02
26.00	0.41E-03	-0.14E-07	0.14E-02	0.45E-03	0.36E-02	0.31E-02
30.00	0.61E-03	-0.12E-07	0.11E-02	0.19E-03	0.33E-02	0.22E-02
35.00	0.00E+00	0.12E-07	0.62E-03	0.67E-04	0.22E-02	0.16E-02
60.00	0.00E+00	0.34E-08	0.79E-03	0.41E-06	0.13E-02	0.38E-03

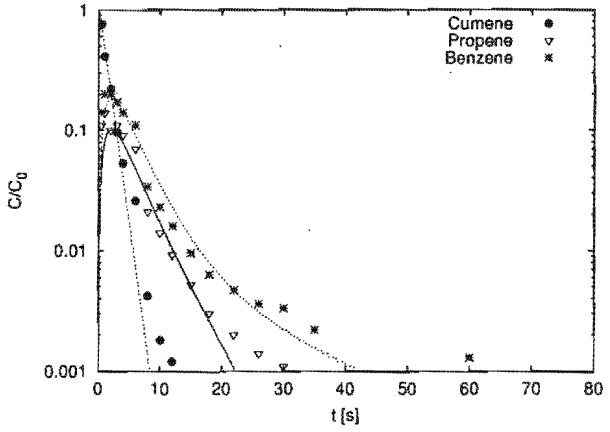

Appendix L. Cumene pulse experiments over E1-E3 extrudates

Run Conditions react86

T_R [°C]	F(STP) [ml/min]	R_y [cm]	V_{cat} [ml]	τ [s]
350	411	0.075	0.432	3.12

Errors of C(t)

	Cumene	Propene	Benzene
Least Err	0.13E+00	0.11E+00	0.96E-01
R^2	0.989	0.966	0.975
Min Err% (@ time)	6.86(0.5)	0.58(18.0)	0.38(2.0)
Max Err% (@ time)	34.08(6.0)	127.19(80.0)	48.00(80.0)

Parameter Estimates

	Low Estimate	Estimate	High Estimate
$K_c(Propene)$	23	55	133
$K_c(Benzene)$	37	123	407
$D_{Cumene}[cm^2/s]$	0.25E-02	0.51E-02	0.11E-01
$\alpha(Propene)$	0.11E-01	0.56E-01	0.27E+00
$\alpha(Benzene)$	0.27E-02	0.18E-01	0.12E+00
ϕ	44	65	94

Model Parameters

	Cumene	Propene	Benzene
$k_{eff}[1/s]$	0.25E+04		
$D_y[cm^2/s]$	0.51E-02	0.89E-02	0.63E-02
$K_c[/]$	0	55	123
α	0.28E+01	0.56E-01	0.18E-01
β	0.24E-01	0.42E-01	0.30E-01

Experiment versus Model

	CUMENE		PROPENE		BENZENE	
t[s]	Exp	Mod	Exp	Mod	Exp	Mod
0.50	0.68E+00	0.66E+00	0.88E-01	0.52E-01	0.11E+00	0.91E-01
1.00	0.40E+00	0.44E+00	0.12E+00	0.82E-01	0.17E+00	0.15E+00
2.00	0.23E+00	0.19E+00	0.12E+00	0.98E-01	0.18E+00	0.18E+00
3.00	0.11E+00	0.86E-01	0.10E+00	0.90E-01	0.15E+00	0.17E+00
6.00	0.26E-01	0.74E-02	0.65E-01	0.46E-01	0.10E+00	0.89E-01
8.00	0.50E-02	0.14E-02	0.22E-01	0.28E-01	0.36E-01	0.55E-01
10.00	0.23E-02	0.28E-03	0.14E-01	0.17E-01	0.25E-01	0.34E-01
12.00	0.11E-02	0.56E-04	0.90E-02	0.11E-01	0.16E-01	0.22E-01
15.00	0.78E-03	0.52E-05	0.48E-02	0.55E-02	0.95E-02	0.12E-01
18.00	0.73E-03	0.74E-06	0.32E-02	0.31E-02	0.70E-02	0.76E-02
22.00	0.52E-03	0.77E-07	0.19E-02	0.15E-02	0.51E-02	0.45E-02
26.00	0.49E-03	-0.30E-07	0.12E-02	0.79E-03	0.38E-02	0.30E-02
30.00	0.47E-03	0.18E-07	0.85E-03	0.42E-03	0.28E-02	0.21E-02
45.00	0.00E+00	-0.13E-07	0.64E-03	0.42E-04	0.22E-02	0.83E-03
60.00	0.00E+00	0.28E-08	0.83E-03	0.44E-05	0.13E-02	0.37E-03
80.00	0.00E+00	0.51E-10	0.12E-02	0.22E-06	0.23E-02	0.13E-03

Appendix L. Cumene pulse experiments over E1-E3 extrudates

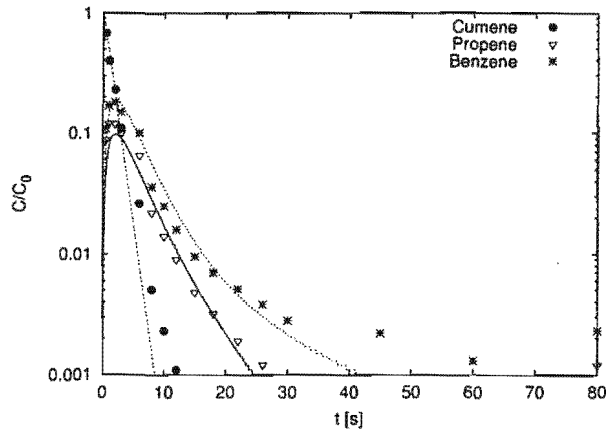

Appendix L. Cumene pulse experiments over E1-E3 extrudates

Run Conditions react87

T_R [°C]	F(STP) [ml/min]	R_y [cm]	V_{cat} [ml]	τ [s]
350	411	0.075	0.432	3.12

Errors of C(t)

	Cumene	Propene	Benzene
Least Err	0.13E+00	0.13E+00	0.69E-01
R^2	0.992	0.918	0.969
Min Err% (@ time)	4.53(2.0)	0.76(2.0)	0.29(22.0)
Max Err% (@ time)	43.21(6.0)	65.67(22.0)	15.11(0.5)

Parameter Estimates

	Low Estimate	Estimate	High Estimate
$K_c(Propene)$	14	31	69
$K_c(Benzene)$	22	73	245
$D_{Cumene}[cm^2/s]$	0.19E-02	0.50E-02	0.13E-01
$\alpha(Propene)$	0.17E-01	0.97E-01	0.54E+00
$\alpha(Benzene)$	0.34E-02	0.29E-01	0.25E+00
ϕ	41	66	106

Model Parameters

	Cumene	Propene	Benzene
$k_{eff}[1/s]$	0.25E+04		
$D_y[cm^2/s]$	0.50E-02	0.87E-02	0.62E-02
$K_c[/]$	0	31	73
α	0.28E+01	0.97E-01	0.29E-01
β	0.24E-01	0.41E-01	0.29E-01

Experiment versus Model

	CUMENE		PROPENE		BENZENE	
t[s]	Exp	Mod	Exp	Mod	Exp	Mod
0.50	0.63E+00	0.67E+00	0.80E-01	0.54E-01	0.13E+00	0.97E-01
1.00	0.38E+00	0.44E+00	0.11E+00	0.84E-01	0.20E+00	0.16E+00
2.00	0.21E+00	0.20E+00	0.10E+00	0.10E+00	0.20E+00	0.19E+00
3.00	0.11E+00	0.87E-01	0.84E-01	0.92E-01	0.17E+00	0.18E+00
4.00	0.67E-01	0.39E-01	0.72E-01	0.76E-01	0.15E+00	0.15E+00
6.00	0.33E-01	0.76E-02	0.55E-01	0.47E-01	0.12E+00	0.91E-01
10.00	0.30E-02	0.30E-03	0.12E-01	0.16E-01	0.29E-01	0.33E-01
12.00	0.14E-02	0.59E-04	0.61E-02	0.98E-02	0.17E-01	0.21E-01
22.00	0.22E-03	0.36E-07	0.14E-01	0.88E-03	0.37E-02	0.36E-02
26.00	0.31E-03	-0.17E-07	0.40E-03	0.35E-03	0.26E-02	0.22E-02
30.00	0.00E+00	0.12E-07	0.38E-03	0.14E-03	0.22E-02	0.15E-02
35.00	0.00E+00	-0.30E-07	0.24E-03	0.44E-04	0.15E-02	0.92E-03
45.00	0.00E+00	-0.84E-08	0.39E-03	0.47E-05	0.11E-02	0.38E-03

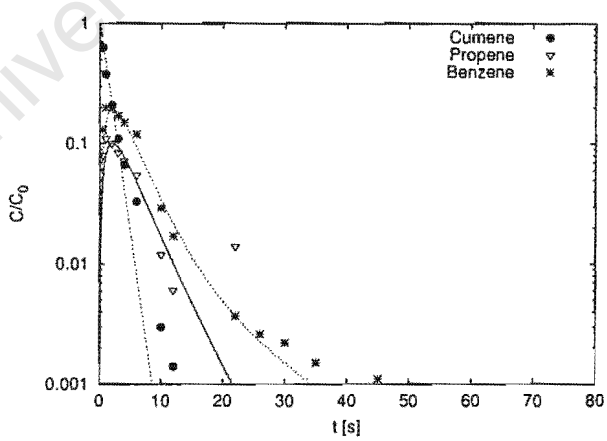

Appendix L. Cumene pulse experiments over E1-E3 extrudates

Run Conditions react88

T_R [°C]	F(STP) [ml/min]	R_y [cm]	V_{cat} [ml]	τ [s]
350	411	0.075	0.432	3.12

Errors of C(t)

	Cumene	Propene	Benzene
Least Err	0.17E+00	0.55E-01	0.67E-01
R^2	0.990	0.963	0.967
Min Err% (@ time)	2.65(1.0)	1.96(12.0)	0.36(22.0)
Max Err% (@ time)	56.82(6.0)	8.31(0.5)	18.78(8.0)

Parameter Estimates

	Low Estimate	Estimate	High Estimate
$K_c(Propene)$	0	8	126
$K_c(Benzene)$	34	68	134
$D_{Cumene}[cm^2/s]$	0.29E-02	0.62E-02	0.13E-01
$\alpha(Propene)$	0.14E-01	0.44E+00	0.71E+01
$\alpha(Benzene)$	0.93E-02	0.40E-01	0.17E+00
ϕ	88	59	87

Model Parameters

	Cumene	Propene	Benzene
$k_{eff}[1/s]$	0.25E+04		
$D_y[cm^2/s]$	0.62E-02	0.11E-01	0.77E-02
$K_c[/]$	0	8	68
α	0.34E+01	0.44E+00	0.40E-01
β	0.29E-01	0.51E-01	0.36E-01

Experiment versus Model

	CUMENE		PROPENE		BENZENE	
t[s]	Exp	Mod	Exp	Mod	Exp	Mod
0.50	0.69E+00	0.65E+00	0.79E-01	0.64E-01	0.13E+00	0.11E+00
1.00	0.41E+00	0.42E+00	0.11E+00	0.97E-01	0.20E+00	0.17E+00
2.00	0.24E+00	0.18E+00	0.10E+00	0.11E+00	0.20E+00	0.20E+00
4.00	0.66E-01	0.31E-01	0.71E-01	0.82E-01	0.14E+00	0.15E+00
6.00	0.36E-01	0.55E-02	0.57E-01	0.48E-01	0.12E+00	0.93E-01
8.00	0.91E-02	0.97E-03	0.23E-01	0.27E-01	0.88E-01	0.56E-01
10.00	0.24E-02	0.17E-03	0.11E-01	0.15E-01	0.24E-01	0.34E-01
12.00	0.15E-02	0.31E-04	0.72E-02	0.79E-02	0.18E-01	0.22E-01
15.00	0.69E-03	0.27E-05	0.36E-02	0.32E-02	0.11E-01	0.12E-01
18.00	0.55E-03	0.22E-06	0.17E-02	0.13E-02	0.65E-02	0.69E-02
22.00	0.37E-03	0.45E-07	0.75E-03	0.37E-03	0.38E-02	0.37E-02
26.00	0.00E+00	0.33E-07	0.42E-03	0.11E-03	0.25E-02	0.22E-02
30.00	0.00E+00	-0.80E-08	0.59E-03	0.33E-04	0.27E-02	0.13E-02
35.00	0.00E+00	-0.19E-07	0.67E-03	0.72E-05	0.16E-02	0.74E-03